The role of inflammation in cardiac and vascular remodelling
Jong, R.C.M. de

Citation

Jong, R. C. M. de. (2019, January 31). *The role of inflammation in cardiac and vascular remodelling*. Retrieved from https://hdl.handle.net/1887/68468

Note: To cite this publication please use the final published version (if applicable).

Cover Page

Universiteit Leiden

Author: Jong, R.C.M. de
Title: The role of inflammation in cardiac and vascular remodelling
Issue Date: 2019-01-31

The role of inflammation in cardiac and vascular remodelling
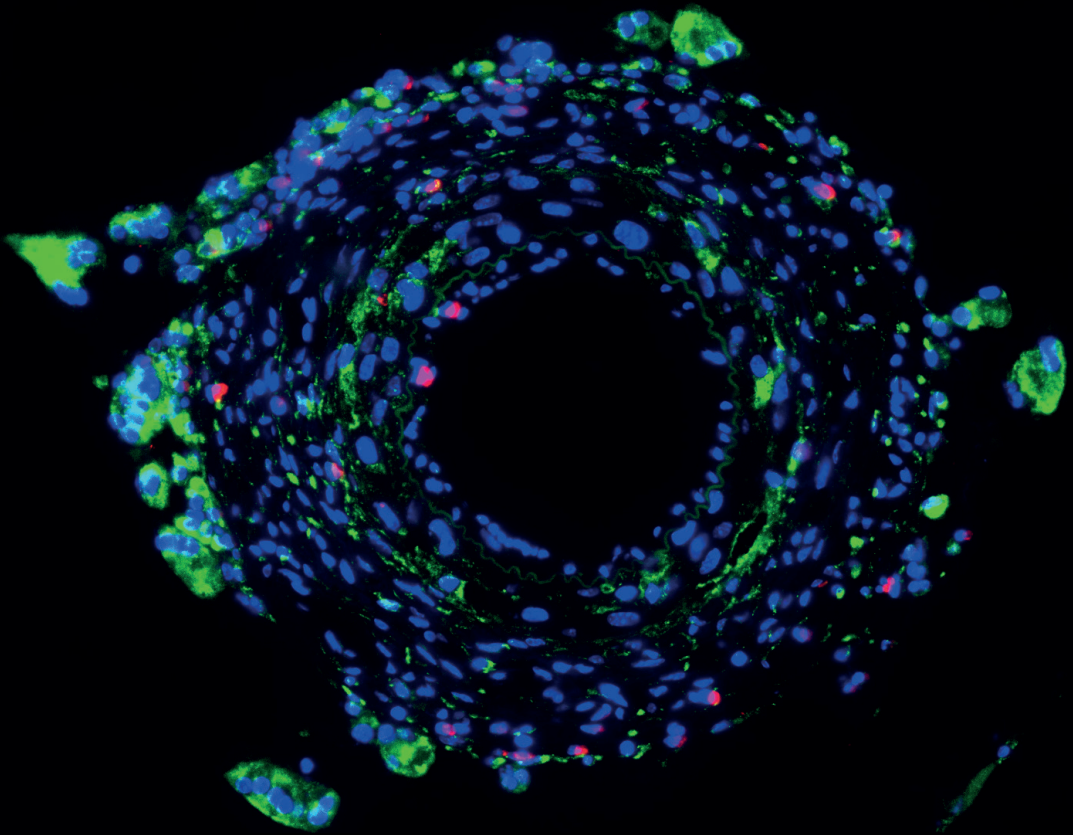
Rob de Jong

The role of inflammation in cardiac and vascular remodelling

Rob de Jong

The role of inflammation in cardiac and vascular remodelling

Proefschrift

ter verkrijging van
de graad van Doctor aan de Universiteit Leiden,
op gezag van Rector Magnificus prof. mr. C.J.J.M. Stolker,
volgens besluit van het College voor Promoties
te verdedigen op donderdag 31 januari 2019
klokke 15:00 uur

door

Robbert Cornelis Maria de Jong

Geboren te Leidschendam
in 1985

Promotores: Prof. dr. P.H.A. Quax
                      Prof. dr. J.W. Jukema

Co-promotor: Dr. M.R. de Vries

Leden promotiecommissie: Prof. dr. M.J.T.H. Goumans
                      Prof. dr. P.C.N. Rensen
                      Dr. S.C.A. de Jager (UMC Utrecht)
                      Dr. I. Bot (LACDR, Leiden University)

Table of contents

Chapter 1

General introduction and outline of thesis

Introduction

Atherosclerosis is a lipid-driven chronic inflammation of the vessel wall, which can lead to formation of an atherosclerotic plaque[1]. This can lead to various clinical manifestations like stable angina, acute coronary syndrome and heart failure[1], but also stroke[2] and peripheral artery occlusive disease[3]. As a consequence is atherosclerosis and its subsequent clinical manifestations one of the leading causes of morbidity and mortality worldwide[4, 5].

Acute coronary syndrome

Acute coronary syndrome can be divided in unstable angina and myocardial infarction (MI). In case of unstable angina the coronary artery is partially blocked, while during a MI the coronary artery is completely blocked, for example due to rupture of an atherosclerotic plaque[6]. In both situations the myocardium downstream of the (partially) occlusion is excluded from oxygen supply and becomes hypoxic, while waste products like carbon dioxide accumulate in that hypoxic area. Subsequently, this leads to death of cardiomyocytes or even worse, cardiac arrest and death[6]. In case of survival of the patient, the loss of viable cardiomyocytes leads to cardiac remodelling, which can ultimately lead to heart failure[7].

Last decades many improvements are realized in revascularization strategies following acute coronary syndrome. Balloon angioplasty, usually in combination with stenting, is commonly used, but coronary artery bypass grafting is also used, especially in patients with multivessel disease[6]. Although these revascularization strategies resulted in a decreased morbidity and mortality rate, a significant part of the patients suffer from complications like restenosis, accelerated atherosclerosis and heart failure. It is of high importance that the ischemia time is kept as short as possible, preferable less than 60 minutes, since ischemia time is shown to correlate with morbidity and mortality[6]. Furthermore, one can imagine that a short ischemic period reduces the amount of adverse cardiac remodelling.

Cardiac remodelling

Cardiac remodelling can be described as a change in shape, size and function of the heart. This can be the result of exercise, in which cardiac function is often increased, or following injury of the heart muscle, for example after a MI, in which cardiac function is decreased. The latter is also termed adverse cardiac remodelling[8]. Following a MI adverse cardiac remodelling is the response to a sudden loss of cardiomyocytes in which the heart tries to compensate for the dead tissue and to maintain its function[9]. This leads to a decreased left ventricle (LV) wall thickness in the infarct zone due to the loss of

cardiomyocytes, which are replaced by a collagen scar[10]. In the non-infarct zone the LV wall thickness is increased due to hypertrophy of cardiomyocytes which is a response to hypertensive stress. This initially results in maintained cardiac function, and thus called a compensatory response, however, on the long run, cardiac hypertrophy is an independent risk factor for cardiovascular pathologies[8]. Furthermore, the LV becomes progressively dilated, and together with the expansion of connective tissue throughout the ventricle wall, which cause ventricular stiffness, this leads to loss of cardiac function and subsequently pathological conditions like heart failure[9].

Adverse cardiac remodelling is a process that can be divided into different phases (Figure 1). First after a MI tissue injury, reactive oxygen species and necrosis initiate the inflammatory phase, in which neutrophils and macrophages remove dead cells and matrix debris. This phase is followed by the reparative and proliferative phase (in some cases these two phase are considered two different phases), in which the inflammatory response shifts to inflammation resolution, myofibroblasts are activated leading to scar formation and wound healing[7].
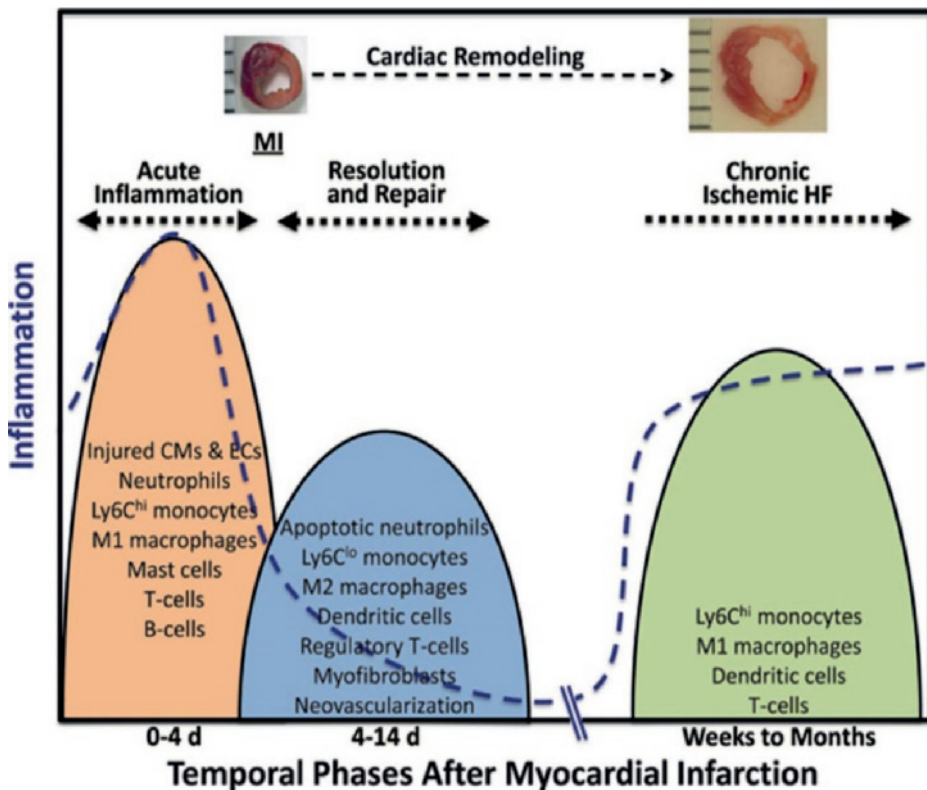
Figure 1. An overview of the different phases in cardiac remodelling following MI. Figure adapted from Prabhu *et al*[7].

Inflammatory phase

Inflammation plays a critical role in the different phases after a MI. The next paragraphs describe in brief the role of different immune cells and different molecules that influence inflammation following a MI. Further details regarding the role of inflammation following MI can be found in different reviews[7, 11, 12].

During the inflammatory phase cardiomyocytes in the infarct area become necrotic and release so-called damage associated molecular patterns (DAMPs), like high mobility group box-1(HMGB1), fibronectin extra domain A, heat shock proteins, singe-stranded RNA, double-stranded RNA and many more[7]. DAMPS are recognized by pattern recognition receptors (PRRs), like toll-like receptors (TLRs), nucleotide-binding oligomerization domain-lie receptors (NLRs) and receptor for advanced glycation end-products (RAGE)[7]. Binding of a DAMP with a PRR leads to downstream signalling and following a MI this signalling may activate several pathways that stimulate leukocyte infiltration and other pro-inflammatory mechanisms.

Binding of DAMP to endothelial cells leads to an increase in the expression of adhesion molecules like E-selectin and P-selectin[13], and subsequently the leukocyte infiltration is increased. Furthermore, due to the ischemic event vessel wall integrity is affected leading to increased leukocyte infiltration in the infarct area[14]. Leukocyte infiltration is also enhanced by the expression of chemokines. Chemokines are cytokines that attract immune cells to injured tissue, examples of chemokines are: chemokine (C-C motif) ligand 2 (CCL2), which is known to attract mainly mononuclear cells, like monocytes, and chemokine (C-X-C motif) ligand 8 (CXCL8; also known as interleukin 8 (IL-8)), which attracts mainly neutrophils[15].

Neutrophils are the first immune cells that arrive in the infarct area and they play an important role in clearing the infarct site from matrix debris and dead cells[11]. Neutrophils help clear the infarct site by phagocytic activity, but also by releasing extra cellular matrix (ECM)-digesting enzymes which helps in the removal of DAMP containing molecules[13]. Furthermore, it is believed that neutrophils stimulate leukocyte infiltration by releasing azurocidin, cathepsin G and a complex of interleukin 6 (IL-6) and its soluble receptor16, and expression of triggering receptor expressed on myeloid cells-1 (TREM-1)[17].

Shortly after the neutrophil infiltration, pro-inflammatory monocytes infiltrate into the injured myocardium. Especially Ly6C^{high} monocytes are abundantly present in the inflammatory phase of cardiac repair[18]. Ly6C^{high} monocytes clear the infarct area from dead cells and matrix debris by their phagocytic actions and expressing of proteolytic mediators, like cathepsins and urokinase-type plasminogen activator[19]. Furthermore, Ly6C^{high} monocytes amplify the inflammatory response by expressing pro-inflammatory cytokines like, tumour necrosis factor α (TNF-α), interleukin 1β (IL-1β) and IL-6[19]. Pro-inflammatory macrophages, also known as M1 macrophages, display comparable

functions as Ly6C^{high} monocytes following a MI in infarct healing. This seems plausible since the main part of the cardiac macrophage pool are derived from infiltrated monocytes[20, 21]. However, not all cardiac macrophages are derived from monocytes, about 8% of all cardiac cells are resident macrophages in healthy myocardium[21]. The exact functions of these resident macrophages in the inflammatory phase of infarct healing are not known yet.

Emerging evidence suggest that both T and B lymphocytes play a role in the early phase of infarct healing. It is believed that cytotoxic (CD8^{+}) T cells infiltrate the infarct area and exhibit undesirable cytotoxic effects on healthy cardiomyocytes[22]. Furthermore, it has been shown that mature B lymphocytes recruit Ly6C^{high} monocytes by expression of chemokine (C-C motif) ligand 7 (CCL7)[23].

Reparative and proliferative phase

The inflammatory phase of infarct healing is followed by the reparative and proliferative phase. This phase is characterized by inhibition and resolution of the inflammatory response, neovascularization and the formation of a scar[7]. The shift from a pro-inflammatory response to an anti-inflammatory response involves a whole range of (immune) cells. Neutrophils, which cleared the infarct area from dead cells and matrix debris, undergo apoptosis and the apoptotic neutrophils are phagocytized by macrophages. Uptake of apoptotic neutrophils by macrophages is followed by a phenotypic shift from pro-inflammatory macrophages to anti-inflammatory macrophages. These anti-inflammatory macrophages express cytokines and growth factors that promote tissue repair and neovascularization, like interleukin 10 (IL-10), transforming growth factor β (TGF-β) and vascular endothelial growth factor (VEGF)[7].

Whereas Ly6C^{high} monocytes where mainly recruited to the infarct site in the inflammatory phase, it are the LyC6^{low} monocytes that are recruited during the reparative and proliferative phase. Ly6C^{low} monocytes express, just like anti-inflammatory macrophages, cytokines and growth factors that promote tissue repair and neovascularization. Furthermore, a part of the anti-inflammatory macrophages are derived from Ly6C^{low} monocytes[20]. It should be noted that macrophages cannot simply categorized to pro- or anti-inflammatory macrophages, but a broad spectrum of different macrophage subsets is involved in infarct healing. Future research will probably discover more macrophage subsets, all with their specific phenotypes and functions.

Dendritic cells (DCs) seem to play an important role during the reparative and proliferative phase of infarct healing. DCs infiltrate into the myocardium following a MI and with a peak seven days post infarction. Furthermore, it has been shown that DC ablation leads to adverse ventricular remodelling and reduced cardiac function, most likely caused by increased Ly6Chigh monocyte infiltration[24].

During the reparative and proliferative phase of infarct healing different T-cells subsets of are involved. For example, Foxp3^{+} CD4^{+} regulatory T cells (Tregs) influence inflammation resolution and wound healing, and thereby improve infarct healing[25]. Furthermore, it has been shown that activation of natural killer T cells leads to a reduction in adverse ventricular remodelling and cardiac failure, through increased expression of IL-10[26].

Myocardial ischemia reperfusion injury

As mentioned before many improvements have been made the last decades regarding revascularization following a MI. Undoubtedly, restoring the blood flow (reperfusion) to the ischemic area is the best treatment to save as much cardiomyocytes as possible, and currently it is clinical routine to perform revascularization therapy directly after a MI. However, reperfusion following a MI also causes myocardial ischemia-reperfusion (MI-R) injury. MI-R injury results in vascular leakage, no reflow phenomenon, cell death, transcriptional reprogramming, autoimmunity and increase of the inflammatory response[14].

Reactive oxygen species (ROS), which are produced in response to the sudden re-oxygenation of ischemic tissue, are in part responsible for the increase in inflammatory response[27]. These ROS act on several pathways related to pro-inflammatory cytokine and chemokine production, like the nuclear factor kappa B (NFκB) pathway, mitogen-activated protein kinase (MAPK) pathway and type 1 interferon pathway[27]. Taken together, it seems that the ultimate goal following a MI should be: fast revascularization in combination with treatment against MI-R injury. In the first part of this thesis we focus on anti-inflammatory therapy to treat MI-R injury and MI without reperfusion.

Vascular remodelling

Vascular remodelling is a response to environmental changes, which leads to structural changes in the vessel wall. It involves at least four processes, namely cell migration, cell growth, cell death and production or degradation of ECM[28]. Just like cardiac remodelling, vascular remodelling can be divided in beneficial and adverse vascular remodelling. In beneficial vascular remodelling, the vascular changes result in creation (e.g. vasculogenesis during embryonic development) or restoration of blood flow (e.g. neovascularization following ischemia). In adverse vascular remodelling, on the other hand, the changes in the vessel wall result in reduced blood flow (e.g. atherosclerosis and restenosis), which subsequently can lead to several clinical manifestations.

Restenosis

In case of ischemic problems caused by narrowing or obstruction of a vessel, the preferred

therapy is percutaneous coronary intervention (PCI) like, balloon angioplasty, often in combination with placement of a stent. A major drawback of PCI is restenosis, which is the re-narrowing of the opened vessel leading to new clinical symptoms[29]. Intimal hyperplasia and accelerated atherosclerosis (Figure 2) are the two main contributors of restenosis. In case of intimal hyperplasia the increase in the intimal layer of the vessel consist mainly of vascular smooth muscle cells (VSMCs), while in case of accelerated atherosclerosis the enlarged intima consists of VSMCs, macrophages and foam cells.
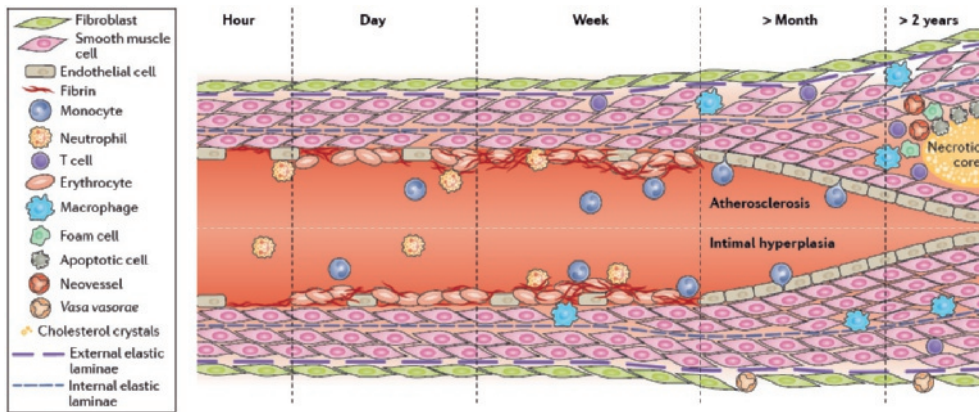
Figure 2. An overview of the development of both atherosclerosis and intimal hyperplasia. Figure adapted from de Vries *et al*[34].

Intimal hyperplasia is caused by local tissue injury during PCI. During the interventional procedure the vessel wall is de-endothelialized or the remaining endothelium is activated. Platelets and fibrinogen bind to the de-endothelialized vessel wall and they express different adhesion molecules like, P-selectin and glycoprotein Ib-α. The damaged endothelial cells also express adhesion molecules and thereby both de-endothelialization and endothelial injury lead to increased leukocyte infiltration of the vessel wall[30]. These leukocytes express cytokine and chemokines, like IL-6, TNF-α and CCL2, that further boost the inflammatory response[31]. Furthermore, leukocytes and activated platelets also release growth factors like, TGF-β[32], and matrix metalloproteinases (MMPs), which lead to ECM remodelling and migration of VSMCs from the media to the intima[31]. As mentioned before, the newly formed neointima consists mainly of VSMCs and they release, together with leukocytes, several growth factors and MMPs, which leads to more proliferation of VSMCs and thus further increase of intimal thickening[31].

Under hypercholesterolemic conditions lipoproteins, like oxidized low density lipoprotein (oxLDL), are formed within the vessel wall. When this occurs at an injured site of the vessel wall, this will lead to a further increase in inflammatory response. Furthermore, macrophages in the vessel wall will recognize and phagocytize oxLDL particles, leading to the formation of foam cells[33]. Therefore, we refer to accelerated atherosclerosis, instead of intimal hyperplasia,

when we study intimal thickening under hypercholesterolemic conditions.

Animal models

To study cardiac remodelling we used two different mouse models, namely a mouse model for MI and MI-R[35]. Basically these models are quite similar to each other. In our MI mouse model (Figure 3) we permanently ligate the left anterior descending (LAD) coronary artery, simulating a permanent MI. In the MI-R mouse model the ligation of the LAD is removed after 45 minutes ischemia, simulating MI-R injury. Both models were used in combination with magnetic resonance imaging (MRI), which is in our belief the most reliable method to study cardiac function in vivo.
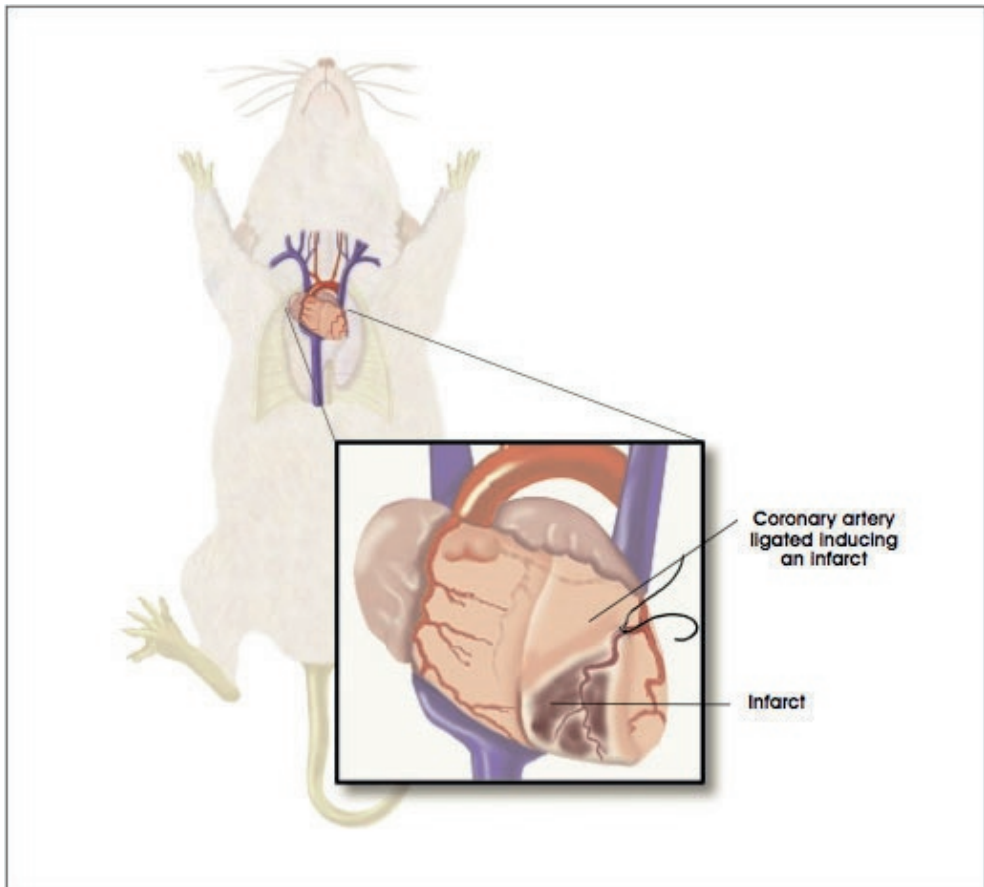
Figure 3. A schematic overview of the MI mouse model.

To mimic the clinical situation often experienced by patients suffering from MI and MI-R injury hypercholesterolemic ApoE*3-Leiden mice were used[36]. These mice experience hypercholesterolemia when fed an high fat diet, but not when fed a chow diet. Other

hypercholesterolemic mouse strains, like ApoE^{-/-} and LDLR^{-/-} are also often used to study cardiac and vascular remodelling. However, ApoE^{-/-} mice already experience hypercholesterolemia on a chow diet and LDLR^{-/-} mice have a cholesterol metabolism which is less comparable to the human situation compared to the cholesterol metabolism of ApoE*3-Leiden mice. Therefore ApoE*3-Leiden mice experience, in our opinion, the best resemblance of the clinical situation of most patients regarding hypercholesterolemia.

To study post-interventional intimal hyperplasia we used the femoral artery cuff mouse model, in which we place a non-constrictive cuff around the femoral artery. The local injury inflicted during this procedure resembles the local injury inflicted during PCI. In response to this injury a VSMC-rich neointima is formed within three weeks if this model is used under normocholesterolemic conditions[37].

Different mouse models were used to study accelerated atherosclerosis, namely the femoral artery cuff model and the carotid collar model (Figure 4), both under hypercholesterolemic conditions. To perform the femoral artery cuff mouse model under hypercholesterolemic conditions, we used ApoE*3-Leiden mice on a high fat diet[37]. In this situation a neointima, which consists of VSMCs, macrophages and other leukocytes, will develop within two weeks. In the carotid collar model we used ApoE^{-/-} mice on a high fat diet. In this model, a semi-constrictive collar is placed around both the left and right carotid artery[38]. Disturbed flow and increased shear stress lead to damage and activation of the endothelial cells. Together with the hypercholesterolemic conditions this leads to development of an atherosclerotic plaque, which consist of a necrotic core, ECM, VSMCs and leukocytes, within four weeks.
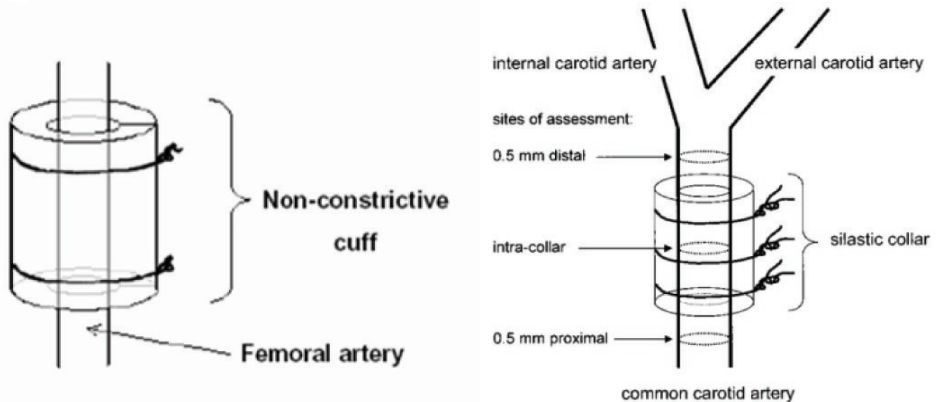
Figure 4. Schematic overview of different mouse models for accelerated atherosclerosis. Left a schematic overview of the femoral artery cuff model and right the carotid collar model.

Non-interventional therapies

Currently, non-interventional therapies focus mainly on prevention of cardiovascular diseases, for example by lowering LDL cholesterol levels using statins and proprotein convertase subtilisin/kexin type 9 (PCSK9) inhibitors. Furthermore, several immunomodulatory therapies showed promising results in animal models, but in most clinical trials these therapies were not as successful as expected. One important reason for the failure of current immunomodulatory therapies is that they are focussed on single factors or pathways, which are not able to sufficiently modulate the complex inflammatory process. Therefore, new potential therapies should focus on targets that can modulate multiple processes. The next paragraphs describe several molecules/proteins that are able to modulate multiple processes.

Phosphorylcholine

Phosphorylcholine (PC) is the polar headgroup of a major membrane component, phosphatidylcholine. Phosphatidylcholines are not only vital for all eukaryotic cells, but they are also a membrane component of prokaryote microorganisms, like Streptococcus pneumoniae, and they are also present in lipoproteins, like LDL. PC is a so-called cryptic epitope, which means that eukaryotic cells and lipid molecules have to be modified before they are recognized by the innate immune system[39]. Therefore, viable cells are not recognized in a PC-dependent manner. However, if cells undergo apoptosis, a process in which ROS cause oxidation of molecules, like phospholipids, the PC epitope is modified. This oxidation-induced modification during apoptosis makes the PC epitope accessible for the innate immune system, therefore it is also called an oxidation specific epitope (OSE). In native LDL the PC epitope also remains hidden until it becomes oxidized, which results in the formation of the atherogenic lipid molecule oxLDL[40].

Apoptotic cells and oxLDL, which contain OSEs are immunogenic and pro-inflammatory[39]. Therefore, blocking the PC epitope may be an interesting target for treatment of adverse cardiac and vascular remodelling. Natural antibodies against PC, such as the EO6 or T15 antibodies[41], have anti-inflammatory properties[39, 42] and they inhibit the uptake of apoptotic cells and oxLDL by macrophages in vitro[43, 44]. In vivo it has been shown that B-1a and B-1b cells produce OSE specific antibodies, which display atheroprotective properties[45-47]. Furthermore, sterile inflammation in the spleen triggers splenic B-cells to produce OSE specific antibodies which reduce the development of atherosclerosis[48]. In patients suffering from cardiovascular diseases, low levels of natural IgM antibodies against PC are associated with a worsened prognosis[49]. Furthermore, low levels of natural anti-PC IgM antibodies itself are associated with development of cardiovascular diseases[50-53]. Using different experimental mouse models it has been shown that active and passive immunization with anti-PC IgM antibodies reduces atherosclerosis

development[54, 55] and reduces vein graft disease[56]. Taken together, these data indicate that the use of anti-PC antibodies may be an interesting therapeutic agent against vascular and cardiac remodelling.

A major drawback for using IgM antibodies as a therapeutic agent is that they are relatively expensive and difficult to produce. To overcome this problem our group participated in the development of a fully humanized anti-PC IgG antibody, further referred as PC-mAb, which is compared to IgM antibodies easier to produce and less expensive. Using the femoral artery cuff model in hypercholesterolemic ApoE*3-Leiden mice, we have shown that PC-mAb treatment inhibits accelerated atherosclerosis development and has anti-inflammatory properties. Therefore, PC-mAb treatment may have beneficial effects against adverse cardiac remodelling following MI and MI-R injury , which is described in chapter 2 and 3.

Annexin A5

Annexins are a family of proteins which bind reversibly to negatively charged phospholipids in a calcium dependant manner[57]. One member, Annexin A5 (AnxA5), is known for its ability to bind to phosphatidylserine (PS), which is expressed by activated platelets during the blood coagulation process. PS binds to factor Va, factor Xa and prothrombin leading to the formation of the prothrombinase complex, which ultimately leads to formation of a blood clot[58]. Extracellular AnxA5 binds to PS on activated platelets, thereby it competes with factor Va, factor Xa and prothrombin and preventing formation of a blood clot[58]. In addition to this anti-thrombotic effects[59, 60], AnxA5 is also known to affect apoptosis and inflammation.

In viable cells PS is expressed at the inner plasma membrane leaflet, however during early apoptosis PS is externalized and thus expressed at the outer plasma membrane leaflet[58]. Upon apoptosis several mechanisms are responsible for PS expression on the outer leaflet of the cell membrane which might be cell and signal specific[61]. When PS is expressed at the surface of apoptotic cells it functions as an "eat me" signal which ensures phagocytosis by specialized leukocytes[61]. AnxA5 binding to PS on apoptotic cells has been used diagnostic tool to visualize cell death[60] and even to assess atherosclerotic plaque vulnerability[62].

AnxA5 binds to PS forming two-dimensional crystals, which may shield PS from recognition by leukocytes and subsequently prevent the resulting inflammatory response[58]. Furthermore it has been shown that AnxA5 interacts with the interferon (IFN)-γ receptor modulating the downstream IFN-γ signalling[63]. In addition, it has been shown that treatment with human AnxA5 inhibits the pro-inflammatory response in LPS challenged mice[64]. Previously, our group found that AnxA5 treatment inhibits the post-interventional pro-inflammatory response leading to reduced development of intimal hyperplasia[65] and accelerated atherosclerosis[66]. Taken together these results

indicate that AnxA5 can be used as an anti-inflammatory agent.

In addition to the anti-inflammatory properties of AnxA5 it also affects apoptosis. Upon apoptosis, for example after MI-R injury, cells express PS. It has been found that following an ischemic event cardiomyocytes express PS for at least six hours on their outer membrane. Treatment with AnxA5 resulted in PS internalization restoring the membrane composition regarding PS asymmetry with no PS expression left on the outer membrane, thereby possibly reversing the apoptotic process[67]. Furthermore, it has been reported that following a MI plasma levels of endogenous AnxA5 are increased[68] and that AnxA5 is taken up in the infarct area in patients with an acute MI[69]. Taken together, due to its anti-inflammatory and anti-apoptotic properties, AnxA5 may be an interesting therapeutic agent against MI-R injury. The effects of AnxA5 treatment against MI-R injury are described in chapter 4.

PCAF

Epigenetic factors are proteins that modulate gene expression in response to environmental changes without changing the DNA sequence, for example by regulating histone acetylation and de-acetylation. Chromatin is a complex which consists of proteins, mainly histones, and DNA, and chromatin can be divided in the more loosely packed euchromatin and the more densely packed heterochromatin. The degree of compactness of the chromatin directly influences gene expression, since the DNA is better accessible for transcription factors in the more loosely packed euchromatin[70]. Acetylation of lysine residues, by lysine acetyltransferases (KATs), on histone proteins leads to the formation of euchromatin, and thus activation of genes. On the other hand, de-acetylation, by lysine deacetylases (KDACs), lead to the formation of heterochromatin and subsequently silencing of genes. Therefore, the balance between KAT and KDAC activity are important in gene regulation[71].

P300/CPB-associated factor (PCAF) is such a KAT, which plays an important role in gene activation, and especially inflammatory gene activation[72]. By acetylation of histone proteins at the site of nuclear factor kappa-beta (NFκB), which is an important transcription factor of many inflammatory related genes, PCAF regulates expression of NFκB-regulated genes, like cyclooxygenase-2 (COX-2) and TNF-α[73]. In addition, PCAF is also known for its ability to acetylate non-histone proteins and thereby modulate inflammatory gene expression. NFκB consists of two subunits, namely p50 and p65, and requires a complex of coactivators to induce NFκB-mediated gene expression. It has been shown that PCAF is an important protein of the coactivator complex required for activation of the p65 subunit and subsequent NF-κB-mediated gene expression[74]. Furthermore, it has been shown, in a model for inflammation induced neovascularization, that the absence of PCAF results in 3505 differentially expressed genes, and more importantly, impaired induction of different pro-inflammatory genes[75].

Additionally, in vitro studies have shown that PCAF knockdown downregulates pro-inflammatory gene expression, including intercellular adhesion molecule-1 (ICAM-1), vascular cell adhesion molecule-1 (VCAM-1) and CCL2[76].

Many NFκB-regulated inflammatory genes, like TNF-α and COX-2, are also known to be involved in development of restenosis[77] and atherosclerosis[78]. Furthermore, three large prospective studies have shown an association between the -2481C variant allele in the promotor region of the PCAF gene and reduced risk of vascular morbidity and mortality[79-82]. In a mouse model for restenosis it was shown that Pcaf mRNA levels were elevated upon vascular injury[82]. The role of PCAF in vascular inflammation is investigated in chapter 5.

MicroRNAs

MicroRNAs (Figure 5) are short endogenous RNA molecules, usually about 22 nucleotides long, which are capable to regulate gene expression[83]. MicroRNAs are
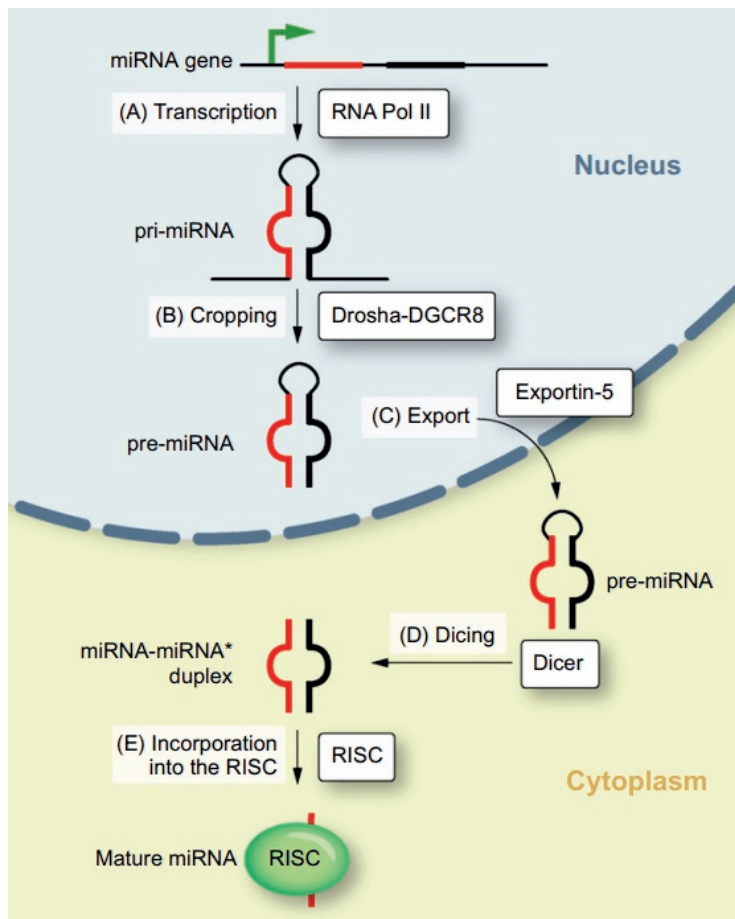
Figure 5. An overview of microRNA biogenesis. Figure adapted from Borel *et al*[87].

transcribed in the nucleus as primary microRNAs, which are subsequently cleaved to form pre-microRNAs by different enzymes, like Drosha and the cofactor DGCR8[84]. These pre-microRNAs are exported from the nucleus to the cytoplasm by the protein Exportin-5. In the cytoplasm pre-microRNAs are further processed by the enzyme Dicer into mature microRNA duplexes[85]. These mature microRNA duplexes are incorporated into the RNA inducing silencing complex (RISC), where they can bind to the 3' untranslated region of their target mRNAs. Perfect complementary binding of the microRNA with its target mRNA will lead to degradation, while imperfect binding will lead to translational repression of the target mRNA[86]. In both situations binding of a microRNA to a target mRNA will lead to downregulation of the target gene.

The fact that microRNAs can target up to several hundred mRNAs means that they can fine-tune a large set of target genes and thereby can have a major impact on multifactorial processes like vascular remodelling. Several microRNAs are found to influence restenosis and atherosclerosis and their specific role is described in several reviews[88, 89]. The 14q32 gene cluster, located on chromosome 14 in human and chromosome 12F1 in mice, contains one of the largest microRNAs clusters, which is highly conserved in mammals[90]. Due to the high degree of homology of the microRNA genes in this cluster, it is an relevant cluster to investigate in mouse models. The 14q32 cluster contains 54 human and 59 murine microRNA genes and previously several microRNAs of the 14q32 gene cluster were investigated regarding their effect on vascular remodelling. It has been shown that inhibition of 14q32 microRNA-329, -487b, -494 and -495 results in increased neovascularization in a hind limb ischemia mouse model[91]. Furthermore, inhibition of microRNA-494 leads to decreased accelerated atherosclerosis development and decreased cholesterol levels[92]. Additionally, other microRNAs of the 14q32 cluster (microRNA-431, -668 and -758) are upregulated in atherosclerotic aortas of ApoE^{-/-} mice[93]. Finally, extensive hypomethylation of 14q32 microRNAs was observed in human atherosclerotic plaques, resulting in the upregulation of several 14q32 microRNAs[94]. The effect of 14q31 microRNA-329, -494 and -495 inhibition on restenosis is discussed in chapter 6.

Outline of the thesis

The aim of this thesis was to further unravel the role of inflammation in cardiac and vascular remodelling, as well as to investigate potential therapeutic agents to treat cardiovascular diseases.

The first part of this thesis focuses on potential immunomodulatory therapeutic agents for the treatment of adverse cardiac remodelling following a MI or MI-R injury.

In **chapter 2** we investigate the therapeutic potential of a humanized IgG antibody against PC (PC-mAb). Using a mouse model for MI in combination with MRI assessment

of infarct size (IS) and cardiac function, we found that PC-mAb treatment reduces LV dilatation and IS by inhibiting both the early and late inflammatory response.

Chapter 3 describes the effect of PC-mAb treatment on adverse cardiac remodelling following MI-R injury. In a mouse model with permanent reperfusion following 45 minutes ischemia, we found that PC-mAb treatment leads to preservation of cardiac function. Furthermore, IS was decreased in PC-mAb treated mice compared to vehicle treated mice. Both the early and late inflammatory response was attenuated following PC-mAb treatment.

In **chapter 4** we study the therapeutic potential of the anti-apoptotic and anti-inflammatory protein AnxA5 against MI-R injury. Administration of AnxA5 resulted in reduced LV dilatation, preservation of ejection fraction and decreased IS. This reduction in adverse cardiac remodelling was accompanied by a reduced early and late inflammatory response.

In the second part of this thesis we focus on epigenetic manipulation against adverse vascular remodelling.

In **chapter 5** we investigate the role of the epigenetic factor PCAF, which is known for its ability to acetylate lysine residues on histone proteins, on vascular inflammation and intimal hyperplasia development. Using the femoral artery cuff mouse model, we found that PCAF deficiency lead to a reduction in intimal hyperplasia development. Using hypercholesterolemic ApoE*3-Leiden mice, we found that the pharmacological PCAF inhibitor garcinol reduces injury-induced vascular inflammation. In addition, in vitro experiments showed that both PCAF deficiency and garcinol downregulate protein expression of several pro-inflammatory proteins.

Chapter 6 zooms in on the role of different microRNA members of the 14q32 gene cluster, namely microRNA-329, -494 and -495, on vascular remodelling. Using the femoral artery cuff mouse model we found that inhibition of microRNA-495 reduced intimal hyperplasia development. This reduction in intimal hyperplasia was accompanied with a reduction of macrophage influx and VSMC proliferation. In a mouse model for accelerated atherosclerosis we showed that inhibition of microRNA-495 leads to smaller atherosclerotic plaque size, while plaque stability was increased. Furthermore, microRNA-495 inhibition led to reduced plasma cholesterol levels, via reduction of the VLDL-fraction.

Finally, **chapter 7** summarizes the results of this thesis and future perspectives are discussed.

References

1.   Boudoulas, K.D., F. Triposciadis, et al., Coronary Atherosclerosis: Pathophysiologic Basis for Diagnosis and Management. Progress in cardiovascular diseases, 2016. 58(6): p. 676-692.

2.   Banerjee, C. and M.I. Chimowitz, Stroke Caused by Atherosclerosis of the Major Intracranial Arteries. Circulation research, 2017. 120(3): p. 502-513.

3.   Mascarenhas, J.V., M.A. Albayati, et al., Peripheral arterial disease. Endocrinology and metabolism clinics of North America, 2014. 43(1): p. 149-166.

4.   Townsend, N., L. Wilson, et al., Cardiovascular disease in Europe: epidemiological update 2016. European heart journal, 2016. 37(42): p. 3232-3245.

5.   Benjamin, E.J., M.J. Blaha, et al., Heart Disease and Stroke Statistics-2017 Update: A Report From the American Heart Association. Circulation, 2017.

6.   Reed, G.W., J.E. Rossi, and C.P. Cannon, Acute myocardial infarction. Lancet (London, England), 2017. 389(10065): p. 197-210.

7.   Prabhu, S.D. and N.G. Frangogiannis, The Biological Basis for Cardiac Repair After Myocardial Infarction: From Inflammation to Fibrosis. Circulation research, 2016. 119(1): p. 91-112.

8.   Shimizu, I. and T. Minamino, Physiological and pathological cardiac hypertrophy. Journal of molecular and cellular cardiology, 2016. 97: p. 245-262.

9.   Jugdutt, B.I., Ventricular remodeling after infarction and the extracellular collagen matrix: when is enough enough? Circulation, 2003. 108(11): p. 1395-1403.

10.   Talman, V. and H. Ruskoaho, Cardiac fibrosis in myocardial infarction-from repair and remodeling to regeneration. Cell and tissue research, 2016. 365(3): p. 563-581.

11.   Frangogiannis, N.G., Regulation of the inflammatory response in cardiac repair. Circulation research, 2012. 110(1): p. 159-173.

12.   Chen, B. and N.G. Frangogiannis, Immune cells in repair of the infarcted myocardium. Microcirculation (New York, N.Y. : 1994), 2017. 24(1).

13.   Kolaczkowska, E. and P. Kubes, Neutrophil recruitment and function in health and inflammation. Nature reviews. Immunology, 2013. 13(3): p. 159-175.

14.   Eltzschig, H.K. and T. Eckle, Ischemia and reperfusion--from mechanism to translation. Nature medicine, 2011. 17(11): p. 1391-1401.

15.   Cavalera, M. and N.G. Frangogiannis, Targeting the chemokines in cardiac repair. Current pharmaceutical design, 2014. 20(12): p. 1971-1979.

16.   Soehnlein, O. and L. Lindbom, Phagocyte partnership during the onset and resolution of inflammation. Nature reviews. Immunology, 2010. 10(6): p. 427-439.

17.   Boufenzer, A., J. Lemarie, et al., TREM-1 Mediates Inflammatory Injury and Cardiac Remodeling Following Myocardial Infarction. Circulation research, 2015. 116(11): p. 1772-1782.

18.   Nahrendorf, M., F.K. Swirski, et al., The healing myocardium sequentially mobilizes two monocyte subsets with divergent and complementary functions. The Journal of experimental medicine, 2007. 204(12): p. 3037-3047.

19.   Shinagawa, H. and S. Frantz, Cellular immunity and cardiac remodeling after myocardial infarction: role of neutrophils, monocytes, and macrophages. Current heart failure reports, 2015. 12(3): p. 247-254.

20.   Gombozhapova, A., Y. Rogovskaya, et al., Macrophage activation and polarization in post-infarction cardiac remodeling. Journal of biomedical science, 2017. 24(1): p. 13.

21.   Heidt, T., G. Courties, et al., Differential contribution of monocytes to heart macrophages in steady-state and after myocardial infarction. Circulation research, 2014. 115(2): p. 284-295.

22.   Varda-Bloom, N., J. Leor, et al., Cytotoxic T lymphocytes are activated following myocardial infarction and can recognize and kill healthy myocytes in vitro. Journal of molecular and cellular cardiology, 2000. 32(12): p. 2141-2149.

23.   Zouggari, Y., H. Ait-Oufella, et al., B lymphocytes trigger monocyte mobilization and impair heart function after acute myocardial infarction. Nature medicine, 2013. 19(10): p. 1273-1280.

24.   Anzai, A., T. Anzai, et al., Regulatory role of dendritic cells in postinfarction healing and left ventricular remodeling. Circulation, 2012. 125(10): p. 1234-1245.

25.   Weirather, J., U.D. Hofmann, et al., Foxp3+ CD4+ T cells improve healing after myocardial infarction by modulating monocyte/macrophage differentiation. Circulation research, 2014. 115(1): p. 55-67.

26.   Sobirin, M.A., S. Kinugawa, et al., Activation of natural killer T cells ameliorates postinfarct cardiac remodeling and failure in mice. Circulation research, 2012. 111(8): p. 1037-1047.

27.   Bagheri, F., V. Khori, et al., Reactive oxygen species-mediated cardiac-reperfusion injury: Mechanisms and therapies. Life sciences, 2016. 165: p. 43-55.

28.   Gibbons, G.H. and V.J. Dzau, The emerging concept of vascular remodeling. The New England journal of medicine,

1994. 330(20): p. 1431-1438.

29.   Jukema, J.W., J.J. Verschuren, et al., Restenosis after PCI. Part 1: pathophysiology and risk factors. Nature reviews. Cardiology, 2011. 9(1): p. 53-62.

30.   Inoue, T., K. Croce, et al., Vascular inflammation and repair: implications for re-endothelialization, restenosis, and stent thrombosis. JACC. Cardiovascular interventions, 2011. 4(10): p. 1057-1066.

31.   Simon, D.I., Inflammation and vascular injury: basic discovery to drug development. Circulation journal : official journal of the Japanese Circulation Society, 2012. 76(8): p. 1811-1818.

32.   Suwanabol, P.A., K.C. Kent, and B. Liu, TGF-beta and restenosis revisited: a Smad link. The Journal of surgical research, 2011. 167(2): p. 287-297.

33.   Hansson, G.K., Inflammation, atherosclerosis, and coronary artery disease. The New England journal of medicine, 2005. 352(16): p. 1685-1695.

34.   de Vries, M.R., K.H. Simons, et al., Vein graft failure: from pathophysiology to clinical outcomes. Nature reviews. Cardiology, 2016. 13(8): p. 451-470.

35.   Michael, L.H., C.M. Ballantyne, et al., Myocardial infarction and remodeling in mice: effect of reperfusion. The American journal of physiology, 1999. 277(2 Pt 2): p. H660-668.

36.   van den Maagdenberg, A.M., M.H. Hofker, et al., Transgenic mice carrying the apolipoprotein E3-Leiden gene exhibit hyperlipoproteinemia. The Journal of biological chemistry, 1993. 268(14): p. 10540-10545.

37.   Lardenoye, J.H., D.J. Delsing, et al., Accelerated atherosclerosis by placement of a perivascular cuff and a cholesterol-rich diet in ApoE*3Leiden transgenic mice. Circulation research, 2000. 87(3): p. 248-253.

38.   von der Thusen, J.H., T.J. van Berkel, and E.A. Biessen, Induction of rapid atherogenesis by perivascular carotid collar placement in apolipoprotein E-deficient and low-density lipoprotein receptor-deficient mice. Circulation, 2001. 103(8): p. 1164-1170.

39.   Chang, M.K., C.J. Binder, et al., Apoptotic cells with oxidation-specific epitopes are immunogenic and proinflammatory. The Journal of experimental medicine, 2004. 200(11): p. 1359-1370.

40.   Miller, Y.I., S.H. Choi, et al., Oxidation-specific epitopes are danger-associated molecular patterns recognized by pattern recognition receptors of innate immunity. Circulation research, 2011. 108(2): p. 235-248.

41.   Palinski, W., S. Horkko, et al., Cloning of monoclonal autoantibodies to epitopes of oxidized lipoproteins from apolipoprotein E-deficient mice. Demonstration of epitopes of oxidized low density lipoprotein in human plasma. The Journal of clinical investigation, 1996. 98(3): p. 800-814.

42.   Huber, J., A. Vales, et al., Oxidized membrane vesicles and blebs from apoptotic cells contain biologically active oxidized phospholipids that induce monocyte-endothelial interactions. Arteriosclerosis, thrombosis, and vascular biology, 2002. 22(1): p. 101-107.

43.   Horkko, S., D.A. Bird, et al., Monoclonal autoantibodies specific for oxidized phospholipids or oxidized phospholipid-protein adducts inhibit macrophage uptake of oxidized low-density lipoproteins. The Journal of clinical investigation, 1999. 103(1): p. 117-128.

44.   Chang, M.K., C. Bergmark, et al., Monoclonal antibodies against oxidized low-density lipoprotein bind to apoptotic cells and inhibit their phagocytosis by elicited macrophages: evidence that oxidation-specific epitopes mediate macrophage recognition. Proceedings of the National Academy of Sciences of the United States of America, 1999. 96(11): p. 6353-6358.

45.   Kyaw, T., C. Tay, et al., B1a B lymphocytes are atheroprotective by secreting natural IgM that increases IgM deposits and reduces necrotic cores in atherosclerotic lesions. Circulation research, 2011. 109(8): p. 830-840.

46.   Rosenfeld, S.M., H.M. Perry, et al., B-1b Cells Secrete Atheroprotective IgM and Attenuate Atherosclerosis. Circulation research, 2015. 117(3): p. e28-39.

47.   Tsiantoulas, D., S. Gruber, and C.J. Binder, B-1 cell immunoglobulin directed against oxidation-specific epitopes. Frontiers in immunology, 2012. 3: p. 415.

48.   Grasset, E.K., A. Duhlin, et al., Sterile inflammation in the spleen during atherosclerosis provides oxidation-specific epitopes that induce a protective B-cell response. Proceedings of the National Academy of Sciences of the United States of America, 2015. 112(16): p. E2030-2038.

49.   Caidahl, K., M. Hartford, et al., IgM-phosphorylcholine autoantibodies and outcome in acute coronary syndromes. International journal of cardiology, 2013. 167(2): p. 464-469.

50.   de Faire, U., J. Su, et al., Low levels of IgM antibodies to phosphorylcholine predict cardiovascular disease in 60-year old men: effects on uptake of oxidized LDL in macrophages as a potential mechanism. Journal of autoimmunity, 2010. 34(2): p. 73-79.

51.   Gleissner, C.A., C. Erbel, et al., Low levels of natural IgM antibodies against phosphorylcholine are independently associated with vascular remodeling in patients with coronary artery disease. Clinical research in cardiology : official journal of the German Cardiac Society, 2015. 104(1): p. 13-22.

52.   Gronlund, H., G. Hallmans, et al., Low levels of IgM antibodies against phosphorylcholine predict development of acute myocardial infarction in a population-based cohort from northern Sweden. European journal of cardiovascular

prevention and rehabilitation : official journal of the European Society of Cardiology, Working Groups on Epidemiology & Prevention and Cardiac Rehabilitation and Exercise Physiology, 2009. 16(3): p. 382-386.

53. Gigante, B., K. Leander, et al., Low levels of IgM antibodies against phosphorylcholine are associated with fast carotid intima media thickness progression and cardiovascular risk in men. Atherosclerosis, 2014. 236(2): p. 394-399.

54. Caligiuri, G., J. Khallou-Laschet, et al., Phosphorylcholine-targeting immunization reduces atherosclerosis. Journal of the American College of Cardiology, 2007. 50(6): p. 540-546.

55. Binder, C.J., S. Horkko, et al., Pneumococcal vaccination decreases atherosclerotic lesion formation: molecular mimicry between Streptococcus pneumoniae and oxidized LDL. Nature medicine, 2003. 9(6): p. 736-743.

56. Faria-Neto, J.R., K.Y. Chyu, et al., Passive immunization with monoclonal IgM antibodies against phosphorylcholine reduces accelerated vein graft atherosclerosis in apolipoprotein E-null mice. Atherosclerosis, 2006. 189(1): p. 83-90.

57. Reutelingsperger, C.P. and W.L. van Heerde, Annexin V, the regulator of phosphatidylserine-catalyzed inflammation and coagulation during apoptosis. Cellular and molecular life sciences : CMLS, 1997. 53(6): p. 527-532.

58. van Genderen, H.O., H. Kenis, et al., Extracellular annexin A5: functions of phosphatidylserine-binding and two-dimensional crystallization. Biochimica et biophysica acta, 2008. 1783(6): p. 953-963.

59. Thiagarajan, P. and C.R. Benedict, Inhibition of arterial thrombosis by recombinant annexin V in a rabbit carotid artery injury model. Circulation, 1997. 96(7): p. 2339-2347.

60. Boersma, H.H., B.L. Kietselaer, et al., Past, present, and future of annexin A5: from protein discovery to clinical applications. Journal of nuclear medicine : official publication, Society of Nuclear Medicine, 2005. 46(12): p. 2035-2050.

61. Fadok, V.A., D.L. Bratton, et al., The role of phosphatidylserine in recognition of apoptotic cells by phagocytes. Cell death and differentiation, 1998. 5(7): p. 551-562.

62. Laufer, E.M., M.H. Winkens, et al., Molecular imaging of macrophage cell death for the assessment of plaque vulnerability. Arteriosclerosis, thrombosis, and vascular biology, 2009. 29(7): p. 1031-1038.

63. Leon, C., D. Nandan, et al., Annexin V associates with the IFN-gamma receptor and regulates IFN-gamma signaling. Journal of immunology (Baltimore, Md. : 1950), 2006. 176(10): p. 5934-5942.

64. Arnold, P., X. Lu, et al., Recombinant human annexin A5 inhibits proinflammatory response and improves cardiac function and survival in mice with endotoxemia. Critical care medicine, 2014. 42(1): p. e32-41.

65. Ewing, M.M., M.R. de Vries, et al., Annexin A5 therapy attenuates vascular inflammation and remodeling and improves endothelial function in mice. Arteriosclerosis, thrombosis, and vascular biology, 2011. 31(1): p. 95-101.

66. Ewing, M.M., J.C. Karper, et al., Annexin A5 prevents post-interventional accelerated atherosclerosis development in a dose-dependent fashion in mice. Atherosclerosis, 2012. 221(2): p. 333-340.

67. Kenis, H., H.R. Zandbergen, et al., Annexin A5 uptake in ischemic myocardium: demonstration of reversible phosphatidylserine externalization and feasibility of radionuclide imaging. Journal of nuclear medicine : official publication, Society of Nuclear Medicine, 2010. 51(2): p. 259-267.

68. Matsuda, R., N. Kaneko, et al., Clinical significance of measurement of plasma annexin V concentration of patients in the emergency room. Resuscitation, 2003. 57(2): p. 171-177.

69. Hofstra, L., I.H. Liem, et al., Visualisation of cell death in vivo in patients with acute myocardial infarction. Lancet (London, England), 2000. 356(9225): p. 209-212.

70. Wu, C., Chromatin remodeling and the control of gene expression. The Journal of biological chemistry, 1997. 272(45): p. 28171-28174.

71. Kuo, M.H. and C.D. Allis, Roles of histone acetyltransferases and deacetylases in gene regulation. BioEssays : news and reviews in molecular, cellular and developmental biology, 1998. 20(8): p. 615-626.

72. Pons, D., F.R. de Vries, et al., Epigenetic histone acetylation modifiers in vascular remodelling: new targets for therapy in cardiovascular disease. European heart journal, 2009. 30(3): p. 266-277.

73. Miao, F., I.G. Gonzalo, et al., In vivo chromatin remodeling events leading to inflammatory gene transcription under diabetic conditions. The Journal of biological chemistry, 2004. 279(17): p. 18091-18097.

74. Sheppard, K.A., D.W. Rose, et al., Transcriptional activation by NF-kappaB requires multiple coactivators. Molecular and cellular biology, 1999. 19(9): p. 6367-6378.

75. Bastiaansen, A.J., M.M. Ewing, et al., Lysine acetyltransferase PCAF is a key regulator of arteriogenesis. Arteriosclerosis, thrombosis, and vascular biology, 2013. 33(8): p. 1902-1910.

76. Huang, J., D. Wan, et al., Histone acetyltransferase PCAF regulates inflammatory molecules in the development of renal injury. Epigenetics, 2015. 10(1): p. 62-72.

77. Monraats, P.S., N.M. Pires, et al., Tumor necrosis factor-alpha plays an important role in restenosis development. FASEB journal : official publication of the Federation of American Societies for Experimental Biology, 2005. 19(14): p. 1998-2004.

78. Narasimha, A.J., J. Watanabe, et al., Absence of myeloid COX-2 attenuates acute inflammation but does not influence development of atherosclerosis in apolipoprotein E null mice. Arteriosclerosis, thrombosis, and vascular biology, 2010. 30(2): p. 260-268.

79.   Monraats, P.S., N.M. Pires, et al., Genetic inflammatory factors predict restenosis after percutaneous coronary interventions. Circulation, 2005. 112(16): p. 2417-2425.

80.   Shepherd, J., S.M. Cobbe, et al., Prevention of coronary heart disease with pravastatin in men with hypercholesterolemia. West of Scotland Coronary Prevention Study Group. The New England journal of medicine, 1995. 333(20): p. 1301-1307.

81.   Shepherd, J., G.J. Blauw, et al., Pravastatin in elderly individuals at risk of vascular disease (PROSPER): a randomised controlled trial. Lancet (London, England), 2002. 360(9346): p. 1623-1630.

82.   Pons, D., S. Trompet, et al., Genetic variation in PCAF, a key mediator in epigenetics, is associated with reduced vascular morbidity and mortality: evidence for a new concept from three independent prospective studies. Heart (British Cardiac Society), 2011. 97(2): p. 143-150.

83.   Bartel, D.P., MicroRNAs: genomics, biogenesis, mechanism, and function. Cell, 2004. 116(2): p. 281-297.

84.   Lee, Y., C. Ahn, et al., The nuclear RNase III Drosha initiates microRNA processing. Nature, 2003. 425(6956): p. 415-419.

85.   Krol, J., I. Loedige, and W. Filipowicz, The widespread regulation of microRNA biogenesis, function and decay. Nature reviews. Genetics, 2010. 11(9): p. 597-610.

86.   Doench, J.G. and P.A. Sharp, Specificity of microRNA target selection in translational repression. Genes & development, 2004. 18(5): p. 504-511.

87.   Borel, F., P. Konstantinova, and P.L. Jansen, Diagnostic and therapeutic potential of miRNA signatures in patients with hepatocellular carcinoma. Journal of hepatology, 2012. 56(6): p. 1371-1383.

88.   Welten, S.M., E.A. Goossens, et al., The multifactorial nature of microRNAs in vascular remodelling. Cardiovascular research, 2016. 110(1): p. 6-22.

89.   Fang, Y.C. and C.H. Yeh, Role of microRNAs in Vascular Remodeling. Current molecular medicine, 2015. 15(8): p. 684-696.

90.   Benetatos, L., E. Hatzimichael, et al., The microRNAs within the DLK1-DIO3 genomic region: involvement in disease pathogenesis. Cellular and molecular life sciences : CMLS, 2013. 70(5): p. 795-814.

91.   Welten, S.M., A.J. Bastiaansen, et al., Inhibition of 14q32 MicroRNAs miR-329, miR-487b, miR-494, and miR-495 increases neovascularization and blood flow recovery after ischemia. Circulation research, 2014. 115(8): p. 696-708.

92.   Wezel, A., S.M. Welten, et al., Inhibition of MicroRNA-494 Reduces Carotid Artery Atherosclerotic Lesion Development and Increases Plaque Stability. Annals of surgery, 2015. 262(5): p. 841-847; discussion 847-848.

93.   Han, H., Y.H. Wang, et al., Differentiated miRNA expression and validation of signaling pathways in apoE gene knockout mice by cross-verification microarray platform. Experimental & molecular medicine, 2013. 45: p. e13.

94.   Aavik, E., H. Lumivuori, et al., Global DNA methylation analysis of human atherosclerotic plaques reveals extensive genomic hypomethylation and reactivation at imprinted locus 14q32 involving induction of a miRNA cluster. European heart journal, 2015. 36(16): p. 993-1000.

Chapter 2

Anti phosphorylcholine antibodies reduce infarct size and left ventricular dilatation by inhibiting the early and late inflammatory response following myocardial infarction

Submitted for publication

Rob C. M. de Jong[1,2*]

Niek J. Pluijmert[3*]

Margreet R. de Vries[1,2]

Knut Pettersson[4]

Douwe E. Atsma[3]

J. Wouter Jukema[1,3]

Paul H. A. Quax[1,2]

[*]Authors contributed equally to this work

[1]Department of Surgery, Leiden University Medical Center, Leiden, the Netherlands

[2]Einthoven Laboratory for Experimental Vascular Medicine, Leiden University Medical Center, Leiden, the Netherlands

[3]Department of Cardiology, Leiden University Medical Center, Leiden, the Netherlands

[4]Athera Biotechnologies, Stockholm, Sweden

Abstract

Background: PC-mAb is a human IgG1 directed against phosphorylcholine that has anti-inflammatory properties. In this study, we hypothesized PC-mAb treatment would reduce adverse cardiac remodeling and infarct size (IS) following myocardial infarction (MI).

Methods: MI was induced by permanent ligation of the LAD coronary artery in hypercholesterolemic ApoE*3-Leiden mice. Cardiac function and IS were assessed using cardiac magnetic resonance imaging (MRI). Using (immuno)histological analysis we determined left ventricle (LV) fibrous content, LV wall thickness and leukocyte infiltration. ELISA and FACS analyses were used to study the systemic inflammatory response.

Results: We found a 21% reduced LV diastolic volume and 31% reduced IS following PC-mAb treatment after three weeks compared to untreated mice. The decreased IS was confirmed histologically, since LV fibrous content was decreased, and LV wall thickness was preserved. CCL2 concentrations were decreased two days after MI induction, while no difference was observed three weeks post MI. Furthermore, percentage of circulating monocytes were decreased two days post MI. Finally, leukocyte influx was decreased three weeks post MI, but not after two days.

Conclusions: PC-mAb treatment reduces local and systemic inflammatory response resulting in limitation of adverse cardiac remodeling and IS following MI. This indicates that PC-mAb might be a promising therapeutic agent following MI and subsequent cardiac remodeling.

Introduction

Over the last decades much improvements have been made to treat patients suffering MI, using percutaneous coronary interventions[1] or coronary artery bypass grafting[2]. However, revascularization is not possible in a significant portion of the patients suffering from chronic coronary artery disease[3], due to anatomical or clinical complications or simply because the possibilities for providing this kind of clinical care are not available. Therefore, it is still relevant in these times where most of the studies focus on ischemia reperfusion studies in relation to myocardial infarction, to study the effects permanent ischemia on post infarctional cardiac remodeling. MI can lead to adverse left ventricular (LV) remodeling, characterized by LV dilatation and reduced LV wall thickness, which successively leads to heart failure[4], one of the leading causes of death worldwide[5].

Following a MI, an intense inflammatory response is triggered, which helps to clear the injured myocardium from dead cardiomyocytes and matrix debris, and ultimately leads to infarct healing and scar formation[6]. However, when the inflammatory response is extended it may cause viable cardiomyocytes to die[7]. Necrotic cardiomyocytes release damage-associated molecular patterns (DAMPs), like high mobility group box-1 (HMBG1), heat shock protein (HSP), interleukin-1α (IL-1α) and extracellular RNA (eRNA), which trigger the innate immune system[7] via TLR activation[8-10]. The role of apoptotic cells seems to be more complicated. Uptake of apoptotic cells by macrophages might have anti-inflammatory effects[11], on the other hand it has been suggested that apoptotic cells are immunogenic and pro-inflammatory[12]. Wan and colleagues found that effective efferocytosis of apoptotic cardiomyocytes, promotes the resolution of inflammation after a MI[13]. However, the main part of apoptotic cells in the healing infarct are non-cardiomyocytes. For instance apoptotic neutrophils represent a large part of the apoptotic cells in the healing infarct, and their role in inflammation resolution is not yet known[7].

Following a MI, the production of reactive oxygen species (ROS) by endothelial cells, circulating phagocytes and cardiomyocytes is increased as a result of the ischemic event[14]. These ROS are responsible for generating oxidative damage, and thereby producing oxidation-specific epitopes (OSEs) on apoptotic cells, which can act as DAMPs and are recognized by innate immunity[15]. Further research revealed that the polar headgroup, phosphorylcholine (PC), of oxidized phospholipids (oxPLs), is an important OSE, which is present on apoptotic cells, but not on viable cells[12]. Moreover, PC is present on oxidized LDL (oxLDL), a key player in atherogenesis because of its pro-inflammatory properties[16]. It has been shown that a specific clone of IgM autoantibodies against PC, termed EO6 or T15 antibodies[17], can inhibit the uptake of both apoptotic cells[18] and oxLDL[19], and has anti-inflammatory properties[12]. Furthermore, it has been shown that B-1a and B-1b cells produce OSE specific IgM antibodies which protect against atherosclerosis[20-22] and it has been found that splenic B-cells display an OSE

associated atheroprotective effect which is initiated through sterile inflammation[23].
Low levels of natural IgM anti-PC antibodies are associated with increased risk for cardiovascular events[24-28] and resulted in a worsened prognosis regarding patients with an acute coronary syndrome[29]. In addition, both active and passive immunization with antibodies against PC ameliorates atherosclerosis development and is proven to be atheroprotective[30-32]. Taken together, these data show that blocking PC might be an interesting therapeutic approach to treat cardiovascular disease. However, IgM antibodies are not optimal for therapeutic use, particularly because of its difficulty to produce recombinant IgM antibodies with their pentamer structures.

We previously developed a fully human IgG type1 directed against human PC (PC-mAb), which has anti-inflammatory properties, blocks oxLDL uptake by macrophages and inhibits vascular remodeling in a mouse model for accelerated atherosclerosis[33]. In the current study we aimed to investigate the effect of PC-mAb treatment on cardiac function, LV remodeling and the inflammatory response following MI. To study this, we administrated PC-mAb to hypercholesterolemic APOE*3-Leiden mice after induction of a permanent MI.

Methods

Animals and diets
All animal experiments were approved by the Institutional Committee for Animal Welfare of the Leiden University Medical Center (LUMC) and in compliance with Dutch government guidelines and the Directive 2010/63/EU of the European Parliament. Transgenic female APOE*3-Leiden mice[34], aged 8-10 weeks at the start of a dietary run-in period were used for this experiment. Mice were fed a semisynthetic Western-type diet supplemented with 0.4% cholesterol (AB Diets, Woerden, The Netherlands) four weeks prior to surgery which was continued throughout the complete experiment. Mice were housed under standard conditions in conventional cages and received food and water ad libitum.

Plasma lipid analysis
Plasma levels of total cholesterol (TC) and triglycerides (TG) were determined for randomization one week before surgery. After a four hours fasting period, plasma was obtained via tail vein bleeding (approximately 50 μL) and assayed for total cholesterol (TC) and triglycerides (TG) levels using commercially available enzymatic kits according to the manufacturer's protocols (11489232; Roche Diagnostics, Mannheim, Germany, and 11488872; Roche Diagnostics, Mannheim, Germany, respectively)

Induction of myocardial infarction and PC-mAb treatment
Myocardial infarction (MI) was induced by ligation of the left anterior descending (LAD) coronary artery at day 0 in 12-14 weeks old female APOE*3-Leiden mice as described

previously[35,36]. Briefly, mice were pre-anesthetized with 5% isoflurane in a gas mixture of oxygen and placed in a supine position on a heating pad (37°C). After endotracheal intubation and ventilation (rate 160 breaths/min, stroke volume 190µL; Harvard Apparatus, Holliston, MA, USA), mice were kept anesthetized with 1.5-2% isoflurane. Subsequently a left thoracotomy was performed in the 4th intercostal space and the LAD coronary artery was permanently ligated using a 7-0 prolene suture. Subsequently, the thorax was closed in layers with 5-0 prolene suture and mice were allowed to recover. Analgesia was obtained with buprenorfine s.c. (0.1mg/kg) pre-operative and 12h post-operative.

After surgery animals were randomly grouped to receive administration of i.p. injections with 10 mg/kg PC-mAb (Athera, Biotechnologies, Solna, Sweden) every 3rd day or NaCl 0.9% w/v (vehicle) as a control (Figure 1B). Sham operated animals were operated similarly but without ligation of the LAD and received i.p. injections with NaCl 0.9% w/v (sham).

After two days or three weeks were euthanized by bleeding and explantation of the heart under general anesthesia with 1.5-2% isoflurane. Hearts were immersion-fixated in 4% paraformaldehyde for 24 hours and embedded in paraffin. Blood samples were collected and used for serum analysis. The heart and body weights were measured from all animals using a digital scale.

Cardiac magnetic resonance imaging

Left ventricular (LV) dimensions, function and infarct size (IS) were assessed two days and three weeks after surgery (Figure 1A) by using a 7-Tesla magnetic resonance imaging (MRI) (Bruker Biospin, Ettlingen, Germany) to obtain contrast-enhanced and cine MRI images. Mice were pre-anesthetized with 5% isoflurane in a gas mixture of oxygen and kept anesthetized with 1.5-2% isoflurane. Respiratory rate was monitored by a respiration detection cushion, which was place underneath the thorax and connected to a gating module to monitor respiratory rate (SA Instruments, Inc., Stony Brook, NY). Image reconstruction was performed using Bruker ParaVision 5.1 software.

Infarct size

Infarct size was determined with contrast-enhanced MR imaging after injection of 150 µl (0.5 mmol/ml) of gadolinium-DPTA (Gd-DPTA, Dotarem, Guerbet, The Netherlands) via the tail vein. A gradient echo sequence (FLASH) was used to acquire a set of 14 contigious 0.7 mm contrast-enhanced slices in short-axis orientation. Imaging parameters were: echo time of 1.9 ms, repetition time of 84.16 ms, field of view of 33 mm^2, and a matrix size of 192x256.

Left ventricular function

Left ventricular function was assessed with a high resolution 2D FLASH cine sequence

to acquire a set of 9 contigious 1 mm slices in short axis orientation covering the entire heart. Imaging parameters were: echo time of 1.49 ms, repetition time of 5.16 ms, field of view of 26 mm^2, and a matrix size of 144x192.

Image analysis

Image analysis was performed with the MR Analytical Software System (MASS) for mice (MEDIS, Leiden, The Netherlands). LV endo- and epicardial borders were delineated manually and a reference point was positioned by an investigator blinded to treatment. End-diastolic and end-systolic phases and the contrast enhanced areas were identified automatically, and the percentage of infarcted myocardium, LV end-diastolic volume (EDV), LV end-systolic volume (ESV), and LV ejection fraction (EF) were computed.

LV fibrous content and LV wall thickness

Five μm thick transverse sections were made along the entire long-axis of the LV and every 50th section was stained with Sirius Red. Collagen deposition was used as an indicator of the fibrotic area and LV fibrous content was determined by planimetric measurements of all sections and calculated as fibrotic area divided by the total LV wall surface area.

LV wall thickness was analyzed in five different sections centralized in the infarct area. Per section wall thickness was measured at three places in the infarct area, both border zones, and at two places in the intraventricular septum. All measurements were performed using the ImageJ 1.47v software program (NIH, USA).

Local inflammatory response

For analysis of the cardiac inflammatory response a subpopulation was selected, and sections were stained using antibodies against leukocytes (anti-CD45, 550539; BD Pharmingen, San Diego, CA, USA). The number of leukocytes was expressed as a number per 0.25 mm^2 in the septum (2 areas), border zones (2 areas), and infarcted myocardium (3 areas).

FACS analysis

To examine the effect of PC-mAb therapy on the acute inflammatory response, mice were sacrificed and blood samples were collected at day two. To study the systemic effects whole blood was analyzed for monocytosis. Total circulating leukocytes were determined using a semi-automatic hematology analyzer F-820 (Sysmex; Sysmex Corporation, Etten-Leur, The Netherlands).

For FACS analysis, 35μL of whole blood was incubated for 30 min on ice with directly conjugated antibodies directed against Ly6C-FITC (AbD Serotec, Dusseldorf, Germany), Ly6G-PE (BD Pharmingen, San Diego, CA, USA), CD11b-APC (BD Pharmingen, San Diego, CA, USA), and CD115-PerCP (R&D Systems, Minneapolis, MN, USA). Monocytes were

gated based on their expression profile: CD11b-positive, Ly6G-negative, and CD115-positive. Data was analyzed using FlowJo software (Tree Star Inc.)

CCL2 and PC-mAb ELISA
A PC-mAb ELISA kit (Athera Biotechnologies, Solna, Sweden) was used to determine serum PC-mAb concentrations. To study the effects of PC-mAb on systemic inflammation, inflammatory cytokine concentration of chemokine (C-C motif) ligand 2 (CCL2) was determined using an ELISA kit (Cat. No. 555260, BD Biosciences, San Diego, CA, USA).

TLR4 and PC co-localization
The presence of Toll-like receptor 4 (TLR4) and PC co-localization in the infarct area, was investigated by immunohistochemistry. TLR4 was stained using specific antibodies against TLR4 (anti-CD284, AHP1822, Bio-Rad Laboratories Inc.). PC was stained using the same antibody (Athera, Biotechnologies, Solna, Sweden) as was used for treatment.

Statistical analysis
Values were expressed as mean ± SEM. Comparisons of parameters between the sham, PC-mAb, and vehicle groups were made using 1-way analysis of variance (ANOVA) with Tukey's correction or 2-way ANOVA with repeated measures and Tukey's posttest in case of multiple time points. Comparisons between PC-mAb and vehicle were made using unpaired t-tests. A value of P≤0.05 was considered to represent a significant difference. Statistical procedures were performed using IBM SPSS 23.0.0 (SPSS Inc – IBM, Armonk, NY, USA) and Graphpad Prism 6.02 (Graphpad software Inc, La Jolla, CA, USA).

Results

Animal characteristics
No differences in bodyweight (BW) were observed following PC-mAb (20.4±0.3 g) treatment compared to vehicle (20.5±0.4 g) and sham (19.6±0.3 g). Possible cardiac hypertrophy was assessed by determining heart weight (HW) and heart to body weight (HW-BW) ratio. Following PC-mAb treatment both HW (134±5 mg) and HW-BW ratio (6.6±0.3) were reduced compared to vehicle (HW: 167±9 mg, P<0.01; HW-BW ratio: 8.2±0.4, P<0.01), to levels similar to those observed in the sham group (HW: 144±8 mg; HW-BW ratio: 7.3±0.3) (Table 1).

PC-mAb concentrations
To validate that the observed data is the result of PC-mAb treatment, we determined serum PC-mAb concentrations using ELISA. PC-mAb levels were only detectable in PC-mAb treated mice (32±8 μg/ml after two days, and 36±6 μg/ml after three weeks) but

not in vehicle or sham-operated animals after both two days and three weeks following MI.

Table 1: Plasma lipids & animal characteristics

	T (wk)	sham	MI PC-mAb	MI vehicle
N		13	14	16
TC (mmol/L)	0	17.5±1.7	15.0±1.4	14.8±1.0
TG (mmol/L)	0	2.5±0.2	3.0±0.2	2.8±0.1
BW (g)	0	20.7±0.5	21.1±0.3	20.9±0.5
	3	19.6±0.3	20.4±0.3	20.5±0.4
HW (mg)	3	144±8	134±5[##]	167±9
HW/BW ratio (mg/g)	3	7.3±0.3	6.6±0.3[##]	8.2±0.4

Table 1: Plasma lipid levels and animal characteristics: plasma total cholesterol (TC), triglycerides (TG), body weight (BW), heart weight (HW). Values are means ± SEM. [##]$P<0.01$ vehicle.

TLR4 and PC co-localization

Since our rationale for using PC-mAb to treat adverse cardiac remodeling following MI was to inhibit the pro-inflammatory response, we investigated if TLR4 was localized at the same areas as PC. As can be appreciated from Figure 1 TLR4 staining is indeed localized at comparable areas in the infarct area as is PC staining.
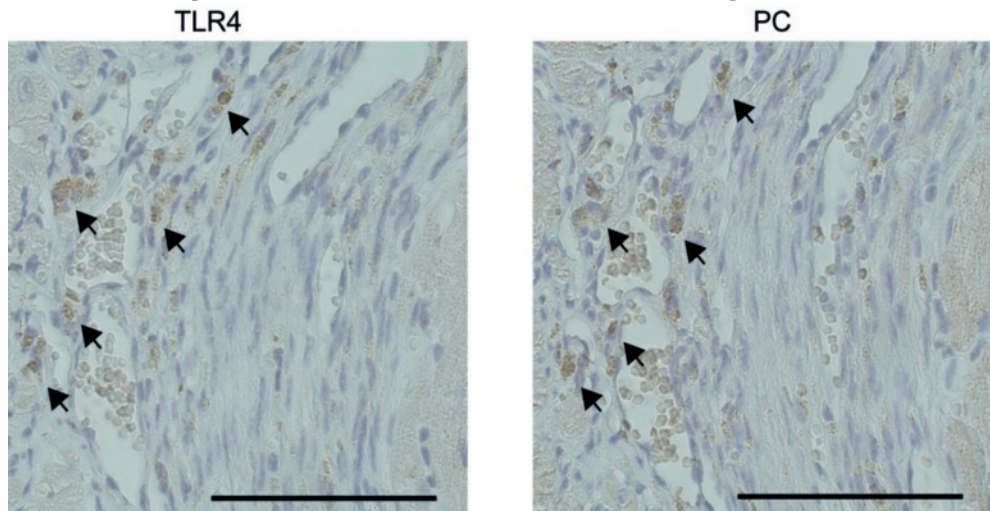
Figure 1: TLR4 and PC co-localization. Representative images of TLR4 (left) and PC (right) staining in the infarct area of an untreated mice. Scale bar = 50 μm.

PC-mAb reduces contrast-enhanced MRI assessed LV infarct size

Baseline infarct size (IS) was assessed using contrast-enhanced MRI two days post MI. No differences in IS could be observed between the PC-mAb treated group and the vehicle group at baseline (30.9±3.2% vs. 36.7±2.7%). However, three weeks post MI, PC-mAb treated mice showed significantly smaller IS compared to vehicle treated mice
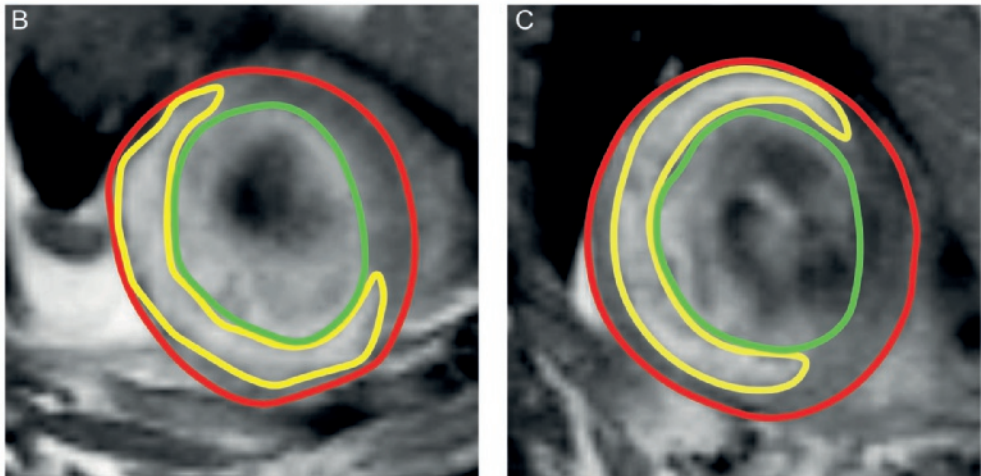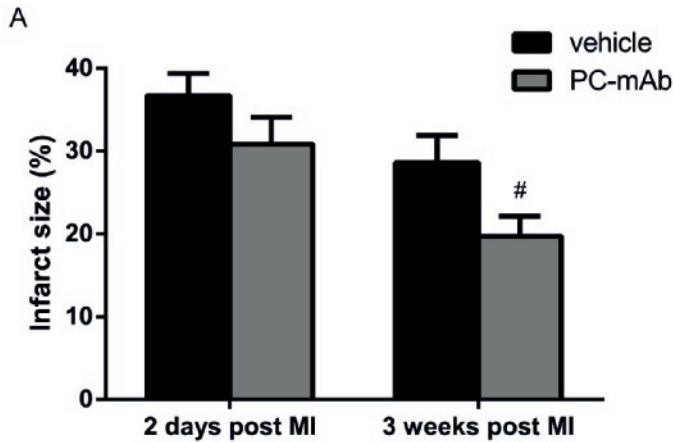
Figure 2: Quantification of infarct size using contrast-enhanced MR imaging. Infarct size was measured at baseline (two days post MI) and at sacrifice (three weeks post MI) and quantified as percentage of the LV mass (A). Representative Gd-DPTA-enhanced MR images 2 days post MI of vehicle (B) and PC-mAb treated (C) mice. Red line indicates epicardial border, green line indicates endocardial border and yellow line indicates infarct area. Data are mean ± SEM. #P≤0.05 vs. vehicle.

(19.7±2.4% vs. 28.6±3.3%, P<0.01; Figure 2A).

Interestingly, IS was significantly smaller three weeks post MI compared to two days post MI in both the vehicle and PC-mAb group, indicating some amount of infarct healing and loss of acute infarct edema took place in both groups.

PC-mAb reduces LV dilatation, but does not affect LV function

To investigate the effect of PC-mAb treatment on LV dilatation serial cardiac cine MRI images were made two days and three weeks following MI. Two days post MI no differences could be observed between vehicle and PC-mAb treatment regarding EDV

(39.7±2.8 µl vs. 36.7±2.2 µl; Figure 3A) and ESV (25.7±3.1 µl vs. 23.5±2.7 µl; Figure 3B). Three weeks post MI ESV was not significantly different in the PC-mAb group compared to the vehicle group (32.9±5.5 µl vs. 44.0±7.0 µl; Figure 3B). Interestingly, PC-mAb treated animals showed a significantly smaller EDV three weeks post MI compared to untreated animals (48.6±4.7 µl vs. 61.3±6.3 µl, P=0.05; Figure 3A), indicating a reduction in LV dilatation in the PC-mAb treated group compared to the vehicle group.

Next, ejection fraction (EF) was measured as indication of LV function. No differences could be observed between PC-mAb treated mice and untreated mice two days post MI (38.3±4.0% vs. 37.8±4.1%) and three weeks post MI (37.4±4.7% vs. 34.4±5.1%), indicating PC-mAb treatment does not affect LV function (Figure 3C).
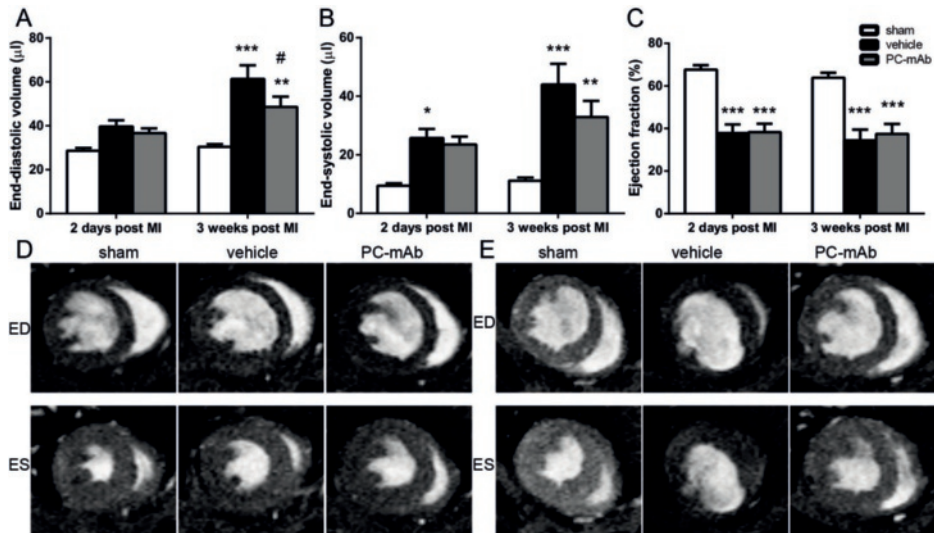
Figure 3: Quantification of LV volumes and function using cardiac MR imaging. LV volumes, EDV (A) and ESV (B), and function, EF (C), were assessed two days and three weeks after MI (n=12-16 per group). Representative transversal short-axis MR images at end-diastole (ED) and end-systole (ES) two days (D) and three weeks (E) post MI in the sham, vehicle and PC-mAb groups. Data are mean ± SEM. #P≤0.05 vs. vehicle, *P≤0.05, **P≤0.01, ***P≤0.001 all vs. sham.

PC-mAb reduces LV fibrous content and ameliorates LV wall thickness

To validate the decreased IS by immunohistochemistry, cross-sections from the hearts were stained with Sirius Red to measure fibrous content of the LV as a measure for IS. PC-mAb treated animals showed a strong trend towards decreased LV fibrous content compared to untreated animals (18.6±1.4% vs 25.5±3.4%, P=0.07; Figure 4A), confirming the decreased IS measured with contrast-enhanced MRI.

Next, we assessed the LV wall thickness in different areas of the heart; the septum, the border zones and the infarct area. LV wall thickness was significantly increased in the septum of both the PC-mAb (1.22±0.04 mm, P<0.001) and the vehicle group (1.10±0.05

mm, P<0.01) compared to sham (0.85±0.04 mm; Figure 4B). This indicates compensatory cardiac hypertrophy in this area, suggesting the viable myocardium to compensate for the infarcted myocardium. Interestingly, LV wall thickness was increased in the border zone and infarct area in the PC-mAb treated animals compared to untreated animals (border zones: 1.17±0.03 mm vs. 0.99±0.06 mm, P<0.05; infarct area: 0.66±0.06 mm vs. 0.45±0.08 mm, P<0.05; Figure 4B). The increased LV wall thickness in the border zone is likely the result of cardiac hypertrophy, since it is also significantly increased compared to the sham group (1.01±0.03 mm). Since the LV wall thickness in the infarct area was significantly decreased in both the PC-mAb and vehicle group compared to sham, the observed reduced decrease in the PC-mAb treated animals compared to untreated animals indicates preserved LV wall thickness following PC-mAb treatment.
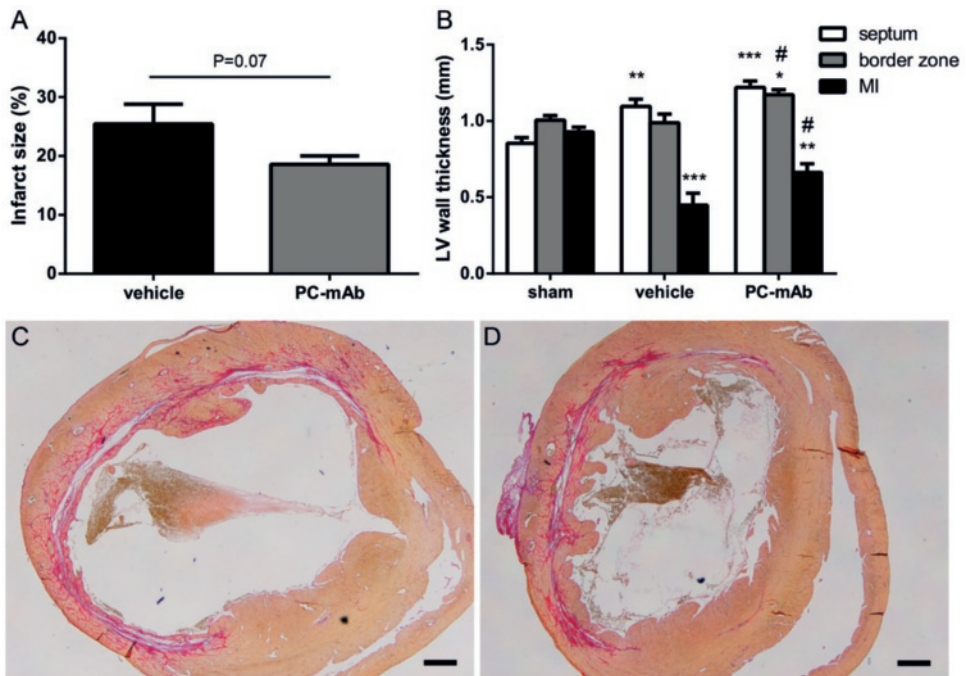
Figure 4: Histological quantification of LV fibrous content and LV wall thickness three weeks post MI. LV fibrous content (A) was measured by Sirius red staining and quantified as the area of the LV occupied by collagen (n=9-10 per group). LV wall thickness (B) was assessed in 3 specific areas: interventricular septum, border zone and infarct area (n=9-10 per group). Representative images of Sirius Red staining of untreated (C) and PC-mAb treated (D) mice. Scale bar = 500 μm. Data are mean ± SEM. #P≤0.05 vs. vehicle, *P≤0.05, **P≤0.01, ***P≤0.001 all vs. sham.

PC-mAb causes reduction of the local inflammatory response

To investigate the local inflammatory response, cross-sections from the hearts were immune-stained for CD45 (leukocyte marker), and the number of CD45 positive cells

were counted in the septum, border zones and infarct area. We observed a striking decrease in number of leukocytes in all areas following PC-mAb treatment compared to the vehicle group three weeks after MI induction (septum: 1.2±0.2 vs. 3.0±0.6, P<0.01; border zones: 1.4±0.2 vs. 3.3±0.7, P<0.05 and infarct area: 1.3±0.2 vs. 3.4±0.7 per 0.25 mm^2, P<0.01; Figure 5B), suggesting PC-mAb treatment reduces the local inflammatory response following MI. Moreover, numbers of leukocytes in the PC-mAb group were comparable with the sham group (septum: 1.2±0.3, border zones: 1.0±0.2, and infarct area: 0.8±0.1 per 0.25 mm^2), suggesting, to some degree, an accelerated and better resolution of the inflammatory response.

Since the acute phase of the inflammatory response is crucial in MI we investigated the number of leukocytes that infiltrated the cardiac tissue two days post MI. In the infarct area an increased number of leukocytes was observed in the vehicle group compared to the sham group (20.5±4.0 vs. 4.9±0.4 per 0.25 mm^2, P<0.01), while no difference was observed between the PC-mAb group and the sham group (11.3±3.3 vs. 4.9±0.4 per 0.25 mm^2, P=0.33; Figure 5A), suggesting that PC-mAb treatment dampened the acute local inflammatory response. In all other areas no differences could be detected between the PC-mAb and vehicle group (Figure 5A).
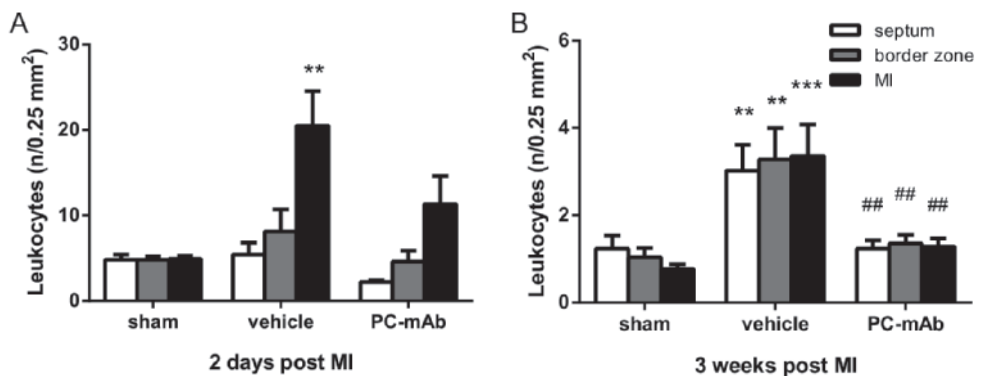
Figure 5: Histological quantification of the local inflammatory response. The number of CD45 positive cells (leukocytes) were counted per specific area: interventricular septum, border zone and infarct area, as measure of local inflammation. Each bar represents the average number of leukocytes per field of view in the specific areas three weeks post MI (A; n-9-10 per group) and two days post MI (B; n=4-5 per group). Data are mean ± SEM. $^{##}$P≤0.01 vs. vehicle, **P≤0.01, ***P≤0.001 both vs. sham.

PC-mAb attenuates the systemic inflammatory response

To further unravel the effect of PC-mAb treatment following MI, we investigated the systemic inflammatory response. Serum concentrations of CCL2 (a pro-inflammatory cytokine) were measured two days and three weeks after MI induction. Two days post MI CCL2 concentrations were significantly reduced in the PC-mAb group (18.3±13.7 pg/ml) compared to both the sham (80.5±14.5 pg/ml, P<0.01) and vehicle group (96.8±4.4

pg/ml, P<0.01; Figure 6A), suggesting that PC-mAb treatment reduces the systemic inflammatory response. However, three weeks post MI no significant differences could be observed in serum CCL2 concentrations between all groups suggesting a transient effect on the systemic inflammatory process (Figure 6B).

Furthermore, we investigated the effect of PC-mAb treatment on circulating monocytes two days after induction of MI using FACS analysis. We found a decrease in percentage of circulating monocytes following PC-mAb treatment compared to the vehicle group (1.6±0.2% vs. 4.4±0.7%, P<0.01; Figure 6C). Moreover, percentage of circulating monocytes was comparable to the sham group (2.0±0.5%). Taken together these data demonstrate that PC-mAb treatment attenuates monocytosis.
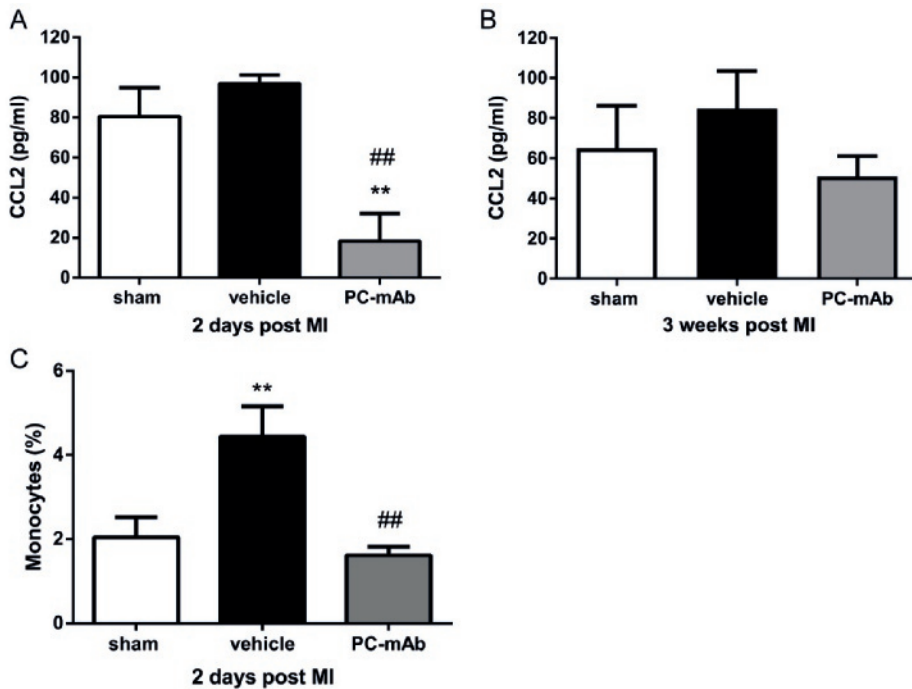
Figure 6: Quantification of the systemic inflammatory response. Serum levels of CCL2 were determined using ELISA as measure of systemic inflammation, two days post MI (A; n=6-8 per group) and three weeks post MI (B; n=9-10 per group). Circulating monocytes were determined two days post MI using FACS analysis and expressed as percentage of total leukocytes (C; n=6-8 per group). Data are mean ± SEM. ##P≤0.01 vs. vehicle, **P≤0.01 vs. sham.

Discussion

PC-mAb is a human IgG directed against PC with anti-inflammatory properties[33]. This study demonstrates a beneficial effect of PC-mAb treatment following permanent MI. We show that PC-mAb treatment decreases HW, infarct size and LV dilatation, while

preserving LV wall thickness. This effect is most likely due to the reduced systemic inflammatory response two days post MI and the reduced local inflammatory response after three weeks.

Adverse left ventricular remodeling is one of the mechanisms responsible for development of heart failure[4], which is one of the leading causes of morbidity and mortality worldwide[5]. We demonstrate a reduction of adverse LV remodeling following administration of PC-mAb, as observed by restricted LV dilatation. Furthermore, we found that HW and HW/BW ratio was reduced following PC-mAb treatment, indicating reduced compensatory cardiac hypertrophy, which is another hallmark of adverse cardiac remodeling and heart failure[37]. Moreover, PC-mAb treatment decreases IS and it has been postulated that IS can be directly linked to heart failure and mortality following MI[38]. These results suggest PC-mAb treatment might be a promising therapeutic agent against heart failure in ischemic heart disease.

Inflammation plays an important role following MI, being responsible for removing necrotic and apoptotic cells, thereby improving infarct healing and scar formation[6]. On the other side, extensive inflammation may cause death of viable cardiomyocytes and enhances LV remodeling[7]. We demonstrate that PC-mAb treatment reduces the local inflammatory response, indicated by reduced leukocyte infiltration, three weeks post MI, but not two days after MI. This suggests that PC-mAb treatment does not inhibit the early beneficial local inflammatory response, but interestingly, it inhibits the deleterious extensive inflammatory response, limiting adverse LV remodeling[7].

Although context dependent, it has been shown that oxPLs are agonists for TLR4 signaling resulting in production of cytokines and chemokines like, CCL2, interleukin- 6 (IL-6) and interleukin (IL-8)[39,40]. Here we show that TLR4 and PC are localized at similar areas in the infarct area following MI, supporting a role of PC as a ligand for TLR4 signaling in the infarcted myocardium. This justifies our choice to use PC-mAb as potential therapy following MI. By expressing anti-inflammatory properties PC-mAb seems to reduce LV remodeling as shown by decreased IS and LV dilatation, while preserving LV wall thickness. Following MI a portion of the cardiomyocytes undergo apoptosis[6]. Apoptotic cells express oxidized lipids on their outer membrane[41], which is immunogenic[12]. It has been demonstrated that natural and monoclonal EO6/T15 antibodies against PC bind to apoptotic cells[18,41], thereby reducing the inflammatory response[12]. Therefore, we suggest that the observed reduced IS is the result of a dampened inflammatory response, thereby sparing viable cardiomyocytes. The preserved LV wall thickness might also be a result of the dampened inflammatory response, but it can also be a direct result of the decreased LV dilatation[42].

CCL2 is a chemoattractant known for its ability to attract inflammatory leukocytes to sites of tissue injury[43], for example after a MI followed by reperfusion[44]. Although it is believed that these attracted leukocytes promote removal of dead tissue and infarct healing, it has been shown that CCL2 null mice show decreased macrophage recruitment

to the infarcted myocardium that coincides with decreased LV remodeling following myocardial ischemia-reperfusion (MI-R)[44]. This is in agreement with our finding of decreased CCL2 serum concentration, and decreased LV remodeling. Interestingly, CCL2 serum concentrations in the PC-mAb treated group were also decreased compared to the sham group indicating PC-mAb reduces both surgery-induced systemic inflammation and infarction-induced local inflammation.

Previously, we showed PC-mAb to reduce CCL2 levels produced by human monocytes stimulated with oxLDL *in vitro* and in our model for accelerated atherosclerosis local expression of CCL2 in the vessel wall was inhibited[33]. Furthermore, it is known that blood CCL2 levels are increased in ApoE*3-Leiden mice when fed a high fat diet[45]. We suggest PC-mAb treatment reduces the systemic inflammatory response by binding to PC on apoptotic cells and/or oxLDL, which might contribute to the reduced LV remodeling, as observed in reduced serum CCL2 concentrations.

Hypercholesterolemia causes a pro-inflammatory state which is characterized by a monocytosis[46]. This increase in monocytes is mainly caused by an increase in the pro-inflammatory Ly6C^{hi} subset. It has been shown that following MI in hypercholesterolemic ApoE$^{-/-}$ mice more Ly6C^{hi} monocytes are recruited into the infarct area which resulted in decreased LV function[47] and impaired infarct healing[48]. In the current study we found a reduction of total monocytes in the PC-mAb treated group, accompanied with a decrease in IS and LV dilatation. However, the reduction of total monocytes could not be assigned to one of the different monocyte subsets (Ly6C^{hi}, Ly6C^{med} and Ly6C^{low}; data not shown).

In conclusion, PC-mAb treatment following permanent MI reduces adverse cardiac remodeling and IS, likely by reducing the inflammatory response. Therefore PC-mAb treatment might be a potential therapy to reduce inflammation and adverse cardiac remodeling, thereby preventing heart failure in ischemic heart disease.

References

1   Hibbard, M. D. et al. Percutaneous transluminal coronary angioplasty in patients with cardiogenic shock. Journal of the American College of Cardiology 19, 639-646 (1992).

2   Deb, S. et al. Coronary artery bypass graft surgery vs percutaneous interventions in coronary revascularization: a systematic review. Jama 310, 2086-2095, doi:10.1001/jama.2013.281718 (2013).

3   Seiler, C., Stoller, M., Pitt, B. & Meier, P. The human coronary collateral circulation: development and clinical importance. European heart journal 34, 2674-2682, doi:10.1093/eurheartj/eht195 (2013).

4   Jessup, M. & Brozena, S. Heart failure. The New England journal of medicine 348, 2007-2018, doi:10.1056/NEJMra021498 (2003).

5   Lloyd-Jones, D. et al. Heart disease and stroke statistics--2010 update: a report from the American Heart Association. Circulation 121, e46-e215, doi:10.1161/circulationaha.109.192667 (2010).

6   Frangogiannis, N. G. The immune system and cardiac repair. Pharmacological research : the official journal of the Italian Pharmacological Society 58, 88-111, doi:10.1016/j.phrs.2008.06.007 (2008).

7   Frangogiannis, N. G. Inflammation in cardiac injury, repair and regeneration. Current opinion in cardiology 30, 240-245, doi:10.1097/hco.0000000000000158 (2015).

8   Timmers, L. et al. Toll-like receptor 4 mediates maladaptive left ventricular remodeling and impairs cardiac function after myocardial infarction. Circulation research 102, 257-264, doi:10.1161/circresaha.107.158220 (2008).

9   Arslan, F. et al. Lack of fibronectin-EDA promotes survival and prevents adverse remodeling and heart function deterioration after myocardial infarction. Circulation research 108, 582-592, doi:10.1161/circresaha.110.224428 (2011).

10   Karper, J. C. et al. Toll-like receptor 4 is involved in human and mouse vein graft remodeling, and local gene silencing reduces vein graft disease in hypercholesterolemic APOE*3Leiden mice. Arteriosclerosis, thrombosis, and vascular biology 31, 1033-1040, doi:10.1161/atvbaha.111.223271 (2011).

11   Fürnrohr, B. G. et al. Signals, receptors, and cytokines involved in the immunomodulatory and anti-inflammatory properties of apoptotic cells. Signal Transduction 5, 356-365, doi:10.1002/sita.200500071 (2005).

12   Chang, M. K. et al. Apoptotic cells with oxidation-specific epitopes are immunogenic and proinflammatory. The Journal of experimental medicine 200, 1359-1370, doi:10.1084/jem.20031763 (2004).

13   Wan, E. et al. Enhanced efferocytosis of apoptotic cardiomyocytes through myeloid-epithelial-reproductive tyrosine kinase links acute inflammation resolution to cardiac repair after infarction. Circulation research 113, 1004-1012, doi:10.1161/circresaha.113.301198 (2013).

14   Misra, M. K., Sarwat, M., Bhakuni, P., Tuteja, R. & Tuteja, N. Oxidative stress and ischemic myocardial syndromes. Medical science monitor : international medical journal of experimental and clinical research 15, Ra209-219 (2009).

15   Miller, Y. I. et al. Oxidation-specific epitopes are danger-associated molecular patterns recognized by pattern recognition receptors of innate immunity. Circulation research 108, 235-248, doi:10.1161/circresaha.110.223875 (2011).

16   Navab, M. et al. The oxidation hypothesis of atherogenesis: the role of oxidized phospholipids and HDL. Journal of lipid research 45, 993-1007, doi:10.1194/jlr.R400001-JLR200 (2004).

17   Palinski, W. et al. Cloning of monoclonal autoantibodies to epitopes of oxidized lipoproteins from apolipoprotein E-deficient mice. Demonstration of epitopes of oxidized low density lipoprotein in human plasma. The Journal of clinical investigation 98, 800-814, doi:10.1172/jci118853 (1996).

18   Chang, M. K. et al. Monoclonal antibodies against oxidized low-density lipoprotein bind to apoptotic cells and inhibit their phagocytosis by elicited macrophages: evidence that oxidation-specific epitopes mediate macrophage recognition. Proceedings of the National Academy of Sciences of the United States of America 96, 6353-6358 (1999).

19   Horkko, S. et al. Monoclonal autoantibodies specific for oxidized phospholipids or oxidized phospholipid-protein adducts inhibit macrophage uptake of oxidized low-density lipoproteins. The Journal of clinical investigation 103, 117-128, doi:10.1172/jci4533 (1999).

20   Kyaw, T. et al. B1a B lymphocytes are atheroprotective by secreting natural IgM that increases IgM deposits and reduces necrotic cores in atherosclerotic lesions. Circulation research 109, 830-840, doi:10.1161/circresaha.111.248542 (2011).

21   Rosenfeld, S. M. et al. B-1b Cells Secrete Atheroprotective IgM and Attenuate Atherosclerosis. Circulation research 117, e28-39, doi:10.1161/circresaha.117.306044 (2015).

22   Tsiantoulas, D., Gruber, S. & Binder, C. J. B-1 cell immunoglobulin directed against oxidation-specific epitopes. Frontiers in immunology 3, 415, doi:10.3389/fimmu.2012.00415 (2012).

23   Grasset, E. K. et al. Sterile inflammation in the spleen during atherosclerosis provides oxidation-specific epitopes that induce a protective B-cell response. Proceedings of the National Academy of Sciences of the United States of America 112, E2030-2038, doi:10.1073/pnas.1421227112 (2015).

24   Gronlund, H. et al. Low levels of IgM antibodies against phosphorylcholine predict development of acute myocardial infarction in a population-based cohort from northern Sweden. European journal of cardiovascular prevention

and rehabilitation : official journal of the European Society of Cardiology, Working Groups on Epidemiology & Prevention and Cardiac Rehabilitation and Exercise Physiology 16, 382-386, doi:10.1097/HJR.0b013e32832a05df (2009).

25   Sjoberg, B. G. et al. Low levels of IgM antibodies against phosphorylcholine-A potential risk marker for ischemic stroke in men. Atherosclerosis 203, 528-532, doi:10.1016/j.atherosclerosis.2008.07.009 (2009).

26   de Faire, U. et al. Low levels of IgM antibodies to phosphorylcholine predict cardiovascular disease in 60-year old men: effects on uptake of oxidized LDL in macrophages as a potential mechanism. Journal of autoimmunity 34, 73-79, doi:10.1016/j.jaut.2009.05.003 (2010).

27   Gigante, B. et al. Low levels of IgM antibodies against phosphorylcholine are associated with fast carotid intima media thickness progression and cardiovascular risk in men. Atherosclerosis 236, 394-399, doi:10.1016/j.atherosclerosis.2014.07.030 (2014).

28   Gleissner, C. A. et al. Low levels of natural IgM antibodies against phosphorylcholine are independently associated with vascular remodeling in patients with coronary artery disease. Clinical research in cardiology : official journal of the German Cardiac Society 104, 13-22, doi:10.1007/s00392-014-0750-y (2015).

29   Caidahl, K. et al. IgM-phosphorylcholine autoantibodies and outcome in acute coronary syndromes. International journal of cardiology 167, 464-469, doi:10.1016/j.ijcard.2012.01.018 (2013).

30   Binder, C. J. et al. Pneumococcal vaccination decreases atherosclerotic lesion formation: molecular mimicry between Streptococcus pneumoniae and oxidized LDL. Nature medicine 9, 736-743, doi:10.1038/nm876 (2003).

31   Faria-Neto, J. R. et al. Passive immunization with monoclonal IgM antibodies against phosphorylcholine reduces accelerated vein graft atherosclerosis in apolipoprotein E-null mice. Atherosclerosis 189, 83-90, doi:10.1016/j.atherosclerosis.2005.11.033 (2006).

32   Caligiuri, G. et al. Phosphorylcholine-targeting immunization reduces atherosclerosis. Journal of the American College of Cardiology 50, 540-546, doi:10.1016/j.jacc.2006.11.054 (2007).

33   Ewing, M. M. et al. Optimized anti-phosphorylcholine IgG for therapeutic inhibition of inflammatory vascular disease. European heart journal 34, P5703-P5703, doi:10.1093/eurheartj/eht310.P5703 (2013).

34   van den Maagdenberg, A. M. et al. Transgenic mice carrying the apolipoprotein E3-Leiden gene exhibit hyperlipoproteinemia. The Journal of biological chemistry 268, 10540-10545 (1993).

35   Michael, L. H. et al. Myocardial infarction and remodeling in mice: effect of reperfusion. The American journal of physiology 277, H660-668 (1999).

36   Louwe, M. C. et al. RP105 deficiency aggravates cardiac dysfunction after myocardial infarction in mice. International journal of cardiology 176, 788-793, doi:10.1016/j.ijcard.2014.07.086 (2014).

37   Shimizu, I. & Minamino, T. Physiological and pathological cardiac hypertrophy. Journal of molecular and cellular cardiology 97, 245-262, doi:10.1016/j.yjmcc.2016.06.001 (2016).

38   McAlindon, E., Bucciarelli-Ducci, C., Suleiman, M. S. & Baumbach, A. Infarct size reduction in acute myocardial infarction. Heart (British Cardiac Society) 101, 155-160, doi:10.1136/heartjnl-2013-304289 (2015).

39   Walton, K. A. et al. Receptors involved in the oxidized 1-palmitoyl-2-arachidonoyl-sn-glycero-3-phosphorylcholine-mediated synthesis of interleukin-8. A role for Toll-like receptor 4 and a glycosylphosphatidylinositol-anchored protein. The Journal of biological chemistry 278, 29661-29666, doi:10.1074/jbc.M300738200 (2003).

40   Imai, Y. et al. Identification of oxidative stress and Toll-like receptor 4 signaling as a key pathway of acute lung injury. Cell 133, 235-249, doi:10.1016/j.cell.2008.02.043 (2008).

41   Chou, M. Y. et al. Oxidation-specific epitopes are dominant targets of innate natural antibodies in mice and humans. The Journal of clinical investigation 119, 1335-1349, doi:10.1172/jci36900 (2009).

42   Olivetti, G., Capasso, J. M., Sonnenblick, E. H. & Anversa, P. Side-to-side slippage of myocytes participates in ventricular wall remodeling acutely after myocardial infarction in rats. Circulation research 67, 23-34 (1990).

43   Gillitzer, R. & Goebeler, M. Chemokines in cutaneous wound healing. Journal of leukocyte biology 69, 513-521 (2001).

44   Dewald, O. et al. CCL2/Monocyte Chemoattractant Protein-1 regulates inflammatory responses critical to healing myocardial infarcts. Circulation research 96, 881-889, doi:10.1161/01.RES.0000163017.13772.3a (2005).

45   Murphy, N. et al. Dietary antioxidants decrease serum soluble adhesion molecule (sVCAM-1, sICAM-1) but not chemokine (JE/MCP-1, KC) concentrations, and reduce atherosclerosis in C57BL but not apoE*3 Leiden mice fed an atherogenic diet. Disease markers 21, 181-190 (2005).

46   Swirski, F. K. et al. Ly-6Chi monocytes dominate hypercholesterolemia-associated monocytosis and give rise to macrophages in atheromata. The Journal of clinical investigation 117, 195-205, doi:10.1172/jci29950 (2007).

47   Panizzi, P. et al. Impaired infarct healing in atherosclerotic mice with Ly-6C(hi) monocytosis. Journal of the American College of Cardiology 55, 1629-1638, doi:10.1016/j.jacc.2009.08.089 (2010).

48   Nahrendorf, M. et al. The healing myocardium sequentially mobilizes two monocyte subsets with divergent and complementary functions. The Journal of experimental medicine 204, 3037-3047, doi:10.1084/jem.20070885 (2007).

Chapter 3

Anti phosphorylcholine antibodies preserve cardiac function and reduce infarct size by attenuation of the inflammatory response following myocardial ischemia-reperfusion injury

Submitted for publication

Niek J. Pluijmert[1*]

Rob C. M. de Jong[2,3*]

Margreet R. de Vries[2,3]

Knut Pettersson[4]

Douwe E. Atsma[1]

J. Wouter Jukema[1,3]

Paul H. A. Quax[2,3]

[*]Authors contributed equally to this work

[1]Department of Cardiology Leiden University Medical Center, Leiden, the Netherlands

[2]Department of Surgery, Leiden University Medical Center, Leiden, the Netherlands

[3]Einthoven Laboratory for Experimental Vascular Medicine, Leiden University Medical Center, Leiden, the Netherlands

[4]Athera Biotechnologies, Stockholm, Sweden

Abstract

Background: Myocardial infarction is preceded by atherosclerosis and followed by a post-ischemic inflammatory process. Antibodies against phosphorylcholine (PC) are known to have anti-inflammatory properties.

Objectives: This study aimed to investigate the modulatory effects of a fully humanized IgG monoclonal antibody directed against phosphorylcholine (PC-mAb) in myocardial remodeling and cardiac function following myocardial ischemia-reperfusion (MI-R) injury.

Methods: In hypercholesterolemic ApoE*3-Leiden mice the LAD coronary artery was occluded for 45 minutes followed by permanent reperfusion and treatment with PC-mAb or vehicle. Two days and three weeks post reperfusion left ventricular (LV) function and infarct size (IS) were assessed by cardiac magnetic resonance imaging. LV fibrous content, LV wall thickness and leukocyte infiltration were evaluated (immuno) histologically. The systemic inflammatory response was analyzed using ELISA and FACS.

Results: Contrast-enhanced MRI assessed IS as well as histologically assessed LV fibrous content were reduced following PC-mAb treatment compared to vehicle three weeks post reperfusion. This resulted in reduced end-diastolic and end-systolic volumes by 24% and 42% respectively, leading to an increased ejection fraction by 33% in the PC-mAb group. These observations could be explained by a reduced systemic inflammatory response two days after reperfusion as observed by decreased CCL2 levels and circulating $Ly6C^{hi}$ monocytes, resulting in reduced leukocyte infiltration and preservation of LV wall thickness after three weeks.

Conclusions: PC-mAb treatment attenuates the post-ischemic inflammatory response, leading to a reduction in adverse cardiac remodeling and preservation of cardiac function in hypercholesterolemic ApoE*3-Leiden mice. Therefore, PC-mAb therapy may be a valid therapeutic approach against MI-R injury.

Introduction

Ischemic heart disease remains one of the leading causes of death worldwide[1]. Currently, the preferred therapy to treat acute myocardial infarction is revascularization therapy to salvage myocardium[2]. However, revascularization causes a subsequent problem of myocardial ischemia-reperfusion (MI-R) injury, in which an additional wave of damage is inflicted to the myocardium due to an increased inflammatory response[3] and generation of reactive oxygen species (ROS)[4], ultimately leading to increased cell death. In a clinical perspective, MI-R injury contributes to adverse cardiac remodeling which subsequently leads to chronic heart failure, known as an important contributor of morbidity and mortality worldwide[3]. Currently, ameliorating this post-ischemic inflammatory process and healing of ischemic myocardium to inhibit LV remodelling remains a challenge.

The increased inflammatory response during MI-R injury is partially responsible for the increased generation of ROS[4]. These ROS are, at their turn, responsible for the formation of oxidation-damaged molecules, which can be recognized by the innate immune system[5]. Oxidation-damaged molecules are recognized by the innate immune system via so-called oxidation specific epitopes (OSEs), which can act as damage associated molecular patterns (DAMPs)[5] and trigger toll-like receptors which play an important role in post MI remodeling[6,7]. In this way inflammation and ROS generation increase each other's adverse effects following MI-R injury.

Following MI-R injury apoptotic cells express OSE on their outer membrane in the form of oxidized membrane phospholipids8. Phosphorylcholine (PC) is the polar head group of the membrane phospholipid phosphatidylcholine and an example of such an OSE, which is expressed on apoptotic cells, but interestingly not on viable cells[8]. Furthermore, apoptotic cells expressing PC, or other OSEs, are known for their immunogenic and pro-inflammatory properties[8]. Interestingly, PC is also expressed by oxidized LDL (oxLDL), an important lipoprotein in the development of atherosclerosis due to its pro-inflammatory properties[5]. Plasma levels of oxPL are in turn related to an increased risk of coronary artery disease events[9]. These PC containing proteins are targeted by innate immunity through recognition by scavenger receptors and natural antibodies[10].

Natural antibodies against PC, also known as EO6 or T15 antibodies[11], are capable to inhibit oxLDL and apoptotic cell uptake by macrophages *in vitro*[12,13]. Furthermore, it has been shown that EO6/T15 antibodies block the pro-inflammatory effects of PC expressing oxidation-damaged molecules[8,14]. In addition, it has been shown that B-1a and B-1b cells produce atheroprotective OSE specific antibodies[15-17], and sterile inflammation in the spleen initiates OSE specific antibody production by splenic B-cells which reduce the development of atherosclerosis[18]. Low concentrations of natural IgM anti-PC antibodies are associated with increased risk for cardiovascular diseases[19-22] and acute coronary syndrome patients with low anti-PC antibody levels experience a

worsened prognosis[23]. Active and passive immunization with antibodies against PC reduces atherosclerosis development[24,25] and vein graft plaque size[26]. Altogether, these data indicate that blocking PC using IgM antibodies may be an interesting approach to treat cardiovascular disease. However, IgM antibodies are not optimal for therapeutic use, because they are, compared to IgG antibodies, relatively expensive and difficult to produce.

Previously we developed PC-mAb, a fully humanized IgG against human PC with anti-inflammatory properties which reduces accelerated atherosclerosis development[27]. In this study we used PC-mAb to investigate its effect against MI-R injury. This study was performed in a model trying to simulate the clinical setting of patients suffering from MI-R injury as a result of revascularization therapy. Therefore we used hypercholesterolemic ApoE*3-Leiden mice starting treatment after reperfusion and using a follow-up of three weeks.

Methods

Myocardial ischemia-reperfusion (MI-R) injury was induced in 12-14 weeks old female ApoE*3-Leiden mice as described previously[28]. Subsequently mice were treated with 10 mg/kg PC-mAb every 3rd day or NaCl 0.9% w/v as a control (vehicle) intraperitoneally. Sham operated animals were operated similarly but without ligation of the LAD, and received injections with NaCl 0.9% w/v. After two days and three weeks LV function and IS were assessed by cardiac MRI. Three weeks post reperfusion LV fibrous content and LV wall thickness were evaluated histologically. Local inflammatory response was investigated two days and three weeks after MI-R injury using immunohistochemistry. The systemic inflammatory response was analyzed using ELISA and FACS. For further details see the Online Appendix.

Statistical analysis

Values were expressed as mean±SEM. Comparisons of parameters between the sham, PC-mAb, and vehicle groups were made using 1-way analysis of variance (ANOVA) with Tukey's correction or 2-way ANOVA with repeated measures and Tukey's post-test in case of multiple time points. Comparisons between PC-mAb and vehicle were made using unpaired t-tests. A value of $p < 0.05$ was considered to represent a significant difference. All statistical procedures were performed using IBM SPSS 23.0.0 (SPSS Inc – IBM, Armonk, NY, USA) and GraphPad Prism 6.02 (GraphPad Software Inc, La Jolla, CA, USA).

Results

Animal characteristics

Body weight (BW), heart weight (HW), total plasma cholesterol (TC) and triglyceride

(TG) concentrations were not affected following PC-mAb treatment (Table 1). HW/BW ratio was decreased following PC-mAb treatment compared to vehicle (5.9±0.1 vs. 6.9±0.3 mg/g, p=0.025). This suggest a reduction in cardiac hypertrophy following PC-mAb treatment.

Table 1: Plasma lipid profiles and animal characteristics

	T (wk)	sham	MI-R PC-mAb	MI-R vehicle
N		13	14	15
TC (mmol/L)	0	17.5±1.7	17.4±1.0	16.8±1.3
TG (mmol/L)	0	2.5±0.2	3.0±0.2	2.6±0.2
BW (g)	0	20.7±0.5	21.5±0.3	21.1±0.4
	3	19.6±0.3	20.8±0.3	20.2±0.4
HW (mg)	3	144±8	123±2	140±7
HW/BW ratio (mg/g)	3	7.3±0.3	5.9±0.1[#]**	6.9±0.3

Table 1: Plasma lipid levels and animal characteristics: plasma total cholesterol (TC), triglycerides (TG), body weight (BW), heart weight (HW). Values are means ± SEM. [#]P<0.05, vs. vehicle, **P<0.01 vs. sham.

PC-mAb concentrations

To confirm the observed effects are indeed the result of PC-mAb treatment, we measured circulating PC-mAb levels two days and three weeks after MI-R injury. PC-mAb was not detectable in the sham and vehicle group both two days and three weeks after MI-R injury. In the PC-mAb treated group PC-mAb levels were 45±10 µg/ml after two days and 40±10 µg/ml after three weeks.

Contrast-enhanced MRI assessed infarct size

First, we assessed baseline IS two days post MI-R injury using contrast-enhanced MRI. No difference was observed between PC-mAb treated animals compared to vehicle animals (28.3±1.4% vs. 30.6±2.1%; Figure 1A). Three weeks after MI-R injury IS was significantly reduced in PC-mAb treated animals compared to vehicle animals (12.8±1.2% vs. 18.3±1.1%, p=0.002). Absolute IS was not different two days after MI-R injury between PC-mAb and vehicle treated animals (16.2±1.0 mg vs. 16.7±1.3 mg; Figure 1B), but three weeks after MI-R injury absolute IS was significantly reduced in PC-mAb treated animals compared to vehicle animals (6.3±0.6 mg vs. 8.6±0.5 mg, p=0.006). Non-infarcted myocardium (Figure 1C) was not significantly different between PC-mAb and vehicle animals at both two days (40.8±1.4 mg vs. 37.9±2.5 mg) and three weeks (42.5±1.4 mg vs. 38.8±2.1 mg). Taken together, this indicates IS significantly decreased following PC-mAb treatment when compared to vehicle animals three weeks after MI-R injury.

As expected some amount of infarct healing was observed in both groups, since IS was significantly smaller three weeks after MI-R injury when compared to two days after MI-R injury (p<0.001) as a result of transitory early infarct edema.
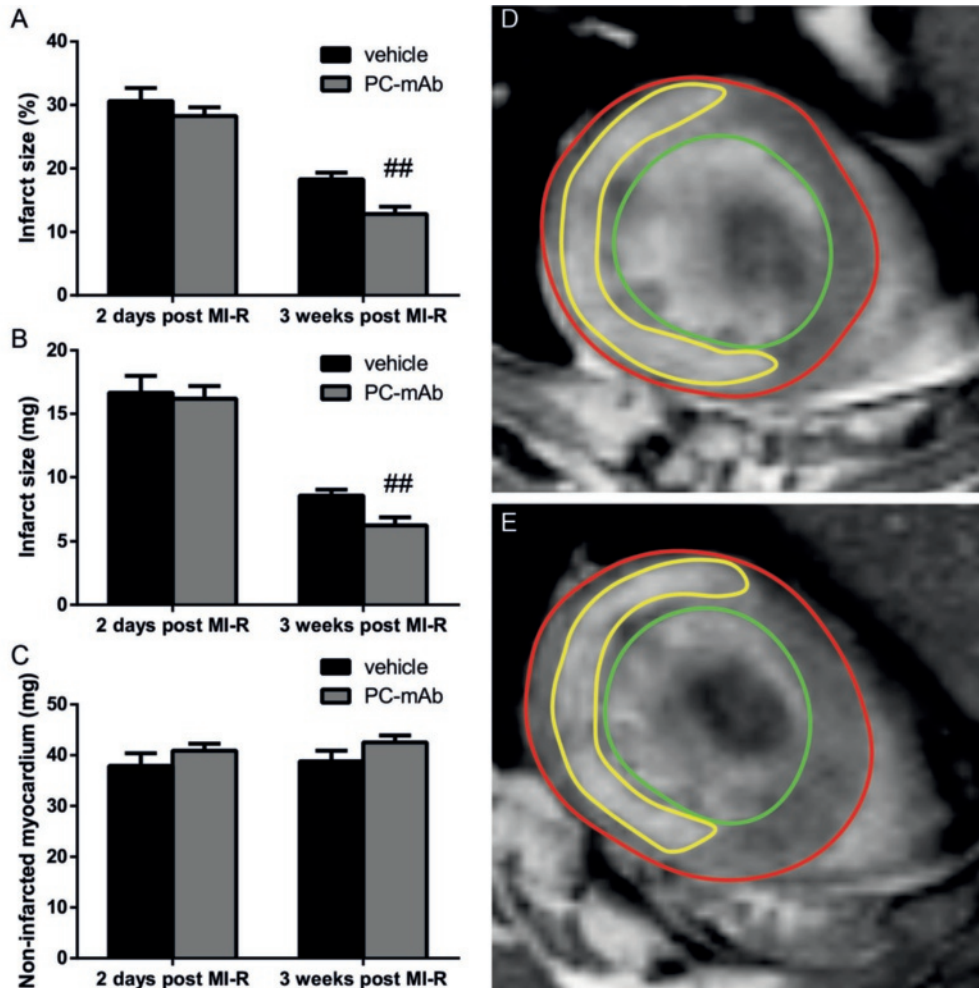
Figure 1: Quantification of infarct size using contrast-enhanced MR imaging. Infarct size was measured at baseline (two days post MI-R) and at sacrifice (three weeks post MI-R), infarct size is quantified as percentage of the LV mass (A), or as absolute mass (mg) of the infarcted myocardium (B; n=14-15 per group). (C) Absolute mass of the non-infarcted myocardium (mg). Representative Gd-DPTA-enhanced MR images two days post MI-R injury of vehicle (D) and PC-mAb treated (E) mice. Red line indicates epicardial border, green line indicates endocardial border and yellow line indicates infarct area. Data are mean±SEM. ##p<0.01 vs. vehicle.

LV dilation and function

To investigate the effect of PC-mAb treatment on LV dilatation and function, we made serial cine MRI images two days and three weeks post MI-R injury. Two days after MI-R injury EDV (Figure 2A) was not affected following PC-mAb treatment (30.8±0.9 µl) when compared to sham (28.7±1.2 µl) and vehicle (34.4±2.3 µl). However, three weeks after MI-R injury PC-mAb treatment resulted in significantly smaller EDV compared to vehicle animals (33.7±1.4 µl vs. 44.4±2.4 µl, p<0.001), which was statistically not

different from the EDV of sham animals (30.4±1.2 µl). ESV (Figure 2B) was significantly increased two days after MI-R injury in both the vehicle (19.4±2.0 µl, p<0.001) and PC-mAb group (14.7±0.7 µl, p=0.047) compared to the sham group (9.4±0.8 µl), while no difference could be observed between the vehicle and PC-mAb group. Interestingly, three weeks post MI-R injury ESV was significantly smaller following PC-mAb treatment (15.5±0.9 µl) compared to vehicle animals (26.6±2.2 µl, p<0.001), while no difference was observed when compared to the sham group (11.2±1.0 µl). Taken together, these results suggest PC-mAb treatment prevents LV dilatation to a level comparable to animals without MI-R injury.

EF as a measure of LV function (Figure 2C) was significantly decreased two days post MI-R injury in both the vehicle (44.7±3.0%, p<0.001) and PC-mAb group (52.1±1.8%, p<0.001) when compared to the sham group (67.6±2.1%), while no difference was observed between vehicle and PC-mAb group. Three weeks post MI-R injury EF was still decreased in both vehicle (40.8±2.9%, p<0.001) and PC-mAb group (54.1±1.8%, p=0.02) when compared to sham (63.9±2.3%). However, PC-mAb treatment significantly increased EF compared to vehicle animals (p<0.001), indicating preservation of LV function by PC-mAb treatment, whereas EF further decreased in the vehicle group compared to the day two time point.
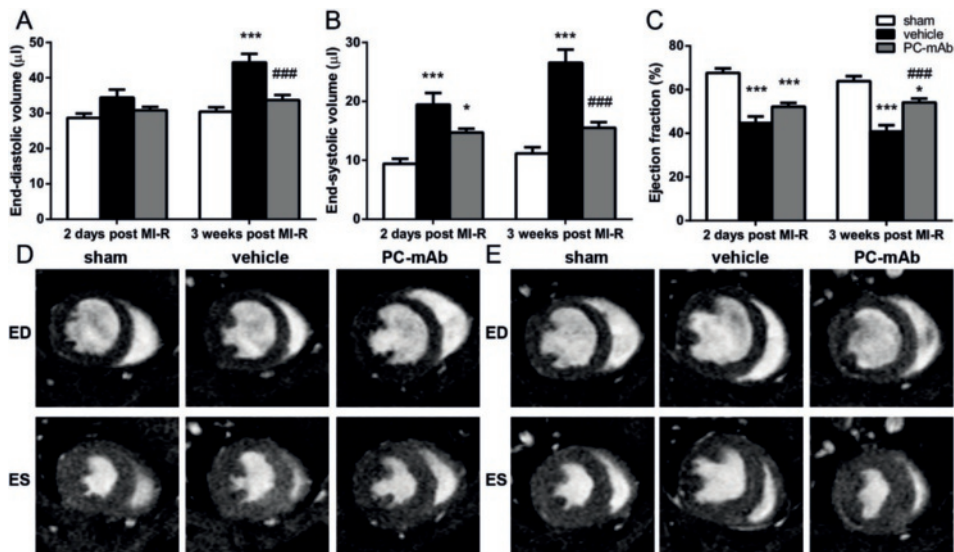
Figure 2: Quantification of LV volumes and function using cardiac MR imaging. LV volumes, EDV (A) and ESV (B), and function, EF (C), were assessed two days and three weeks after MI-R (n=12-15 per group). Representative transversal short-axis MR images at end-diastole (ED) and end-systole (ES) two days (D) and three weeks (E) post MI-R in the sham, vehicle and PC-mAb groups. Data are mean±SEM. ###p<0.05 vs. vehicle, *p<0.05, ***p<0.001 both vs. sham.

LV fibrous content and LV wall thickness

To confirm the effect of PC-mAb on contrast-enhanced MRI assessed IS, we measured LV fibrous content, as a measure for IS, using Sirius Red staining. LV fibrous content was significantly reduced following PC-mAb treatment (12.9±1.0%) compared to vehicle animals (19.8±1.8%, p=0.004; Figure 3A), confirming the earlier observed decreased IS. Accordingly, three weeks after MI-R, LV wall thickness in the PC-mAb compared to the vehicle group was increased in the infarct area (0.87±0.03 mm vs. 0.75±0.04 mm, p=0.045) and border zones (1.13±0.02 mm vs. 1.03±0.03 mm, p=0.041). LV wall thickness in the interventricular septum was significantly increased in both the PC-mAb (1.18±0.04 mm) and vehicle group (1.10±0.04 mm) compared to the sham group (0.85±0.04 mm, both p<0.001). These results indicate cardiac hypertrophy, probably caused by compensation of healthy cardiomyocytes to maintain cardiac function.
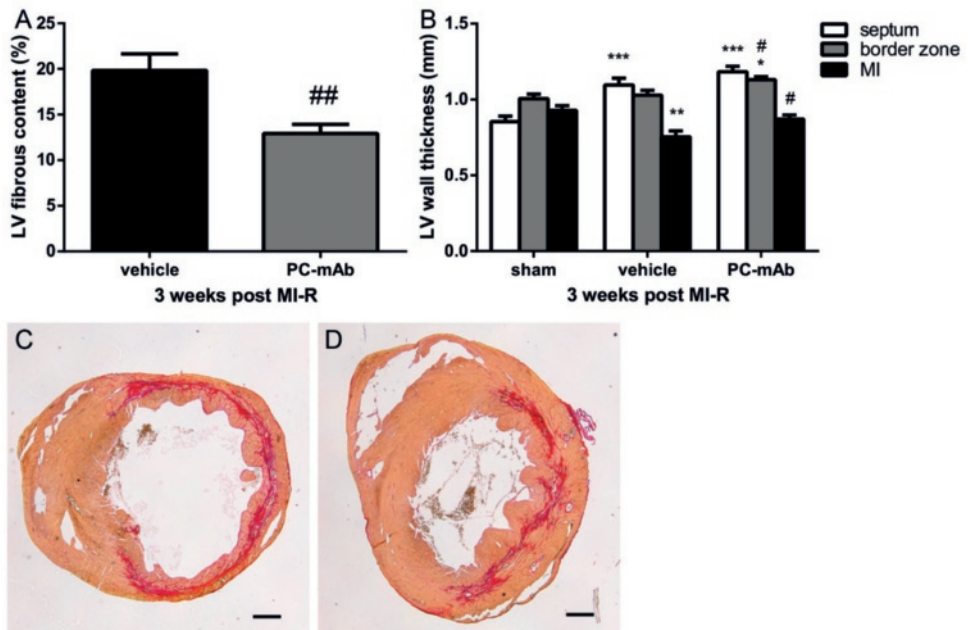
Figure 3: Histological quantification of LV fibrous content and LV wall thickness three weeks post MI-R. LV fibrous content (A) was measured by Sirius red staining and quantified as the area of the LV occupied by collagen. LV wall thickness (B) was assessed in 3 specific areas: interventricular septum, border zone and infarct area (n=9-10 per group). Representative images of Sirius Red staining of vehicle (C) and PC-Mab treated (D) mice. Scale bar = 500 μm. Data are mean±SEM. #p<0.05, ##p<0.01 both vs. vehicle, *p<0.05, **p<0.01, ***p<0.001 all vs. sham.

Local inflammatory response

To unravel the mechanism of PC-mAb treatment against MI-R injury, we investigated leukocyte infiltration two days and three weeks after MI-R injury using immunohistochemistry. First, we studied the early leukocyte infiltration two days post

MI-R injury in different areas of the LV wall namely: the interventricular septum, the border zones and in the infarct area (Figure 4A). In the interventricular septum (sham: 4.8±0.7, vehicle: 3.3±1.1 and PC-mAb: 2.7±0.6 leukocytes per 0.25 mm^2) no differences were observed between all groups. However, in the border zones we observed a near significant (p=0.08) reduction of leukocyte infiltration following PC-mAb treatment (4.2±0.6 leukocytes per 0.25 mm^2) compared to vehicle animals (7.7±2.2 leukocytes per 0.25 mm^2), but not compared to corresponding areas of the normal myocardium in sham animals (4.8±0.4 leukocytes per 0.25 mm^2). In the infarct area we observed no significant difference between PC-mAb and vehicle treated mice (PC-mAb: 9.5±1.5 vs. vehicle: 15.8±4.7 leukocytes per 0.25 mm^2), but we did observe a significant increase in leukocyte infiltration in vehicle treated mice compared to sham (4.9±0.4 leukocytes per 0.25 mm^2, p=0.01).

Next, we investigated the leukocyte infiltration three weeks post MI-R injury in the same areas as mentioned before (Figure 4B). We observed a significant reduction of leukocyte infiltration in all areas following PC-mAb treatment compared to vehicle animals (septum: 0.8±0.1 vs. 3.2±0.7, p=0.001, border zones: 1.1±0.3 vs. 3.1±0.4, p<0.001, infarct area: 0.8±0.2 vs. 3.4±0.7, p<0.001, leukocytes per 0.25 mm^2), while no difference was observed between the PC-mAb and sham group (septum: 1.2±0.3, border zones: 1.0±0.2, infarct area: 0.8±0.1 leukocytes per 0.25 mm^2). Taken together, these results indicate that PC-mAb treatment reduces leukocyte infiltration.
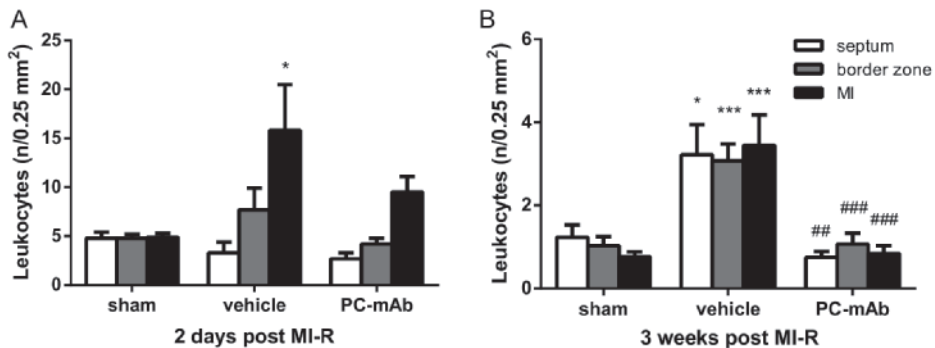
Figure 4: Histological quantification of the local inflammatory response. The number of CD45 positive cells (leukocytes) were counted per specific area: interventricular septum, border zone and infarct area, as measure of local inflammation. Each bar represents the average number of leukocytes per field of view in the specific areas 2 days post MI-R (A; n=3-5 per group) and three weeks post MI-R (B; n= 9-10 per group). Data are mean±SEM. ##P<0.01, ###p<0.001 both vs. vehicle, *p<0.01, ***p<0.001 both vs. sham.

Systemic inflammatory response

To investigate the effect of PC-mAb treatment on the systemic inflammatory response after MI-R injury, we analyzed serum chemokine (C-C motif) ligand 2 (CCL2) levels two

days and three weeks post MI-R injury. Two days after MI-R injury PC-mAb treatment significantly reduces CCL2 levels compared to both vehicle and sham animals (PC-mAb: 13.4±10.0 pg/ml, vehicle: 74.3±6.6 pg/ml, p=0.007, sham: 80.5±14.5 pg/ml, p=0.002; Figure 5A). Three weeks after MI-R injury the effect of PC-mAb treatment on CCL2 levels was less obvious. CCL2 levels were decreased, although not significantly, following
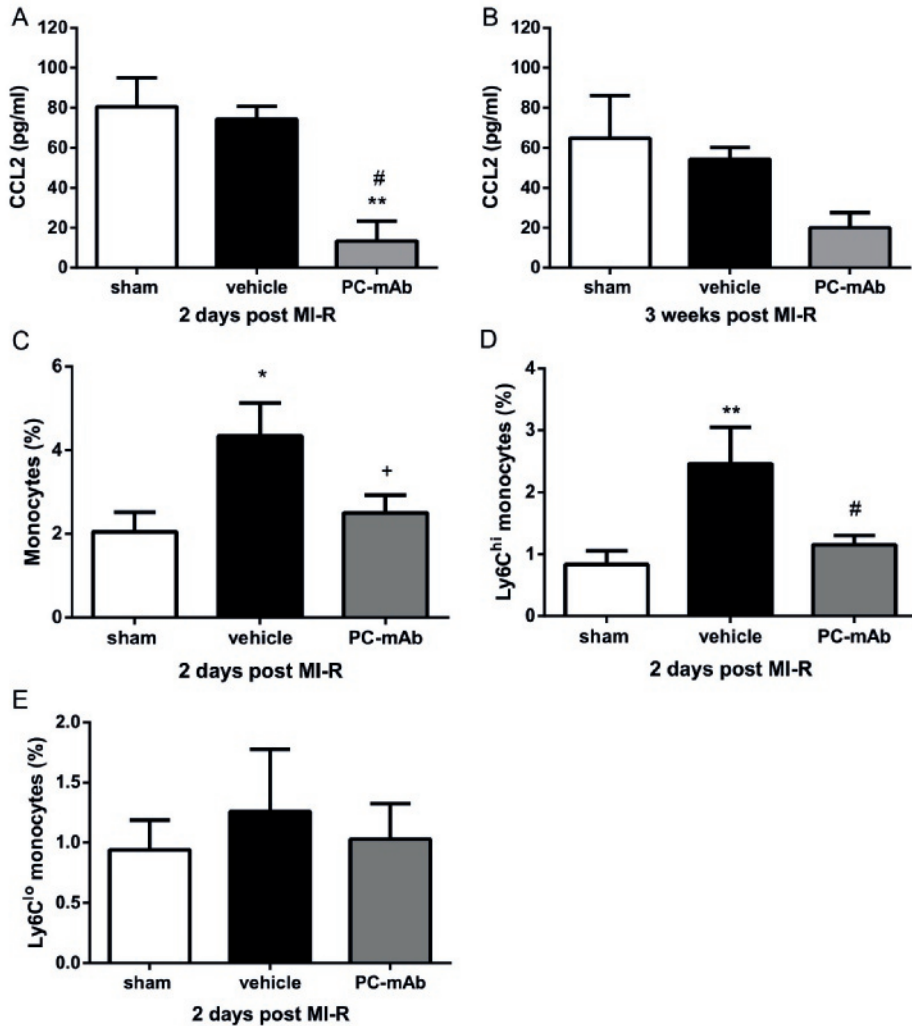
Figure 5: Quantification of the systemic inflammatory response. Serum levels of CCL2 were determined using ELISA as measure of systemic inflammation, two days post MI-R (A; n=4-8 per group) and three weeks post MI-R (B; n=9-10 per group). Circulating monocytes (C) and different monocyte subsets, Ly6C^{hi} (D) Ly6C^{lo} (E), were determined two days post MI-R using FACS analysis and expressed as percentage of total leukocytes (n=4-8 per group). Data are mean±SEM. +p=0.09, $^{#}$p<0.05 both vs. vehicle, **p<0.01 vs. sham.

PC-mAb treatment (20.0±7.5 pg/ml; Figure 5B) compared to vehicle (54.2±6.0 pg/ml) and sham animals (64.9±21.3 pg/ml). Finally, we investigated the effect of PC-mAb treatment on circulating monocytes two days after MI-R injury. The percentage circulating monocytes (of total leukocytes) was near significantly (p=0.09) reduced following PC-mAb treatment (2.5±0.4%) compared to vehicle animals (4.3±0.8%), but not compared to sham animals (2.0±0.5%; Figure 5C). Furthermore, the percentage circulating pro-inflammatory Ly6C^{hi} monocytes (of total leukocytes) was significantly reduced in the PC-mAb treated group (1.2±0.2%) compared to the vehicle group (2.5±0.6%, p=0.02), while no significant difference was observed when compared to the sham group (0.8±0.2%; Figure 5D). Regarding the Ly6C^{lo} monocytes (Figure 5E) no significant differences were observed between all groups (sham: 0.9±0.2%; vehicle: 1.3±0.5%; PC-mAb: 1.0±0.3% (percentage of total leukocytes)). Taken together, these results suggest that PC-mAb treatment especially reduces the early inflammatory response following MI-R injury.

Discussion

This study shows a therapeutic effect of PC-mAb treatment after MI-R injury. Administration of PC-mAb after MI-R injury attenuated the early systemic inflammatory response, by reduction of serum CCL2 levels and circulating Ly6C^{hi} monocytes after two days, as well as the late local inflammatory response by decreased myocardial leukocyte infiltration after three weeks. This resulted in a decreased IS and preservation of LV wall thickness which eventually caused restricted LV dilation and preserved LV function.

Post-ischemic LV remodeling and function
Adverse cardiac remodeling after a MI is characterized by an increase of both EDV and ESV, normally followed by a reduced EF[29]. In this study we assessed EDV, ESV and EF and found PC-mAb treatment to significantly restrict EDV and ESV increase following MI-R injury accompanied by a significant increase in EF, thereby suggesting limitation of adverse cardiac remodeling with preservation of LV function.

We investigated the effect of PC-mAb treatment on IS using contrast-enhanced MRI and showed PC-mAb treatment to significantly decrease IS three weeks after MI-R injury. Previous research showed that IS is directly related to LV remodeling and clinical outcome following MI[30-32]. This suggests the observed preservation of LV function to be the result of improved infarct healing as demonstrated by the reduced IS. In addition, we histologically supported this observation demonstrating a decreased LV fibrous content as a measure of IS and increased LV wall thickness following PC-mAb treatment. LV wall thickness is affected following a MI because of the loss of viable cardiomyocytes which are replaced by collagen[33]. The preservation of LV wall thickness might indicate that

PC-mAb treatment restricts loss off viable cardiomyocytes. Furthermore, we observed an increase in LV wall thickness in the interventricular septum in both the PC-mAb and vehicle group, most likely the result of cardiac hypertrophy caused by compensation of healthy cardiomyocytes to maintain cardiac function[34].

Post-ischemic inflammatory response

Inflammation plays an important role in the repair process following MI leading to formation of a scar[35]. Reperfusion itself causes additional damage to the myocardium by the formation of ROS[4] and accelerates cell membrane damage of cardiomyocytes[36] making ischemic-reperfused myocardium amenable to anti-inflammatory interventions. We assessed the effect of PC-mAb treatment on the post-reperfusion inflammatory response by quantification of local infiltration of leukocytes in the LV wall, which was significantly decreased following PC-mAb treatment after three weeks. Infarct healing following MI-R injury can be divided into two phases, first the early inflammatory phase in which leukocytes play an important role by removing dead cells and matrix debris before they trigger the innate immune system, followed by a reparative phase in which the scar is formed[35]. Our results suggest PC-mAb treatment to reduce the adverse long term inflammatory response, while the beneficial early inflammatory response is less affected as demonstrated by a non-significant difference in early leukocyte infiltration after two days.

CCL2 is an important chemokine responsible for the recruitment of leukocytes to injured tissue[37]. Even though leukocytes remove possible immunogenic cell components and promote infarct healing after MI, CCL2 knock-out mice experience reduced macrophage recruitment to the infarcted myocardium, which resulted in decreased adverse ventricular remodeling following MI-R injury[38]. In agreement with the above-mentioned study, we found that PC-mAb treatment resulted in significant reduction of CCL2 serum levels two days after MI-R injury. Previously, we demonstrated PC-mAb to reduce CCL2 production of monocytes stimulated with oxLDL *in vitro* and expression of CCL2 in cuffed femoral arteries *in vivo*[27]. Systemic CCL2 levels are increased in ApoE*3-Leiden mice when fed a high fat diet[39]. We suppose PC-mAb is capable of binding to apoptotic cells and/or oxLDL thereby reducing the systemic inflammatory response, as observed by reduced CCL2 levels, which subsequently may contribute to the reduction in adverse ventricular remodeling and preservation of cardiac function.

In addition, we observed a decrease of the percentage of monocytes in blood following PC-mAb treatment two days after reperfusion. As mentioned before, infarct healing can be divided in two different phases and in both phases a different subset of monocytes play their own specific role[35]. In the inflammatory phase, pro-inflammatory Ly6C^{hi} monocytes, which can differentiate into pro-inflammatory M1 macrophages, contribute by clearing the infarct site from necrotic cells and matrix debris[35]. In the reparative phase, anti-inflammatory Ly6C^{lo} monocytes, which can differentiate into repair associated

M2 macrophages, play an important role in scar formation and infarct healing[35]. In this study we observed a decrease in Ly6C^{hi} monocytes, but not in Ly6C^{lo} monocytes. Thus, despite Ly6C^{hi} monocytes play an important role in clearing the infarct site from cell debris, we found a beneficial effect on infarct healing and LV function following a PC-mAb induced reduction of circulating Ly6C^{hi} monocytes. In agreement, it has been shown that hypercholesterolemia results in increased numbers of Ly6C^{hi} monocytes[40], subsequently leading to reduced EF[41] and impaired infarct healing[42].

Upon a myocardial ischemic event, affected cardiomyocytes can undergo apoptosis[43], thereby expressing oxidized molecules, like PC, on their outer membrane[44], which is immunogenic[8]. Previous research showed that natural and monoclonal EO6/T15 antibodies against PC are capable to bind to apoptotic cells and oxLDL[12,13,44] thereby dampening the inflammatory response[8]. Therefore, we postulate that our PC-mAb antibodies reduce the inflammatory response following MI-R injury by binding to apoptotic cells before they trigger the innate immune system, subsequently leading to reduced adverse cardiac remodeling leading to preservation of cardiac function.

We performed this study in a clinically relevant setting by starting treatment after reperfusion and by using hypercholesterolemic mice. Most studies performed on possible therapeutic agents against MI-R injury used a strategy in which treatment was started before reperfusion was realized. In our opinion that is not really mimicking the clinical treatment of revascularized patients. Furthermore, hypercholesterolemia affects MI-R injury in mice[45-47] and it is an important risk factor for MI in human[48]. Vice versa, MI has been shown to accelerate atherosclerosis[49] indicating important interactions between both inflammatory processes. This makes them both amenable to anti-inflammatory and immunomodulatory treatment[50]. We used ApoE*3-Leiden mice in this study, which develop hypercholesterolemia when fed a high cholesterol diet, but not when fed a chow diet[51], mimicking the situation often observed in MI patients. The fact that we used a clinical relevant mouse model adds even more value to the already impressive cardioprotective effects of PC-mAb.

Conclusions

PC-mAb treatment attenuates the post-ischemic inflammatory response following myocardial ischemia reperfusion as demonstrated by a reduction of systemic CCL2 levels and circulating Ly6C^{hi} monocytes resulting in impaired myocardial leukocyte infiltration and preservation of LV wall thickness. In a translational animal model mimicking the clinical setting this resulted in limited adverse cardiac remodeling with a decreased infarct size causing reduced LV end-diastolic and end-systolic volumes accompanied by a preserved LV function. Therefore, PC-mAb therapy may be a valid therapeutic approach against MI-R injury.

References

1   McAloon, C. J. et al. The changing face of cardiovascular disease 2000-2012: An analysis of the world health organisation global health estimates data. International journal of cardiology 224, 256-264, doi:10.1016/j.ijcard.2016.09.026 (2016).

2   Bagai, A., Dangas, G. D., Stone, G. W. & Granger, C. B. Reperfusion strategies in acute coronary syndromes. Circulation research 114, 1918-1928, doi:10.1161/circresaha.114.302744 (2014).

3   Ibanez, B., Heusch, G., Ovize, M. & Van de Werf, F. Evolving therapies for myocardial ischemia/reperfusion injury. Journal of the American College of Cardiology 65, 1454-1471, doi:10.1016/j.jacc.2015.02.032 (2015).

4   Bagheri, F. et al. Reactive oxygen species-mediated cardiac-reperfusion injury: Mechanisms and therapies. Life sciences, doi:10.1016/j.lfs.2016.09.013 (2016).

5   Miller, Y. I. et al. Oxidation-specific epitopes are danger-associated molecular patterns recognized by pattern recognition receptors of innate immunity. Circulation research 108, 235-248, doi:10.1161/circresaha.110.223875 (2011).

6   Timmers, L. et al. Toll-like receptor 4 mediates maladaptive left ventricular remodeling and impairs cardiac function after myocardial infarction. Circulation research 102, 257-264, doi:10.1161/circresaha.107.158220 (2008).

7   Arslan, F. et al. Lack of fibronectin-EDA promotes survival and prevents adverse remodeling and heart function deterioration after myocardial infarction. Circulation research 108, 582-592, doi:10.1161/circresaha.110.224428 (2011).

8   Chang, M. K. et al. Apoptotic cells with oxidation-specific epitopes are immunogenic and proinflammatory. The Journal of experimental medicine 200, 1359-1370, doi:10.1084/jem.20031763 (2004).

9   Tsimikas, S. et al. Oxidation-specific biomarkers, lipoprotein(a), and risk of fatal and nonfatal coronary events. Journal of the American College of Cardiology 56, 946-955, doi:10.1016/j.jacc.2010.04.048 (2010).

10   Shaw, P. X. et al. Natural antibodies with the T15 idiotype may act in atherosclerosis, apoptotic clearance, and protective immunity. The Journal of clinical investigation 105, 1731-1740, doi:10.1172/jci8472 (2000).

11   Palinski, W. et al. Cloning of monoclonal autoantibodies to epitopes of oxidized lipoproteins from apolipoprotein E-deficient mice. Demonstration of epitopes of oxidized low density lipoprotein in human plasma. The Journal of clinical investigation 98, 800-814, doi:10.1172/jci118853 (1996).

12   Horkko, S. et al. Monoclonal autoantibodies specific for oxidized phospholipids or oxidized phospholipid-protein adducts inhibit macrophage uptake of oxidized low-density lipoproteins. The Journal of clinical investigation 103, 117-128, doi:10.1172/jci4533 (1999).

13   Chang, M. K. et al. Monoclonal antibodies against oxidized low-density lipoprotein bind to apoptotic cells and inhibit their phagocytosis by elicited macrophages: evidence that oxidation-specific epitopes mediate macrophage recognition. Proceedings of the National Academy of Sciences of the United States of America 96, 6353-6358 (1999).

14   Huber, J. et al. Oxidized membrane vesicles and blebs from apoptotic cells contain biologically active oxidized phospholipids that induce monocyte-endothelial interactions. Arteriosclerosis, thrombosis, and vascular biology 22, 101-107 (2002).

15   Kyaw, T. et al. B1a B lymphocytes are atheroprotective by secreting natural IgM that increases IgM deposits and reduces necrotic cores in atherosclerotic lesions. Circulation research 109, 830-840, doi:10.1161/circresaha.111.248542 (2011).

16   Rosenfeld, S. M. et al. B-1b Cells Secrete Atheroprotective IgM and Attenuate Atherosclerosis. Circulation research 117, e28-39, doi:10.1161/circresaha.117.306044 (2015).

17   Tsiantoulas, D., Gruber, S. & Binder, C. J. B-1 cell immunoglobulin directed against oxidation-specific epitopes. Frontiers in immunology 3, 415, doi:10.3389/fimmu.2012.00415 (2012).

18   Grasset, E. K. et al. Sterile inflammation in the spleen during atherosclerosis provides oxidation-specific epitopes that induce a protective B-cell response. Proceedings of the National Academy of Sciences of the United States of America 112, E2030-2038, doi:10.1073/pnas.1421227112 (2015).

19   de Faire, U. et al. Low levels of IgM antibodies to phosphorylcholine predict cardiovascular disease in 60-year old men: effects on uptake of oxidized LDL in macrophages as a potential mechanism. Journal of autoimmunity 34, 73-79, doi:10.1016/j.jaut.2009.05.003 (2010).

20   Gleissner, C. A. et al. Low levels of natural IgM antibodies against phosphorylcholine are independently associated with vascular remodeling in patients with coronary artery disease. Clinical research in cardiology : official journal of the German Cardiac Society 104, 13-22, doi:10.1007/s00392-014-0750-y (2015).

21   Gronlund, H. et al. Low levels of IgM antibodies against phosphorylcholine predict development of acute myocardial infarction in a population-based cohort from northern Sweden. European journal of cardiovascular prevention and rehabilitation : official journal of the European Society of Cardiology, Working Groups on Epidemiology & Prevention and Cardiac Rehabilitation and Exercise Physiology 16, 382-386, doi:10.1097/HJR.0b013e32832a05df (2009).

22   Gigante, B. et al. Low levels of IgM antibodies against phosphorylcholine are associated with fast carotid intima media thickness progression and cardiovascular risk in men. Atherosclerosis 236, 394-399, doi:10.1016/j.

atherosclerosis.2014.07.030 (2014).

23   Caidahl, K. et al. IgM-phosphorylcholine autoantibodies and outcome in acute coronary syndromes. International journal of cardiology 167, 464-469, doi:10.1016/j.ijcard.2012.01.018 (2013).

24   Caligiuri, G. et al. Phosphorylcholine-targeting immunization reduces atherosclerosis. Journal of the American College of Cardiology 50, 540-546, doi:10.1016/j.jacc.2006.11.054 (2007).

25   Binder, C. J. et al. Pneumococcal vaccination decreases atherosclerotic lesion formation: molecular mimicry between Streptococcus pneumoniae and oxidized LDL. Nature medicine 9, 736-743, doi:10.1038/nm876 (2003).

26   Faria-Neto, J. R. et al. Passive immunization with monoclonal IgM antibodies against phosphorylcholine reduces accelerated vein graft atherosclerosis in apolipoprotein E-null mice. Atherosclerosis 189, 83-90, doi:10.1016/j.atherosclerosis.2005.11.033 (2006).

27   Ewing, M. M. et al. Optimized anti-phosphorylcholine IgG for therapeutic inhibition of inflammatory vascular disease. European heart journal 34, P5703-P5703, doi:10.1093/eurheartj/eht310.P5703 (2013).

28   Michael, L. H. et al. Myocardial infarction and remodeling in mice: effect of reperfusion. The American journal of physiology 277, H660-668 (1999).

29   Galli, A. & Lombardi, F. Postinfarct Left Ventricular Remodelling: A Prevailing Cause of Heart Failure. Cardiology research and practice 2016, 2579832, doi:10.1155/2016/2579832 (2016).

30   Wu, E. et al. Infarct size by contrast enhanced cardiac magnetic resonance is a stronger predictor of outcomes than left ventricular ejection fraction or end-systolic volume index: prospective cohort study. Heart (British Cardiac Society) 94, 730-736, doi:10.1136/hrt.2007.122622 (2008).

31   Masci, P. G. et al. Relationship between location and size of myocardial infarction and their reciprocal influences on post-infarction left ventricular remodelling. European heart journal 32, 1640-1648, doi:10.1093/eurheartj/ehr064 (2011).

32   McAlindon, E., Bucciarelli-Ducci, C., Suleiman, M. S. & Baumbach, A. Infarct size reduction in acute myocardial infarction. Heart (British Cardiac Society) 101, 155-160, doi:10.1136/heartjnl-2013-304289 (2015).

33   Sutton, M. G. & Sharpe, N. Left ventricular remodeling after myocardial infarction: pathophysiology and therapy. Circulation 101, 2981-2988 (2000).

34   Shimizu, I. & Minamino, T. Physiological and pathological cardiac hypertrophy. Journal of molecular and cellular cardiology 97, 245-262, doi:10.1016/j.yjmcc.2016.06.001 (2016).

35   Prabhu, S. D. & Frangogiannis, N. G. The Biological Basis for Cardiac Repair After Myocardial Infarction: From Inflammation to Fibrosis. Circulation research 119, 91-112, doi:10.1161/circresaha.116.303577 (2016).

36   Hori, M. & Nishida, K. Oxidative stress and left ventricular remodelling after myocardial infarction. Cardiovascular research 81, 457-464, doi:10.1093/cvr/cvn335 (2009).

37   Gillitzer, R. & Goebeler, M. Chemokines in cutaneous wound healing. Journal of leukocyte biology 69, 513-521 (2001).

38   Dewald, O. et al. CCL2/Monocyte Chemoattractant Protein-1 regulates inflammatory responses critical to healing myocardial infarcts. Circulation research 96, 881-889, doi:10.1161/01.RES.0000163017.13772.3a (2005).

39   Murphy, N. et al. Dietary antioxidants decrease serum soluble adhesion molecule (sVCAM-1, sICAM-1) but not chemokine (JE/MCP-1, KC) concentrations, and reduce atherosclerosis in C57BL but not apoE*3 Leiden mice fed an atherogenic diet. Disease markers 21, 181-190 (2005).

40   Swirski, F. K. et al. Ly-6Chi monocytes dominate hypercholesterolemia-associated monocytosis and give rise to macrophages in atheromata. The Journal of clinical investigation 117, 195-205, doi:10.1172/jci29950 (2007).

41   Panizzi, P. et al. Impaired infarct healing in atherosclerotic mice with Ly-6C(hi) monocytosis. Journal of the American College of Cardiology 55, 1629-1638, doi:10.1016/j.jacc.2009.08.089 (2010).

42   Nahrendorf, M. et al. The healing myocardium sequentially mobilizes two monocyte subsets with divergent and complementary functions. The Journal of experimental medicine 204, 3037-3047, doi:10.1084/jem.20070885 (2007).

43   Frangogiannis, N. G. The immune system and cardiac repair. Pharmacological research 58, 88-111, doi:10.1016/j.phrs.2008.06.007 (2008).

44   Chou, M. Y. et al. Oxidation-specific epitopes are dominant targets of innate natural antibodies in mice and humans. The Journal of clinical investigation 119, 1335-1349, doi:10.1172/jci36800 (2009).

45   Girod, W. G., Jones, S. P., Sieber, N., Aw, T. Y. & Lefer, D. J. Effects of hypercholesterolemia on myocardial ischemia-reperfusion injury in LDL receptor-deficient mice. Arteriosclerosis, thrombosis, and vascular biology 19, 2776-2781 (1999).

46   Scalia, R. et al. Simvastatin exerts both anti-inflammatory and cardioprotective effects in apolipoprotein E-deficient mice. Circulation 103, 2598-2603 (2001).

47   Jones, S. P., Girod, W. G., Marotti, K. R., Aw, T. Y. & Lefer, D. J. Acute exposure to a high cholesterol diet attenuates myocardial ischemia-reperfusion injury in cholesteryl ester transfer protein mice. Coronary artery disease 12, 37-44 (2001).

48   Yusuf, S. et al. Effect of potentially modifiable risk factors associated with myocardial infarction in 52 countries (the INTERHEART study): case-control study. Lancet (London, England) 364, 937-952, doi:10.1016/s0140-6736(04)17018-

9 (2004).

49   Dutta, P. et al. Myocardial infarction accelerates atherosclerosis. Nature 487, 325-329, doi:10.1038/nature11260 (2012).

50   Frostegard, J. Immunity, atherosclerosis and cardiovascular disease. BMC medicine 11, 117, doi:10.1186/1741-7015-11-117 (2013).

51   Lardenoye, J. H. et al. Accelerated atherosclerosis by placement of a perivascular cuff and a cholesterol-rich diet in ApoE*3Leiden transgenic mice. Circulation research 87, 248-253 (2000).

Supplemental material

Methods

Animals and diets
All animal experiments were approved by the Institutional Committee for Animal Welfare of the Leiden University Medical Center (LUMC) and in compliance with Dutch government guidelines and the Directive 2010/63/EU of the European Parliament. Transgenic female ApoE*3-Leiden mice[1], backcrossed for more than 40 generations on a C57Bl/6J background (bred in the animal facility of the LUMC), aged 8-10 weeks at the start of a dietary run-in period were used for this experiment. Mice were fed a semisynthetic Western-type diet supplemented with 0.4% cholesterol (AB Diets, Woerden, The Netherlands) four weeks prior to surgery which was continued throughout the complete experiment. Mice were housed under standard conditions in conventional cages and received food and water ad libitum.

Plasma lipid analysis
Plasma levels of total cholesterol (TC) and triglycerides (TG) were determined for randomization one week before surgery. After a 4-hour fasting period, plasma was obtained via tail vein bleeding and assayed for total cholesterol (TC) and triglycerides (TG) levels using commercially available enzymatic kits according to the manufacturer's protocols (11489232; Roche Diagnostics, Mannheim, Germany, and 11488872; Roche Diagnostics, Mannheim, Germany, respectively).

Surgical myocardial infarction models and PC-mAb injections
Myocardial ischemia-reperfusion (MI-R) injury was induced at day 0 in 12-14 weeks old female ApoE*3-Leiden mice as described previously[2]. Briefly, mice were pre-anesthetized with 5% isoflurane in a gas mixture of oxygen and room air and placed in a supine position on a heating pad. After endotracheal intubation and ventilation (rate 160 breaths/min, stroke volume 190 µL; Harvard Apparatus, Holliston, MA, USA), mice were kept anesthetized with 1.5-2% isoflurane. Subsequently, a left thoracotomy was performed in the 4th intercostal space and the left anterior descending (LAD) coronary artery was ligated during 45 minutes using a 7-0 prolene suture knotted on a 2 mm section of a plastic tube. Ischemia was confirmed by myocardial blanching. After 45 minutes of ischemia, permanent reperfusion was established. Subsequently, the thorax was closed in layers with 5-0 prolene suture and mice were allowed to recover. Analgesia was obtained with buprenorfine s.c. (0.1 mg/kg) pre-operative and 10-12 hours post-operative. After surgery, animals were randomly grouped to receive intraperitoneal injections with 10 mg/kg PC-mAb every 3rd day or NaCl 0.9% w/v as a control (vehicle). Sham operated animals were operated similarly but without ligation of the LAD, and

received intraperitoneal injections with NaCl 0.9% w/v. Injections were administered direct after surgery (approximately 15 minutes after reperfusion) and between 12:00 p.m. and 2:00 p.m. every 3rd day thereafter.

After two days or three weeks mice were euthanized by bleeding and explantation of the heart under general anesthesia with 1.5-2% isoflurane and heart weight (HW) was determined using a digital scale. Next, hearts were immersion-fixated in 4% paraformaldehyde for 24 hours and embedded in paraffin. Blood samples were collected and used for serum analysis. The heart and body weights were measured from all animals.

Cardiac magnetic resonance imaging

Left ventricular (LV) dimensions and function were assessed two and three weeks after surgery by using a 7-Tesla magnetic resonance imaging (MRI) (Bruker Biospin, Ettlingen, Germany) to obtain contrast-enhanced and cine MRI images. Mice were pre-anesthetized with 5% isoflurane and maintained anesthetized at 1-2% isoflurane. Respiratory rate was monitored by a respiration detection cushion, which was place underneath the thorax and connected to a gating module to monitor respiratory rate (SA Instruments, Inc., Stony Brook, NY). Image reconstruction was performed using Bruker ParaVision 5.1 software.

Infarct size

To distinguish for any possible treatment effect initial baseline IS was determined at day two using contrast-enhanced MR imaging after injection of a 150 µL (0.05 mmol/ml) bolus of gadolinium-DPTA (Gd-DPTA, Dotarem, Guerbet, The Netherlands) via the tail vein. A high-resolution 2D FLASH cine sequence was used to acquire a set of 14 contiguous 0.5 mm slices in short-axis orientation covering the entire heart. Imaging parameters were: echo time of 1.9 ms, repetition time of 84.16 ms, field of view of 33 mm^2, and a matrix size of 192x256.

Mice without visible contrast were excluded from the study as being failed MI procedure. Therapeutic effects regarding IS were determined by repetition of contrast-enhanced MRI at day 21.

LV dimensions and function

LV dimensions were measured at day two and after three weeks with a high-resolution 2D fast gradient echo (FLASH) sequence to acquire a set of contiguous 1 mm slices in short-axis orientation covering the entire long-axis of the heart. Imaging parameters were: echo time of 1.49 ms, repetition time of 5.16 ms, field of view of 26 mm^2, and a matrix size of 144x192.

Image analysis

MRI images were converted to DICOM format and analyzed with the MR Analytical Software System (MASS) for mice (MEDIS, Leiden, The Netherlands). LV endo- and epicardial borders were delineated manually by an investigator blinded to the experimental groups. End-diastolic and end-systolic phases and the contrast enhanced areas were identified automatically, and the percentage of infarcted myocardium, LV end-diastolic volume (EDV), LV end-systolic volume (ESV), and LV ejection fraction (EF) were computed.

LV fibrous content and LV wall thickness

Paraffin-embedded hearts were cut into serial transverse sections of 5 μm along the entire long-axis of the LV. To analyze collagen deposition as an indicator of the fibrotic area, every 50th section of each heart was stained with Sirius Red. LV fibrous content was determined by planimetric measurement of all sections and calculated as fibrotic area divided by the total LV wall surface area including the interventricular septum.

LV wall thickness was measured in five different sections centralized in the infarct area. Per section, wall thickness was analyzed at 3 places equally distributed in the infarcted area, both border zones, and 2 places of the interventricular septum. Measurements were performed perpendicular to the ventricular wall. Corresponding areas were used for measurements in the non-infarcted sham group. All measurements were performed by an observer blinded to the groups, using the ImageJ 1.47v software program (NIH, USA).

Myocardial inflammatory response

For analysis of the cardiac inflammatory response a subpopulation was selected, and sections of the mid-infarct region of the heart were stained using antibodies against leukocytes (anti-CD45, 550539; BD Pharmingen, San Diego, CA, USA). The number of leukocytes was expressed as a number per 0.25 mm^2 in the septum (2 areas), border zones (2 areas), and infarcted myocardium (3 areas). Corresponding areas were used for measurements in the non-infarcted sham group.

FACS analysis

To examine the effect of PC-mAb therapy on the acute inflammatory response, mice were euthanized and blood samples were collected at day two. To study the systemic effects whole blood was analyzed for monocytosis. White blood cell counts (WBC, x106/mL) were measured using a semi-automatic hematology analyzer F-820 (Sysmex; Sysmex Corporation, Etten-Leur, The Netherlands). For FACS analysis, 35 μL of whole blood was incubated for 30 min on ice with directly conjugated antibodies directed against Ly6C-FITC (AbD Serotec, Dusseldorf, Germany), Ly6G-PE (BD Pharmingen, San Diego, CA, USA), CD11b-APC (BD Pharmingen, San Diego, CA, USA), and CD115-PerCP (R&D Systems, Minneapolis, MN, USA). Monocytes were gated based on their expression

profile: CD11b-positive, Ly6G-negative, and CD115-positive. Data was analyzed using FlowJo software (Tree Star Inc.)

CCL2 and PC-mAb ELISA

An PC-mAb ELISA kit (Athera Biotechnologies, Solna, Sweden) was used to determine serum PC-mAb concentrations. To study the effects of PC-mAb on systemic inflammation, an ELISA kit (Cat. No. 555260, BD Biosciences, San Diego, CA, USA) for cytokine concentration of chemokine (C-C motif) ligand 2 (CCL2) was used.

Statistical analysis

Values were expressed as mean ± SEM. Comparisons of parameters between the sham, PC-mAb, and vehicle groups were made using 1-way analysis of variance (ANOVA) with Tukey's correction or 2-way ANOVA with repeated measures and Tukey's posttest in case of multiple time points. Comparisons between PC-mAb and vehicle were made using unpaired t-tests. A value of $p < 0.05$ was considered to represent a significant difference. All statistical procedures were performed using IBM SPSS 23.0.0 (SPSS Inc – IBM, Armonk, NY, USA) and GraphPad Prism 6.02 (GraphPad Software Inc, La Jolla, CA, USA).

References

1   van den Maagdenberg, A. M. et al. Transgenic mice carrying the apolipoprotein E3-Leiden gene exhibit hyperli-poproteinemia. The Journal of biological chemistry 268, 10540-10545 (1993).
2   Michael, L. H. et al. Myocardial infarction and remodeling in mice: effect of reperfusion. The American journal of physiology 277, H660-668 (1999).

Chapter 4

Annexin A5 reduces infarct size and improves cardiac function after myocardial ischemia-reperfusion injury by suppression of the cardiac inflammatory response

Rob C. M. de Jong[1,2]

Niek J. Pluijmert[3]

Margreet R. de Vries[1,2]

Knut Pettersson[4]

Douwe E. Atsma[3]

J. Wouter Jukema[1,3]

Paul H. A. Quax[1,2]

[1]Department of Surgery, Leiden University Medical Center, Leiden, the Netherlands

[2]Einthoven Laboratory for Experimental Vascular Medicine, Leiden University Medical Center, Leiden, the Netherlands

[3]Department of Cardiology, Leiden University Medical Center, Leiden, the Netherlands

[4]Athera Biotechnologies, Stockholm, Sweden

Abstract

Annexin A5 (AnxA5) is known to have anti-inflammatory and anti-apoptotic properties. Inflammation and apoptosis are key processes in post-ischemic cardiac remodeling. In this study, we investigated the effect of AnxA5 on left ventricular (LV) function and remodeling three weeks after myocardial ischemia-reperfusion (MI-R) injury in hypercholesterolemic ApoE*3-Leiden mice. Using a mouse model for MI-R injury, we demonstrate AnxA5 treatment resulted in a 27% reduction of contrast-enhanced MRI assessed infarct size (IS). End-diastolic and end-systolic volumes were decreased by 22% and 38%, respectively. LV ejection fraction was increased by 29% in the AnxA5 group compared to vehicle. Following AnxA5 treatment LV fibrous content after three weeks was reduced by 42%, which was accompanied by an increase in LV wall thickness of the infarcted area by 17%. Two days and three weeks after MI-R injury the number of cardiac macrophages was significantly reduced in both the infarct area and border zones following AnxA5 treatment compared to vehicle treatment. Finally, we found that AnxA5 stimulation leads to a reduction of IL-6 production in bone-marrow derived macrophages *in vitro*. AnxA5 treatment attenuates the post-ischemic inflammatory response and ameliorates LV remodeling which improves cardiac function three weeks after MI-R injury in hypercholesterolemic ApoE*3-Leiden mice.

Introduction

Acute myocardial infarction (MI) initiates a massive inflammatory response[1,2] and cell death[3]. To limit myocardial damage due to these processes and salvage ischemic myocardium, primary percutaneous coronary intervention is the preferred clinical therapy to achieve reperfusion[4]. However, post-ischemic reperfusion itself causes reperfusion injury with the formation of reactive oxygen species which cause direct cell death and stimulation of signal transduction to generate inflammatory cytokines[5]. Furthermore, it has been shown that reperfusion induces and in particular aggravates apoptosis[6,7]. Through binding and ingestion of dying cells, myeloid cells can markedly influence immune responses by enhancing or suppressing inflammation indicating close interaction between cell death and inflammation[8]. In line with this affecting apoptosis and inflammation to mitigate cellular damage might result in new clinical therapies.

Myocardial ischemia-reperfusion (MI-R) induced apoptosis results in different (intra) cellular changes including loss of the asymmetric distribution of plasma membrane phospholipids. Normally, the choline-containing lipid phosphatidylcholine is present on both the outer and inner membrane leaflet while aminophospholipids, like phosphatidylserine (PS), are concentrated on the inner membrane leaflet of viable cells. During early apoptosis and inflammatory cell activation, PS is externalized to the outer cell surface as a result of the activated proteolytic enzyme caspase-3, where it functions as an "eat me" signal to ensure early recognition and phagocytosis[9,10]. Annexins are a family of phospholipid-binding proteins and in particular annexin A5 (AnxA5) binds reversibly, specifically and with high affinity to PS-expressing cells[11]. In addition to the first discovered anti-thrombotic effects of AnxA5[12,13], it is also known to have possible diagnostic properties in visualizing cell death[14] including assessment of atherosclerotic plaque vulnerability[15].

MI is reported to cause increased endogenous AnxA5 plasma levels[16] and uptake in the infarct area[17] in patients. After an ischemic event, cardiomyocytes were found to express PS on their cell surface for at least 6 hours. Administration of exogenous AnxA5 resulted in cytoplasmic internalization and restored sarcolemmal PS asymmetry with no externalized PS remaining, thereby possibly reversing the apoptotic process[18]. Furthermore, a reduced post-interventional inflammatory response was observed following AnxA5 treatment resulting in a potential therapeutic effect against post-interventional intimal hyperplasia[19] and accelerated atherosclerosis[20].

Taken together, the anti-apoptotic and anti-inflammatory effects of AnxA5, can provide a possible role of human recombinant AnxA5 as a therapeutic agent to decrease post-ischemic left ventricular (LV) remodeling and improve cardiac function. A previous study showed beneficial effects of Diannexin, a dimer of AnxA5, treatment in rabbits on post-ischemic blood flow following ischemia and reperfusion[21]. In the current study we demonstrate the beneficial effects of AnxA5 treatment on infarct size (IS) and post-

infarctional cardiac remodeling in a clinically more relevant setting, namely by starting the treatment post-reperfusion and using a follow-up up to three weeks. Cardiac function and IS were assessed three weeks post reperfusion. Moreover, the experiments are performed under hypercholesterolemic conditions by using ApoE*3-Leiden mice on a Western-type diet. Furthermore, we investigate the effect of AnxA5 treatment on the post ischemic-reperfused inflammatory response.

Results

Annexin A5 accumulates in the infarct area
First, AnxA5 accumulation in the infarct area following AnxA5 treatment was evaluated using immunohistochemistry. Two days post MI-R AnxA5 staining, using a specific AnxA5 antibody, was clearly more intense in the infarct area of AnxA5 treated when compared to vehicle treated mice (Fig. 1), suggesting AnxA5 accumulation in the infarct area. Furthermore, as can be appreciated from the images of sham operated mice, AnxA5 protein is present in the healthy myocardium. However, compared the infarcted myocardium, healthy myocardium shows AnxA5 staining which is evenly distributed throughout the tissue. Moreover, the exogenously added AnxA5 accumulates especially in the infarcted area with a spot-wise pattern. Total plasma cholesterol concentration, triglyceride levels and body weight were not affected by AnxA5 treatment (Supplementary Table S1).

Annexin A5 reduces contrast-enhanced MRI assessed LV infarct size
Infarct size as assessed by contrast-enhanced MRI was significantly reduced after three weeks in AnxA5 treated mice compared to the vehicle group (13.4±1.8% vs. 18.3±1.1%, P=0.022; Fig. 2A), while initial IS, two days after MI-R, was comparable in both groups (27.0±2.3% vs. 30.6±2.1%, P=0.249; Fig. 2A). Interestingly, IS was significantly smaller (Supplementary Fig. S1A) three weeks post-reperfusion compared to two days post-reperfusion indicating infarct healing and resorption of acute infarct edema. This observation was confirmed by the absolute numbers of IS and viable myocardium. IS was decreased in both the vehicle and AnxA5 group after three weeks when compared to two days (Supplementary Fig. S1B), while viable myocardium was unchanged in time (Supplementary Fig. S1C). Reduced IS does not affect heart weight, since heart weight was comparable in all three groups (AnxA5: 145±5 mg, vehicle: 140±7 mg, and sham 144±8 mg; Supplementary Table S1).

Annexin A5 improves LV function
MRI analyses showed that the reduced scar expansion after MI-R due to AnxA5 treatment was accompanied by a limitation of LV dilation and preserved LV function after three weeks. No differences were observed at day two (EDV: 31.0±2.0 µl vs.
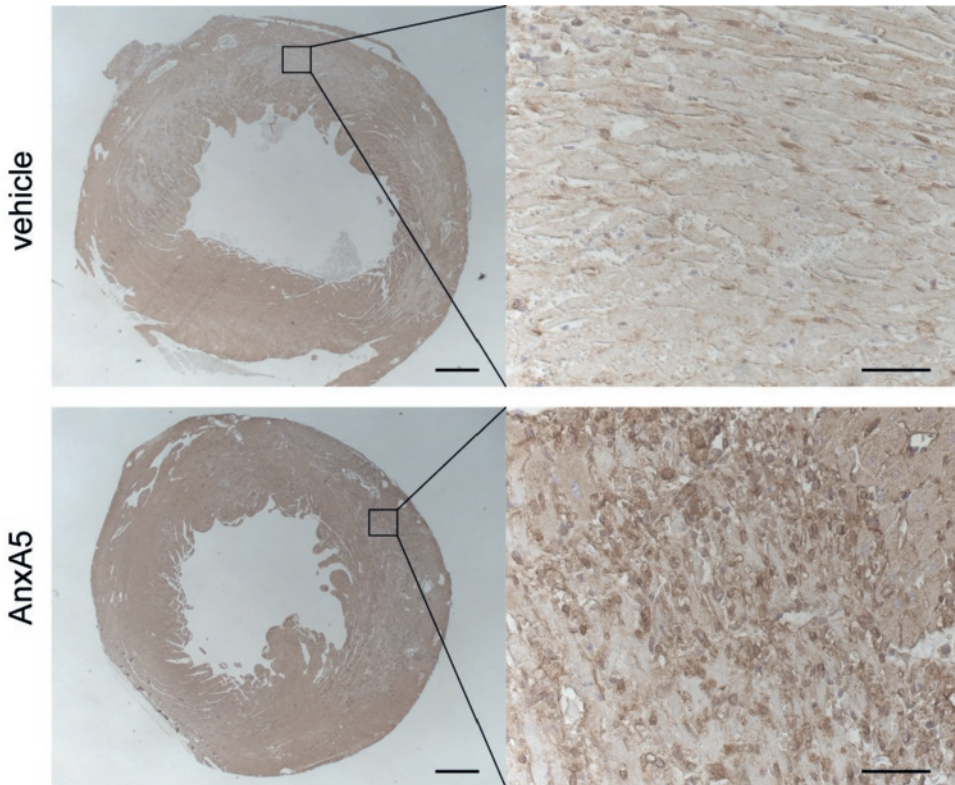
Figure 1: Annexin A5 staining. Representative images of cross-sections from the whole heart (left) or the infarct area (right) two days after MI-R stained for human annexin A5 using a specific AnxA5 antibody, while counterstaining was performed using haematoxilin. AnxA5 treated mice showed a more intense staining compared to vehicle and sham mice. Left panel scale bar: 500μm, right panel scale bar: 20μm.

34.4±2.3 μl, P=1.000; Fig. 3A, and ESV: 14.2±1.5 μl vs. 19.4±2.0 μl, P=0.153; Fig. 3B). However, after three weeks EDV was significantly smaller in the AnxA5 group as compared with vehicle (34.5±2.2 μl vs. 44.4±2.4 μl, P=0.004; Fig. 3A). Furthermore, ESV was significantly smaller in the AnxA5 group as compared with vehicle (16.5±1.4 μl vs. 26.6±2.2 μl, P<0.001; Fig. 3B).

AnxA5 seemed to have a preventive effect with respect to post-ischemic LV dilation according to nearly equal LV volumes as compared to the sham group after three weeks (EDV: 30.4±1.2 μl, P=1.000; Fig. 3A, and ESV: 11.2±1.0 μl, P=0.188; Fig. 3B), in contrast to vehicle treatment which caused obvious LV dilation (both P<0.001; Fig. 3A and 3B).

The limited LV dilation was associated with a significantly better LV function, as expressed by preserved EF in the AnxA5 group compared to vehicle (52.5±2.4% vs. 40.8±2.9%, P=0.019; Fig. 3C) while no significant difference was observed after two days (54.6±3.5% vs. 44.7±3.0%, P=0.074; Fig. 3C).
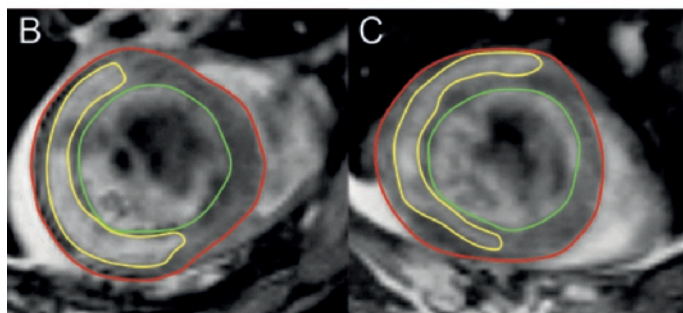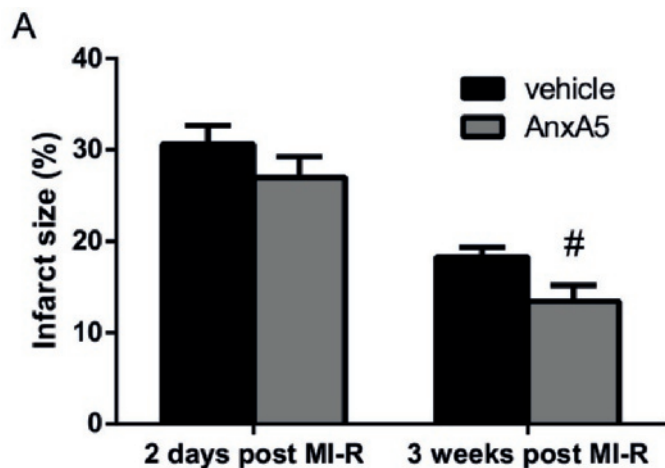
Figure 2: Contrast-enhanced MR imaging. Two days after MI-R no difference in infarct size was observed between the groups (n=13-15). However, after three weeks the AnxA5 group displayed a reduced infarct size as compared to the vehicle group (A). Representative Gd-DPTA-enhanced MR images (B) two days and three weeks after MI-R of the vehicle and AnxA5 group, red line indicates epicardial border, green line indicates endocardial border and yellow line indicates infarct area. Data are mean±SEM. #P<0.05 vs. vehicle.

Annexin A5 reduces LV fibrous content and preserves LV wall thickness

Histological evaluation of LV fibrous content endorsed the aforementioned results as assessed by cardiac MRI. AnxA5 administration caused a reduction of LV fibrous content three weeks after MI-R as compared to the vehicle group (11.4±1.1% vs. 19.8±1.8%; P=0.001, Fig. 4A). This was accompanied by an increased wall thickness of the infarcted LV wall in the AnxA5 compared to the vehicle group (0.90±0.04 mm vs. 0.75±0.04 mm, P=0.041; Fig. 4C). Wall thickness of the border zone area (1.02±0.02 mm vs. 1.03±0.03 mm, P=1.000) and interventricular septum (1.00±0.04 mm vs. 1.10±0.04 mm, P=0.326) were not affected by AnxA5 therapy as compared to vehicle (Fig. 4C).

Furthermore, LV wall thickness in the infarct area was decreased in the vehicle group compared to the sham group (0.93±0.03 mm; P=0.008), while LV wall thickness in the infarct area was preserved in the AnxA5 group (P=1.000) when compared to the sham group (Fig. 4C). Besides, both the AnxA5 (P=0.047) and vehicle (P=0.001) group showed

an increased wall thickness of the interventricular septum compared to the sham group (0.85±0.04 mm) indicating compensatory concentric hypertrophy (Fig. 4C).
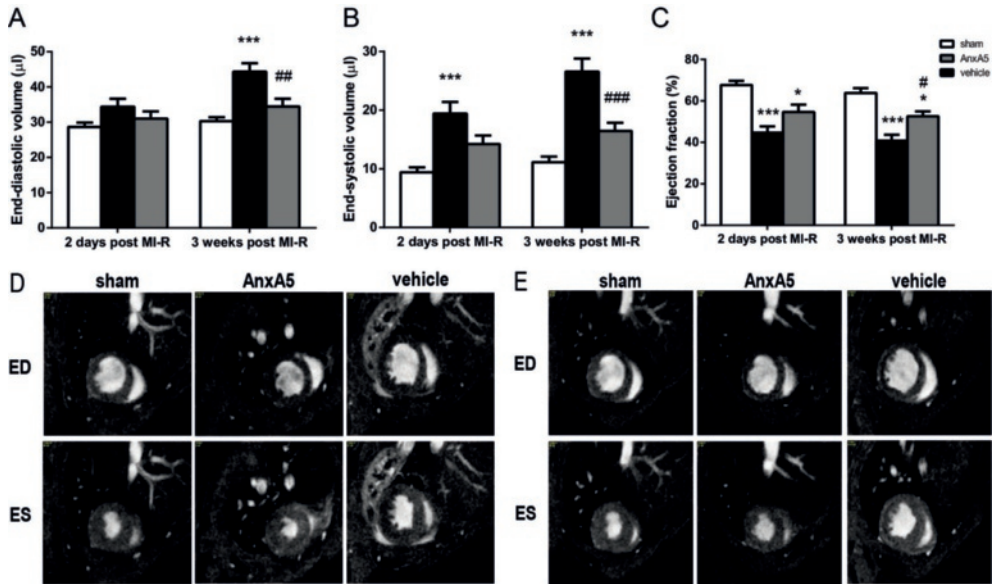
Figure 3: Cardiac MR imaging of LV volumes and function. Assessment of LV volumes and function two days and three weeks after MI-R (n=12-15). AnxA5 therapy prevented the increase in end-diastolic volume (EDV) (A) and end-systolic volume (ESV) (B) accompanied by a preserved ejection fraction (EF) (C) as compared to vehicle three weeks post MI-R. Representative transversal short-axis MR images at end-diastole (ED) and end-systole (ES) two days (D) and three weeks (E) following MI-R in the sham, AnxA5 and vehicle groups, red line indicates epicardial border and green line indicates endocardial border. Data are mean±SEM. #P<0.05, ##P<0.01, ###P<0.001 all vs. vehicle, *P<0.05 and ***P<0.001 both vs. sham.

Annexin A5 causes reduction of the local inflammatory response

Histological analysis two days after MI-R showed a significant increase in cardiac macrophages in both the vehicle (P<0.001) and AnxA5 (P<0.05) treated group when compared to sham mice, indicating an increase of the local inflammatory response following MI-R injury (Fig. 5A). Interestingly, the number of cardiac macrophages was reduced following AnxA5 treatment compared to vehicle in the infarct area (134.5±21.3 vs. 306.4±63.1 per mm^2, P=0.007), border zones (124.9±14.1 vs. 243.0±18.4 per mm^2, P<0.001) and interventricular septum (59.1±8.4 vs. 101.9±12.4 per mm^2, P=0.037). Taken together, this suggests, although increased compared to sham, AnxA5 treatment results in a reduction of the post-ischemic inflammatory response.

Three weeks after MI-R injury the number of cardiac macrophages is increased in both the vehicle (P<0.001) and AnxA5 (P<0.05) group when compared to the sham group, indicating the local inflammatory response is still increased following MI-R

injury at this time point (Fig. 5G). Intriguingly, the number of cardiac macrophages was reduced following AnxA5 treatment compared to vehicle treated mice in the infarct area (240.6±25.1 vs. 376.2±47.3 per mm^2, P=0.029) and border zones (154.1±9.9 vs. 274.6±43.1 per mm^2, P=0.018), but not in the interventricular septum (39.3±5.3 vs. 40.0±8.7 per mm^2, P=1.000). Taken together, this means AnxA5 treatment not only reduces the early inflammatory response, but also the extended chronic inflammatory response.
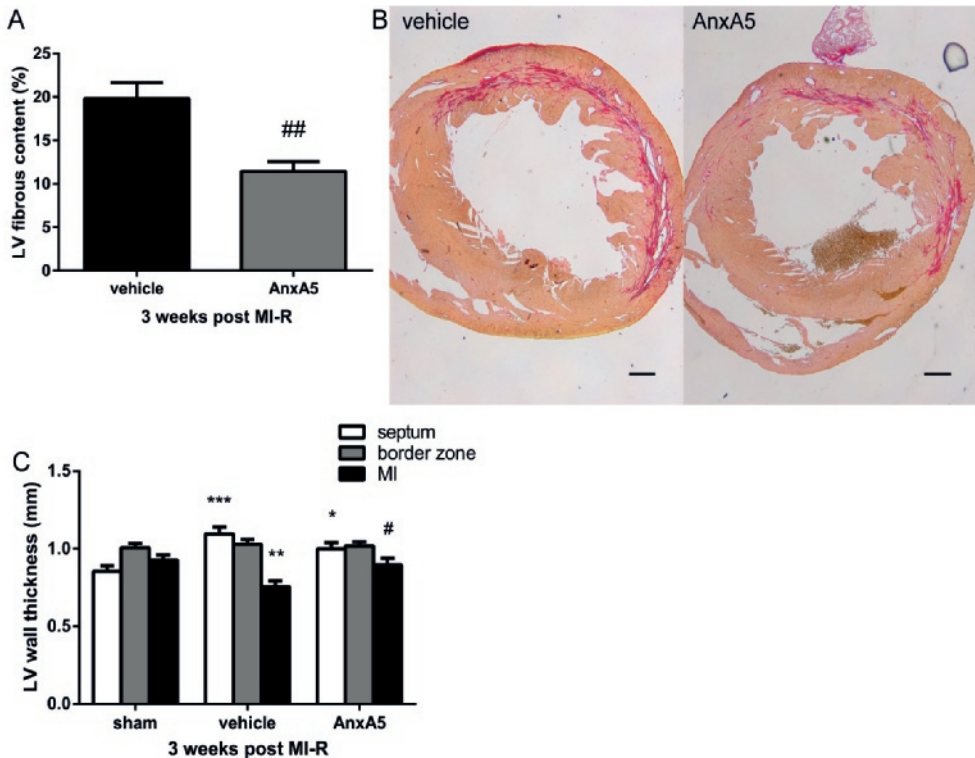
Figure 4: LV fibrous content and LV wall thickness. Histological analysis after three weeks (n=9-10) showed a significant reduced LV fibrous content in the AnxA5 group compared to the vehicle group (A). Representative images (B) of Sirius red staining of cross-sections of the whole heart in the vehicle group and the AnxA5 group. Scale bar: 500µm. LV wall thickness was significantly increased in the infarct area after AnxA5 treatment (C). Data are mean±SEM. #P<0.05 vs. vehicle, *P<0.05, **P<0.01, ***P<0.001 all vs. sham.

AnxA5 treatment reduces the number of proliferating macrophages

To further investigate the mechanism behind the observed reduced inflammatory response, serum CCL2 concentrations two and three weeks port MI-R injury were measured. No significant differences were observed between all groups regarding serum CCL2 concentrations at both time points (Supplementary Fig. S2).
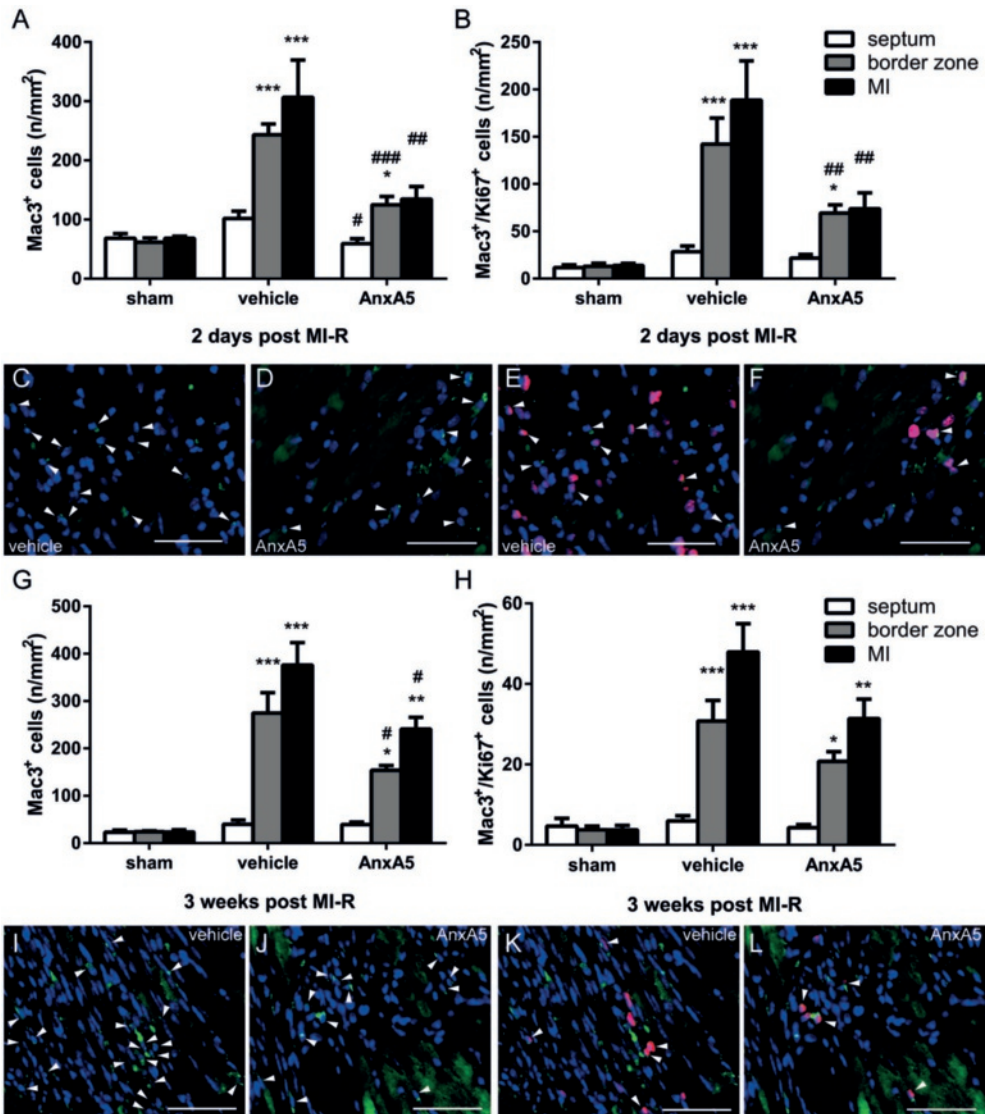
Figure 5: Local inflammatory response and macrophage proliferation. Quantification of the number of infiltrated macrophages showed an decreased number of infiltrated macrophages in the border zones and infarct area two days (n=3-5) following MI-R in the AnxA5 group (A). Mac3/Ki67 double staining revealed a significant reduction in the number of proliferating macrophages in the border zones and infarct area after two days in the AnxA5 treated mice as compared to vehicle (n=5-6; B). Three weeks after MI-R the number of infiltrated macrophages is significantly reduced in the border zones and infarct area upon AnxA5 treatment (G). No differences were observed regarding the number of proliferating macrophages three weeks after MI-R between AnxA5 and vehicle groups (H). Representative images of Mac3 staining (C, D, I and J) and Mac3/Ki67 double staining (E, F, K and L) of the infarct area. Nuclei are shown in blue, Mac3 staining in green and Ki67 in red, arrowheads indicate positive cells. Scale bar: 50μm. Data are mean±SEM. #P,0.05, ##P<0.01, ###P<0.001 all vs. vehicle, *P<0.05, **P<0.01 and ***P<0.001 all vs. sham.

Next, the number of proliferating macrophages (Mac3^{+}/Ki67^{+} cells) was quantified. Two days post MI-R injury the number of proliferating macrophages is significantly reduced in the infarct area and border zones, but not in the interventricular septum in AnxA5 treated mice compared to vehicle treated mice (infarct area: 73.8±17.0 vs. 188.6±41.7, P=0.009; border zones: 69.3±8.6 vs. 142.2±27.5, P=0.008 and septum: 21.8±3.7 vs. 28.5±6.0 per mm^2, P=0.852; Fig. 5B). Compared to sham (infarct area: 13.9±2.3, border zones: 12.9±3.4 and septum: 11.5±3.0 per mm^2), vehicle treated mice show a significant increase in proliferating macrophages in the infarct area (P<0.001) and border zones (P<0.001) of the LV wall, while AnxA5 treated mice only show an increased number of proliferating macrophages in the border zones (P=0.015).

Three weeks post MI-R injury no differences in proliferating macrophages could be observed between AnxA5 treated mice and vehicle treated mice (Fig. 5H). In the infarct area and border zones the number of proliferating macrophages was significantly increased in both the AnxA5 and vehicle group compared to the sham group (infarct area: AnxA5: 31.4±4.9, P=0.008,and vehicle: 47.9±7.0, P<0.001 both vs. sham: 3.7±1.1 per mm^2; border zones: AnxA5: 20.8±2.4, P=0.015 and vehicle: 30.8±5.2, P<0.001 both vs. sham: 3.8±0.9 per mm^2).

AnxA5 stimulation reduces IL-6 production by macrophages *in vitro*
Finally, we investigated the effect of AnxA5 stimulation on cytokine production of bone-marrow derived macrophages (Figure 6). AnxA5 stimulation reduces IL-6 production significantly compared to vehicle (1071±28 vs. 1455±65 pg/ml; P<0.001).
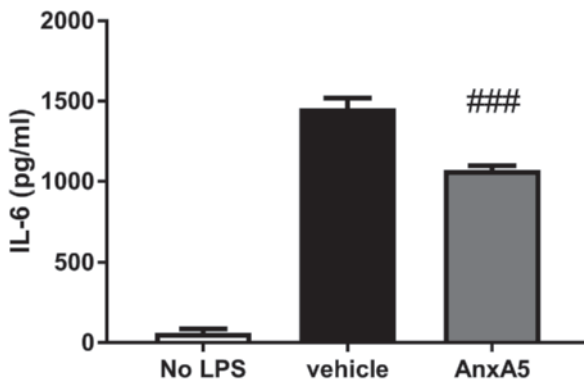
Figure 6: *In vitro* effect of AnxA5 stimulation on bone-marrow derived macrophages. IL-6 production was significantly reduced following AnxA5 stimulation (n=5) compared to vehicle. Data are mean±SEM. ###P<0.001 vs. vehicle.

Discussion

This study shows a beneficial therapeutic effect of human recombinant AnxA5 administration following MI-R injury. By using hypercholesterolemic conditions and administering treatment directly after reperfusion results can be interpreted as clinically relevant. AnxA5 treatment resulted in accumulation of AnxA5 in the infarct area subsequently leading to a reduced infarct size, most likely mediated by attenuation of the inflammatory response. These results translated into limited LV dilation and improved cardiac function three weeks after MI-R. To our knowledge this is the first time that such a huge therapeutic effect (a 28.6% increase in EF) is shown after a follow-up of three weeks and treatment was started post-reperfusion. Although other groups have reported strong beneficial effects on EF of several compounds[22-24], these studies started the therapeutic intervention before reperfusion, a setting that does not really mimics the situation seen in clinical treatment of patients. We found a striking increase in EF by 28.6% following post-reperfusion AnxA5 treatment.

Since infarct healing can be seen as a biphasic process with an inflammatory phase followed by a reparative and proliferative phase[25], therapeutic effects are ideally analyzed after completion of both phases. Therefore we analyzed the effects of AnxA5 at two days and three weeks after MI-R. The fact that especially after three weeks AnxA5 treatment resulted in improved cardiac function and reduced infarct sizes, is very promising for the eventual translation of AnxA5 treatment to a clinical setting in which long term effects are desired.

Hypercholesterolemia is a primary risk factor for MI in human[26] and it affects IS following MI-R injury in mice[27-29] making the condition of value to implement in translational animal models. ApoE*3-Leiden mice develop hypercholesterolemia with subsequent atherosclerosis when fed a high-cholesterol diet, but not following a chow diet[30]. In our study we found a cardioprotective effect of AnxA5 treatment following MI-R in hypercholesterolemic ApoE*3-Leiden mice, although AnxA5 had no effects on plasma cholesterol levels. These mice mimic the clinical situation of most MI patients regarding hypercholesterolemia, and thereby adding more value to the found cardioprotective effect of AnxA5.

We demonstrated a reduced infarct size following MI-R injury as a result of AnxA5 treatment which was accompanied by preserved LV wall thickness of the infarcted area after three weeks. This might explain the improved cardiac function, since attenuation of post-ischemic LV remodeling is a prerequisite to improve LV function and finally attain prolonged survival[31]. In line with our results Hale et al. reported that therapeutic administration of Diannexin caused significantly smaller areas of no-reflow and obviously reduced infarct size within hours following severe myocardial ischemia in rabbits[21]. Diannexin, a 73 kDa recombinant dimer of the endogenous human Annexin A5 protein, has also been reported to have anti-thrombotic activities. Diannexin and

annexin A5 bind PS with K(D) values of 0.6 and 5 nm, respectively, and both bind to the same subpopulation of PS-exposing platelets, thus inhibiting both the adverse effects of PS. Annexin A5 (35.7 kDa) is rapidly cleared from the circulation. In contrast to Annexin A5 which is rapidly cleared from the circulation, Diannexin, has an extended half-life, probably due to the higher molecular weight and the decreased renal clearance rate[21,32,33]. However, in this study we focus on the effects on natural occurring Annexin A5.

Molecular MR imaging with an annexin-labeled magnetofluorescent nanoparticle in combination with delayed-enhancement MRI has been shown to distinguish cardiomyocyte apoptosis from necrosis in vivo within 4 to 6 hours following MI-R injury[34]. Large areas of apoptotic but viable myocardium were revealed emphasizing its susceptibility to pharmacological intervention and salvation of apoptotic myocardium[34]. During the early phase of apoptosis in cardiomyocytes, endogenous AnxA5 is translocated and externalized[35,36]. Reversibility of this apoptotic process was demonstrated, as exogenous AnxA5 binds to externalized PS, thereby shielding of the "eat me" signal[18]. We suggest that treatment with AnxA5, like we performed in the current study, affects the exposed PS and thus attenuate the pro-apoptotic, but also the pro-inflammatory status of the myocardium. Up to at least 6 hours after a solitary MI-R insult AnxA5 binding to externalized PS resulted in restored sarcolemmal PS asymmetry after AnxA5 internalization[18], which might be one of the mechanisms behind the observed decrease in IS after AnxA5 treatment.

Following AnxA5 treatment, the number of cardiac macrophages was dramatically decreased both two days and three weeks post MI-R compared to vehicle treatment. Macrophages play a dual role following MI-R injury, in the early phase after an infarction they help to clear the infarct area from cell debris and matrix components, which can act like damage associated molecular patterns, before they trigger the innate immune response[37] as shown by Figure 5 where an increase of cardiac macrophages can be found after MI-R in both AnxA5 and vehicle groups in comparison to the sham group. On the other hand, macrophages themselves can produce cytokines, which increase the inflammatory response[1,38]. This is one of the reasons for the disappointing results of present anti-inflammatory therapies in clinical trials, despite promising pre-clinical studies[39]. Therefore it seems plausible that rather than total abolishment of the inflammatory response, suppression of inflammation is beneficial following MI-R injury. This explains the observed striking beneficial results regarding IS and cardiac function following AnxA5 treatment, while the number of cardiac macrophages is increased compared to sham mice.

The cardiac macrophage population is maintained by both monocyte infiltration and local proliferation of macrophages. We found no differences in serum CCL2 concentrations, a critical player in monocyte recruitment to sites with tissue injury, following AnxA5 treatment. Therefore, we focused on the role of AnxA5 treatment on

macrophage proliferation following MI-R injury. Interestingly, number of proliferating macrophages was significantly reduced two days post MI-R injury following AnxA5 treatment. However, the percentage proliferating macrophages was comparable in both the vehicle and AnxA5 group. Immediately following MI-R injury the resident macrophage population in the infarct area undergoes apoptosis and is replaced by mainly Ly6C^{high} monocytes, which differentiate into pro-inflammatory macrophages[40]. This population of pro-inflammatory macrophages is maintained by both recruitment of Ly6C^{high} monocytes as well as proliferation of the pro-inflammatory macrophages[41]. Since we did not observe differences in CCL2 concentrations and percentage proliferating macrophages was unaffected, the mechanism by which AnxA5 treatment reduces the number of cardiac macrophages is subject of future research.

We observed a decrease in IL-6 production by bone-marrow derived macrophages following AnxA5 stimulation. Recently, it has been shown that IL-6-deficient mice show reduced acute MI-R injury[42]. Furthermore, a correlation between IL-6 concentrations and myocardial damage was found in patients suffering from ischemic events[43]. This is in line with our results regarding IL-6 production by macrophages and the cardioprotective effect of AnxA5 in vivo. However, the exact mechanism by which AnxA5 regulates IL-6 production in this setting is subject for future research.

Radiolabeled AnxA5 is rapidly cleared from blood and accumulates in apoptotic tissue[20]. Previously, we have shown AnxA5 treatment leads to accumulation of AnxA5 at sites of injured vessel wall after systemic treatment, while AnxA5 is rapidly cleared from the blood[19]. In the current study, we show accumulation of AnxA5 in the infarct area following systemic AnxA5 treatment. The short half-life in blood, accumulation in the infarct area and cardioprotective effect suggests that AnxA5 is a safe and promising therapeutic agent.

Taken together, we showed a potential therapeutic role for human recombinant AnxA5 against MI-R injury in a clinical relevant setting. By suppression of the inflammatory response, AnxA5 attenuates long term adverse LV remodeling and improve cardiac function. A recent study by Ziegler *et al.*, directed at the inhibition of inflammation using CD39 showed similar inhibitory effects on adverse post MI-R remodeling[44]. This underscores the new therapeutic potential of inhibiting inflammation in post MI-R remodeling.

Methods

Animals and diets

This study was performed in compliance with Dutch government guidelines and the Directive 2010/63/EU of the European Parliament. All animal experiments were approved by the Institutional Committee for Animal Welfare of the Leiden University Medical Center (LUMC). Transgenic female ApoE*3-Leiden mice[45], backcrossed for more

than 40 generations on a C57Bl/6J background (bred in the animal facility of the LUMC), aged 8-10 weeks at the start of a dietary run-in period were used for this experiment. Mice were fed a semisynthetic Western-type diet supplemented with 0.4% cholesterol (AB Diets, Woerden, The Netherlands) 4 weeks prior to surgery, which was continued throughout the complete experiment. Mice were housed under standard conditions in conventional cages and received food and water ad libitum.

Plasma lipid analysis

Plasma levels of total cholesterol (TC) and triglycerides (TG) were determined for randomization one week before surgery and at the end of the experiment. After a 4 hours fasting period, plasma was obtained via tail vein bleeding (~50μL) and assayed for total cholesterol (TC) and triglycerides (TG) levels using commercially available enzymatic kits according to the manufacturer's protocols (11489232 and 11488872, respectively; Roche Diagnostics, Mannheim, Germany).

Surgical myocardial ischemia-reperfusion model and Annexin A5 administration

MI was induced by MI-R at day 0 in 12-14 weeks old female ApoE*3-Leiden mice as described previously[46]. Briefly, mice were pre-anesthetized with 5% isoflurane in a gas mixture of oxygen and room air and placed in a supine position on a heating pad (37°C). After endotracheal intubation and ventilation (rate 160 breaths/min, stroke volume 190 μL; Harvard Apparatus, Holliston, MA, USA), mice were kept anesthetized with 1.5-2% isoflurane. Subsequently, a left thoracotomy was performed in the 4th intercostal space and the left anterior descending (LAD) coronary artery was ligated during 45 minutes using a 7-0 prolene suture knotted on a 2 mm section of a plastic tube followed by permanent reperfusion. Ischemia was confirmed by myocardial blanching. During this period muscle flaps were folded back and covered with a pre-warmed wet surgical mesh. Body temperature was kept constant between 35-37°C. After 35 minutes of ischemia mice received an intraperitoneal injection of lidocain (6 mg/kg) to prevent cardiac arrhythmias caused by reperfusion. After 45 minutes of ischemia, permanent reperfusion was established. Subsequently, the thorax was closed in layers with 5-0 prolene suture and mice were allowed to recover. Analgesia was obtained with buprenorfine s.c. (0.1 mg/kg) pre-operative and 10-12h post-operative. After surgery, animals were randomly grouped to receive daily administration of intraperitoneal injections with 1 mg/kg human recombinant annexin A5 (AnxA5; Athera Biotechnologies) in a volume of 200 μl, or NaCl 0.9% w/v (vehicle) as a control. Sham operated animals were operated similarly but without ligation of the LAD, and received intraperitoneal injections with NaCl 0.9% w/v. Injections were administered direct after surgery and between 12:00 p.m. and 2:00 p.m. the days thereafter. After two days or three weeks, mice were euthanized by bleeding and explantation of heart under general anesthesia with 1.5-2% isoflurane in a gas mixture of oxygen and room air.

Hearts were quickly excised, immersion-fixated in 4% paraformaldehyde for 24 hours and embedded in paraffin. The heart and body weight were measured from all animals

Cardiac magnetic resonance imaging
Cardiac parameters were assessed two days and three weeks post MI-R using a 7-Tesla MRI (Bruker Biospin, Ettlingen, Germany) equipped with a combined gradient and shim coil, which is inserted into the magnet bore. Mice were pre-anesthetized as described above and kept anesthetized with 1.5-2% isoflurane. Respiratory rate was monitored by a respiration detection cushion, which was placed underneath the thorax and connected to a gating module to monitor respiratory rate (SA Instruments, Inc., Stony Brook, NY). Image reconstruction was performed using Bruker ParaVision 5.1 software.

Infarct size
To determine infarct size, contrast enhanced MR imaging was performed after injection of a 150 µL bolus (0.5 mmol/ml) of gadolinium-DPTA (Gd-DPTA, Dotarem, Guerbet, the Netherlands) via the tail vein. A gradient echo sequence (FLASH) was used to acquire a set of 14 contiguous 0.7 mm contrast-enhanced slices in short-axis orientation covering the entire heart. Imaging parameters were: echo time of 1.9 ms, repetition time of 84.16 ms, field of view (33 mm^2), and a matrix size of 192x256.

Left ventricular function
Assessment of cardiac function was performed with a high-resolution 2D FLASH cine sequence to acquire a set of 9 contiguous 1 mm slices in short-axis orientation covering the entire heart. Imaging parameters were: echo time of 1.49 ms, repetition time of 5.16 ms, field of view (26 mm^2), and a matrix size of 144x192.

Image analysis
All MR image data was analyzed with the MASS for mice software package (MEDIS, Leiden, the Netherlands). The endocardial and epicardial borders were manually delineated and a reference point was positioned by an investigator blinded to treatment. Subsequently, the infarcted area of the LV, end-diastolic volume (EDV), end-systolic volume (ESV), ejection fraction (EF) were computed automatically.

LV fibrous content and LV wall thickness
Paraffin-embedded hearts were cut into serial transverse sections of 5 µm along the entire long-axis of the LV and mounted on slides. To analyze collagen deposition as an indicator of the fibrotic area, every 50th section of each heart was stained with Sirius Red. LV fibrous content, as a representation of IS, was determined by planimetric measurement of all sections and calculated as fibrotic area divided by the total LV wall surface area including the interventricular septum.

LV wall thickness was measured in five different sections centralized in the infarct area. Per section, wall thickness was analyzed at 3 places equally distributed in the infarcted area, both border zones, and 2 places of the interventricular septum. Measurements were performed perpendicular to the ventricular wall. Corresponding areas were used for measurements in the non-infarcted sham group. All measurements were performed by an observer blinded to the groups, using the ImageJ 1.47v software program (NIH, USA).

Immunohistochemistry

To evaluate AnxA5 accumulation in the infarct area paraffin section of the mid-infarct region of the heart were stained using antibodies against AnxA5 (anti-human annexin V, 3357-100, Biovision, Milpitas, CA, USA), while counterstaining was performed using haematoxylin.

For analysis of the cardiac inflammatory response paraffin sections of the mid-infarct region of the heart were stained using antibodies against macrophages (anti-Mac3, 550292; BD Pharmingen, San Diego, CA, USA) and to quantify the number of proliferating macrophages antibodies against proliferation marker Ki67 were used (anti-Ki67, ab16667; Abcam, Cambridge, UK). The number of macrophages and proliferating macrophages was expressed as a number per mm^2 in the septum (2 areas), border zones (2 areas), and infarcted myocardium (3 areas).

Bone-marrow derived macrophages

Bone-marrow derived cells were isolated from ApoE*3-Leiden mice and subjected to murine macrophage colony-stimulating factor (M-CSF) (20 ng/μl; Miltenyi Biotec) to stimulate differentiation into macrophages.

Macrophages were stimulated by exposure to 8% heat-inactivated FCS in the presence and absence of AnxA5 (2 μM). The cells were incubated overnight at 37°C in 5% $CO2$ atmosphere. Next, bone marrow derived macrophage were stimulated with or without LPS (10 ng/ml) for six hours and the supernatants were collected. Subsequently, IL-6 production by these bone marrow-derived macrophages was analyzed by ELISA.

ELISA

To study the effects of AnxA5 on systemic inflammation, an ELISA kit (Cat. No. 555260, BD Biosciences, San Diego, CA, USA) for cytokine concentration of chemokine (C-C motif) ligand 2 (CCL2) was used. Furthermore, the IL-6 production by bone-marrow derived macrophages in vitro was measured using an ELISA kit (Cat. No. 555240 (IL-6), BD Biosciences, San Diego, CA, USA), according to the manufacturer's instructions.

Statistical analysis

Values were expressed as mean ± SEM. Comparisons of parameters between the sham,

AnxA5, and vehicle groups were made using 1-way analysis of variance (ANOVA) with Bonferroni's correction or 2-way ANOVA with repeated measures and Bonferroni's post-test in case of multiple time points. Comparisons between AnxA5 and vehicle were made using (un)paired t-tests. A value of $P<0.05$ was considered to represent a significant difference. Statistical procedures were performed using IBM SPSS 23.0.0 (SPSS Inc – IBM, Armonk, NY, USA) and GraphPad Prism 6.02 (GraphPad Software Inc, La Jolla, CA, USA).

References

1   Frangogiannis, N. G., Smith, C. W. & Entman, M. L. The inflammatory response in myocardial infarction. Cardiovasc Res 53, 31-47, (2002).

2   Frangogiannis, N. G. Regulation of the inflammatory response in cardiac repair. Circ Res 110, 159-173, (2012).

3   Konstantinidis, K., Whelan, R. S. & Kitsis, R. N. Mechanisms of cell death in heart disease. Arterioscler Thromb Vasc Biol 32, 1552-1562, (2012).

4   Schomig, A., Kastrati, A., Dirschinger, J., Mehilli, J., Schricke, U., Pache, J., Martinoff, S., Neumann, F. J. & Schwaiger, M. Coronary stenting plus platelet glycoprotein IIb/IIIa blockade compared with tissue plasminogen activator in acute myocardial infarction. Stent versus Thrombolysis for Occluded Coronary Arteries in Patients with Acute Myocardial Infarction Study Investigators. N Engl J Med 343, 385-391, (2000).

5   Hori, M. & Nishida, K. Oxidative stress and left ventricular remodelling after myocardial infarction. Cardiovasc Res 81, 457-464, (2009).

6   Badalzadeh, R., Mokhtari, B. & Yavari, R. Contribution of apoptosis in myocardial reperfusion injury and loss of cardioprotection in diabetes mellitus. J Physiol Sci 65, 201-215, (2015).

7   Eefting, F., Rensing, B., Wigman, J., Pannekoek, W. J., Liu, W. M., Cramer, M. J., Lips, D. J. & Doevendans, P. A. Role of apoptosis in reperfusion injury. Cardiovasc Res 61, 414-426, (2004).

8   Savill, J., Dransfield, I., Gregory, C. & Haslett, C. A blast from the past: clearance of apoptotic cells regulates immune responses. Nat Rev Immunol 2, 965-975, (2002).

9   Fadok, V. A., Bratton, D. L., Frasch, S. C., Warner, M. L. & Henson, P. M. The role of phosphatidylserine in recognition of apoptotic cells by phagocytes. Cell Death Differ 5, 551-562, (1998).

10   van Genderen, H. O., Kenis, H., Hofstra, L., Narula, J. & Reutelingsperger, C. P. Extracellular annexin A5: functions of phosphatidylserine-binding and two-dimensional crystallization. Biochim Biophys Acta 1783, 953-963, (2008).

11   Reutelingsperger, C. P. & van Heerde, W. L. Annexin V, the regulator of phosphatidylserine-catalyzed inflammation and coagulation during apoptosis. Cell Mol Life Sci 53, 527-532, (1997).

12   Thiagarajan, P. & Benedict, C. R. Inhibition of arterial thrombosis by recombinant annexin V in a rabbit carotid artery injury model. Circulation 96, 2339-2347, (1997).

13   van Heerde, W. L., Sakariassen, K. S., Hemker, H. C., Sixma, J. J., Reutelingsperger, C. P. & de Groot, P. G. Annexin V inhibits the procoagulant activity of matrices of TNF-stimulated endothelium under blood flow conditions. Arterioscler Thromb 14, 824-830, (1994).

14   Boersma, H. H., Kietselaer, B. L., Stolk, L. M., Bennaghmouch, A., Hofstra, L., Narula, J., Heidendal, G. A. & Reutelingsperger, C. P. Past, present, and future of annexin A5: from protein discovery to clinical applications. J Nucl Med 46, 2035-2050, (2005).

15   Laufer, E. M., Winkens, M. H., Narula, J. & Hofstra, L. Molecular imaging of macrophage cell death for the assessment of plaque vulnerability. Arterioscler Thromb Vasc Biol 29, 1031-1038, (2009).

16   Matsuda, R., Kaneko, N., Kikuchi, M., Chiwaki, F., Toda, M., Ieiri, T., Horikawa, Y., Shimizu, M. & Shimamoto, K. Clinical significance of measurement of plasma annexin V concentration of patients in the emergency room. Resuscitation 57, 171-177, (2003).

17   Hofstra, L., Liem, I. H., Dumont, E. A., Boersma, H. H., van Heerde, W. L., Doevendans, P. A., De Muinck, E., Wellens, H. J., Kemerink, G. J., Reutelingsperger, C. P. & Heidendal, G. A. Visualisation of cell death in vivo in patients with acute myocardial infarction. Lancet 356, 209-212, (2000).

18   Kenis, H., Zandbergen, H. R., Hofstra, L., Petrov, A. D., Dumont, E. A., Blankenberg, F. D., Haider, N., Bitsch, N., Gijbels, M., Verjans, J. W., Narula, N., Narula, J. & Reutelingsperger, C. P. Annexin A5 uptake in ischemic myocardium: demonstration of reversible phosphatidylserine externalization and feasibility of radionuclide imaging. J Nucl Med 51, 259-267, (2010).

19   Ewing, M. M., de Vries, M. R., Nordzell, M., Pettersson, K., de Boer, H. C., van Zonneveld, A. J., Frostegard, J., Jukema, J. W. & Quax, P. H. Annexin A5 therapy attenuates vascular inflammation and remodeling and improves endothelial function in mice. Arterioscler Thromb Vasc Biol 31, 95-101, (2011).

20   Ewing, M. M., Karper, J. C., Sampietro, M. L., de Vries, M. R., Pettersson, K., Jukema, J. W. & Quax, P. H. Annexin A5 prevents post-interventional accelerated atherosclerosis development in a dose-dependent fashion in mice. Atherosclerosis 221, 333-340, (2012).

21   Hale, S. L., Allison, A. C. & Kloner, R. A. Diannexin reduces no-reflow after reperfusion in rabbits with large ischemic myocardial risk zones. Cardiovasc Ther 29, e42-52, (2011).

22   Oerlemans, M. I., Liu, J., Arslan, F., den Ouden, K., van Middelaar, B. J., Doevendans, P. A. & Sluijter, J. P. Inhibition of RIP1-dependent necrosis prevents adverse cardiac remodeling after myocardial ischemia-reperfusion in vivo. Basic Res Cardiol 107, 270, (2012).

23   Velotta, J. B., Kimura, N., Chang, S. H., Chung, J., Itoh, S., Rothbard, J., Yang, P. C., Steinman, L., Robbins, R. C. & Fischbein, M. P. alphaB-crystallin improves murine cardiac function and attenuates apoptosis in human endothelial cells

exposed to ischemia-reperfusion. Ann Thorac Surg 91, 1907-1913, (2011).

24   Arslan, F., Smeets, M. B., O'Neill, L. A., Keogh, B., McGuirk, P., Timmers, L., Tersteeg, C., Hoefer, I. E., Doevendans, P. A., Pasterkamp, G. & de Kleijn, D. P. Myocardial ischemia/reperfusion injury is mediated by leukocytic toll-like receptor-2 and reduced by systemic administration of a novel anti-toll-like receptor-2 antibody. Circulation 121, 80-90, (2010).

25   Prabhu, S. D. & Frangogiannis, N. G. The Biological Basis for Cardiac Repair After Myocardial Infarction: From Inflammation to Fibrosis. Circ Res 119, 91-112, (2016).

26   Yusuf, S., Hawken, S., Ounpuu, S., Dans, T., Avezum, A., Lanas, F., McQueen, M., Budaj, A., Pais, P., Varigos, J. & Lisheng, L. Effect of potentially modifiable risk factors associated with myocardial infarction in 52 countries (the INTERHEART study): case-control study. Lancet 364, 937-952, (2004).

27   Girod, W. G., Jones, S. P., Sieber, N., Aw, T. Y. & Lefer, D. J. Effects of hypercholesterolemia on myocardial ischemia-reperfusion injury in LDL receptor-deficient mice. Arterioscler Thromb Vasc Biol 19, 2776-2781, (1999).

28   Jones, S. P., Girod, W. G., Marotti, K. R., Aw, T. Y. & Lefer, D. J. Acute exposure to a high cholesterol diet attenuates myocardial ischemia-reperfusion injury in cholesteryl ester transfer protein mice. Coron Artery Dis 12, 37-44, (2001).

29   Scalia, R., Gooszen, M. E., Jones, S. P., Hoffmeyer, M., Rimmer, D. M., 3rd, Trocha, S. D., Huang, P. L., Smith, M. B., Lefer, A. M. & Lefer, D. J. Simvastatin exerts both anti-inflammatory and cardioprotective effects in apolipoprotein E-deficient mice. Circulation 103, 2598-2603, (2001).

30   Lardenoye, J. H., Delsing, D. J., de Vries, M. R., Deckers, M. M., Princen, H. M., Havekes, L. M., van Hinsbergh, V. W., van Bockel, J. H. & Quax, P. H. Accelerated atherosclerosis by placement of a perivascular cuff and a cholesterol-rich diet in ApoE*3Leiden transgenic mice. Circ Res 87, 248-253, (2000).

31   Wu, E., Ortiz, J. T., Tejedor, P., Lee, D. C., Bucciarelli-Ducci, C., Kansal, P., Carr, J. C., Holly, T. A., Lloyd-Jones, D., Klocke, F. J. & Bonow, R. O. Infarct size by contrast enhanced cardiac magnetic resonance is a stronger predictor of outcomes than left ventricular ejection fraction or end-systolic volume index: prospective cohort study. Heart 94, 730-736, (2008).

32   Kuypers, F. A., Larkin, S. K., Emeis, J. J. & Allison, A. C. Interaction of an annexin V homodimer (Diannexin) with phosphatidylserine on cell surfaces and consequent antithrombotic activity. Thromb Haemost 97, 478-486, (2007).

33   Rand, M. L., Wang, H., Pluthero, F. G., Stafford, A. R., Ni, R., Vaezzadeh, N., Allison, A. C., Kahr, W. H., Weitz, J. I. & Gross, P. L. Diannexin, an annexin A5 homodimer, binds phosphatidylserine with high affinity and is a potent inhibitor of platelet-mediated events during thrombus formation. J Thromb Haemost 10, 1109-1119, (2012).

34   Sosnovik, D. E., Garanger, E., Aikawa, E., Nahrendorf, M., Figuiredo, J. L., Dai, G., Reynolds, F., Rosenzweig, A., Weissleder, R. & Josephson, L. Molecular MRI of cardiomyocyte apoptosis with simultaneous delayed-enhancement MRI distinguishes apoptotic and necrotic myocytes in vivo: potential for midmyocardial salvage in acute ischemia. Circ Cardiovasc Imaging 2, 460-467, (2009).

35   Monceau, V., Belikova, Y., Kratassiouk, G., Charue, D., Camors, E., Communal, C., Trouve, P., Russo-Marie, F. & Charlemagne, D. Externalization of endogenous annexin A5 participates in apoptosis of rat cardiomyocytes. Cardiovasc Res 64, 496-506, (2004).

36   Monceau, V., Belikova, Y., Kratassiouk, G., Robidel, E., Russo-Marie, F. & Charlemagne, D. Myocyte apoptosis during acute myocardial infarction in rats is related to early sarcolemmal translocation of annexin A5 in border zone. Am J Physiol Heart Circ Physiol 291, H965-971, (2006).

37   Frangogiannis, N. G. Inflammation in cardiac injury, repair and regeneration. Curr Opin Cardiol 30, 240-245, (2015).

38   Frangogiannis, N. G. The mechanistic basis of infarct healing. Antioxid Redox Signal 8, 1907-1939, (2006).

39   Seropian, I. M., Toldo, S., Van Tassell, B. W. & Abbate, A. Anti-inflammatory strategies for ventricular remodeling following ST-segment elevation acute myocardial infarction. J Am Coll Cardiol 63, 1593-1603, (2014).

40   Heidt, T., Courties, G., Dutta, P., Sager, H. B., Sebas, M., Iwamoto, Y., Sun, Y., Da Silva, N., Panizzi, P., van der Laan, A. M., Swirski, F. K., Weissleder, R. & Nahrendorf, M. Differential contribution of monocytes to heart macrophages in steady-state and after myocardial infarction. Circ Res 115, 284-295, (2014).

41   Hilgendorf, I., Gerhardt, L. M., Tan, T. C., Winter, C., Holderried, T. A., Chousterman, B. G., Iwamoto, Y., Liao, R., Zirlik, A., Scherer-Crosbie, M., Hedrick, C. C., Libby, P., Nahrendorf, M., Weissleder, R. & Swirski, F. K. Ly-6Chigh monocytes depend on Nr4a1 to balance both inflammatory and reparative phases in the infarcted myocardium. Circ Res 114, 1611-1622, (2014).

42   Jong, W. M., Ten Cate, H., Linnenbank, A. C., de Boer, O. J., Reitsma, P. H., de Winter, R. J. & Zuurbier, C. J. Reduced acute myocardial ischemia-reperfusion injury in IL-6-deficient mice employing a closed-chest model. Inflamm Res 65, 489-499, (2016).

43   Sawa, Y., Ichikawa, H., Kagisaki, K., Ohata, T. & Matsuda, H. Interleukin-6 derived from hypoxic myocytes promotes neutrophil-mediated reperfusion injury in myocardium. J Thorac Cardiovasc Surg 116, 511-517, (1998).

44   Ziegler, M., Hohmann, J. D., Searle, A. K., Abraham, M. K., Nandurkar, H. H., Wang, X. & Peter, K. A single-chain antibody-CD39 fusion protein targeting activated platelets protects from cardiac ischaemia/reperfusion injury. Eur Heart J 39, 111-116, (2018).

45   van den Maagdenberg, A. M., Hofker, M. H., Krimpenfort, P. J., de Bruijn, I., van Vlijmen, B., van der Boom, H.,

Havekes, L. M. & Frants, R. R. Transgenic mice carrying the apolipoprotein E3-Leiden gene exhibit hyperlipoproteinemia. J Biol Chem 268, 10540-10545, (1993).

46   Michael, L. H., Ballantyne, C. M., Zachariah, J. P., Gould, K. E., Pocius, J. S., Taffet, G. E., Hartley, C. J., Pham, T. T., Daniel, S. L., Funk, E. & Entman, M. L. Myocardial infarction and remodeling in mice: effect of reperfusion. Am J Physiol 277, H660-668, (1999).

Supplementary information

Supplementary table

Supplementary Table S1: plasma lipids & animal characteristics

	T (wk)	sham	AnxA5	vehicle
N		13	14	15
TC (mmol/L)	0	17.5±1.7	15.6±1.8	16.8±1.3
	3	13.1±1.1	15.8±1.2	14.0±1.2
TG (mmol/L)	0	2.5±0.2	2.5±0.2	2.6±0.2
	3	2.4±0.2	1.9±0.2	1.8±0.2
BW (g)	0	20.7±0.5	21.0±0.4	21.1±0.4
	3	19.6±0.3	20.6±0.3	20.2±0.4
HW (mg)	3	144±8	145±5	140±7
HW/BW ratio (mg/g)		7.3±0.3	7.2±0.2	6.9±0.3

Supplemental table I: Plasma lipid profiles and animal characteristics: plasma total cholesterol (TC), triglycerides (TG), body weight (BW), heart weight (HW).

Supplementary figures
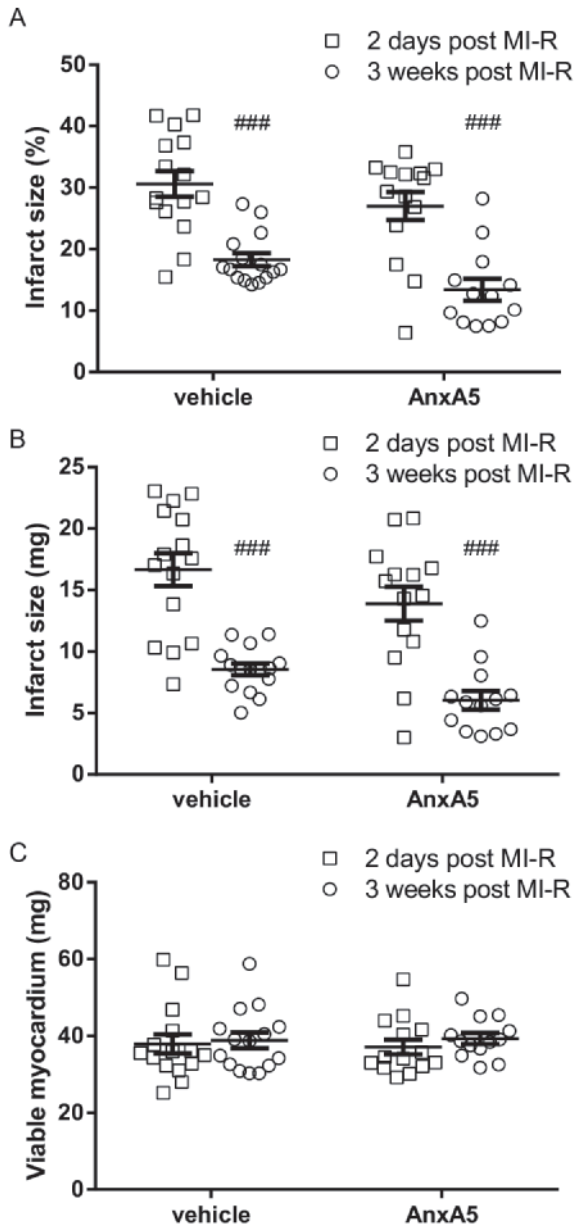
Supplementary figure S1: Absolute numbers contrast-enhanced MR imaging. Three weeks after MI-R IS was significantly smaller in both the vehicle as the AnxA5 group compared to two days after MI-R (A and B). However, viable myocardium remained unchanged in both groups (D). Data are means ± SEM. ###P<0.01 vs. 2 days post MI-R.
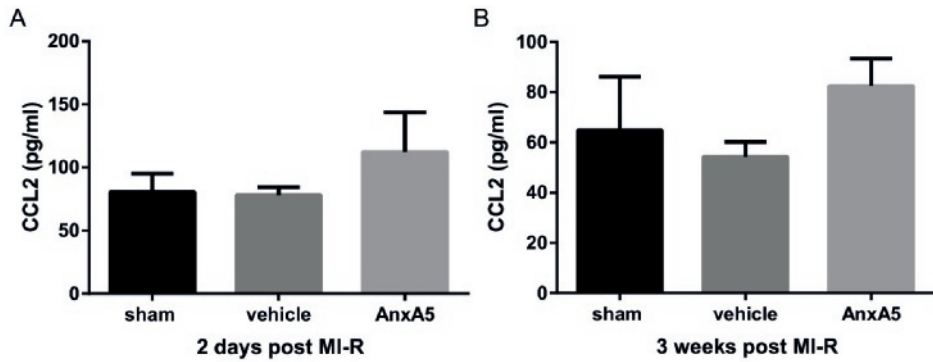
Supplementary figure S2: Serum CCL2 concentrations. Both two days (A) and three weeks (B) post MI-R injury no differences could be observed in serum CCL2 concentrations between all groups.
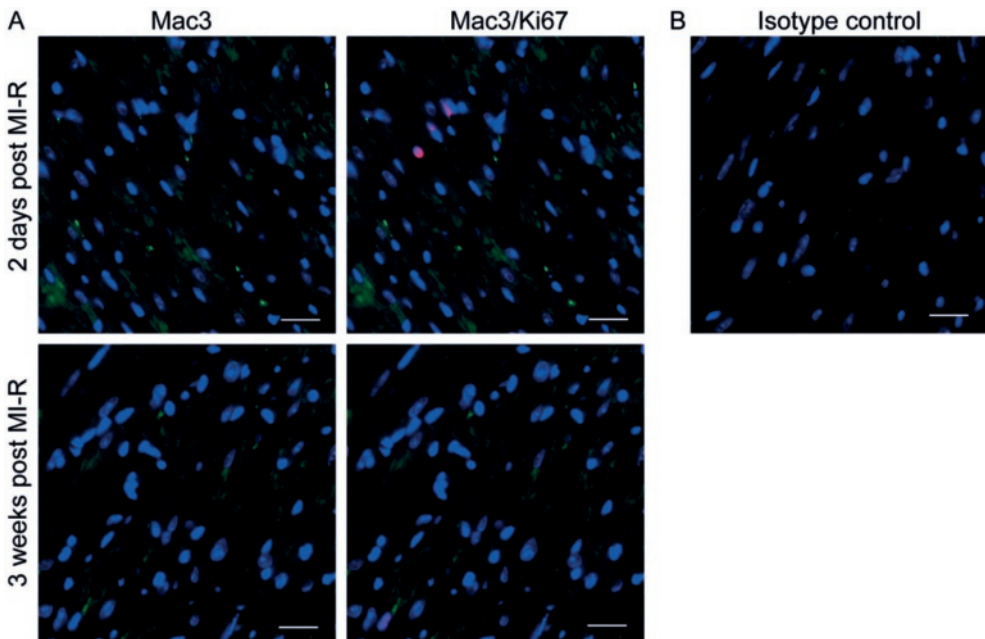
Supplemental figure S3: Representative images of Mac/Ki67 staining. Representative images of Mac3 staining (left) and Mac3/Ki67 double staining (right) of the sham group infarct area (A). Nuclei are shown in blue, Mac3 staining in green and Ki67 in red, arrowheads indicate positive cells. Representative image of isotype control (B). Scale bar: 20 μm.

Chapter 5

The epigenetic factor PCAF regulates vascular inflammation and is essential for intimal hyperplasia development

Rob C. M. de Jong[1,2]

Mark M. Ewing[1,3]

Margreet R. de Vries[1,2]

Jacco C. Karper[1,2]

Antonius J. N. M. Bastiaansen[1,2]

Erna A. B. Peters[1,2]

Fabiana Baghana[1,2]

Peter J. van den Elsen[4,5]

Celine Gongora[5,6]

J. Wouter Jukema[1,3]

Paul H. A. Quax[1,2]

[1]Department of Surgery, Leiden University Medical Center, Leiden, the Netherlands

[2]Einthoven Laboratory for Experimental Vascular Medicine,
Leiden University Medical Center, Leiden, the Netherlands

[3]Department of Cardiology, Leiden University Medical Center, Leiden, the Netherlands

[4]Department of Immunohematology and Blood Transfusion,
Leiden University Medical Center (LUMC), Leiden, The Netherlands

[5]Department of Pathology, VU University Medical Center, Amsterdam, the Netherlands

[6]Université de Montpellier 2, 34095 Montpellier, France,

[7]Institut de Recherche en Cancérologie de Montpellier INSERM U 89, 34298, Montpellier, France

Abstract

Objective Genetic P300/CBP-associated factor (PCAF) variation affects restenosis-risk in patients. PCAF has lysine acetyltransferase activity and promotes nuclear factor kappa-beta (NFκB)-mediated inflammation, which drives post-interventional intimal hyperplasia development. We studied the contributing role of PCAF in post-interventional intimal hyperplasia.

Methods and Results PCAF contribution to inflammation and intimal hyperplasia was assessed in leukocytes, macrophages and vascular smooth muscle cells (vSMCs) in vitro and in a mouse model for intimal hyperplasia, in which a cuff is placed around the femoral artery. PCAF deficiency downregulate CCL2, IL-6 and TNF-alpha expression, as demonstrated on cultured vSMCs, leukocytes and macrophages. PCAF KO mice showed a 71.8% reduction of vSMC-rich intimal hyperplasia, a 73.4% reduction of intima/media ratio and a 63.7% reduction of luminal stenosis after femoral artery cuff placement compared to wild type (WT) mice. The association of PCAF and vascular inflammation was further investigated using the potent natural PCAF inhibitor garcinol. Garcinol treatment reduced CCL2 and TNF-alpha expression, as demonstrated on cultured vSMCs and leukocytes.

To assess the effect of garcinol treatment on vascular inflammation we used hypercholesterolemic ApoE*3-Leiden mice. After cuff placement, garcinol treatment resulted in reduced arterial leukocyte and macrophage adherence and infiltration after three days compared to untreated animals.

Conclusions These results identify a vital role for the lysine acetyltransferase PCAF in the regulation of local inflammation after arterial injury and likely the subsequent vSMC proliferation, responsible for intimal hyperplasia.

Introduction

Percutaneous coronary intervention (PCI) remains the main choice of revascularization therapy for coronary artery disease. However, intimal hyperplasia is a common complication and inflammation plays a pivotal role in its development[1-4]. Despite the introduction of (drug-eluting) stents, this problem remains in part of the patients. Endothelial injury during PCI promotes leukocyte attachment and extravasation[1,3,5]. Subsequently, leukocytes and vascular smooth muscle cells (vSMCs) produce pro-inflammatory cytokines which lead to vSMC migration, proliferation and extracellular matrix formation[1].

Nuclear factor kappa-beta (NFκB) is an important transcription factor which regulates the expression of many inflammatory related genes involved in cardiovascular disease[6]. Gene-environmental interactions that stimulate NFκB expression are regulated by epigenetic factors that strongly modulate gene expression patterns without DNA sequence modification, for example by regulating histone acetylation and de-acetylation[7,8]. Inflammatory gene expression is the result of the counterbalancing and reversible actions of lysine acetyltransferases (KATs) and lysine deacetylases (KDACs), which together determine chromatin structure modification and accessibility to transcription factors[9].

P300/CBP associated factor (PCAF/KAT2B) is a transcriptional co-activator with intrinsic HAT-activity and is involved in lysine acetylation of histones at the site of NFκB-regulated genes[9-11]. Thereby PCAF regulates the NFκB-mediated increase in tumor necrosis factor (TNF)-alpha expression[10] and TNF-alpha regulates the inflammatory response that lead to intimal hyperplasia[12]. Previously, our group found that following hind limb ischemia PCAF-deficient mice differentially express 3505 genes in their adductor muscle group when compared to wild type mice[13]. Furthermore, Huang *et. al.* found that PCAF regulates the expression of inflammatory genes upon renal injury[14].

Previously, association between the -2481C variant allele of the PCAF gene and reduced vascular mortality was shown in three independent large prospective studies[15-17], identifying PCAF as possible diagnostic marker for CHD mortality and restenosis[18]. Increased intravascular Pcaf mRNA levels after injury suggested PCAF involvement in inflammatory-mediated remodelling, although the nature of this elevation remained unexplored[18]. Recently, it has been shown that PCAF expression was increased in abdominal aortic aneurysm tissue when compared to healthy aorta tissue[19].

Few natural inhibitors of PCAF have been described, of which only the natural inhibitor garcinol, derived from the Garcinia Indica fruit rind, has been shown to be extremely potent[20]. It inactivates PCAF activity rapid[21] and has strong apoptosis-inducing effect on leukemia cell lines[22], and also on prostate and pancreatic cancer cells[23] through inhibition of NFκB-DNA binding. These properties make garcinol an extremely potent inhibitor of PCAF-regulated inflammation, although garcinol may be not completely

PCAF specific[24].

In the present study, the well characterized PCAF knock-out mice[25, 26] were used to investigate the contribution of PCAF to the inflammatory response following vascular injury in a reactive intimal hyperplasia mouse model[27,28]. Furthermore, garcinol was used to investigate the effect of pharmaceutical PCAF inhibition on vascular inflammation in a hypercholesterolemic setting.

Materials and Methods

Mice

This study was performed in compliance with Dutch government guidelines and the Directive 2010/63/EU of the European Parliament. All animal experiments were approved by the Institutional Committee for Animal Welfare of the Leiden University Medical Center (approval reference numbers 09094 and 09224). The generation of PCAF knockout (PCAF KO) mice has been described previously[29] and were kindly provided by Dr. C. Gongora. Male C57BL/6 PCAF KO mice and wild type (WT) C57BL/6 controls were used, as were transgenic male ApoE*3-Leiden mice (both bred in our own laboratory), backcrossed for more than 20 generations on a C57BL/6 background. ApoE*3-Leiden (at the start of a dietary run-in period) and WT and PCAF KO mice aged 10-12 weeks, were used for femoral artery cuff experiments.

Diet

PCAF KO and WT mice received chow diet. Transgenic male ApoE*3-Leiden mice were fed a Western-type diet containing 1% cholesterol and 0.05% cholate to induce hypercholesterolemia (AB Diets). The diet was given three weeks prior to surgery and was continued throughout the experiment. All animals received food and water ad libitum during the entire experiment.

Femoral artery cuff mouse model

To investigate the role of PCAF in intimal hyperplasia development, WT and PCAF KO mice underwent a non-constrictive cuff placement around the femoral artery to induce vascular inflammation and remodeling as previously described[27]. Mice were anesthetized before surgery with an i.p. injection of midazolam (8 mg/kg, Roche Diagnostics), medetomidine (0.5 mg/kg, Orion) and fentanyl (0.05 mg/kg, Janssen Pharmaceutica). To investigate short term inflammatory cell influx, cuff placement was performed on hypercholesterolemic ApoE*3-Leiden mice treated with garcinol or vehicle.

After 21 days (WT and PCAF KO mice) or after 3 days (ApoE*3-Leiden mice) mice were anesthetized as before and sacrificed via perfusion. The thorax was opened and pressure-perfusion (100mm Hg) with PBS was performed for 3 minutes by cardiac puncture of

the left ventricle. After perfusion with 3.7% formaldehyde the cuffed femoral arteries were harvested, fixed for 5 hours in formaldehyde and paraffin-embedded.

In vivo garcinol treatment

During non-constrictive cuff placement, ApoE*3-Leiden mice were treated with 10 µl pluronic gel F127 (40%, maintained at 0°C, Sigma Aldrich) ± 25 mg/ml garcinol (Enzo Life Sciences). In this way, garcinol was slowly released over a period of a couple of days at the site of injury. The pluronic gel with or without garcinol was lubricated around the isolated femoral artery and was allowed to harden out and settle around the cuff, which occurred within 20 seconds after application.

Plasma analysis and ELISA

Total plasma cholesterol concentration (Roche Diagnostics, kit 1489437) was measured enzymatically. Inflammatory cytokine concentration of chemokine (C-C motif) ligand 2 (CCL2), interleukin-6 (IL-6) and TNF-alpha were determined using ELISA kits (555260, 555240 and 558534, Becton Dickinson), according to the manufacturer's instructions.

(Immuno)histochemistry (IHC)

To detect the presence of inflammatory cells, vessel wall characteristics and effects of garcinol therapy, IHC was performed on paraffin-embedded sections of cuffs harvested after 3 days (ApoE*3-Leiden) or 21 days respectively (PCAF KO and WT mice). Weigert's elastin staining was used to visualize elastic laminae. Inflammatory cell presence in the vascular wall was visualized using antibodies against leukocytes (anti-CD45 clone 30-F11, BD Pharmingen) and macrophages (anti-Mac3 clone M3/84, BD Pharmingen). Vascular SMCs were stained using anti-smooth muscle actin (SMA, clone 1A4, Dako) antibodies, PCAF was stained using anti-PCAF (ab12188, Abcam) antibodies and CCL2 was stained using anti-CCL2 (clone M-18, Santa Cruz) antibodies.

Morphometric analysis

All quantifications in this study were performed on six equally spaced serial stained perpendicular cross-sections throughout the entire length of the vessel, as described previously[30]. Using image analysis software (Qwin, Leica), total cross-sectional medial area (between both elastic laminae), neointimal area (between internal elastic lamina and lumen) and luminal area was measured. These values were used to calculate the intima / media ratio and percentage luminal stenosis. In the short term study (3 days) the number of leukocytes, macrophages and CCL2 positive cells and after 21 days in PCAF KO vs. WT macrophages were counted manually and expressed as a percentage of the total number of cells (stained with hematoxylin). CCL2 and vSMC content after 21 days is analyzed using Qwin and CCL2 is expressed as the percentage of total medial and intimal area stained positive for CCL2. Vascular SMC content is expressed as both the

percentage and the area (µm2) of total medial and intimal area stained positive for SMA.

In vitro immune response

Whole blood-derived leukocytes:

Blood was drawn from PCAF KO and WT mice via tail vein bleeding. The blood was diluted 1:25 with RPMI 1640 (Invitrogen) supplemented with 1% penicillin/streptomycin (Invitrogen). Blood was incubated in the presence and absence of lipopolysaccharide (LPS) from Escherichia coli K-235 L2018 (Sigma Aldrich) alone or together with garcinol. The cells were incubated overnight at 37°C in 5% CO_2 atmosphere. After 24 hours incubation the supernatants were collected and analyzed by ELISA.

Vascular smooth muscle cells:

Murine aortas were harvested from PCAF KO and WT mice. The aortas were cut longitudinally to expose the luminal side. The endothelial cells were removed by gently scraping. The aortas were cut in small pieces and placed on gelatin-coated culture dishes. The explants were cultured in DMEM (PAA laboratories) containing 20% FCS heat-inactivated (Lonza), 1% penicillin/streptomycin (Invitrogen) and 1% NEAA (PAA laboratories). Cells were cultured and used for experiments at passages 2 to 4. It should be noted that, by using this method, SMA positive myofibroblasts may be isolated as well. To evaluate the effects of inflammation on inflammatory cytokine expression, confluent layers of vSMC were seeded out in DMEM supplemented with 8% FCS heat-inactivated and 1% penicillin/streptomycin and cultured for 24 hours. Vascular SMCs were stimulated by exposure to 8% FCS heat-inactivated in the presence and absence of LPS alone or together with garcinol. The cells were incubated overnight at 37°C in 5% CO_2 atmosphere. After 24 hours incubation the supernatants were collected and analyzed by ELISA.

Pcaf silencing in vSMCs:

Vascular SMCs were transfected using Lipofectamine 2000 (Invitrogen) according to the manufacturer's instructions with control short-interfering RNA (scrambled siRNA; Qiagen) or a combination of 4 siRNAs directed towards *Pcaf* (Qiagen) for 4 hours. Subsequently vSMCs were stimulated with LPS (1 ng/ml) for 24 hours and supernatants were collected and analyzed by ELISA. To confirm *Pcaf* knockdown, qPCR was used to analyze *Pcaf* expression. RNA was isolated using RNeasy minikits (Qiagen) and qPCR was performed on ABI7500 Fast system using Taqman gene expression assays for *Hprt1* and *Pcaf*.

Bone-marrow derived macrophages:

Bone-marrow (BM) derived cells were isolated from PCAF KO and WT mice and subjected to murine macrophage colony-stimulating factor (M-CSF) (20 ng/µl; Miltenyi

Biotec) to stimulate differentiation into macrophages.

Macrophages were stimulated by exposure to 8% FCS heat-inactivated in the presence and absence LPS alone or together with garcinol. The cells were incubated overnight at 37°C in 5% CO_2 atmosphere. After 24 hours incubation the supernatants were collected and analyzed by ELISA.

Cell viability assay

Since garcinol can affect cellular viability in high concentrations due to aspecific effects, garcinol-induced apoptosis in ex vivo whole blood was assessed in heparinized venous whole blood drawn from WT mice. Blood was diluted 1:25 in RPMI together with (0, 2.5, 10, 15, 20, 30, 50, 100 or 250 µM) garcinol for 24h at 37°C in 5% CO_2 atmosphere. After 24h incubation, red blood cells were lysed and the medium was refreshed with RPMI supplemented with 8% FCS and 10% (vol/vol) Alamar blue (Invitrogen). The optical density of each well was measured in a Millipore CytoFluor 2300 plate-reading Fluor meter with excitation at 560 nm and emission at 615 nm when medium in untreated samples turned pink (±4h). Cell viability (%) was calculated compared with positive (untreated) control cells.

Statistical analysis

Data are expressed as mean ± SEM. Two-tailed Student's t-tests were used to compare groups. A level of $P<0.05$ was considered significant.

Results

PCAF deficiency leads to reduced inflammatory cytokine production *in vitro*

To investigate whether PCAF has a specific effect on cytokine production, we determined the effect of PCAF deficiency on inflammatory cytokine production *in vitro*. TNF-alpha production in whole blood derived leukocytes of PCAF KO mice was significantly reduced 24 hours after stimulation with LPS, when compared to whole blood derived leukocytes of WT mice (Fig 1A). Also in PCAF KO BM derived macrophages TNF-alpha production reduced compared to WT macrophages upon LPS stimulation although not significantly (Figure 1B), whereas IL-6 production was significantly reduced after stimulation with 31.25 and 62.5 ng/ml LPS (Fig 1C). CCL2 production of PCAF KO compared to WT vSMCs was already reduced without LPS stimulation (Fig 1D). This reduction was even bigger after stimulation with 0.1 and 1 ng/ml LPS.

Intimal hyperplasia is reduced in PCAF KO mice

To confirm PCAF deficiency of our PCAF KO mice we performed an immunohistochemical staining using specific anti-PCAF antibodies. As can be observed in Fig 2A, clear PCAF
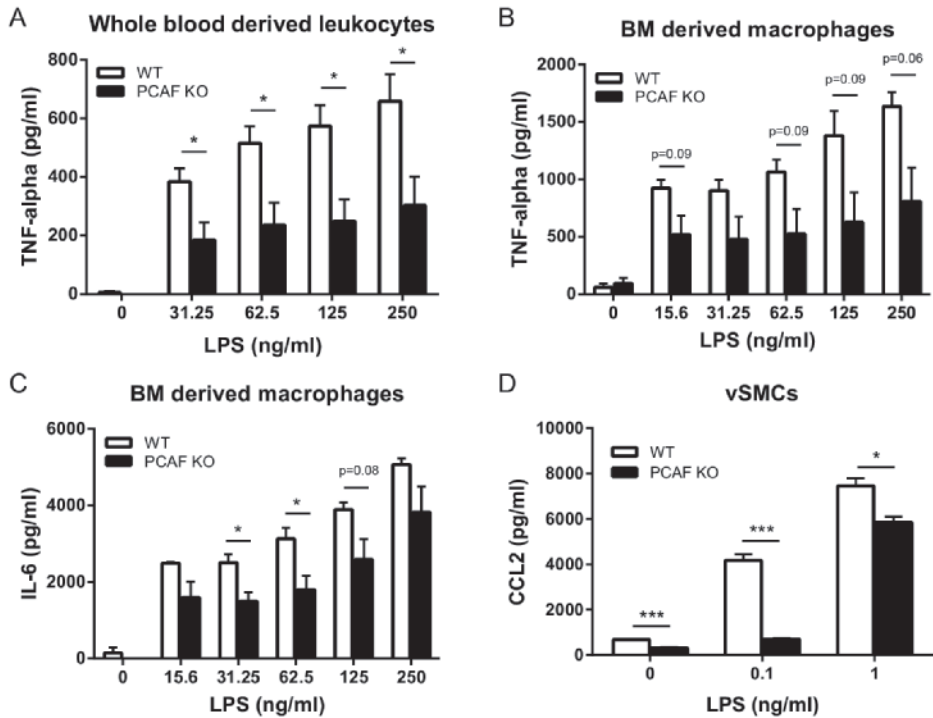
Figure 1. Effect of PCAF deficiency on inflammatory cytokine expression in vitro. (A) TNF-alpha production of whole blood derived leukocytes (n=5) from WT and PCAF KO mice 24 hours after LPS (0-250 ng/ml) stimulation. *$P<0.05$. TNF-alpha(B) and IL-6 (C) production of bone marrow derived macrophages (n=3) from WT and PCAF KO mice 24 hours after LPS (0-250 ng/ml) stimulation. *$P<0.05$. (D) CCL2 production of vascular smooth muscle cells (n=3) from WT and PCAF KO mice 24 hours after LPS (0-1 ng/ml) stimulation. *$P<0.05$, ***$P<0.001$. Results are mean±SEM.

staining is present in the femoral artery segments of WT mice, while it is completely absent in the PCAF KO mice. Having shown a reduction of inflammatory cytokine production in PCAF deficient cells in vitro, we next demonstrated the effect of PCAF deficiency on intimal hyperplasia of cuffed femoral artery segments of C57Bl/6 control and PCAF KO mice using Weigert's elastin staining. Quantitative analysis revealed a significant reduction of intimal hyperplasia of 71.8% in PCAF KO mice when compared to WT mice (Figs 2B and E). Since the media area was comparable between groups, this was accompanied by a significantly reduced intima/media ratio by 73.4% (Figure 2C) and luminal stenosis by 63.7% after 21 days (Fig 2D).

The lesion of both the WT as the PCAF KO mice mainly consists of vSMCs as can be observed in Fig 2H. Total area of intimal SMA expressing cells was significantly decreased in PCAF KO mice compared to WT mice (Fig 2F), whereas total area of the medial SMA expressing cells was not affected (Fig 2G). To exclude a difference in vSMC content at baseline, uncuffed arteries of both the WT and PCAF KO mice were stained for
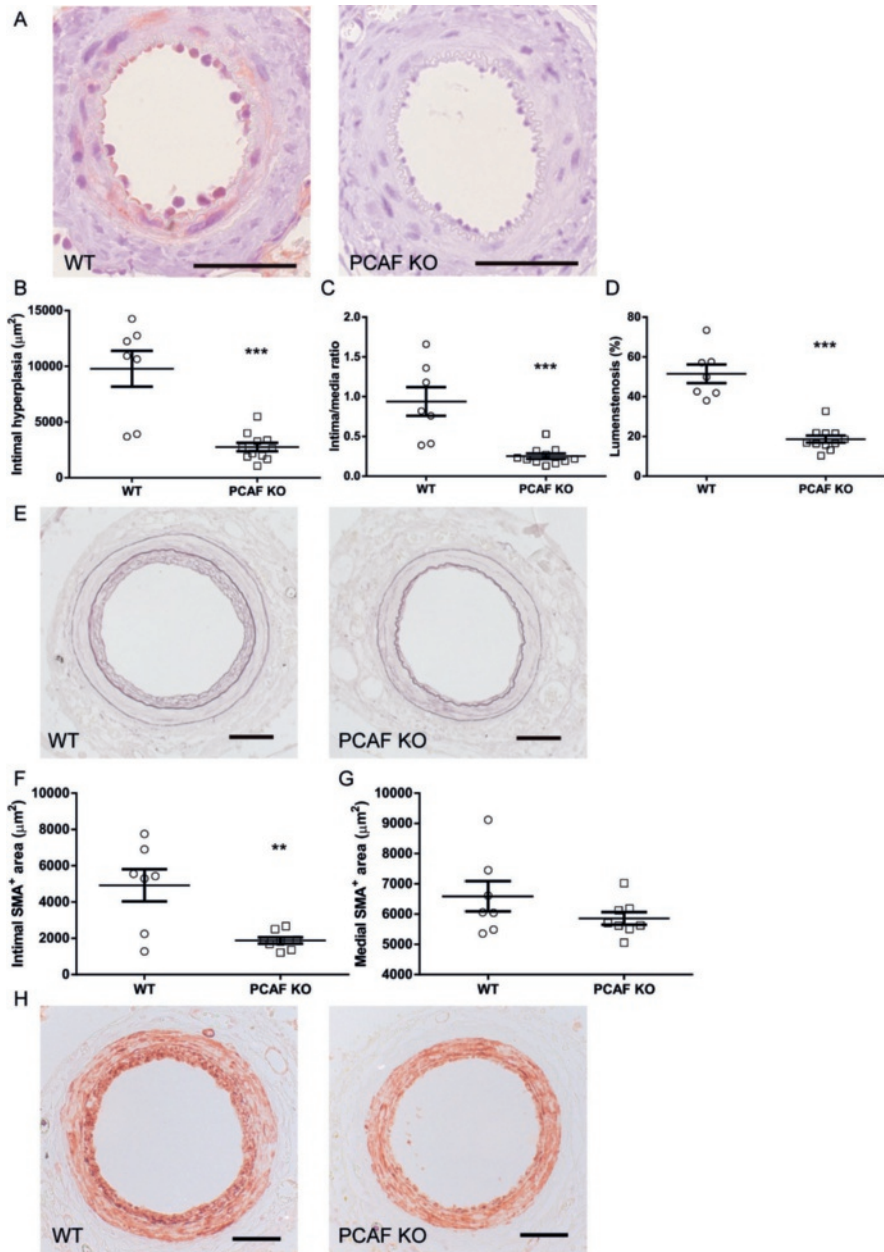
Figure 2. Effect of PCAF deficiency on intimal hyperplasia and vascular smooth muscle cell content *in vivo*. Representative images of PCAF staining (A), scale bar = 100 μm. Quantification of intimal hyperplasia (B), intima/media ratio (C) and lumenstenosis (D) 21 days after cuff placement in WT (n=7) and PCAF KO (n=11) mice. ***$P<0.001$. Representative images of elastin staining (E), scale bar = 50 μm. Quantification intimal (F) and medial (G) smooth muscle cell area (μm2) 21 days after cuff placement in WT (n=7) and PCAF KO (n=8) mice. **$P<0.01$. (H) Representative images of smooth muscle actin (SMA) staining of cuffed femoral arteries, scale bar = 50 μm. Results are mean±SEM.

SMA, and no difference in vSMC content was observed (S1 Fig 1A). The reduced vSMC accumulation in the intima suggests a reduced vSMC migration and/or proliferation in PCAF KO mice. However, the number of Ki67 positive vSMCs was not reduced in both de media (S1 Fig 1B) and intima (S1 Fig 1C) in PCAF KO mice when compared to WT mice. We believe this is due to the time point of 21 days, which might be too late to analyze vSMC proliferation.
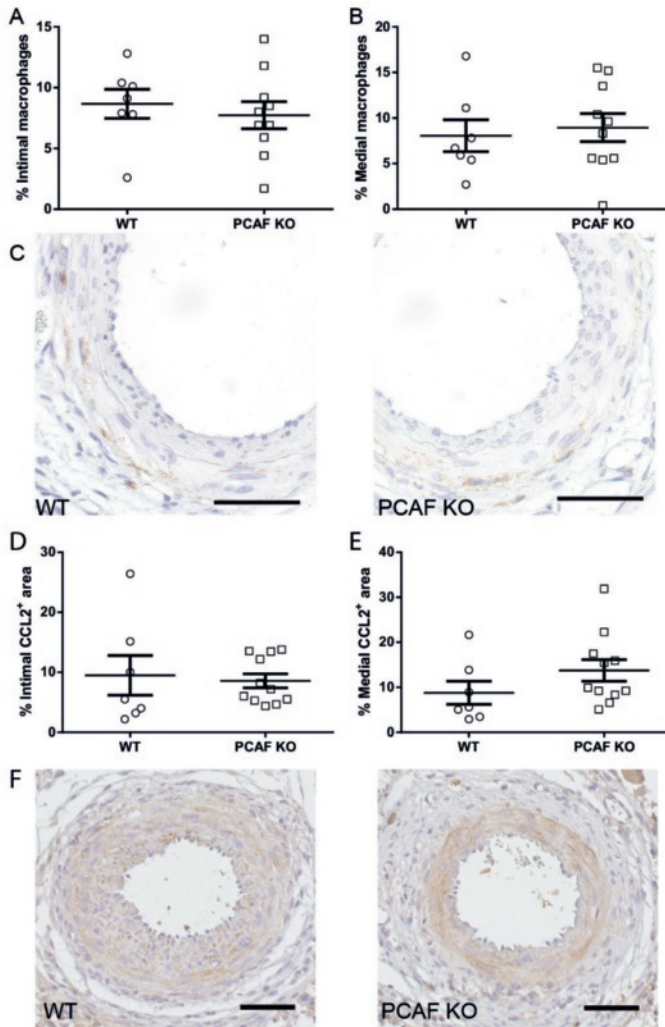
Figure 3. Effect of PCAF deficiency on macrophage influx and CCL2 expression *in vivo*. Quantification of Mac3 positive cells (macrophages) in the intima (A) and media (B) 21 days after cuff placement in WT (n=7) and PCAF KO (n=11) mice. Representative images of Mac3 staining (C), scale bar = 50 μm. Quantification of CCL2 positive area in the intima (D) and media (E) 21 days after cuff placement in WT (n=7) and PCAF KO (n=11) mice. Representative images of CCL2 staining (F), scale bar = 50 μm. Results are mean±SEM.

PCAF deficiency does not lead to reduced macrophage influx and CCL2 expression after 21 days

Next, we investigated the effect of PCAF deficiency on macrophage influx and CCL2 expression. The percentage of intimal and medial macrophages was not affected in PCAF KO mice compared to WT mice (Figs 3 A-C). The percentage of intimal and medial CCL2 expressing cells was also not affected by PCAF deficiency (Figs 3 D-F). Furthermore, medial and intimal TNF-alpha expression was not affected in PCAF KO mice compared to WT mice (S1 Fig 1D).

The inflammatory response following vascular injury is a process that mainly takes place the first couple of days after injury[31]. Analysis of the inflammatory response at 21 days after cuff placement may be too late. Therefore, we investigated the short term inflammatory response using the pharmalogical PCAF inhibitor garcinol, in hypercholesterolemic ApoE*3-Leiden mice, in which the inflammatory response is more explicit.

Garcinol inhibits inflammatory cytokine production *in vitro*

First, we studied the effect of garcinol (0-20 µM) on TNF-alpha production of whole blood derived leukocytes stimulated with LPS (100 ng/ml). TNF-alpha production was significantly reduced when treated with 5 and 10 µM garcinol compared to vehicle (Fig 4A) and TNF-alpha production was totally abolished when treated with 20 µM garcinol. CCL2 production of vSMCs was reduced by 19.2% after LPS stimulation (1 ng/ml) in combination with garcinol treatment (15 µM) compared to vehicle (Fig 4B), but not when treated with lower concentrations of garcinol.

To study possible toxic effects of garcinol, we studied the viability of circulating leukocytes (whole blood) in the presence of garcinol (0-250 µM) using the redox indicator Alamar blue. Fluorescence intensity (FI) remained constant at ~5700 AU (615 nm) at garcinol concentrations 0-20 µM, indicating complete cellular viability comparable to positive controls (Fig 4C), with cytotoxicity at concentrations ≥30 µM (FI: ~900 AU). Furthermore, we used a MTT assay to study the possible toxic effects of garcinol on vSMCs, no detrimental effects of garcinol were found in concentrations range up to 20 µM (S1 Fig 2).

To exclude non-specific effects of garcinol treatment on vSMCs, we transfected vSMCs with specific *Pcaf* siRNAs to induce *Pcaf* knockdown. After transfection qPCR analysis revealed a significant knockdown of *Pcaf* (Fig 4D). CCL2 production was reduced by 25.6% following siRNA-mediated *Pcaf* knockdown compared to vSMCs transfected with a non-specific scrambled siRNA (Fig 4E), suggesting similar effects as observed after garcinol treatment. Moreover, we stimulated PCAF KO VSMCs simultaneously with LPS and 15 µM garcinol or vehicle and measured CCL2 production and no difference in CCL2 production is observed between both groups (S1 Fig 3). This again suggests that garcinol is, at least in the concentration range we use, specific for garcinol.
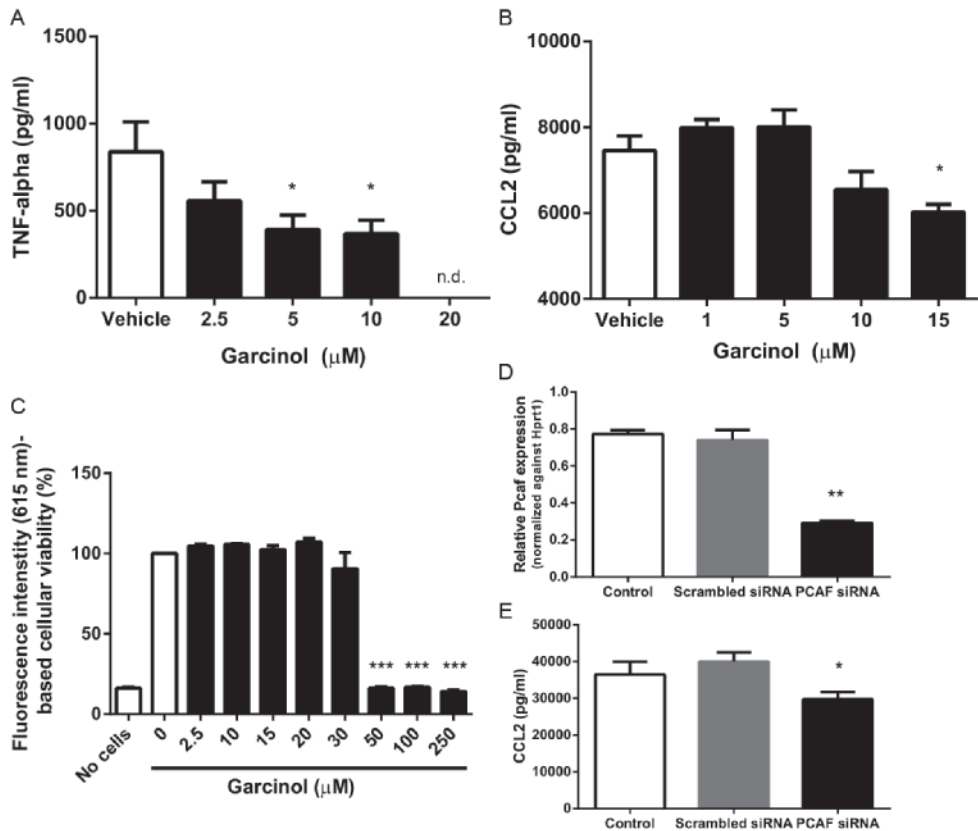
Figure 4. Effect of garcinol treatment and PCAF downregulation on inflammatory cytokine expression *in vitro*. (A) TNF-alpha production of whole blood derived leukocytes (n=5) after 24 hours stimulation with LPS (100 ng/ml) in combination with garcinol (0-20 μM). *$P<0.05$ compared to vehicle (0 μM garcinol), n.d.: non-detectable. (B) CCL2 production of vascular smooth muscle cells (n=3) after 24 hours stimulation with LPS (1 ng/ml) in combination with garcinol (0-15 μM). *$P<0.05$ compared to vehicle (0 μM garcinol). (C) Whole blood derived leukocyte viability (n=4) after 24 hours incubation with garcinol (0-250 μM), expressed as percentage fluorescence intensity. ***$P<0.001$ compared to 0 μM garcinol. (D) Relative *Pcaf* expression of vascular smooth muscle cells (n=3) transfected with scrambled or PCAF siRNA and stimulated with 1 ng/ml for 24 hours. **$P<0.01$ compared to scrambled siRNA. (E) CCL2 production of vascular smooth muscle cells (n=3) transfected with scrambled or PCAF siRNA and stimulated with 1 ng/ml for 24 hours. *$P<0.05$ compared to scrambled siRNA. Results are mean±SEM.

Pharmacological PCAF inhibition reduces injury-induced leukocyte recruitment in vivo

Since garcinol reduces cytokine production in vitro, we treated hypercholesterolemic ApoE*3-Leiden mice with garcinol and investigated leukocyte infiltration 3 days after cuff placement. Short term garcinol treatment significantly reduced intimal leukocytes by 62.2% and medial leukocytes by 60.7% (Fig 5A) after 3 days. Since most of the

leukocytes associated with the vessel wall are of the macrophage subtype, we also quantified these specifically. Intimal macrophages were reduced by 54.8% whereas medial macrophages were reduced by 84.5% compared to the pluronic gel control group (Fig 5B). Next, we studied the effect of garcinol on CCL2 expression, an important chemokine involved in attracting macrophages to sites of injury. Short term garcinol treatment reduced the percentage of cells in the intima that expressed CCL2 by 65.0% and of cells in the media by 57.0% (Fig 5C), suggesting that garcinol reduced leukocyte infiltration by affecting chemo-attracting factors.
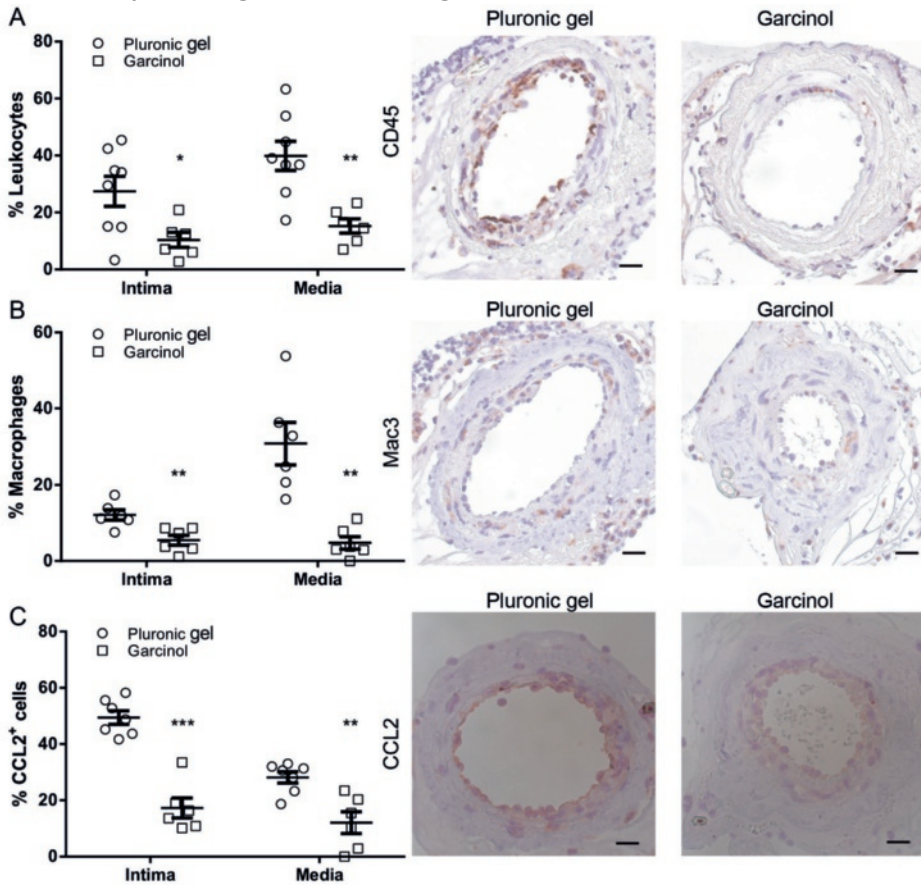
Figure 5. Effect of garcinol treatment on inflammatory cell recruitment and CCL2 expression *in vivo*.
(A) Quantification of CD45 positive cells (leukocytes) in the intima and media 3 days after cuff placement in ApoE*3-Leiden mice treated with garcinol (n=6) or pluronic gel (n=8). *$P<0.05$, **$P<0.01$. (B) Quantification of Mac3 positive cells (macrophages) in the intima and media 3 days after cuff placement in ApoE*3-Leiden mice treated with garcinol (n=6) or pluronic gel (n=6). **$P<0.01$. (C) Quantification of CCL2 positive cells in the intima and media 3 days after cuff placement in ApoE*3-Leiden mice treated with garcinol (n=6) or pluronic gel (n=7). **$P<0.01$, ***$P<0.001$. Representative images of CD45, Mac3 and CCL2 staining of cuffed femoral arteries, scale bar = 20 μm. Results are mean±SEM.

Discussion

In this study we demonstrate that PCAF deficiency reduces the *in vitro* inflammatory response and reduces development of vSMC-rich intimal hyperplasia *in vivo*. The natural PCAF inhibitor garcinol reduces the inflammatory response *in vitro*. Furthermore, we demonstrate that garcinol treatment reduces short term (3 days) leukocyte infiltration and CCL2 expression *in vivo*, following vascular injury in hypercholesterolemic apoE*3-Leiden mice. To our knowledge, this is the first paper to show that PCAF has a contributing role in intimal hyperplasia development, by regulating the inflammatory response and perhaps reducing the subsequent vSMC proliferation.

We used PCAF KO mice to demonstrate clear effects of PCAF deficiency on inflammatory-regulated intimal hyperplasia. Animals developed significantly smaller vSMC-rich lesions with reduced lumenstenosis. PCAF KO cells were used to demonstrate its essential contribution in the production of pro-inflammatory cytokines (CCL2, IL-6 and TNF-alpha) by various cell types including whole blood-derived leukocytes, BM derived macrophages and vSMCs. These results demonstrate an important role for the epigenetic factor PCAF in the post-interventional arterial inflammatory response.

TNF-alpha production was severely compromised in whole blood-derived leukocytes from PCAF deficient animals and in WT whole blood derived leukocytes treated with garcinol. In BM derived macrophages TNF-alpha production was also decreased, although not significantly. Previously it has been shown that lack of TNF-alpha in mice reduces intimal hyperplasia development[12, 32]. TNF-alpha production is regulated by NFκB[6] and PCAF is an important co-activator of NFκB[10]. Therefore, it is likely that the reduced intimal hyperplasia development in PCAF KO mice is, at least in part, caused by reduced TNF-alpha production.

IL-6 production in BM-derived macrophages was significantly decreased in PCAF KO macrophages compared to WT macrophages. Macrophages play an important role in vascular inflammation and one of the cytokines macrophages produce during vascular inflammation is IL-6[33]. Furthermore, it has been shown that IL-6 recruits bone marrow cells to the vessel wall and thereby contributes to intimal hyperplasia[34]. Niida *et al.* showed that nuclear factor of kappa light polypeptide gene enhancer in B-cells inhibitor, delta (IκBNS) inhibits NFκB activity and IL-6 production in a mouse model for restenosis, subsequently leading to reduced intimal hyperplasia development[35]. Since PCAF is a coactivator of NFκB, and thus regulates IL-6 production, it is plausible that the reduced intimal hyperplasia is in part due to reduced IL-6 production.

PCAF deficiency led to reduced CCL2 production in vSMCs *in vitro*. These results were similar in wildtype cells treated with garcinol or subjected to siRNA mediated PCAF knockdown. Furthermore, garcinol treatment reduced CCL2 expression *in vivo* following vascular injury. Previous studies have shown that CCL2 plays an important role in the development of intimal hyperplasia, by regulation of the inflammatory response and

vSMC proliferation[36-38]. In agreement, we found a reduced vSMC-rich intimal lesion size in PCAF KO mice compared to WT mice, which may indicate reduced vSMC proliferation. It is plausible that the effect of PCAF deficiency on CCL2 production is in part responsible for the reduced intimal hyperplasia development. Whether PCAF deficiency acts directly on vSMC proliferation or indirectly via inflammation or a combination of both, remains to be investigated.

Although we found a reduction in inflammatory cytokine production *in vitro* and reduced intimal hyperplasia development upon PCAF deficiency, we could not show a reduction in macrophage influx and CCL2 expression *in vivo*. Most likely this is due to the non-optimal time point to evaluate macrophage influx and CCL2 expression in PCAF KO mice. To overcome this problem we repeated the experiment and evaluated vascular inflammation at an earlier time point in a mouse model in which vascular inflammation is more profound, namely hypercholesterolemic ApoE*3-Leiden mice. Moreover, most patients suffering from coronary artery disease experience elevated cholesterol levels or hypercholesterolemia, which is an well-known risk factor for cardiovascular disease in human[39]. Therefore, we studied the effect of garcinol treatment in hypercholesterolemic ApoE*3-Leiden mice, mimicking the clinical situation regarding cholesterols levels. We found reduced leukocyte infiltration and CCL2 expression 3 days after cuff placement in hypercholesterolemic mice treated with garcinol. These results suggest that PCAF inhibition by garcinol reduces vascular inflammation in a clinical relevant mouse model. One should keep in mind that garcinol could affect other *in vivo* targets next to PCAF, like cyclooxygenase-2 (COX-2)[40], 5-lipoxygenase (5-Lox)[41] and others[24], that might contribute to the observed anti-inflammatory effect of garcinol in our study.

PCAF is involved in regulation of NFκB-mediated transcription of inflammatory genes in two different ways. First, PCAF is capable of acetylation of histone proteins at the site of NFκB-regulated genes, making the DNA at that specific site more accessible for NFκB. Second, PCAF is able to acetylate lysine residues on the p65 unit of NFκB itself, increasing its binding to the DNA[9]. Both mechanisms lead to an increase in transcription of pro-inflammatory genes, like CCL2, TNF-alpha and IL-6. We believe that both these mechanisms are affected in the PCAF KO mice and following garcinol treatment, leading to a decreased expression of pro-inflammatory genes and subsequently attenuation of intimal hyperplasia.

In conclusion, using PCAF KO mice, evidence is provided that PCAF contributes to post-interventional intimal hyperplasia. This could be explained by an as yet uncharacterized direct or indirect effect of PCAF on inflammation and vSMC proliferation, leading to reduced post-interventional intimal hyperplasia. These results shed light on the possible contribution of PCAF as an important epigenetic factor in intimal hyperplasia development in human coronary lesions and identify it as a possible new clinical target against intimal hyperplasia after PCI.

References

1.   Lee MS, David EM, Makkar RR, Wilentz JR. Molecular and cellular basis of restenosis after percutaneous coronary intervention: the intertwining roles of platelets, leukocytes, and the coagulation-fibrinolysis system. The Journal of pathology. 2004;203(4):861-70.

2.   Pires NM, Jukema JW, Daemen MJ, Quax PH. Drug-eluting stents studies in mice: do we need atherosclerosis to study restenosis? Vascular pharmacology. 2006;44(5):257-64.

3.   Pons D, Monraats PS, de Maat MP, Pires NM, Quax PH, van Vlijmen BJ, et al. The influence of established genetic variation in the haemostatic system on clinical restenosis after percutaneous coronary interventions. Thrombosis and haemostasis. 2007;98(6):1323-8.

4.   Simsekyilmaz S, Liehn EA, Militaru C, Vogt F. Progress in interventional cardiology: challenges for the future. Thrombosis and haemostasis. 2015;113(3):464-72.

5.   Hansson GK. Inflammation, atherosclerosis, and coronary artery disease. The New England journal of medicine. 2005;352(16):1685-95.

6.   Van der Heiden K, Cuhlmann S, Luong le A, Zakkar M, Evans PC. Role of nuclear factor kappaB in cardiovascular health and disease. Clinical science (London, England : 1979). 2010;118(10):593-605.

7.   Barnes PJ, Karin M. Nuclear factor-kappaB: a pivotal transcription factor in chronic inflammatory diseases. The New England journal of medicine. 1997;336(15):1066-71.

8.   Vermeulen L, De Wilde G, Notebaert S, Vanden Berghe W, Haegeman G. Regulation of the transcriptional activity of the nuclear factor-kappaB p65 subunit. Biochemical pharmacology. 2002;64(5-6):963-70.

9.   Pons D, de Vries FR, van den Elsen PJ, Heijmans BT, Quax PH, Jukema JW. Epigenetic histone acetylation modifiers in vascular remodelling: new targets for therapy in cardiovascular disease. European heart journal. 2009;30(3):266-77.

10.   Miao F, Gonzalo IG, Lanting L, Natarajan R. In vivo chromatin remodeling events leading to inflammatory gene transcription under diabetic conditions. The Journal of biological chemistry. 2004;279(17):18091-7.

11.   Sheppard KA, Rose DW, Haque ZK, Kurokawa R, McInerney E, Westin S, et al. Transcriptional activation by NF-kappaB requires multiple coactivators. Molecular and cellular biology. 1999;19(9):6367-78.

12.   Monraats PS, Pires NM, Schepers A, Agema WR, Boesten LS, de Vries MR, et al. Tumor necrosis factor-alpha plays an important role in restenosis development. FASEB journal : official publication of the Federation of American Societies for Experimental Biology. 2005;19(14):1998-2004.

13.   Bastiaansen AJ, Ewing MM, de Boer HC, van der Pouw Kraan TC, de Vries MR, Peters EA, et al. Lysine acetyltransferase PCAF is a key regulator of arteriogenesis. Arteriosclerosis, thrombosis, and vascular biology. 2013;33(8):1902-10.

14.   Huang J, Wan D, Li J, Chen H, Huang K, Zheng L. Histone acetyltransferase PCAF regulates inflammatory molecules in the development of renal injury. Epigenetics. 2015;10(1):62-72.

15.   Monraats PS, Pires NM, Agema WR, Zwinderman AH, Schepers A, de Maat MP, et al. Genetic inflammatory factors predict restenosis after percutaneous coronary interventions. Circulation. 2005;112(16):2417-25.

16.   Shepherd J, Cobbe SM, Ford I, Isles CG, Lorimer AR, MacFarlane PW, et al. Prevention of coronary heart disease with pravastatin in men with hypercholesterolemia. West of Scotland Coronary Prevention Study Group. The New England journal of medicine. 1995;333(20):1301-7.

17.   Shepherd J, Blauw GJ, Murphy MB, Bollen EL, Buckley BM, Cobbe SM, et al. Pravastatin in elderly individuals at risk of vascular disease (PROSPER): a randomised controlled trial. Lancet (London, England). 2002;360(9346):1623-30.

18.   Pons D, Trompet S, de Craen AJ, Thijssen PE, Quax PH, de Vries MR, et al. Genetic variation in PCAF, a key mediator in epigenetics, is associated with reduced vascular morbidity and mortality: evidence for a new concept from three independent prospective studies. Heart (British Cardiac Society). 2011;97(2):143-50.

19.   Han Y, Tanios F, Reeps C, Zhang J, Schwamborn K, Eckstein HH, et al. Histone acetylation and histone acetyltransferases show significant alterations in human abdominal aortic aneurysm. Clinical epigenetics. 2016;8:3.

20.   Balasubramanyam K, Altaf M, Varier RA, Swaminathan V, Ravindran A, Sadhale PP, et al. Polyisoprenylated benzophenone, garcinol, a natural histone acetyltransferase inhibitor, represses chromatin transcription and alters global gene expression. The Journal of biological chemistry. 2004;279(32):33716-26.

21.   Arif M, Pradhan SK, Thanuja GR, Vedamurthy BM, Agrawal S, Dasgupta D, et al. Mechanism of p300 specific histone acetyltransferase inhibition by small molecules. Journal of medicinal chemistry. 2009;52(2):267-77.

22.   Matsumoto K, Akao Y, Kobayashi E, Ito T, Ohguchi K, Tanaka T, et al. Cytotoxic benzophenone derivatives from Garcinia species display a strong apoptosis-inducing effect against human leukemia cell lines. Biological & pharmaceutical bulletin. 2003;26(4):569-71.

23.   Ahmad A, Wang Z, Wojewoda C, Ali R, Kong D, Maitah MY, et al. Garcinol-induced apoptosis in prostate and pancreatic cancer cells is mediated by NF- kappaB signaling. Frontiers in bioscience (Elite edition). 2011;3:1483-92.

24.   Liu C, Ho PC, Wong FC, Sethi G, Wang LZ, Goh BC. Garcinol: Current status of its anti-oxidative, anti-inflammatory and anti-cancer effects. Cancer letters. 2015;362(1):8-14.

25.   Duclot F, Jacquet C, Gongora C, Maurice T. Alteration of working memory but not in anxiety or stress response in p300/CBP associated factor (PCAF) histone acetylase knockout mice bred on a C57BL/6 background. Neuroscience letters. 2010;475(3):179-83.

26.   Duclot F, Meffre J, Jacquet C, Gongora C, Maurice T. Mice knock out for the histone acetyltransferase p300/CREB binding protein-associated factor develop a resistance to amyloid toxicity. Neuroscience. 2010;167(3):850-63.

27.   de Vries MR, Seghers L, van Bergen J, Peters HA, de Jong RC, Hamming JF, et al. C57BL/6 NK cell gene complex is crucially involved in vascular remodeling. Journal of molecular and cellular cardiology. 2013;64:51-8.

28.   Lardenoye JH, Delsing DJ, de Vries MR, Deckers MM, Princen HM, Havekes LM, et al. Accelerated atherosclerosis by placement of a perivascular cuff and a cholesterol-rich diet in ApoE*3Leiden transgenic mice. Circulation research. 2000;87(3):248-53.

29.   Yamauchi T, Yamauchi J, Kuwata T, Tamura T, Yamashita T, Bae N, et al. Distinct but overlapping roles of histone acetylase PCAF and of the closely related PCAF-B/GCN5 in mouse embryogenesis. Proceedings of the National Academy of Sciences of the United States of America. 2000;97(21):11303-6.

30.   Ewing MM, Karper JC, Abdul S, de Jong RC, Peters HA, de Vries MR, et al. T-cell co-stimulation by CD28-CD80/86 and its negative regulator CTLA-4 strongly influence accelerated atherosclerosis development. International journal of cardiology. 2013;168(3):1965-74.

31.   Simon DI. Inflammation and vascular injury: basic discovery to drug development. Circulation journal : official journal of the Japanese Circulation Society. 2012;76(8):1811-8.

32.   Zimmerman MA, Selzman CH, Reznikov LL, Miller SA, Raeburn CD, Emmick J, et al. Lack of TNF-alpha attenuates intimal hyperplasia after mouse carotid artery injury. American journal of physiology Regulatory, integrative and comparative physiology. 2002;283(2):R505-12.

33.   Shirai T, Hilhorst M, Harrison DG, Goronzy JJ, Weyand CM. Macrophages in vascular inflammation--From atherosclerosis to vasculitis. Autoimmunity. 2015;48(3):139-51.

34.   Shoji M, Furuyama F, Yokota Y, Omori Y, Sato T, Tsunoda F, et al. IL-6 mobilizes bone marrow-derived cells to the vascular wall, resulting in neointima formation via inflammatory effects. Journal of atherosclerosis and thrombosis. 2014;21(4):304-12.

35.   Niida T, Isoda K, Kitagaki M, Ishigami N, Adachi T, Matsubara O, et al. IkappaBNS regulates interleukin-6 production and inhibits neointimal formation after vascular injury in mice. Cardiovascular research. 2012;93(2):371-9.

36.   Kim WJ, Chereshnev I, Gazdoiu M, Fallon JT, Rollins BJ, Taubman MB. MCP-1 deficiency is associated with reduced intimal hyperplasia after arterial injury. Biochemical and biophysical research communications. 2003;310(3):936-42.

37.   Schepers A, Eefting D, Bonta PI, Grimbergen JM, de Vries MR, van Weel V, et al. Anti-MCP-1 gene therapy inhibits vascular smooth muscle cells proliferation and attenuates vein graft thickening both in vitro and in vivo. Arteriosclerosis, thrombosis, and vascular biology. 2006;26(9):2063-9.

38.   Egashira K, Zhao Q, Kataoka C, Ohtani K, Usui M, Charo IF, et al. Importance of monocyte chemoattractant protein-1 pathway in neointimal hyperplasia after periarterial injury in mice and monkeys. Circulation research. 2002;90(11):1167-72.

39.   Pearson T. Cardiovascular Update: Risk, Guidelines, and Recommendations. Workplace health & safety. 2015;63(9):376-80.

40.   Yoshida K, Tanaka T, Hirose Y, Yamaguchi F, Kohno H, Toida M, et al. Dietary garcinol inhibits 4-nitroquinoline 1-oxide-induced tongue carcinogenesis in rats. Cancer letters. 2005;221(1):29-39.

41.   Chen X, Zhang X, Lu Y, Shim JY, Sang S, Sun Z, et al. Chemoprevention of 7,12-dimethylbenz[a]anthracene (DMBA)-induced hamster cheek pouch carcinogenesis by a 5-lipoxygenase inhibitor, garcinol. Nutrition and cancer. 2012;64(8):1211-8.

Supporting information

Supplemental materials & methods

(Immuno)histochemistry (IHC)

IHC was performed on paraffin-embedded sections of uncuffed arteries or cuffed arteries of PCAF KO and WT mice harvested after 21 days. Vascular SMCs (vSMCs) were stained using anti-smooth muscle actin (SMA, clone 1A4, Dako) antibodies, while proliferating vSMCs were stained using the above mentioned anti-SMA antibodies in combination with anti-Ki67 (Abcam; ab16667) antibodies. TNF-alpha was stained using anti-TNF-alpha antibodies (Abcam; ab6671).

Quantification of proliferating vSMCs

Quantification of Ki67/SMA cells in media (left) and intima (right) of cuffed vessel segments, expressed as mean number per section , minimial six sections per cuffed segment.

MTT assay

At day zero $5.0^{E}+03$ VSMCs were seeded in a 96-wells plate in DMEM supplemented with 10% FCS heat-inactivated and 1% penicillin/streptomycin and cultured for 24 hours. The next day the medium was refreshed with DMEM supplemented with 10% FCS heat-inactivated and 1% penicillin/streptomycin with different concentrations $(0, 5, 10, 20 , 40 \,\mu M)$ garcinol or 20% DMSO as negative control. After 24 hours incubation at 37°C, 10 µl MTT (12 mM) was added directly to the medium. After 4 hours incubation at 37°C, isopropanol was added and incubated for 1.5 hour on a shaker. Optical density was measured at 540 nm and cell viability (%) was calculated compared with positive (untreated) control cells.

In vitro effect of garcinol on PCAF deficient vSMCs

PCAF KO VSMCs were simultaneously stimulated with 0.1 ng LPS and 15 µM garcinol or vehicle for 24 hours and subsequently CCL2 levels were measured using ELISA kit (555260, Becton Dickinson), according to the manufacturer's instructions.

Supplementary figures
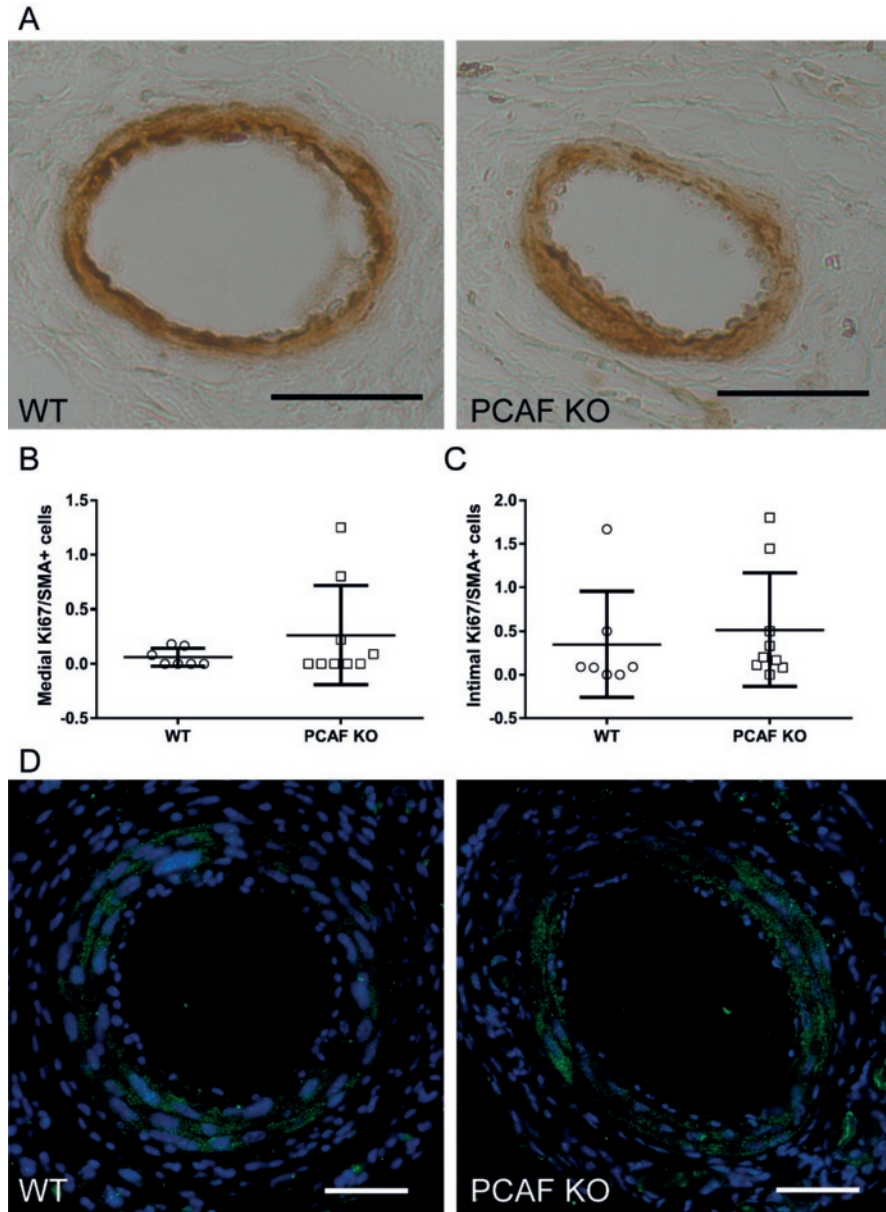
Supplemental Figure 1: Baseline vSMC content and effect of PCAF deficiency on vSMC proliferation and TNF-alpha expression. Representative images of SMA staining in uncuffed arteries (A). Scale bar = 20 µm. Quantification of Ki67/SMA+ cells in the media (B) and neointima (C) of WT (n=7) and PCAF KO (n=9) mice. Results are mean±SEM. Representative images of TNF-alpha staining of cuffed femoral arteries (D). Scale bar = 50 µm.
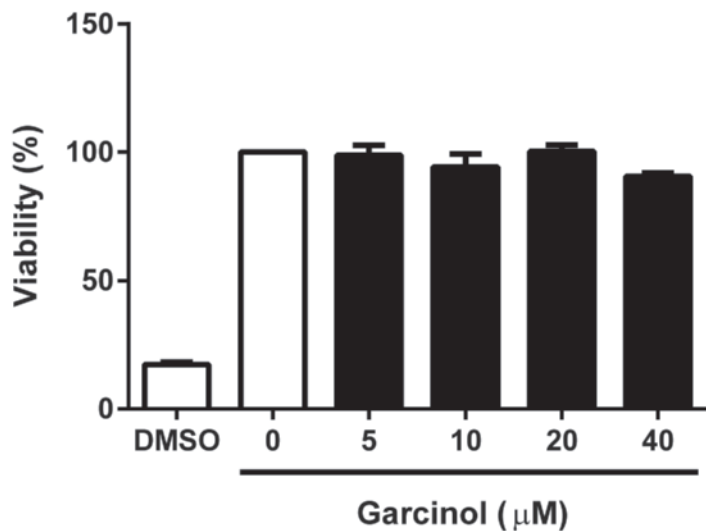
Supplemental Figure 2: Effect of garcinol on VSMC apoptosis *in vitro*. MTT assay assessed viability of VSMCs stimulated with different concentrations garcinol. Results are mean±SEM.
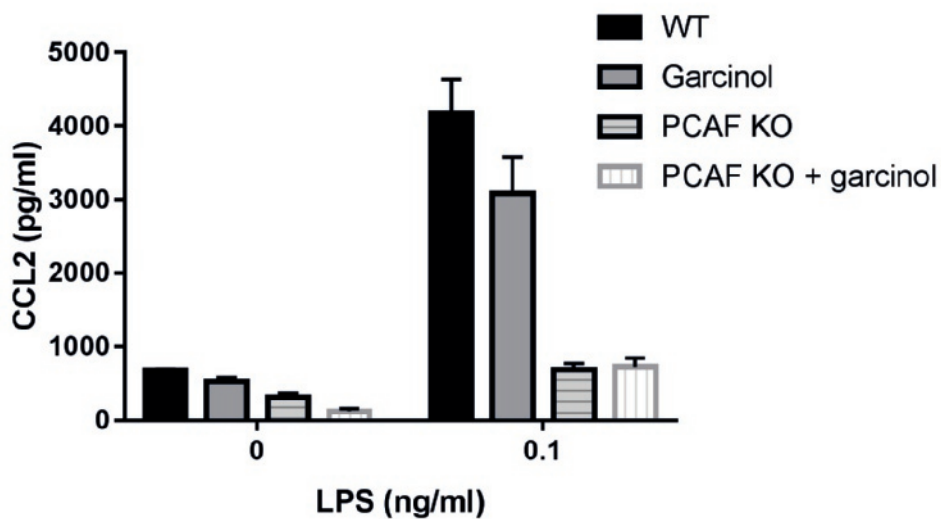
Supplemental Figure 3: Effect of garcinol on CCL production of PCAF deficient vSMCs. CCL2 production of vascular smooth muscle cells (n=3) from WT and PCAF KO mice 24 hours after simultaneous LPS (0-0.1 ng/ml) and garcinol (0-15 µM) stimulation. Results are mean±SEM.
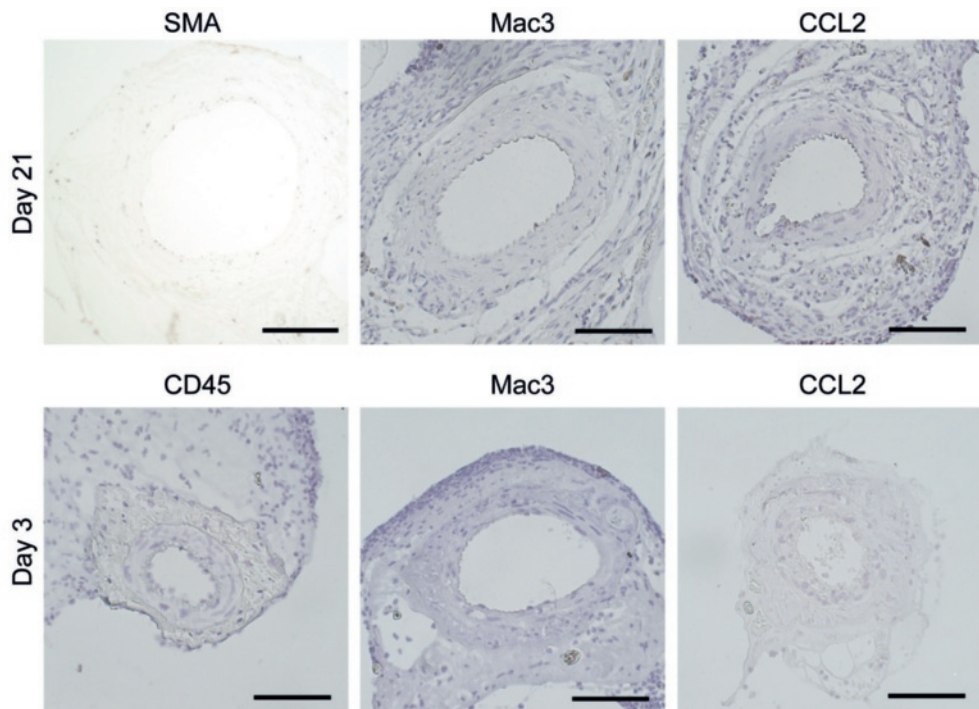
Supplemental Figure 4: No primary antibody controls. Representative images of different no primary antibody controls. Scale bar = 50 µm

Chapter 6

Inhibition of 14q32 microRNA miR-495 reduces lesion formation, intimal hyperplasia and plasma cholesterol levels in experimental restenosis

Rob C. M. de Jong[1,2]

Sabine M. J. Welten[1,2]

Anouk Wezel[1,5]

Margreet R. de Vries[1,2]

Martin C. Boonstra[1]

Laura Parma[1,2]

J. Wouter Jukema[1,3]

Tetje C. van der Sluis[4]

Ramon Arens[4]

Ilze Bot[5]

Sudhir Agrawal[6]

Paul H. A. Quax[1,2 †]

A. Yaël Nossent[1,2 †]

† Authors contributed equally to this work

[1]Department of Surgery, Leiden University Medical Center, Leiden, the Netherlands

[2]Einthoven Laboratory for Experimental Vascular Medicine, Leiden University Medical Center, Leiden, the Netherlands

[3]Department of Cardiology, Leiden University Medical Center, Leiden, the Netherlands

[4]Department of Immunohematology and Blood Transfusion, Leiden University Medical Center (LUMC), Leiden, The Netherlands

[5]Division of Biopharmaceutics, LACDR, Leiden University, Leiden, the Netherlands

[6]Idera Pharmaceuticals, Boston, MA, USA

Abstract

Background and aims: To investigate the role of 14q32 microRNAs in intimal hyperplasia and accelerated atherosclerosis; two major contributors to restenosis. Restenosis occurs regularly in patients treated for coronary artery disease and peripheral arterial disease. We have previously shown that inhibition of 14q32 microRNAs leads to increased post-ischemic neovascularization, and microRNA miR-494 also decreased atherosclerosis, while increasing plaque stability. We hypothesized that 14q32 microRNA inhibition has beneficial effects on intimal hyperplasia, as well as accelerated atherosclerosis.

Methods: Non-constrictive cuffs were placed around both femoral arteries of C57BL/6J mice to induce intimal hyperplasia. Accelerated atherosclerotic plaque formation was induced in hypercholesterolemic ApoE$^{-/-}$ mice by placing semi-constrictive collars around both carotid arteries. 14q32 microRNAs miR-329, miR-494 and miR-495 were inhibited in vivo using Gene Silencing Oligonucleotides (GSOs).

Results: Inhibition of miR-495 led to a 32% reduction of intimal hyperplasia. Moreover, the number of macrophages in the arterial wall of mice treated with GSO-495 was reduced by 55%. Inhibition of miR-329 and miR-494 had less profound effects on intimal hyperplasia. Inhibition of miR-495 also decreased atherosclerotic plaque formation by 52% and plaques of GSO-495 treated animals showed a more stable phenotype. Finally, cholesterol levels were also decreased in GSO-495 treated animals, via reduction of the VLDL-fraction.

Conclusions: Inhibition of miR-495 decreased our primary outcomes, namely intimal hyperplasia and accelerated atherosclerosis. Inhibition of miR-495 also favourably affected multiple secondary outcomes, including macrophage influx, plaque stability and total plasma cholesterol levels. We conclude that 14q32 microRNA miR-495 is a promising target for prevention of restenosis.

Introduction

Severe atherosclerosis can cause narrowing and occlusions of affected arteries, that require endovascular intervention (such as balloon angioplasty with or without stenting) to restore and maintain blood flow. Unfortunately, vascular damage inflicted by these interventions can lead to rapid restenosis of the artery[1]. Intimal hyperplasia is an important contributor to restenosis, which is characterized by extracellular matrix rearrangements, smooth muscle cell (SMC) proliferation and inflammation. On top of that, accelerated atherosclerosis is observed, especially under hypercholesterolemic conditions. Intimal hyperplasia is initiated by damage to the endothelium caused by vascular interventions and results in the activation of endothelial cells (ECs). Subsequently, leukocytes adhere to and infiltrate the vessel wall. These leukocytes secrete inflammatory cytokines and chemokines promoting inflammation and release matrix metalloproteinases and growth factors leading to extracellular matrix remodeling as well as smooth muscle cell (SMC) proliferation and migration. Accelerated atherosclerosis is initiated by severe flow disturbance combined with the uptake of lipids by macrophages in the vessel wall and subsequent formation of foam cells under hypercholesterolemic conditions.

MicroRNAs are short endogenous RNA molecules which, through binding to the 3'UTR of their target mRNA, regulate gene expression by inhibiting translation of the mRNA into protein. A single microRNA is able to regulate numerous, up to several hundred, target genes[2]. The fact that a single microRNA can fine-tune the expression of large sets of target genes and thus genetic programs for specific physiological processes makes microRNAs an interesting therapeutic tool for complex diseases[3].

We have previously shown that several members of a large microRNA gene cluster on human chromosome 14 (14q32) are highly involved in vascular remodeling, targeting multiple processes important for neovascularization and atherosclerosis[4]. The 14q32 cluster encodes over 54 microRNA genes and is highly conserved between mammals. Inhibition of 14q32 microRNAs miR-329, miR-487b, miR-494 and miR-495 improved post-ischemic neovascularization in a hind limb ischemia model[4]. Inhibition of 14q32 microRNA miR-494 also reduced collar-induced plaque size (accelerated atherosclerosis), increased plaque stability and decreased plasma cholesterol levels[5]. Han et al also observed upregulation of other 14q32 microRNAs (namely miR-431, miR-668 and miR-758) in atherosclerotic aortas of ApoE^{-/-} mice compared to healthy aortas of C57BL/6 mice[6]. Moreover, hypomethylation of 14q32 microRNAs was observed in human atherosclerotic plaques, resulting in the upregulation of several 14q32 cluster members[7]. The role of 14q32 microRNAs in restenosis however, is unknown.

The involvement of microRNAs in restenosis has been demonstrated in several studies and was recently reviewed[8]. For example, inhibition of miR-21 decreased neointima formation in rat carotid arteries after angioplasty, whereas overexpression of miR-29b

inhibited the formation of neointima in balloon-injured rat carotid arteries[9,10]. Based on our previous findings, we hypothesized that 14q32 microRNA inhibition would reduce lesion formation in experimental models for restenosis. In this study, we inhibited 14q32 microRNAs miR-329, miR-494 and miR-495 in a model for intimal hyperplasia and subsequently, we inhibited miR-329 and miR-495 in an accelerated atherosclerosis model and examined the effects on primary outcomes of vascular remodeling or arterial stenosis. In addition, we studied the effects of 14q32 microRNA inhibition on secondary outcomes such as target gene regulation, vascular cell proliferation, plaque stability and cholesterol homeostasis.

Materials and Methods

Mice
This study was performed in compliance with Dutch government guidelines and the Directive 2010/63/EU of the European Parliament. All animal experiments were approved by the Institutional Committee for Animal Welfare of the Leiden University Medical Center (approval reference numbers 13119 and 12165). Male C57BL/6J (10 weeks old) animals were purchased from the Jackson Laboratory. Male ApoE^{-/-} (7-14 weeks old at start of diet) were bred in the local animal breeding facility (Gorlaeus Laboratories, Leiden University, Leiden, the Netherlands). C57BL/6J mice received chow diet during the whole experiment. ApoE^{-/-} mice were fed a Western-type diet, containing 0.25% cholesterol and 15% cacao butter (Special Diet Services) for six weeks, two weeks prior to surgery. All animals received food and water ad libitum during the entire experiment. During surgery, mice were anesthetized by intraperitoneal (i.p) injection of midazolam (8 mg/kg, Roche Diagnostics), medetomidine (0.4 mg/kg, Orion) and fentanyl (0.08 mg/kg, Janssen Pharmaceutica). The adequacy of the anaesthesia was monitored by keeping track of the breathing frequency and the response to toe pinching of the mice. After surgery, mice were antagonized with a subcutaneous injection of flumenazenil (0.5 mg/kg; Fresenius Kabi), antesedan (2.5 mg/kg; AST Pharma) and buprenorphine (0.1 mg/kg; MSD Animal Health).

Femoral artery cuff mouse model
Intimal hyperplasia was induced by placement of a non-constrictive cuff around the femoral artery of C57BL/6J mice. The left and right femoral arteries were isolated and a rigid, non-constrictive polyethylene cuff was placed around the artery. Thereafter, the wound was closed by a continuous suture. After 21 days, mice were anesthetized and sacrificed via perfusion. Venous blood was drawn in EDTA collection tubes and centrifuged (6000 rpm for 10 min at 4°C) to obtain plasma. The thorax was opened and mild pressure-perfusion (100 mm/Hg) with PBS was performed for 4 minutes by cardiac puncture in the left ventricle. After perfusion with 3.7% formaldehyde, cuffed

femoral arteries were harvested, fixed 5 hours in formaldehyde and paraffin-embedded.

Carotid collar mouse model

Carotid artery plaque formation was induced by perivascular collar placement as described earlier[11]. In brief, a semi-constrictive cuff collar was placed around both left and right carotid arteries to induce accelerated atherosclerosis (n=15 per group). Four weeks (28 days) after collar placement, mice were anesthetized and sacrificed via perfusion, after which carotid arteries were harvested, fixed overnight in formaldehyde and paraffin-embedded.

Gene Silencing Oligonucleotides (GSOs)

Gene Silencing Oligonucleotides (GSOs) were designed with perfect reverse complementarity to the mature target microRNA sequences and synthesized by Idera Pharmaceuticals (GSOs kindly provided by Idera pharmaceuticals). As a negative control, a scrambled sequence was used, designed not to target any known murine microRNA. GSOs consist of two single-stranded 2'O-methylated DNA strands, linked together at their 5'ends by a phosphothioate-linker to avoid TLR-activation[12]. Sequences of microRNAs and GSOs used are given in Supplemental Table 1.

Uptake of IRDye-800CW labelled GSOs

Two adult male C57BL/6J mice received one non-constrictive cuff around the left femoral artery, while the contra-lateral femoral artery was left unaffected. One day prior to cuff placement, mice were injected intravenously with IRDye-800CW-labelled GSO-329 (0.4 mg/mouse; Idera Pharmaceuticals) or with IRDye-800CW-unlabelled control. Mice were sacrificed by cervical dislocation, 24 hours after cuff placement. Near-InfraRed (NIR) fluorescence measurements were performed using the FLARETM NIR imaging system[13].

Treatment with GSOs in in vivo models

In case of the femoral artery cuff model, mice received a single intravenous injection of 1 mg GSO dissolved in 200 µl PBS, one day before cuff placement. In case of the carotid collar model, mice received a first intravenous injection of 1 mg GSO dissolved in 200 µl PBS, 4 days after collar placement. At day 18 after collar placement, mice received a second injection of 0.5 mg GSO dissolved in 200 µl PBS.

A subset of mice (n=3 per group for cuff model and n=6 per group for collar model) was sacrificed 3 days after the first GSO injection in order to establish downregulation of microRNAs in vivo.

Plasma analysis

Blood was collected from mice prior to surgery, at sacrifice and at indicated timepoints (day 2, day 7, day 21 in cuff model for FACS analysis), by tail bleeding. The concentration of cholesterol in plasma was determined by incubation with 0.025 U/ml cholesterol

oxidase (Sigma) and 0.065 U/ml peroxidase and 15 μg/mL cholesterol esterase (Roche Diagnostics) in polyoxyethylene-9-laurylether, and 7.5% methanol. Precipath (standardized serum; Roche Diagnostics) was used as an internal standard. Absorbance was measured at 490 nm.

For lipid profiling, plasma was pooled (n= 5 pooled samples per group, plasma samples of 3 mice were pooled per sample) and diluted 6 times, after which fractionation of plasma lipoproteins was performed using an AKTA-FPLC. Total cholesterol levels were determined in each fraction and in the original pooled sample using a colorimetric assay (Roche Diagnostics, kit 11489232). Absorbance was measured at 490 nm.

Histology and morphometry

Formaldehyde fixed carotid and femoral arteries were paraffin-embedded and 5 μm thick cross sections of arteries were stained to visualize vessel morphology. Paraffin sections of femoral arteries were stained with Weigert's Elastin to visualize the elastic laminae to determine intimal hyperplasia. Paraffin sections of carotid arteries were stained with hematoxylin-phloxine-saffron (HPS) to determine plaque size. Sirius red staining was used to visualize collagen content.

To visualize macrophages and smooth muscle cells, cross sections of arteries were re-hydrated and endogenous peroxidase activity was blocked. Macrophages and smooth muscle cells were stained using anti-Mac3 (BD Pharmingen, clone M3/84) and anti-smooth muscle actin (SMA; DAKO, clone 1A4) respectively and counterstained using haematoxylin.

To assess proliferation of smooth muscle cells, cross sections of femoral arteries were stained using anti-Ki-67 (proliferation marker) (Abcam, clone SP6) and anti-SMA (DAKO, clone 1A4). Ki-67 was visualized using Alexa 647 conjugated secondary antibody (Invitrogen) and SMA was visualized using Alexa 555 conjugated secondary antibody (Invitrogen). Nuclei were stained using Fluoroshield with DAPI (Sigma).

All quantifications of femoral arteries were performed on six equally spaced cross sections through the cuffed femoral artery by a single blinded observer. Vessel wall parameters, collagen content and smooth muscle cell area were quantified using Qwin (Leica). Macrophage content and the number of Ki-67/SMA positive cells in the cuffed femoral artery of C57Bl6/J mice were counted manually.

Morphometric analysis of carotid arteries was performed on atherosclerotic lesions at the site of maximal stenosis by a single blinded observer. Plaque size, necrotic core, collagen content, smooth muscle cell area and macrophage content were quantified using image analysis software for morphometric analysis (Qwin, Leica).

Cell culture

Bone marrow (BM) cells isolated from C57BL/6J mice were cultured for 7 days in RPMI medium supplemented with 20% inactivated fetal calf serum (FCSi, PAA), 2 mmol/L

l-glutamine (PAA), 100 U/mL penicillin and 100 µg/mL streptomycin and 30% L929 cell-conditioned medium, as the source of macrophage colony-stimulating factor (M-CSF), to generate BM-derived macrophages (BMDMs)[14].

Primary cultured murine vascular smooth muscle cells (vSMC) and cell lines for fibroblasts (3T3) and endothelial cells (H5V) were cultured in complete DMEM GlutaMAXTM medium (Gibco) supplemented with 10% FCSi, 1% penicillin/ streptomycin.

VSMCs, H5V and 3T3 cells were plated in triplicate at a density of 106 cells/mL. GSOs were added overnight at a concentration of 5 µg/mL, after which the cells were lysed for RNA isolation. For BMDMs, GSOs were added immediately after isolation from BM in a concentration of 5 µg/mL. After three days medium was refreshed with a similar addition of GSOs in a concentration of 5 µg/mL. Four days later, medium was removed and cells were lysed for RNA isolation.

RNA isolation, cDNA synthesis and quantitative PCR (qPCR)

For measuring basal femoral artery microRNA expression three paraffin embedded femoral artery segments from 21 days after cuff placement were pooled, paraffin was removed using xyleen and tissue was homogenized by grounding using a Pellet Pestle Cordless Motor (Kimble Chase Life Science). For analysis of microRNA inhibition three fresh femoral artery segments from 3 days after cuff placement were pooled and homogenized by grounding using a Pellet Pestle Cordless Motor (Kimble Chase Life Science). Three carotid artery segments from 7 days after collar placement (3 days after GSO injections) were pooled and homogenized using the same Pellet Pestle Cordless Motor. Liver was isolated and homogenized by grounding with pestle and mortar in liquid nitrogen. Total RNA was extracted using a standard TRIzol-chloroform extraction method. RNA concentration and purity were examined by nanodrop (Nanodrop Technologies). MiR quantification was performed using Taqman® miR assays (Thermo Fisher) following manufacturer's protocol. qPCR was performed on the Viia7 system (Thermo Fisher). Normalization of data was performed using a stably expressed endogenous control (snRNA U6 and mmu-let-7c).

For in vitro and in vivo experiments, total RNA was extracted from cells and tissues using the standard TRIzol-choloform extraction method. RNA was reverse transcribed using high-capacity RNA to cDNA RT kits (Life technologies) and used for quantitative analysis of mouse genes with the Viia7 system (Applied Biosystems). The relative expression of putative miR-495 target genes was quantified using the QuantiTect SYBR® Green technology (Qiagen). Normalization of the data was performed by using stably expressed endogenous controls (Hprt and Rpl27). Primer sequences can be found in Supplemental Table 2.

Cholesterol efflux assay

BMDMs, cultured and treated with GSOs as described above, were plated at a density

of 0.5x106 cells per well. The following day, medium was changed with DMEM containing 10% BSA and 1 µCi/mL 3H-cholesterol (loading medium) to which either GSO-control of GSO-495 was added and cells were treated with 20 mg/mL cholesterol. After 24 hours, loading medium was replaced with DMEM with 10% BSA for 1 hour. Next, medium was changed for control DMEM with 10% BSA or DMEM with 10% BSA supplemented with HDL (50 µg/mL). After 24 hours, radioactivity in the cells and medium was determined by liquid scintillation counting (Packard 1500 Tricard). Cholesterol efflux was defined as $(dpm_{medium}/dpm_{cells}+dpm_{medium})x100\%$ and shown as the percentage of HDL specific efflux, corrected for non-specific efflux to control medium.

Statistical analysis

Data are expressed as mean ± SEM. Comparisons of absolute miR expression were performed using one-way ANOVA, followed by a Tukey's multiple comparison test. Comparisons of multiple treatment groups with the control group were performed using one-way ANOVA, followed by multiple comparisons without correction for multiple t-tests. Two-tailed Student's t-tests were used to compare a single treatment group with the control group. A level of $p<0.05$ was considered significant.

Results

In vivo inhibition of miR-329, miR-494 and miR-495 after GSO treatment in the cuff model

Expression levels of 14q32 microRNAs miR-329, miR-494 and miR-495 were measured in the femoral arteries of wildtype C57BL/6J mice and the carotid arteries of ApoE^{-/-} mice, representing the two models used to study post-interventional intimal hyperplasia and accelerated atherosclerosis. Expression of miR-329, miR-494 and miR-495 was also measured in the aorta of ApoE^{-/-} mice. In the femoral arteries of wildtype mice, expression of miR-329 and miR-495 was highest, followed by miR-494 expression (Figure 1A, left panel). As we have previously established, the expression of miR-495 was highest in the aorta of ApoE^{-/-} mice (Figure 1A, middle panel), whereas in the carotid arteries of these animals, both miR-495 and miR-494 were highly expressed (Figure 1A, right panel)[5].

Next, we measured expression of these microRNAs after GSO treatment in the femoral cuff model. Expression of miR-329, miR-494 and miR-495 was measured at a single timepoint in the femoral artery of in C57BL/6J mice, 3 days after cuff placement, 4 days after GSO injection. MiR-329 was significantly downregulated by 52% in the femoral arteries of C57BL/6J mice compared to GSO-control treated animals. Although not statistically significant at this specific timepoint, microRNA inhibition is a time-dependent process[4] and miR-495 was downregulated by 34% in the femoral arteries of C57BL/6J mice (p=0.22). For miR-494, we could not observe downregulation at this
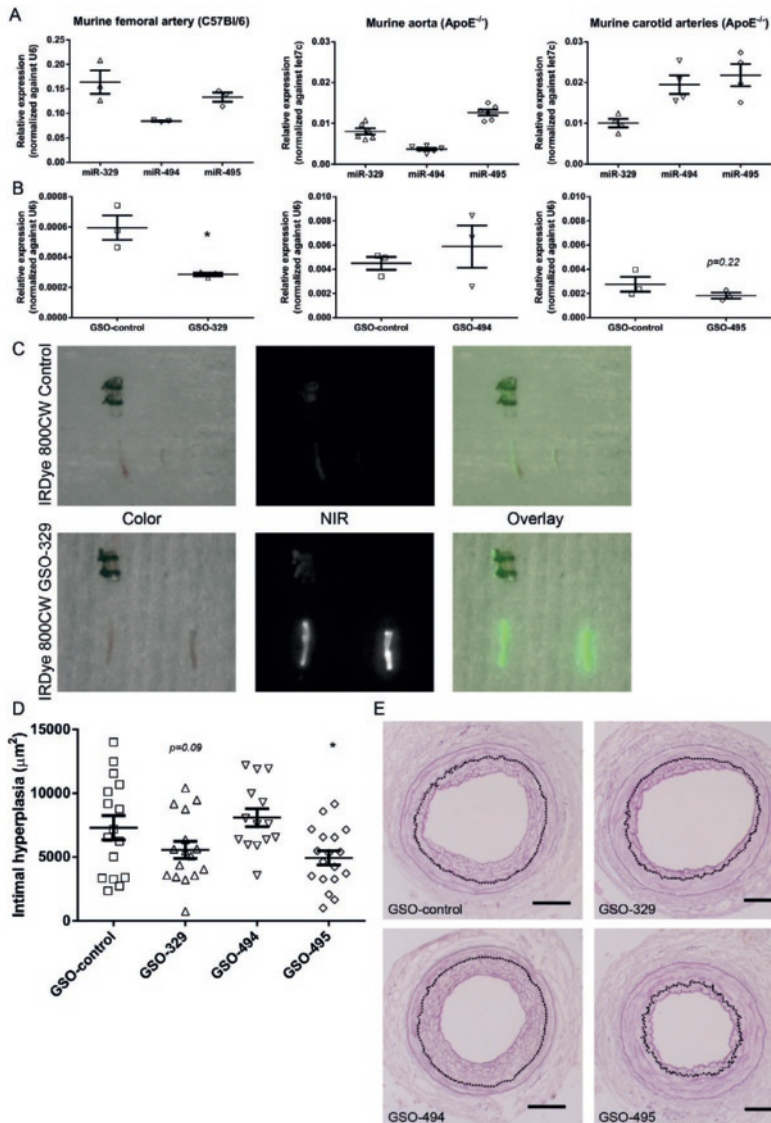
Figure 1. Expression and inhibition of 14q32 microRNAs miR-329, miR-494 and miR-495, and effects of 14q32 microRNA inhibition on intimal hyperplasia. (A) Relative expression levels (±SEM) of miR-329, miR-494 and miR-495 in the femoral artery of C57BL/6J mice (n=3 pooled samples, 3 femoral arteries were pooled for 1 sample), the aorta (n=6) and carotid artery of ApoE^{-/-} mice (n=4 pooled samples, 3 carotids were pooled for 1 sample; data on microRNA expression in ApoE^{-/-} mice was adapted with permission from Wezel *et.al.*[5]). (B) Mean expression levels, relative to U6, of miR-329, miR-494 and miR-495 in cuffed femoral arteries (n=3 pooled samples, 3 femoral arteries were pooled for 1 sample) are shown here 4 days after GSO treatment (±SEM). *$p<0.05$. (C) Uptake of IRDye-800CW-labelled GSO-329 in the cuffed femoral artery. In each micrograph the cuffed femoral artery (cuff removed; left) and contra-lateral non-cuffed femoral artery (right) are displayed. Upper panels show femoral arteries of IDRye-800CW-unlabelled control treated animals and lower panels femoral arteries of IRDye-800CW-labelled GSO-329 treated animals, 24 hours after cuff placement and 48 hours after GSO-injection. Colour images are shown on the left, near-infrared (NIR) images in the middle and an overlay of colour and NIR images is shown on the right. (D) Quantification of intimal hyperplasia 21 days after cuff placement in C57BL/6J mice (n=14-18 per group) treated with GSOs (±SEM). *$p<0.05$ compared to GSO-control. (E) Representative images of elastin staining of cuffed femoral arteries, dashed line represents lamina elastic interna (scale bar = 50 μm).

specific timepoint (Figure 1B).

Uptake of GSOs at site of cuff placement
To visualize uptake of GSOs in the femoral artery, C57BL/6J mice were injected with either IRDye-800CW-labelled GSO-329, or IRDye-800CW-unlabelled control, one day prior to cuff placement. As expression of miR-329 was highest in the femoral artery, we injected mice with IRDye 800CW-labelled GSO-329. Since the GSO chemistry is comparable for GSO-329, GSO-494 and GSO-495, we assume similar uptake of the other GSOs. Uptake of labelled GSO-329 was observed in both cuffed (left) and non-cuffed (right) femoral arteries, whereas minimal uptake was detected in the femoral arteries of mice treated with IRDye-800CW control (Figure 1C). These data demonstrate effective uptake of GSOs in the femoral arteries. Previously, we have shown that GSOs are also taken up specifically in the carotid arteries of ApoE^{-/-} mice, 4 days and 28 days after collar placement[5].

Effects of miR-329, miR-494 and miR-495 inhibition on vascular remodelling in C57BL/6J mice
At 21 days after cuff placement, intimal hyperplasia was significantly reduced by 33% following treatment with GSO-495 compared to GSO-control. Although not statistically significant, treatment with GSO-329 also decreased intimal hyperplasia by 24% (p=0.09), whereas GSO-494 treatment had no effect on intimal hyperplasia (Figure 1D and representative images in Figure 1E). In addition, a decreased intima/media ratio was observed following GSO-495 treatment (35% reduction). This ratio was not decreased in GSO-329 and GSO-494 treated animals (Supplemental Figure 1A). No differences were found regarding luminal area and lumenstenosis following GSO-494 or GSO-495 treatment (Supplemental Figure 1B and 1C). GSO-329 treatment significantly increased luminal area and decreased lumenstenosis in these animals (Supplemental Figure 1B and 1C). These data show a beneficial effect of GSO-495 treatment on intimal hyperplasia in C57BL/6J mice.

Effects of miR-329, miR-494 and miR-495 inhibition on vessel wall composition in C57BL/6J mice
To assess the effect of microRNA inhibition on vessel wall composition following cuff placement, we (immuno-)stained serial sections with SMA, Mac-3 or Sirius red. No differences were observed regarding SMC content in the intima and media of GSO treated groups (Figure 2A and 2B, representative images in Figure 2C). Since GSO-495 treatment reduced intimal hyperplasia, we examined the number of proliferating SMCs in this group by staining for Ki67 and SMA and compared the number of double positive cells (Ki67^{+}/SMA^{+} cells) in GSO-495 treated animals with GSO-control treated animals (Figure 2D and 2E). Inhibition of miR-495 reduced the number of proliferating
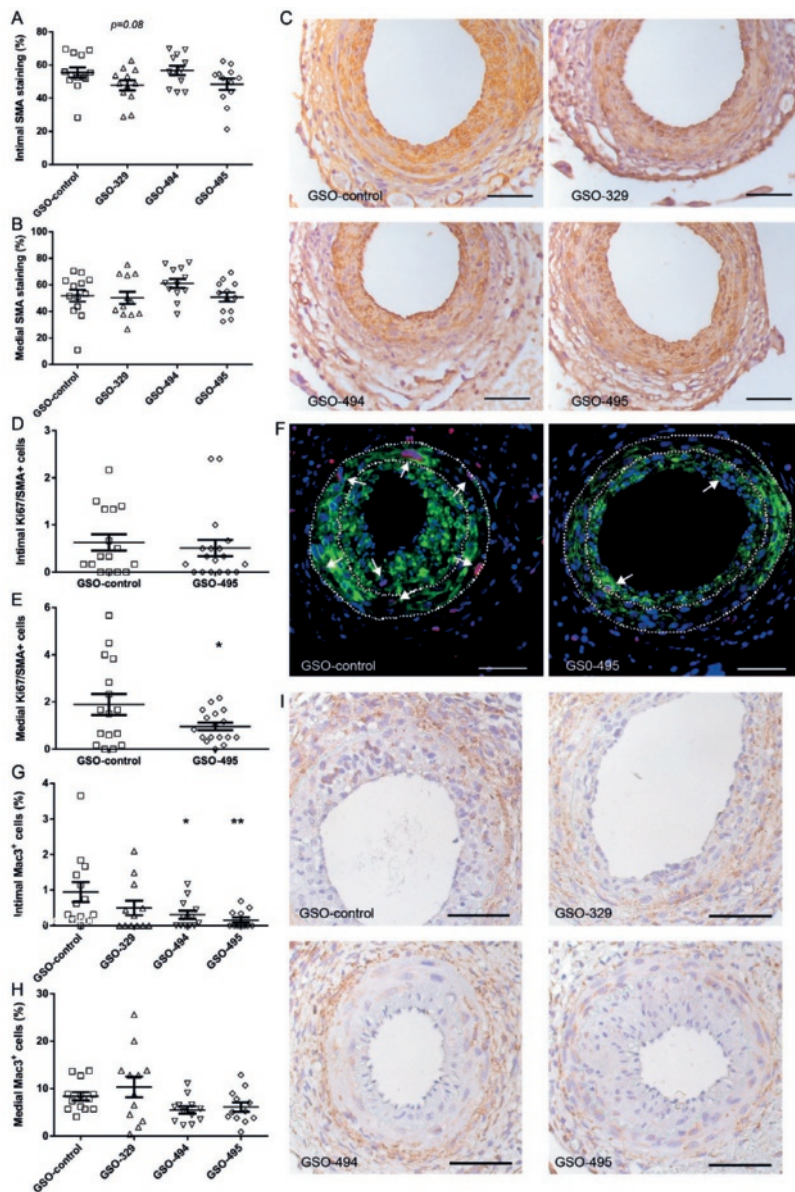
Figure 2. Effect of 14q32 microRNA inhibition on vascular smooth muscle cell proliferation and macrophage influx. Quantification of intimal (A) and medial (B) smooth muscle cell area (%) 21 days after cuff placement in C57BL/6J mice (n=12-13 per group) treated with GSOs (±SEM). (C) Representative images of SMA staining of cuffed femoral arteries (scale bar = 50 μm). Quantification of intimal (D) and medial (E) smooth muscle cell proliferation 21 days after cuff placement in C57BL/6J mice (n=16-17 per group) treated with GSO-495 (±SEM). *p<0.05. (F) Representative images of Ki67/ SMA staining of cuffed femoral arteries, arrows indicate Ki67/SMA positive cells, dashed lines indicate the elastic laminae (scale bar = 50 μm). Nuclei are shown in blue, SMA staining in green and Ki67 in red. Quantification of intimal (G) and medial (H) macrophage influx (%) 21 days after cuff placement in C57BL/6J mice (n=12-13 per group) treated with GSOs (±SEM). *p<0.05, **p<0.01 compared to GSO-control. (I) Representative images of Mac3 staining of cuffed femoral arteries (scale bar = 50 μm).

SMCs by 47% in the media of these animals, but not in the intima (Figure 2D and 2E, representative images in Figure 2F)

Following GSO- 494 and GSO-495 treatment, macrophage influx was significantly reduced by 35% and 78% respectively in the intimal area compared to GSO-control (Figure 2G). Macrophage influx in the medial area was reduced, although not statistically significant, by 35% following GSO-494 (p=0.13) treatment and by 27% following GSO-495 (p=0.23) treatment (Figure 2H, representative images in Figure 2I). MicroRNA inhibition did not alter collagen content in either the intima or the media of GSO treated animals (Supplemental Figure 2A and 2B, representative images in Supplemental Figure 2C).

Effects of miR-495 and miR-329 inhibition in the carotid collar mouse model in ApoE$^{-/-}$ mice

Next, we assessed the effects of 14q32 microRNA miR-329 and miR-495 inhibition on accelerated atherosclerotic plaque formation. Atherosclerotic plaque sizes were significantly decreased with 53% in GSO-495 treated animals (Figure 3A and representative images in Figure 3B). In GSO-329 treated animals, a trend towards a 43% decrease in atherosclerotic plaque size compared to GSO-control animals (p=0.09, Figure 3A, representative images Figure 3B) was observed. In addition to the decreased plaque size, composition of the lesions was also affected by GSO-495 treatment. Inhibition of miR-495 resulted in smaller necrotic core sizes (60% reduction), whereas inhibition of miR-329 had no significant effects on necrotic core size (Figure 4A). In addition, the percentage of macrophage content in the lesions was decreased by 30% in GSO-495 treated animals (Figure 4B), but not in GSO-329 treated animals. No difference was observed in the percentage of SMA positive lesion area between groups (Figure 4C). Inhibition of miR-495, but not miR-329, increased collagen content by 139% (Figure 4D), further increasing plaque stability.

Plasma cholesterol levels in GSO-495 treated animals were significantly decreased with 13% (Figure 3C). Lipid profiling using AKTA-FPLC revealed a reduction in the VLDL fraction after treatment with miR-495 inhibition (Figure 3D). This reduction in plasma cholesterol and VLDL levels was not observed in animals treated with GSO-329 (Figure 3C and 3D). In order to elucidate the mechanism behind the VLDL reduction in GSO-495 treated animals, we investigated the *in vitro* cholesterol efflux in macrophages. We found that treatment of macrophages with GSO-495 significantly increased cholesterol efflux *in vitro* by 96% (Figure 3E).

Target gene regulation after miR-495 inhibition

We investigated the effects of miR-495 inhibition on target gene regulation. We made a selection of putative target genes that have predicted binding sites for miR-495 in their 3'UTR. Although *in vivo* inhibition of miR-495 was not statistically significant at
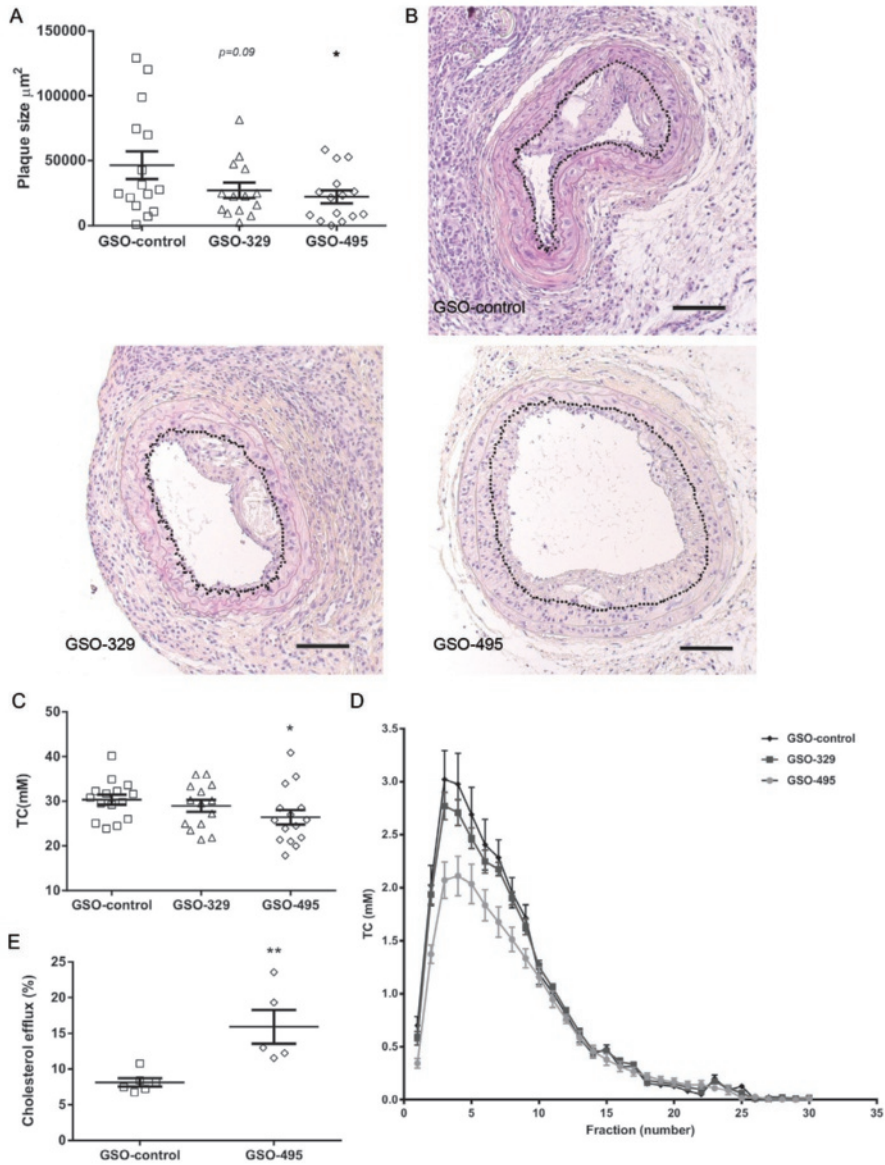
Figure 3. Effect of 14q32 microRNA miR-495 inhibition on plaque size and cholesterol levels.
(A) Quantification of plaque size 28 days after collar placement in ApoE$^{-/-}$ mice (n=14-15 per group) treated with GSO-control, GSO-329 or GSO-495. *$p<0.05$ compared to GSO-control. (B) Representative images of HPS staining of carotid arteries (scale bar = 100 μm). (C) Total cholesterol levels of ApoE$^{-/-}$ mice treated with GSO-control, GSO-329 or GSO-495, 6 weeks after start of the western type diet. *$p<0.05$ compared to GSO-control. (D) Cholesterol profile of GSO treated ApoE$^{-/-}$ mice (n=5 pooled samples per group, plasma samples of 3 animals were pooled per sample) analysed using AKTA-FPLC. (E) Quantification of cholesterol efflux (%) from macrophages treated with GSO-control or GSO-495. **$p<0.01$.
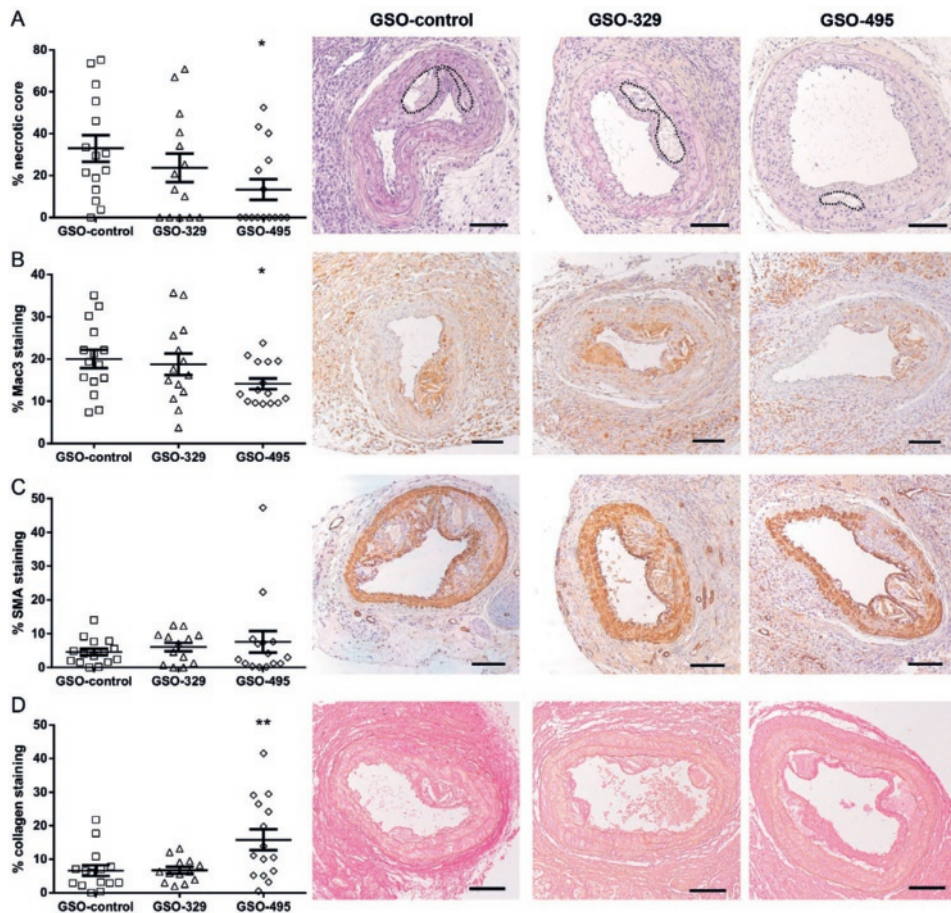
Figure 4. Effects of 14q32 microRNA miR-495 inhibition on lesion composition 28 days after collar placement in ApoE$^{-/-}$ mice. (A) Quantification of necrotic core size. (B) Percentage (%) of macrophage influx. (C) Percentage (%) of smooth muscle cell area. (D) Percentage (%) of collagen content. *p<0.05, **p<0.01 compared to GSO-control. Representative images of (A) HPS staining, (B) Mac3 staining, (C) SMA staining and (D) Sirius red staining are shown (n=13-15 mice per group, scale bar = 100 μm).

this specific timepoint, we could observe upregulation of miR-495 target genes Tgfβ2 and Il13ra1 in the carotid arteries (Figure 5B). Furthermore, expression of target genes Acvr1 (p=0.07) in the carotids and Il10 (p=0.05) in the spleen were upregulated in GSO-495 treated animals (Figure 5B). In addition, we determined the expression of multiple cholesterol metabolism related target genes of miR-495 in the liver but no differences were observed in the expression of Lrp6, Mttp, Ldlr and Abca1 (Supplemental Figure 3). To investigate the effects of miR-495 inhibition on various individual cell types in vascular remodelling, H5V endothelial cells, vSMCs, 3T3 fibroblasts and BMDMs were treated with GSOs against miR-495. Multiple target genes with predicted binding sites

for miR-495 were examined, including cytokines, complement components, lipid-related target genes and tissue inhibitors of metalloproteinases (TIMPs). Inhibition of miR-495 led to upregulation of Tlr7 in H5V cells and vSMCs ($p=0.05$), whereas the anti-inflammatory Il10 was upregulated in 3T3 cells ($p=0.06$) and H5V cells ($p=0.11$) (Supplemental Figure 4). Other genes that were upregulated after miR-495 inhibition included Cdknb1 ($p=0.09$) in 3T3 cells, Cd59 ($p=0.08$) and Ccr2 ($p=0.06$) in BMDMs.
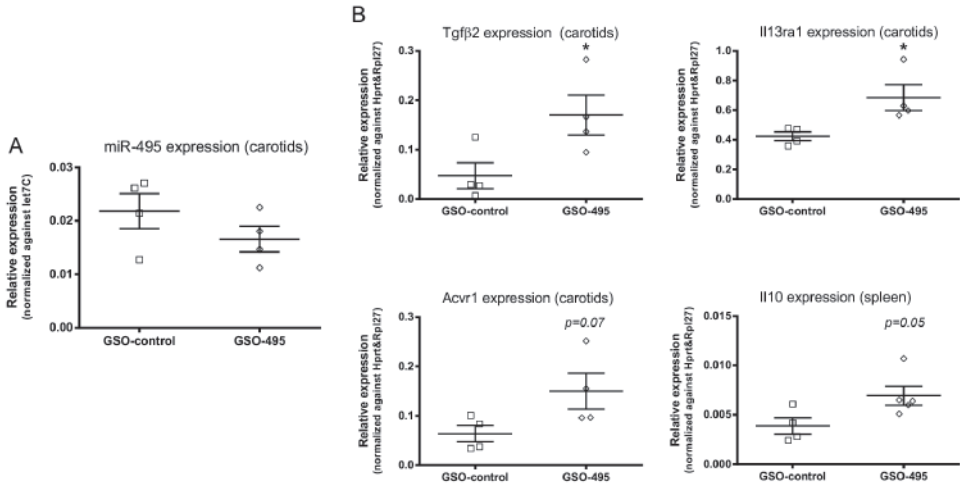
Figure 5. *In vivo* **expresion of miR-495 and putative target genes.** (A) Mean expression levels of miR-495 in carotid arteries, relative to let7c, are shown here 3 days after GSO treatment in ApoE^{-/-} mice (n=4 pooled samples per group, 3 carotids were pooled per sample). (B) Mean expression levels of putative miR-495 target genes Tgfβ2, Il13ra1 and Acvr1 in carotids (n=5 samples per group; 3 carotids were pooled per sample), and Il10 in spleen (n=5 per group), relative to Hprt and Rpl27, are shown here 3 days after GSO treatment in ApoE^{-/-} mice. *$p<0.05$.

Discussion

Here, we hypothesized that inhibition of 14q32 microRNAs would reduce restenosis through decreased intimal hyperplasia and decreased accelerated atherosclerosis. We show that inhibition of miR-495 leads to less intimal hyperplasia following vascular injury and decreased plaque formation in atherosclerosis prone mice, whilst increasing plaque stability in these animals. In addition, we investigated the effects of 14q32 microRNA miR-495 inhibition on secondary outcomes such as target gene regulation, smooth muscle cell proliferation, plaque stability and cholesterol homeostasis. The 14q32 microRNA gene cluster is the largest known mammalian microRNA gene cluster to date and many 14q32 microRNAs have been implicated within human disease[15]. Recently, we have reported the role of multiple microRNAs from this cluster in several aspects of vascular remodelling, including angiogenesis, arteriogenesis and

atherosclerosis[4,5].

MicroRNAs are known for their ability to regulate the expression of numerous genes[16]. Especially miR-495 may have the ability to target a large number of genes; bioinformatics analysis using www.targetscan.org (TargetScan 7.0, consulted January 2016) revealed over 5103 transcripts with in total 7998 putative binding sites for human miR-495 (of which 1015 conserved sites and 6983 poorly conserved sites) and 4879 transcripts with putative binding sites for murine miR-495 (and a total of 7886 sites). It is therefore unlikely that the observed effects are attributable to strong regulation of one target gene in particular, but rather are the sum of modest regulation of multiple target genes involved in all aspects of the processes of vascular remodelling studied here, namely intimal hyperplasia and accelerated atherosclerosis. Moreover, binding of a certain microRNA to its target gene does not completely silence its expression, but rather downtunes its expression[2]. This corresponds to the modest effects that we observed on miR-495 target gene regulation.

In vivo, treatment with GSO-495 led to upregulation of target genes Tgfβ2, Il13ra1 and Il10 and a trend towards upregulation of Acvr1. IL-13, one of the cytokines secreted by CD4+ Th2-cells, inhibits macrophage activation and decreases the production of pro-inflammatory cytokines by activated macrophages[17]. More specifically, the IL-13 receptor alpha 1 chain (Il13ra1) is implicated within the signal transduction route of IL-13 and inhibits interferon-γ induced gene expression in macrophages[18]. We did observed upregulation of Il10 expression specifically in the spleen following systemic treatment with GSO-495. Since it has been shown that splenic-derived IL-10 has anti-inflammatory properties[19,20], it is plausible that the observed increase in splenic Il-10 expression following GSO-495 has a systemic effect on accelerated atherosclerosis. Likewise, IL-10, which is also a Th2 cytokine has anti-inflammatory properties and protects against atherosclerosis and neointima formation by inhibiting macrophage activation and inhibition of matrix metalloproteinases[21-24]. These findings are in line with our results that GSO-495 treatment decreases macrophage numbers within the arterial lesions investigated. Tgfβ2 is known to be an important regulator of collagen synthesis[25]. This is in line with the observed increase in collagen content and upregulation of Tgfβ2 in the carotid artery. Furthermore, it has been shown that inhibition of Tgfβ1, -β2 and -β3 activity induces atherosclerosis and favours development of an unstable plaque phenotype, which suggests Tgfβ2 has atheroprotective properties and could therefore contribute to the reduced plaque formation seen in this study[26]. Despite the observed upregulation in putative target genes of miR-495, we cannot rule out the possibility that the observed upregulation is the result of an indirect effect of miR-495 inhibition instead of a direct effect of miR-495 inhibition.

Inhibition of miR-495 reduced proliferation of SMCs in neointimal lesions of GSO-495 treated animals. Proliferation and migration of vascular SMCs is one of the most important events in intimal hyperplasia[27]. In agreement with the reduced proliferation

of SMCs after miR-495 inhibition, overexpression of miR-495 has previously been shown to increase proliferation of neonatal rat cardiomyocytes[28]. On the other hand, it has also been shown that miR-495 promotes proliferation of HUVECs[29]. These and our findings demonstrate different actions of microRNAs in different cell types, which comes with both benefits and limitations for possible therapeutic uses.

Following GSO-495 treatment we found a reduction of total cholesterol levels of 13%, which could mainly be attributed to a reduction of VLDL. One of the most frequently used therapy against atherosclerosis is the use of statins, which aims for reduction of (V)LDL cholesterol levels in the blood. Statins reduce (V)LDL cholesterol levels in a range of 40 to 60% depending on the dose administered, which subsequently reduces the risk of ischemic heart disease by 61% and of stroke by 17%[30]. Although we cannot explain the reduced plaque size and increased stability of the plaques completely by the modest reduction of VLDL plasma cholesterol levels, it is plausible that this reduction contributes, at least partly, to the reduced plaque size and increased plaque stability. This hypothesis is supported by the observed increase in cholesterol efflux from macrophages *in vitro* following GSO-495 treatment. This suggests GSO-495 can inhibit atherogenesis by facilitating removal of cholesterol from the vessel wall to the liver in an HDL dependent manner.

Inhibition of miR-495 also led to a decrease in necrotic core size and macrophage content, while it increased collagen content in atherosclerotic lesions. A decrease in necrotic core size and macrophage content together with an increase in collagen content are characteristics of increased plaque stability[31]. MiR-495 was thus shown to not only contribute to atherosclerotic lesion formation, but also plaque stability in ApoE$^{-/-}$ mice. To our knowledge, we are the first to report that inhibition of miR-495 leads to therapeutic benefits in two models of vascular remodelling, namely the femoral artery cuff model for intimal hyperplasia and the carotid collar model for accelerated atherosclerosis. Not only were the lesions in these models reduced in size, but the lesions also contained fewer macrophages and in case of the carotid collar model, plaque stability was increased. Atherosclerosis is the most common underlying cause of cardiovascular disease and can lead to, amongst others, myocardial infarction, ischemic stroke and peripheral arterial disease. Restenosis occurs upon endovascular interventions performed to target these atherosclerotic lesions and involves the re-narrowing of arteries. Reducing both intimal hyperplasia and accelerated atherosclerosis is of crucial importance for the prevention of restenosis.

A limitation of this study is the fact that due to the time-dependent regulation of microRNA expression levels, we cannot attribute all the observed biological effects to miR-495 downregulation with absolute certainty; some of the effects may still be indirect, rather than direct consequences of GSO-495 administration. Future studies should therefore include detailed *in vivo* studies of time-dependent microRNA downregulation and target gene upregulation. Taken together however, we conclude that GSO-495 administration

improves both primary and secondary parameters of restenosis. GSO-495 reduces both intimal hyperplasia and accelerated atherosclerosis, which makes miR-495 a highly attractive therapeutic target for patients treated for occlusive arterial disease who are at risk of developing restenosis.

References

1   Clowes, A. W., Reidy, M. A. & Clowes, M. M. Mechanisms of stenosis after arterial injury. Lab Invest 49, 208-215, (1983).

2   E., v. R. & Olson, E. N. MicroRNA therapeutics for cardiovascular disease: opportunities and obstacles. Nat. Rev. Drug Discov 11, 860-872, (2012).

3   Welten, S. M., Goossens, E. A., Quax, P. H. & Nossent, A. Y. The multifactorial nature of microRNAs in vascular remodelling. Cardiovasc. Res 110, 6-22, (2016).

4   Welten, S. M., Bastiaansen, A. J., de Jong, R. C., de Vries, M. R., Peters, E. A., Boonstra, M. C., Sheikh, S. P., Monica, N. L., Kandimalla, E. R., Quax, P. H. & Nossent, A. Y. Inhibition of 14q32 MicroRNAs miR-329, miR-487b, miR-494, and miR-495 increases neovascularization and blood flow recovery after ischemia. Circ. Res 115, 696-708, (2014).

5   Wezel, A., Welten, S. M., Razawy, W., Lagraauw, H. M., de Vries, M. R., Goossens, E. A., Boonstra, M. C., Hamming, J. F., Kandimalla, E. R., Kuiper, J., Quax, P. H., Nossent, A. Y. & Bot, I. Inhibition of MicroRNA-494 Reduces Carotid Artery Atherosclerotic Lesion Development and Increases Plaque Stability. Ann Surg 262, 841-847, (2015).

6   Han, H., Wang, Y. H., Qu, G. J., Sun, T. T., Li, F. Q., Jiang, W. & Luo, S. S. Differentiated miRNA expression and validation of signaling pathways in apoE gene knockout mice by cross-verification microarray platform. Exp. Mol. Med 45, e13, (2013).

7   Aavik, E., Lumivuori, H., Leppanen, O., Wirth, T., Hakkinen, S. K., Brasen, J. H., Beschorner, U., Zeller, T., Braspenning, M., van Criekinge, W., Makinen, K. & Yla-Herttuala, S. Global DNA methylation analysis of human atherosclerotic plaques reveals extensive genomic hypomethylation and reactivation at imprinted locus 14q32 involving induction of a miRNA cluster. Eur Heart J 36, 993-1000, (2015).

8   Gareri, C., S., D. R. & Indolfi, C. MicroRNAs for Restenosis and Thrombosis After Vascular Injury. Circ. Res 118, 1170-1184, (2016).

9   Ji, R., Cheng, Y., Yue, J., Yang, J., Liu, X., Chen, H., Dean, D. B. & Zhang, C. MicroRNA expression signature and antisense-mediated depletion reveal an essential role of MicroRNA in vascular neointimal lesion formation. Circ. Res 100, 1579-1588, (2007).

10   Lee, J., Lim, S., Song, B. W., Cha, M. J., Ham, O., Lee, S. Y., Lee, C., Park, J. H., Bae, Y., Seo, H. H., Seung, M., Choi, E. & Hwang, K. C. MicroRNA-29b Inhibits Migration and Proliferation of Vascular Smooth Muscle Cells in Neointimal Formation. J. Cell Biochem 116, 598-608, (2014).

11   von der Thusen, J. H., van Berkel, T. J. & Biessen, E. A. Induction of rapid atherogenesis by perivascular carotid collar placement in apolipoprotein E-deficient and low-density lipoprotein receptor-deficient mice. Circulation 103, 1164-1170, (2001).

12   Bhagat, L., Putta, M. R., Wang, D., Yu, D., Lan, T., Jiang, W., Sun, Z., Wang, H., Tang, J. X., La Monica, N., Kandimalla, E. R. & Agrawal, S. Novel oligonucleotides containing two 3'-ends complementary to target mRNA show optimal gene-silencing activity. J Med Chem 54, 3027-3036, (2011).

13   Troyan, S. L., Kianzad, V., Gibbs-Strauss, S. L., Gioux, S., Matsui, A., Oketokoun, R., Ngo, L., Khamene, A., Azar, F. & Frangioni, J. V. The FLARE intraoperative near-infrared fluorescence imaging system: a first-in-human clinical trial in breast cancer sentinel lymph node mapping. Ann. Surg. Oncol 16, 2943-2952, (2009).

14   Zhao, Y., Pennings, M., Hildebrand, R. B., Ye, D., Calpe-Berdiel, L., Out, R., Kjerrulf, M., Hurt-Camejo, E., Groen, A. K., Hoekstra, M., Jessup, W., Chimini, G., van Berkel, T. J. & M., V. E. Enhanced foam cell formation, atherosclerotic lesion development, and inflammation by combined deletion of ABCA1 and SR-BI in Bone marrow-derived cells in LDL receptor knockout mice on western-type diet. Circ. Res 107, e20-e31, (2010).

15   Benetatos, L., Hatzimichael, E., Londin, E., Vartholomatos, G., Loher, P., Rigoutsos, I. & Briasoulis, E. The microRNAs within the DLK1-DIO3 genomic region: involvement in disease pathogenesis. Cell Mol Life Sci 70, 795-814, (2013).

16   Rajewsky, N. microRNA target predictions in animals. Nat. Genet 38 Suppl, S8-13, (2006).

17   Doherty, T. M., Kastelein, R., Menon, S., Andrade, S. & Coffman, R. L. Modulation of murine macrophage function by IL-13. J. Immunol 151, 7151-7160, (1993).

18   Sheikh, F., Dickensheets, H., Pedras-Vasconcelos, J., Ramalingam, T., Helming, L., Gordon, S. & Donnelly, R. P. The Interleukin-13 Receptor-alpha1 Chain Is Essential for Induction of the Alternative Macrophage Activation Pathway by IL-13 but Not IL-4. J. Innate. Immun 7, 494-505, (2015).

19   Gotoh, K., Inoue, M., Masaki, T., Chiba, S., Shimasaki, T., Ando, H., Fujiwara, K., Katsuragi, I., Kakuma, T., Seike, M., Sakata, T. & Yoshimatsu, H. A novel anti-inflammatory role for spleen-derived interleukin-10 in obesity-induced inflammation in white adipose tissue and liver. Diabetes 61, 1994-2003, (2012).

20   Gotoh, K., Inoue, M., Masaki, T., Chiba, S., Shimasaki, T., Ando, H., Fujiwara, K., Katsuragi, I., Kakuma, T., Seike, M., Sakata, T. & Yoshimatsu, H. A novel anti-inflammatory role for spleen-derived interleukin-10 in obesity-induced hypothalamic inflammation. J Neurochem 120, 752-764, (2012).

21   Mallat, Z., Besnard, S., Duriez, M., Deleuze, V., Emmanuel, F., Bureau, M. F., Soubrier, F., Esposito, B., Duez, H., Fievet, C., Staels, B., Duverger, N., Scherman, D. & Tedgui, A. Protective role of interleukin-10 in atherosclerosis. Circ. Res 85, e17-e24,

(1999).

22   Holven, K. B., Halvorsen, B., Bjerkeli, V., Damas, J. K., Retterstol, K., Morkrid, L., Ose, L., Aukrust, P. & Nenseter, M. S. Impaired inhibitory effect of interleukin-10 on the balance between matrix metalloproteinase-9 and its inhibitor in mononuclear cells from hyperhomocysteinemic subjects. Stroke 37, 1731-1736, (2006).

23   Wang, P., Wu, P., Siegel, M. I., Egan, R. W. & Billah, M. M. Interleukin (IL)-10 inhibits nuclear factor kappa B (NF kappa B) activation in human monocytes. IL-10 and IL-4 suppress cytokine synthesis by different mechanisms. J. Biol. Chem 270, 9558-9563, (1995).

24   Eefting, D., Schepers, A., de Vries, M. R., Pires, N. M., Grimbergen, J. M., Lagerweij, T., Nagelkerken, L. M., Monraats, P. S., Jukema, J. W., van Bockel, J. H. & Quax, P. H. The effect of interleukin-10 knock-out and overexpression on neointima formation in hypercholesterolemic APOE*3-Leiden mice. Atherosclerosis 193, 335-342, (2007).

25   Wang, X., Smith, P., Pu, L. L., Kim, Y. J., Ko, F. & Robson, M. C. Exogenous transforming growth factor beta(2) modulates collagen I and collagen III synthesis in proliferative scar xenografts in nude rats. J. Surg. Res 87, 194-200, (1999).

26   Mallat, Z., Gojova, A., Marchiol-Fournigault, C., Esposito, B., Kamate, C., Merval, R., Fradelizi, D. & Tedgui, A. Inhibition of transforming growth factor-beta signaling accelerates atherosclerosis and induces an unstable plaque phenotype in mice. Circ. Res 89, 930-934, (2001).

27   Newby, A. C. & Zaltsman, A. B. Molecular mechanisms in intimal hyperplasia. J. Pathol 190, 300-309, (2000).

28   Clark, A. L. & Naya, F. J. MicroRNAs in the Myocyte Enhancer Factor 2 (MEF2)-regulated Gtl2-Dio3 Noncoding RNA Locus Promote Cardiomyocyte Proliferation by Targeting the Transcriptional Coactivator Cited2. J. Biol. Chem 290, 23162-23172, (2015).

29   Liu, D., Zhang, X. L., Yan, C. H., Li, Y., Tian, X. X., Zhu, N., Rong, J. J., Peng, C. F. & Han, Y. L. MicroRNA-495 regulates the proliferation and apoptosis of human umbilical vein endothelial cells by targeting chemokine CCL2. Thromb. Res 135, 146-154, (2015).

30   Law, M. R., Wald, N. J. & Rudnicka, A. R. Quantifying effect of statins on low density lipoprotein cholesterol, ischaemic heart disease, and stroke: systematic review and meta-analysis. BMJ 326, 1423, (2003).

31   Hansson, G. K., Libby, P. & Tabas, I. Inflammation and plaque vulnerability. J. Intern. Med 278, 483-493, (2015).

Supplementary material

Supplemental tables

Supplemental Table 1. Sequences of miRs and GSOs.

MiR	Sequence
hsa/mmu-miR-494	5'-UGAAACAUACACGGGAAACCUC-3'
hsa/mmu-miR-495	5'-AAACAAACAUGGUGCACUUCUU-3'
mmu-miR-329	5'-AACACACCCAGCUAACCUUUUU-3'
GSO	**Sequence**
hsa/mmu-GSO-494	3'-ACTTTGTATGTGCCCTTTGGAG-X-GAGGTTTCCCGTGTATGTTTCA-3'
hsa/mmu-GSO-495	3'-TTTGTTTGTACCACGTGAAGAA-X-AAGAAGTGCACCATGTTTGTTT-3'
mmu-GSO-329	3'-TTGTGTGGGTCGATTGGAAAAA-X-AAAAAGGTTAGCTGGGTGTGTT-3'
negative control GSO	3'-TGTACGACTCCATAACGGT-X-TGGCAATACCTCAGCATGT-3'

'X': Phosphorothioate linker

'-NNN-': 2'-O-methyl-modified nucleotides

Supplemental Table 2. List of primers used for in vivo and in vitro mRNA quantification.

Gene	Forward primer	Reversed primer
Abca1	GGTTTGGAGATGGTTATACAATAGTTGT	TTCCCGGAAACGCAAGTC
Acvr1	GGAAGTCCGCCATTGCCCATC	GGTTGTTTCCCACATCAAGCTGGT
Ccr2	GCTGCCTGCAAAGACCAGAAGAG	TGCCGTGGATGAACTGAGGTAACA
Cd36	ATGGTAGAGATGGCCTTACTTGGG	AGATGTAGCCAGTGTATATGTAGGCTC
Cd59a	TCACTGGCGATCTGAAAAGTGTCTA	GCAGCACTATCTTGAGCCACATC
Cdkn1b	CGGCTGGGTTAGCGGAGCAGTGT	CCAGCGTTCGGGGAACCGTCTGAA
Hprt	TTGCTCGAGATGTCATGAAGGA	AGCAGGTCAGCAAAGAACTTATAG
Il10	GGGTGAGAAGCTGAAGACCCTC	TGGCCTTGTAGACACCTTGGTC
Il13ra1	TTCCAGTCTTTGTCGCAGTGGC	TTGCCAGGATCAGGAATTGGAGGA
Ldlr	TGAGGTTCCTGTCCATCTTCTTCCC	TTGATGTTCTTCAGCCGCCAGTTC
Lrp6	TTTGAACCCACCACCATCGCCTGCC	GCGGTGCAAAGTGCCGGTAGCTGTA
Mttp	TCTCACAGTACCCGTTCTTGGT	GAGAGACATATCCCCTGCCTGT
Rpl27	TGAAAGGTTAGCGGAAGTGC	TTTCATGAACTTGCCCATCTC
Tgfβ2	AGACCCCACATCTCCTGCTAATC	AATCAATGTAAAGAGGGCGAAGGC
Timp2	GTTTATCTACACGGCCCCCTCTT	ATCTTGCCATCTCCTTCTGCCTT
Tlr7	TGCAGGAGCTGGTGGCAAAATTGGA	TGCTGAGCTGTATGCTCTGGGAAAGGT

Supplemental figures
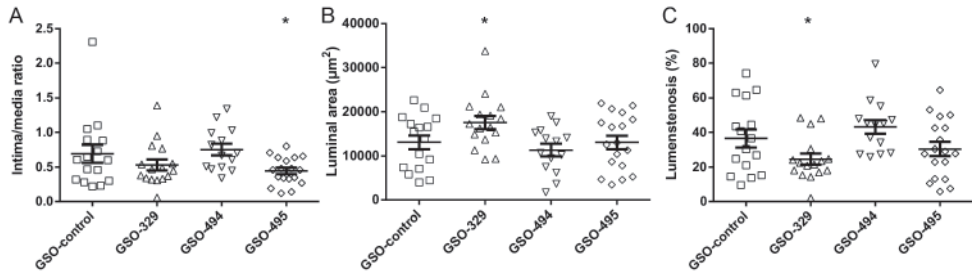
Supplemental figure 1. 14q32 microRNA inhibition in the femoral artery cuff model. (A) Quantification of intima/media ratio, (B) luminal area and (C) lumenstenosis, 21 days after cuff placement in C57Bl/6J mice treated with GSOs (±SEM). *$p<0.05$ compared to GSO-control.
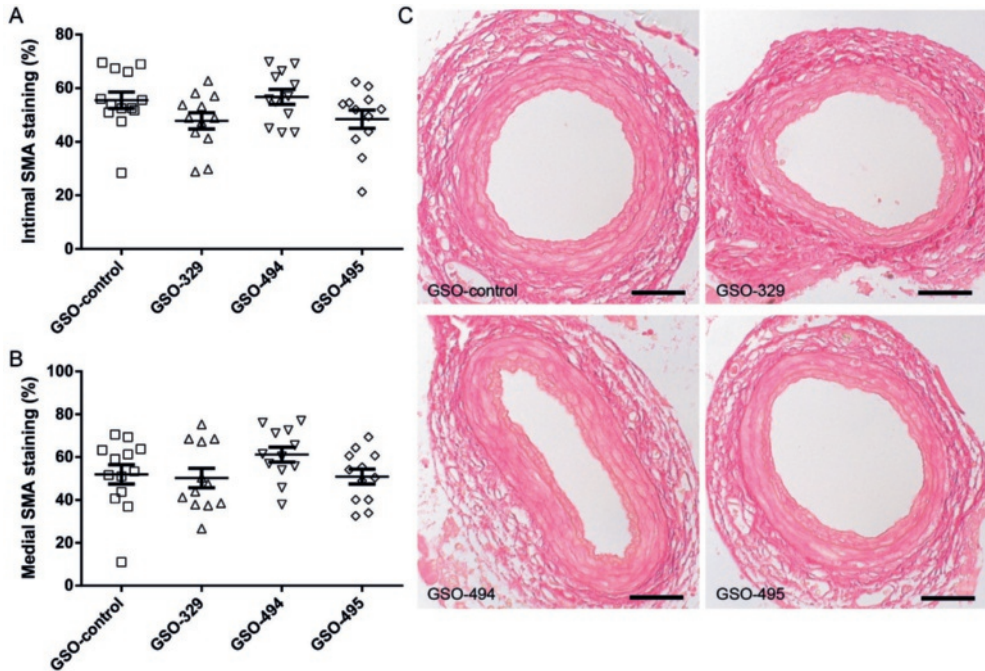
Supplemental figure 2. Effect of 14q32 microRNA inhibition on collagen content. Quantification of intimal (A) and medial (B) collagen content (%) 21 days after cuff placement in C57BL/6J mice (n=10 per group) treated with GSOs (±SEM). (C) Representative images of Sirius Red staining of cuffed femoral arteries (scale bar = 50 μm).
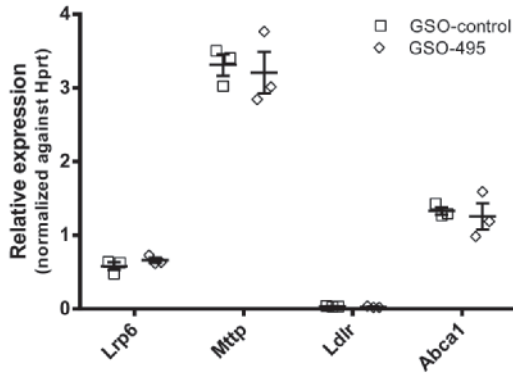
Supplemental figure 3. *In vivo* expression of putative miR-495 target genes in the liver of ApoE^{-/-} mice.
Mean expression levels of cholesterol metabolism related target genes Lrp6, Mttp, Ldlr and Abca1 in liver, relative to Hprt, are shown here 3 days after GSO-495 treatment (±SEM).
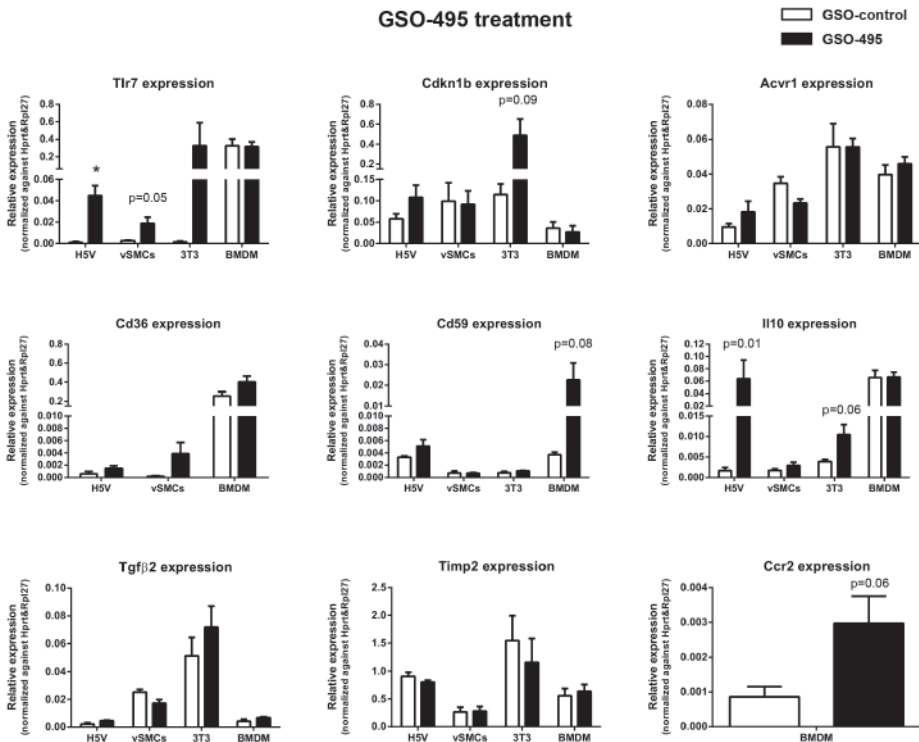
Supplemental figure 4. In vitro expression of putative miR-495 target genes in different cell types.
Mean expression levels of at least 3 independent experiments, relative to Hprt and Rpl27, are shown here (±SEM). Expression of selected genes were measured in H5Vs, vSMCs, 3T3s and BMDMs.*$p<0.05$.
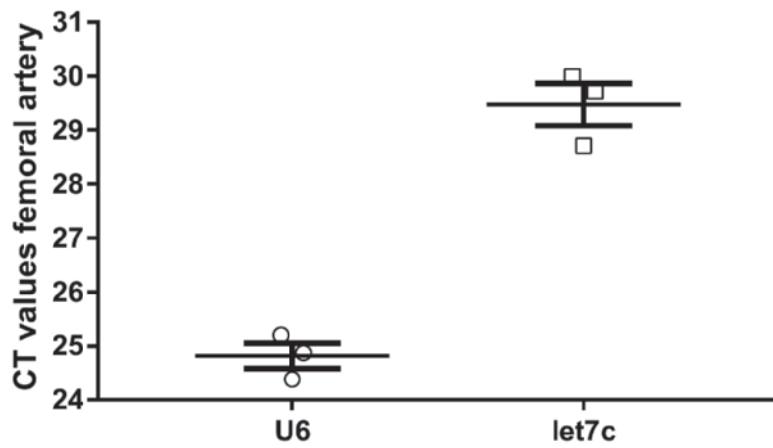
Supplemental figure 5. Expression of housekeeping genes in femoral artery. Average CT value of U6±SEM: 24.8±0.2; CT value of let7c±SEM: 29.5±0.4.

Chapter 7

Summary and general discussion

Summary and general discussion

Cardiovascular disease (CVD) is the collective term for all diseases that involve the heart or circulation, like myocardial infarction (MI), stroke, heart failure and restenosis. The major underlying cause of CVD is atherosclerosis, in which a lipid-driven chronic inflammation of the vessel wall leads to formation of atherosclerotic plaque. Clinical manifestations occur when the atherosclerotic plaque ruptures which subsequently leads to formation of a thrombus, that blocks the blood flow to adjacent tissue. Next to total blockage of the blood flow, it is also possible that clinical problems occur when an atherosclerotic plaque grows to a substantial size, leading to severely reduced blood flow. CVDs are not only one of the leading causes of morbidity and mortality worldwide, but they also are a major economic burden. Understanding the pathophysiology and underlying mechanisms of the different CVDs may offer new potential therapeutic approaches to reduce morbidity and mortality as well as to reduce the economic burden of CVDs.

The aim of thesis was to further investigate the role of inflammation in cardiac and vascular remodelling. This thesis focusses on different types of adverse cardiac and vascular remodelling, namely MI, myocardial ischemia-reperfusion (MI-R) injury, restenosis and accelerated atherosclerosis.

Potential immunomodulatory therapies against adverse cardiac remodelling

Phosphorylcholine (PC) is the polar head group of phosphatidylcholine, which is an important cell membrane phospholipid. PC is an endogenous ligand capable of triggering the innate immune system and it is expressed by apoptotic cells and oxidized LDL[1,2]. In **chapter 2** we investigated the effect of an antibody directed against PC on adverse cardiac remodelling following MI. We previously developed a fully humanized IgG antibody against PC (PC-mAb), which we tested in a mouse model for MI. We found that PC-mAb treatment decreased infarct size (IS) and left ventricular (LV) dilatation. To investigate the mechanism behind this cardioprotective effect of PC-mAb we measured systemic (C-C motif) ligand 2 (CCL2) concentrations and local leukocyte recruitment, and we analysed the circulating leukocytes using FACS. We demonstrated that serum CCL2 concentration was decreased upon PC-mAb treatment two days after MI, but not after three weeks. Interestingly, the number of cardiac leukocytes was decreased following PC-mAb treatment three weeks post MI, but not two days after MI. Finally, we observed an decrease in percentage circulating monocytes two days post MI. Taken together, we suggest PC-mAb treatment reduces adverse cardiac remodelling by attenuating both the early and late inflammatory response.

Reperfusion following a MI not only saves a portion of the cardiomyocytes in the ischemic area, it also boosts the inflammatory response leading to MI-R injury[3]. Therefore, adverse

remodelling following MI-R injury may be more susceptible for the anti-inflammatory effects of PC-mAb treatment than adverse cardiac remodelling following MI. The effect of PC-mAb treatment on adverse cardiac remodelling following MI-R injury was described in **chapter 3**. To study the effect of PC-mAb on adverse cardiac remodelling we used our mouse model for MI-R injury, in which the left anterior descending coronary artery was occluded for 45 minutes followed by permanent reperfusion. Furthermore, we investigated the post-reperfusion inflammatory response by examining CCL2 levels, local leukocyte recruitment and circulating leukocytes. We demonstrated that PC-mAb treatment reduces IS, while it preserves LV wall thickness three weeks post MI-R injury. In addition, PC-mAb treatment reduces LV dilatation leading to preservation of cardiac function. The post-reperfusion inflammatory response was decreased following PC-mAb treatment. Two days post MI-R injury systemic CCL2 level was significantly decreased following PC-mAb treatment, however this decrease in CCL2 concentration was not observed after three weeks. Local leukocyte infiltration was not decreased two days post MI-R injury upon PC-mAb treatment, however after three weeks number of infiltrated leukocytes was decreased in the interventricular septum, border zones and infarct area. Finally, we observed a decreased percentage circulating monocytes in the PC-mAb treated mice two days after MI-R injury. Interestingly, this reduction of circulating monocytes was mainly caused by a decrease of pro-inflammatory Ly6C^{high} monocytes, while anti-inflammatory Ly6C^{low} monocytes were not decreased upon PC-mAb treatment. We concluded that PC-mAb treatment limits adverse cardiac remodelling by attenuation of the early systemic inflammatory response and by reduction of the extended local inflammatory response.

The effect of PC-mAb treatment on adverse cardiac remodelling was investigated in two different mouse models, namely permanent MI and MI-R injury. We observed that PC-mAb treatment was capable to preserve cardiac function following MI-R injury, while this was not the case following permanent MI. We believe that there are several reasons for this difference: 1) in the MI-R injury model a portion of the cardiomyocytes in the ischemic area is saved by reperfusion, leading to a better preserved cardiac function, 2) in the MI-R injury model the inflammatory response is boosted and therefore PC-mAb treatment is better suited to target MI-R injury than permanent MI due to its anti-inflammatory properties.

Cardiac remodelling is a carefully orchestrated process, which can be divided to an inflammatory phase and a reparative and proliferative phase. In the inflammatory phase different pro-inflammatory immune cells remove dead cells and matrix debris from the infarct area, thereby promoting the healing process. In the reparative and proliferative phase the pro-inflammatory response is dampened and partly replaced by anti-inflammatory immune cells that boost scar formation[4]. Therefore, we postulate that rather than total abolishment of the post-infarct inflammatory response, timely suppression is beneficial against adverse cardiac remodelling following MI. In chapter

2 and 3 we show an decrease of the local inflammatory response three weeks after MI, but not two days after the ischemic insult. We suggest PC-mAb treatment reduces the adverse long term inflammatory response, while the necessary early inflammatory response in not affected and thereby reduces adverse cardiac remodelling.

Annexins are phospholipid-binding proteins and especially annexin A5 (AnxA5) is known to bind phosphatidylserine (PS)[5]. PS is expressed by apoptotic cells where it functions as an "eat me" signal for phagocytic cells[6,7]. By shielding of this "eat me" signal, AnxA5 exerts anti-apoptotic and anti-inflammatory properties[5]. In **Chapter 4** we investigated the therapeutic potential of (AnxA5) to treat adverse cardiac remodelling following MI-R injury. Using the same mouse model as described in chapter 3, we found that AnxA5 treatment reduced IS, while preserving LV wall thickness in the infarct area. Subsequently, LV dilatation was limited following AnxA5 treatment, which led to preservation of LV function. Interestingly, we found accumulation of AnxA5 in the infarct area of AnxA5 treated mice two days after MI-R injury, suggests AnxA5 is present at the desired location. Furthermore, to unravel the mechanism behind the cardioprotective effect of AnxA5 we analysed local macrophage infiltration. We found that following AnxA5 treatment, local macrophage infiltration was decreased both two days and three weeks post MI-R injury. Interestingly, a reduction of proliferating macrophages was observed in AnxA5 treated mice two days post MI-R injury, but not after three weeks. However, the percentage proliferating macrophages was comparable in both the vehicle and AnxA5 group. The cardiac macrophage population is maintained by both infiltration of monocytes (controlled in part by CCL2) and local macrophage proliferation[8]. Since we did not find any difference in systemic CCL2 levels and percentage proliferating macrophages was unaffected, the mechanism by which AnxA5 treatment reduces the number of cardiac macrophages is subject of future research. Nevertheless, we conclude that AnxA5 is a potential therapeutic agent against adverse cardiac remodelling by suppressing the inflammatory response.

The potential therapeutic effects of PC-mAb and AnxA5 against adverse cardiac remodelling described in chapter 2, 3 and 4 were studied a clinical relevant setting, namely by starting the treatment post-reperfusion and hypercholesterolemia. Hypercholesterolemia is an important risk factor for MI in human[9] and it has been shown that it affect cardiac remodelling in mice[10,11]. To mimic the clinical situation of most cardiovascular patients, we used hypercholesterolemic ApoE*3-Leiden mice, which only develop hypercholesterolemia when fed a high-fat diet[12]. Although plasma cholesterol levels in these mice are higher than in the clinical situation, we believe that this model is the closest resemblance regarding hypercholesterolemia available.
Most studies on potential therapeutic agents used a treatment strategy in which treatment was started before reperfusion was accomplished. In our opinion

this is not mimicking the clinical situation of MI patients. Therefore, at least in the MI-R injury studies, we used a treatment strategy in which we started treatment immediately after reperfusion. The clinical relevance regarding hypercholesterolemia and treatment strategy used in these studies, adds even more value to the already impressive cardioprotective effects of PC-mAb and AnxA5.

Epigenetic manipulation against adverse vascular remodelling

Epigenetic factors are factors that change gene expression, and thereby the phenotype of an organism, without altering the DNA sequence[13]. In this thesis we focus on two epigenetic systems, namely acetylation and microRNAs.

Acetylation is the introduction of an acetyl group to a chemical compound, while de-acetylation is the opposite, the removal of an acetyl group from a chemical compound. Gene expression can be controlled by the balance of acetylation and de-acetylation of certain proteins, like histones, the proteins around which the DNA is wrapped, but also many non-histone proteins can be acetylated and de-acetylated resulting in altered gene expression. Acetylation of histone proteins results in more loosely wrapped DNA around histones, thereby making the DNA more accessible for transcription, leading to increased gene expression[14]. In case of non-histone proteins, acetylation can lead to both increased and decreased gene expression, depending on the site of acetylation and the resulting fate of the protein, since acetylation of non-histone proteins affect processes, like protein stabilization and localization15. Proteins are usually acetylated and de-acetylated on specific lysine residues by lysine acetyltransferases and lysine deacetylases.

In **Chapter 5** we investigate the role of lysine acetyltransferase P300/CBP associated factor (PCAF) in adverse vascular remodelling. Using a mouse model for intimal hyperplasia in PCAF deficient mice we showed that PCAF deficiency results in decreases intimal hyperplasia development. It is known that PCAF is involved in acetylation of histone acetylation at the site of nuclear factor kappa-beta (NFκB) regulated genes[16-18]. NFκB is an important transcription factor which regulates expression of different pro-inflammatory genes, like tumor necrosis factor α (TNF-α), that are involved in intimal hyperplasia development[19]. Using *in vitro* experiments we showed that different cell types involved in vascular remodelling, reduce their production of pro-inflammatory cytokines, like TNF-α, interleukin-6 (IL-6), and CCL2, upon PCAF deficiency. However, we were not able to show *in vivo* that PCAF deficiency leads to a decreased inflammatory response, probably because the non-optimal time point to evaluate the *in vivo* inflammatory response. To overcome this problem, we studied the *in vivo* inflammatory response in hypercholesterolemic ApoE*3-Leiden mice, in which the inflammatory response is more explicit, at an earlier time point and using the natural PCAF inhibitor garcinol. Indeed, we found a significant reduction of CCL2 expression, and leukocyte and

macrophage infiltration in the vessel wall of mice treated with garcinol. In agreement, we found that garcinol reduced the TNF-α and CCL2 production *in vitro*.

Intimal hyperplasia is not only the result of inflammation, but vascular smooth muscle cell (VSMC) migration and proliferation play also an important role[20]. We observed that PCAF deficiency leads to a decrease of VSMCs in the intimal layer of the vessel wall. Future research is needed to further unravel if PCAF deficiency directly influences VSMC proliferation/migration or that PCAF deficiency impacts VSMC proliferation/migration indirectly via inflammation.

In conclusion, we show that PCAF is involved intimal hyperplasia development and vascular inflammation. This is caused by a direct or indirect effect of PCAF on the inflammatory response, and VSMC proliferation and migration.

MicroRNAs are short endogenous non-coding RNA molecules, which bind to the 3'UTR of their target genes, which can be up to several hundred for a single microRNA and thereby regulate expression of those target genes[21]. Since microRNAs are capable of fine-tuning gene expression of so many targets genes, they can regulate multifactorial processes like adverse vascular remodelling[22]. In **chapter 6** we focus on the role of several members of the 14q32 microRNA cluster in adverse vascular remodelling. Using Gene Silencing Oligonucleotides (GSOs), a relative new microRNA inhibitor with increased specificity and less adverse side effects than the widely used antagomirs, we inhibited expression of microRNA-329, -494 and -495 in a mouse model for intimal hyperplasia. We found that inhibition of microRNA-495 resulted in a decrease in intimal hyperplasia development, while inhibition of microRNA-329 resulted in a near-significant reduction of intimal hyperplasia. Both inflammation and VSMC proliferation play an important role in intimal hyperplasia development[20]. Interestingly, we found that GSO-495 treatment in reduced both macrophage infiltration and VSMC proliferation *in vivo*.

Since no effect on intimal hyperplasia was observed upon microRNA-494, we decided to only investigate the effect of microRNA-329 and -495 inhibition on accelerated atherosclerosis development. We observed a significant reduction of collar-induced atherosclerotic plaque formation upon microRNA-495 inhibition, while treatment with GSO-329 again resulted in a near-significant effect. Atherosclerotic plaque stability is determined by several parameters, namely necrotic core size, macrophage influx, VSMC content and collagen content[23]. We found that inhibition of microRNA-495 led to a reduction in necrotic core size and macrophage infiltration, while collagen content was increased. Taken together this indicates that GSO-495 treatment not only leads to smaller plaques, but the remaining plaque also showed a more stable phenotype.

Since accelerated atherosclerosis was studied in hypercholesterolemic ApoE$^{-/-}$ mice and microRNA-495 has some putative targets involved in cholesterol metabolism we measured cholesterol levels following GSO-495 treatment. Despite no effects were found on expression of the putative target genes (e.g. Lrp6, Mttp, Ldlr and Abca1),

we found that inhibition of microRNA-495 results in decreased plasma cholesterol levels. Moreover, the observed reduction of plasma cholesterol could be attributed to a reduction of very low-density lipoprotein (VLDL), which is, together with LDL, known as the pro-atherosclerotic lipoprotein. We suggest that the reduction of VLDL plasma cholesterol is, at least partly, responsible for the decreased plaque size and increased plaque stability.

Next to the targets mentioned in the paragraph above, we investigated the effect of microRNA-495 inhibition on the expression of several targets putative targets. We found that treatment with GSO-495 led to significant upregulation of Tgfβ2 and Il13ra1, while a modest upregulation was shown for Acvr1 and Il10. Using reversed target prediction a total of 37 putative murine atherosclerosis-related targets genes for microRNA-495 were identified[24]. In our study we were able to show upregulation of only two of the putative targets, which seem unable to result in the observed effect on adverse vascular remodelling. However, in agreement with Van Rooij *et al.*[21], we believe that rather than upregulation of one or two targets genes, it is the sum of many modest upregulated target genes that are responsible for the observed effect on adverse vascular remodelling.

Previously it was shown that microRNA-495 inhibition results in increased therapeutic neovascularization following ischemia[25]. Both therapeutic neovascularization and atherogenesis are influenced by similar cellular mechanisms, like cytokine and adhesion molecule expression. However, factors that increase therapeutic neovascularization usually also increase atherogenesis, this trade-off is also called the Janus phenomenon[26]. The fact that microRNA-495 positively influences both therapeutic neovascularization and adverse vascular remodelling, and thus breaks with the Janus phenomenon, makes it a very interesting potential therapeutic target.

Future perspective

The aim of this thesis was to investigate the role of inflammation in adverse vascular and cardiac remodelling and thereby find new potential therapeutic targets and agents. Potential immunomodulatory therapies are subject of research for decades and in 2017 Ridker *et. al.* showed for the first time that an anti-inflammatory agent reduces CVD[27]. However, the results in most clinical trials are, despite promising pre-clinical studies, disappointing. One of the reasons for the disappointing results is that the immunomodulatory therapies were focussed on single factors and/or factors that take place relatively late in the inflammatory pathway. To overcome this problem we investigated potential targets that influence the inflammatory process earlier in the pathway or factors that are capable to influence multiple processes. In chapter 2, 3 and 4 we investigated PC-mAb and AnxA5 treatment against adverse cardiac remodelling, both potential therapeutic agents capable of binding to endogenous ligands that can trigger the innate immune system. By shielding of endogenous ligands before they

are recognized by the immune system, the inflammatory response is prevented at the earliest time point. In chapter 5 and 6 we described the role of PCAF and microRNA-495 in adverse vascular remodelling, two factors that are capable to influence multiple processes. In the next paragraph the current status of the potential therapeutic agents will be discussed.

Phase 1 clinical trials showed PC-mAb is safe to use in healthy volunteers and peripheral artery disease patients. Therefore, PC-mAb is currently investigated in a phase 2 clinical trial to study efficiency in a relevant patients population. AnxA5 treatment has been shown to be very effective in different mouse models, but AnxA5 therapy is not subject of a clinical trial yet. However, radiolabeled AnxA5 is widely used as a diagnostic tool. Thus, one can imagine that AnxA5 therapy alone likely will not possess severe side effects. In chapter 5 we investigated the role of PCAF in adverse vascular remodelling, in which we used the natural PCAF inhibitor garcinol. Due to its anti-inflammatory and anti–proliferative properties, garcinol treatment is investigated as potential therapy against several diseases, including cancer and bacterial infection, but also against Alzheimer disease. However, clinical data is lacking, therefore, further research regarding pharmacokinetics is required before garcinol can enter a clinical trial. Next to garcinol, many other PCAF inhibitors are under investigation for their therapeutic potential against different diseases, increasing the possibility that a PCAF specific therapy will eventually be found. Miravirsen, a microRNA-122 inhibitor which reduce the replication of hepatitis C virus, is currently the only one microRNA inhibitor that entered a clinical trial[28]. The phase 1 trial showed it is safe to use a microRNA-based treatment in human. However, Miravirsen is a so-called locked nucleic acid, which is chemically different compared to our GSOs. Therefore, further research regarding pharmacokinetics and dosing are necessary should be performed regarding GSO therapy before it can enter clinical trials.

In conclusion, this thesis presents further understanding in the role of inflammation in adverse cardiac and vascular remodelling. Furthermore, the studies included in this thesis identified potential immunomodulatory therapeutic agents against adverse vascular and cardiac remodelling. Future research will show if the potential therapeutic agents can successfully be used in patients suffering from CVD.

References

1   Miller, Y. I., Choi, S. H., Wiesner, P., Fang, L., Harkewicz, R., Hartvigsen, K., Boullier, A., Gonen, A., Diehl, C. J., Que, X., Montano, E., Shaw, P. X., Tsimikas, S., Binder, C. J. & Witztum, J. L. Oxidation-specific epitopes are danger-associated molecular patterns recognized by pattern recognition receptors of innate immunity. Circ Res 108, 235-248, (2011).

2   Chang, M. K., Binder, C. J., Miller, Y. I., Subbanagounder, G., Silverman, G. J., Berliner, J. A. & Witztum, J. L. Apoptotic cells with oxidation-specific epitopes are immunogenic and proinflammatory. J Exp Med 200, 1359-1370, (2004).

3   Ibanez, B., Heusch, G., Ovize, M. & Van de Werf, F. Evolving therapies for myocardial ischemia/reperfusion injury. J Am Coll Cardiol 65, 1454-1471, (2015).

4   Prabhu, S. D. & Frangogiannis, N. G. The Biological Basis for Cardiac Repair After Myocardial Infarction: From Inflammation to Fibrosis. Circ Res 119, 91-112, (2016).

5   Reutelingsperger, C. P. & van Heerde, W. L. Annexin V, the regulator of phosphatidylserine-catalyzed inflammation and coagulation during apoptosis. Cell Mol Life Sci 53, 527-532, (1997).

6   Fadok, V. A., Bratton, D. L., Frasch, S. C., Warner, M. L. & Henson, P. M. The role of phosphatidylserine in recognition of apoptotic cells by phagocytes. Cell Death Differ 5, 551-562, (1998).

7   van Genderen, H. O., Kenis, H., Hofstra, L., Narula, J. & Reutelingsperger, C. P. Extracellular annexin A5: functions of phosphatidylserine-binding and two-dimensional crystallization. Biochim Biophys Acta 1783, 953-963, (2008).

8   Hilgendorf, I., Gerhardt, L. M., Tan, T. C., Winter, C., Holderried, T. A., Chousterman, B. G., Iwamoto, Y., Liao, R., Zirlik, A., Scherer-Crosbie, M., Hedrick, C. C., Libby, P., Nahrendorf, M., Weissleder, R. & Swirski, F. K. Ly-6Chigh monocytes depend on Nr4a1 to balance both inflammatory and reparative phases in the infarcted myocardium. Circ Res 114, 1611-1622, (2014).

9   Yusuf, S., Hawken, S., Ounpuu, S., Dans, T., Avezum, A., Lanas, F., McQueen, M., Budaj, A., Pais, P., Varigos, J. & Lisheng, L. Effect of potentially modifiable risk factors associated with myocardial infarction in 52 countries (the INTERHEART study): case-control study. Lancet 364, 937-952, (2004).

10   Girod, W. G., Jones, S. P., Sieber, N., Aw, T. Y. & Lefer, D. J. Effects of hypercholesterolemia on myocardial ischemia-reperfusion injury in LDL receptor-deficient mice. Arterioscler Thromb Vasc Biol 19, 2776-2781, (1999).

11   Jones, S. P., Girod, W. G., Marotti, K. R., Aw, T. Y. & Lefer, D. J. Acute exposure to a high cholesterol diet attenuates myocardial ischemia-reperfusion injury in cholesteryl ester transfer protein mice. Coron Artery Dis 12, 37-44, (2001).

12   Lardenoye, J. H., Delsing, D. J., de Vries, M. R., Deckers, M. M., Princen, H. M., Havekes, L. M., van Hinsbergh, V. W., van Bockel, J. H. & Quax, P. H. Accelerated atherosclerosis by placement of a perivascular cuff and a cholesterol-rich diet in ApoE*3Leiden transgenic mice. Circ Res 87, 248-253, (2000).

13   Fraga, M. F., Ballestar, E., Paz, M. F., Ropero, S., Setien, F., Ballestar, M. L., Heine-Suner, D., Cigudosa, J. C., Urioste, M., Benitez, J., Boix-Chornet, M., Sanchez-Aguilera, A., Ling, C., Carlsson, E., Poulsen, P., Vaag, A., Stephan, Z., Spector, T. D., Wu, Y. Z., Plass, C. & Esteller, M. Epigenetic differences arise during the lifetime of monozygotic twins. Proc Natl Acad Sci U S A 102, 10604-10609, (2005).

14   Struhl, K. Histone acetylation and transcriptional regulatory mechanisms. Genes Dev 12, 599-606, (1998).

15   Glozak, M. A., Sengupta, N., Zhang, X. & Seto, E. Acetylation and deacetylation of non-histone proteins. Gene 363, 15-23, (2005).

16   Sheppard, K. A., Rose, D. W., Haque, Z. K., Kurokawa, R., McInerney, E., Westin, S., Thanos, D., Rosenfeld, M. G., Glass, C. K. & Collins, T. Transcriptional activation by NF-kappaB requires multiple coactivators. Mol Cell Biol 19, 6367-6378, (1999).

17   Miao, F., Gonzalo, I. G., Lanting, L. & Natarajan, R. In vivo chromatin remodeling events leading to inflammatory gene transcription under diabetic conditions. J Biol Chem 279, 18091-18097, (2004).

18   Pons, D., de Vries, F. R., van den Elsen, P. J., Heijmans, B. T., Quax, P. H. & Jukema, J. W. Epigenetic histone acetylation modifiers in vascular remodelling: new targets for therapy in cardiovascular disease. Eur Heart J 30, 266-277, (2009).

19   Monraats, P. S., Pires, N. M., Schepers, A., Agema, W. R., Boesten, L. S., de Vries, M. R., Zwinderman, A. H., de Maat, M. P., Doevendans, P. A., de Winter, R. J., Tio, R. A., Waltenberger, J., t Hart, L. M., Frants, R. R., Quax, P. H., van Vlijmen, B. J., Havekes, L. M., van der Laarse, A., van der Wall, E. E. & Jukema, J. W. Tumor necrosis factor-alpha plays an important role in restenosis development. Faseb j 19, 1998-2004, (2005).

20   Simon, D. I. Inflammation and vascular injury: basic discovery to drug development. Circ J 76, 1811-1818, (2012).

21   van Rooij, E. & Olson, E. N. MicroRNA therapeutics for cardiovascular disease: opportunities and obstacles. Nat Rev Drug Discov 11, 860-872, (2012).

22   Welten, S. M., Goossens, E. A., Quax, P. H. & Nossent, A. Y. The multifactorial nature of microRNAs in vascular remodelling. Cardiovasc Res 110, 6-22, (2016).

23   Hansson, G. K., Libby, P. & Tabas, I. Inflammation and plaque vulnerability. J Intern Med 278, 483-493, (2015).

24   Wezel, A., Welten, S. M., Razawy, W., Lagraauw, H. M., de Vries, M. R., Goossens, E. A., Boonstra, M. C., Hamming, J. F., Kandimalla, E. R., Kuiper, J., Quax, P. H., Nossent, A. Y. & Bot, I. Inhibition of MicroRNA-494 Reduces Carotid Artery

Atherosclerotic Lesion Development and Increases Plaque Stability. Ann Surg 262, 841-847; discussion 847-848, (2015).

25   Welten, S. M., Bastiaansen, A. J., de Jong, R. C., de Vries, M. R., Peters, E. A., Boonstra, M. C., Sheikh, S. P., La Monica, N., Kandimalla, E. R., Quax, P. H. & Nossent, A. Y. Inhibition of 14q32 MicroRNAs miR-329, miR-487b, miR-494, and miR-495 increases neovascularization and blood flow recovery after ischemia. Circ Res 115, 696-708, (2014).

26   Epstein, S. E., Stabile, E., Kinnaird, T., Lee, C. W., Clavijo, L. & Burnett, M. S. Janus phenomenon: the interrelated tradeoffs inherent in therapies designed to enhance collateral formation and those designed to inhibit atherogenesis. Circulation 109, 2826-2831, (2004).

27   Ridker, P. M. et al. Antiinflammatory Therapy with Canakinumab for Atherosclerotic Disease. The New England journal of medicine 377, 1119-1131, (2017).

28   Simonson, B. & Das, S. MicroRNA Therapeutics: the Next Magic Bullet? Mini Rev Med Chem 15, 467-474, (2015).

Nederlandse samenvatting

Cardiovasculaire ziekten zijn alle aandoeningen met betrekking tot het hart en de bloedvaten, zoals hartinfarct, beroerte, hartfalen en restenose. Atherosclerose, een door vet gedreven chronische ontsteking aan de vaatwand die leidt tot de ontwikkeling van een atherosclerotische plaque, is de belangrijkste achterliggende oorzaak van cardiovasculaire ziekten. Klinische symptomen als gevolg van atherosclerose ontstaan op het moment dat de atherosclerotische plaque scheurt en er een bloedprop ontstaat die de bloedtoevoer voor achterliggend weefsel blokkeert. Daarnaast kunnen er ook klinische symptomen ontstaan zonder dat de atherosclerotische plaque scheurt. In dat geval kan de plaque zo groot worden dat het de bloedtoevoer tot achterliggend weefsel ernstig verminderd. Cardiovasculaire ziekten zijn niet alleen een van de belangrijkste oorzaken van mortaliteit en morbiditeit, maar het is daarnaast ook een enorme economische last. Meer inzicht in de achterliggende mechanismen van cardiovasculaire ziekten kunnen leiden tot nieuwe therapieën, die vervolgens niet alleen kunnen leiden tot minder mortaliteit en morbiditeit, maar ook tot minder economische last.

Het doel van dit proefschrift was om de rol van ontsteking in cardiale en vasculaire remodellering verder te ontrafelen. Er wordt in dit proefschrift onderzoek gedaan naar verschillende typen schadelijke remodellering namelijk: hartinfarct, ischemie-reperfusie schade van het hart, restenose en versnelde atherosclerose.

Potentiele immuun modulerende therapieën tegen schadelijke cardiale remodellering

Phosphorylcholine (PC) is de polaire kop van phosphatidylcholine, een belangrijk cel membraan phospholipide. PC is een endogeen ligand van het aangeboren immuun systeem en het wordt gepresenteerd op apoptotische cellen en geoxideerd LDL. In hoofdstuk 2 hebben we onderzoek gedaan naar het effect van een antilichaam gericht tegen PC tegen schadelijke remodellering als gevolg van een hartinfarct. In een eerder onderzoek hebben wij een gehumaniseerd IgG antilichaam ontwikkeld gericht tegen PC (PC-mAb). Dit antilichaam hebben wij getest in een muismodel waarin we een hartinfarct hebben geïnduceerd. Uit dit onderzoek bleek dat behandeling met PC-mAb ervoor zorgde dat infarctgrootte en linker ventrikel (LV) dilatatie verminderd waren. Om achter het mechanisme van dit beschermende effect van PC-mAb te komen hebben we gekeken naar (C-C motif) ligand 2 (CCL2) waarden in het serum, lokale leukocyten infiltratie en hebben we de leukocyten in het bloed geanalyseerd met FACS. Hieruit bleek dat CCL2 waarden in het serum twee dagen na infarct waren afgenomen als gevolg van behandeling met PC-mAb, drie weken na het infarct konden wij geen verschil in CCL2 waarden aantonen. Wat betreft leukocyten infiltratie in het hartweefsel zagen wij het tegenovergestelde effect namelijk, een sterk verminderd aantal leukocyten drie weken na infarct terwijl er geen verschil aanwezig was twee dagen na het infarct in de met PC-mAb behandelde muizen. Als laatste bleek ook het percentage circulerende monocyten verminderd twee dagen na infarct.

Samenvattend concluderen wij dat behandeling met PC-mAb de schadelijke cardiale remodellering als gevolg van een hartinfarct verminderd doordat het aangrijpt op zowel de vroege als de late ontstekingsreactie.

Meestal wordt een patiënt met een hartinfarct zo snel mogelijk geopereerd met als doel de bloedtoevoer naar het ischemische gebied te herstellen, dit wordt ook wel reperfusie genoemd. Reperfusie zorgt er dan voor dat een deel van de hartspiercellen in het ischemische gebied worden gered. Een nadeel van reperfusie is dat het ook de lokale ontstekingsreactie verhoogd, met als gevolg myocardiaal ischemie-reperfusie (MI-R) schade. Omdat de ontstekingsreactie verhoogd is bij MI-R schade en PC-mAb aangrijpt op de ontstekingsreactie, verwachtten wij dat PC-mAb behandeling schadelijke cardiale remodellering als gevolg van MI-R schade kan verminderen. Dit onderzoek is beschreven in hoofdstuk 3. Om dit te onderzoeken hebben wij gebruik gemaakt van een muismodel voor MI-R schade, waarin we een kransslagader 45 minuten blokkeren gevolgd door permanente reperfusie. Daarnaast hebben we de post MI-R ontstekingsreactie onderzocht door de CCL2 waarden, leukocyten infiltratie en de circulerende leukocyten te analyseren. Uit dit onderzoek bleek dat drie weken na MI-R, PC-mAb behandeling de infarctgrootte verminderd, terwijl de dikte van de LV wand behouden blijft. Daarnaast, werd LV dilatatie verminderd, terwijl de hartfunctie behouden bleef. Wat betreft de post MI-R ontstekingsreactie bleek ook deze verlaagd na behandeling met PC-mAb. Dit kwam tot uiting in verlaagde CCL2 concentraties in het serum twee dagen na MI-R schade als gevolg van PC-mAb behandeling, drie weken na MI-R schade, daarentegen, was de concentratie CCL2 niet verlaagd. Lokale leukocyten infiltratie bleek alleen verlaagd drie weken na MI-R schade als gevolg van PC-mAb behandeling, maar niet twee dagen na MI-R schade. Als laatste hebben we gekeken naar het percentage circulerende monocyten. Behandeling met PC-mAb resulteerde in een lager percentage circulerende monocyten. Nog interessanter was deze vermindering in circulerende monocyten veroorzaakt is door een vermindering van pro-inflammatoire $Ly6C^{high}$ monocyten, terwijl het percentage anti-inflammatoire $Ly6C^{low}$ gelijk bleef na behandeling met PC-mAb.

Deze studie laat zien dat PC-mAb behandeling schadelijke cardiale remodellering als gevolg van MI-R schade vermindert, doordat het zowel de vroege systemische als late lokale inflammatoire reactie verlaagd.

Cardiale remodellering is een zorgvuldig georganiseerd proces, dat onderverdeeld kan worden in verschillende fases, namelijk de inflammatoire fase en de reparatie fase. In de inflammatoire fase worden dode cellen en ander afvalmateriaal verwijderd door verschillende immuun cellen, wat het helingsproces ten goede komt. In de reparatie fase vermindert de pro-inflammatoire reactie en verschijnen er anti-inflammatoire immuun cellen die de ontwikkeling van littekenweefsel bevorderen. Daarom stellen wij dat, om schadelijke cardiale remodellering te reduceren, het beter is om de ontsteking op het juiste moment te verminderen, dan een onmiddellijke totale stopzetting van de ontstekingsreactie. In hoofdstuk 2 en 3 laten wij zien dat PC-mAb behandeling

de lokale ontstekingsreactie drie weken na MI vermindert, terwijl die na twee dagen niet is verminderd. Wij suggereren dat PC-mAb de nadelige langdurige ontstekingsreactie vermindert, terwijl de noodzakelijke acute ontsteking niet wordt aangedaan, waardoor schadelijke cardiale remodellering wordt gereduceerd.

Annexines zijn een groep eiwitten die bekend staan om hun phospholipide-bindende eigenschappen. Van deze annexines, staat annexine A5 (anxA5) bekend om zijn binding met phosphatidylserine (PS). PS komt tot expressie op apoptotische cellen, waar het functioneert als een "eet me op" signaal voor phagocytotische cellen. Door het "eet me op" signaal af te schermen heeft anxA5 een anti-apoptotische en anti-inflammatoire werking. In hoofdstuk 4 onderzoeken we het potentiele therapeutische vermogen van anxA5 tegen schadelijke cardiale remodellering na MI-R schade. Door gebruik te maken van het zelfde muismodel als in hoofdstuk 3, hebben wij uitgezocht dat AnxA5 behandeling infarctgrootte vermindert, terwijl de dikte van de LV wand behouden blijft. Verder was LV dilatatie verminderd, terwijl de hartfunctie behouden bleef. Erg interessant was ook de observatie van ophoping van AnxA5 in het infarct van de met AnxA5 behandelde muizen, waaruit dus blijkt dat AnxA5 daadwerkelijk op de gewenste plek terecht komt. Om meer te weten te komen over het mechanisme achter dit beschermende effect van AnxA5 hebben we de lokale macrofaag infiltratie geanalyseerd. Hieruit bleek dat zowel twee dagen en drie weken na MI-R schade het aantal macrofagen in het hartweefsel was verminderd als gevolg van AnxA5 behandeling. Daarnaast bleek ook het aantal prolifererende macrofagen verminderd in de AnxA5 groep. Dit effect was echter alleen aanwezig twee dagen na MI-R schade en niet na drie weken en bleek het percentage prolifererende macrofagen niet veranderd door AnxA5 behandeling. De populatie van macrofagen in het hart wordt in stand gehouden door infiltratie van monocyten (deels gestuurd door CCL2) en proliferatie van lokale macrofagen. Aangezien wij geen verschil zien in CCL2 concentraties en het percentage prolifererende macrofagen ook niet veranderd was, moet toekomstig onderzoek uitwijzen wat het mechanisme achter de reductie van het aantal macrofagen in het hart door AnxA5 behandeling is. Ondanks dat het mechanisme niet helemaal bekend is, kunnen we concluderen dat AnxA5 een potentieel therapeutisch middel is tegen schadelijke cardiale remodellering door de ontstekingsreactie te onderdrukken.

De potentiele therapeutische effecten van PC-mAb en AnxA5 tegen schadelijke cardiale remodellering beschreven in hoofdstuk 2 tot en met 4 zijn onderzocht in een klinisch relevante setting, namelijk door de behandeling te starten na reperfusie en in een model waarbij verhoogde cholesterolwaardes (ook wel hypercholesterolemie genoemd) geïnduceerd worden. Hypercholesterolemie is een belangrijke risico factor voor MI bij mensen en het blijkt het proces van cardiale remodellering te beïnvloeden. Om de klinische situatie van de meeste hartpatiënten zo goed mogelijk na te bootsen, hebben we gebruik gemaakt van zogenaamde ApoE*3-Leiden muizen, die alleen hypercholesterolemie ontwikkelen op het moment dat ze op een hoog vet dieet gezet worden. De plasma cholesterol waardes zijn weliswaar hoger in deze muizen dan de plasma cholesterol waardes in de meeste hartpatiënten, maar ondanks dat denken wij dat dit model de

klinische situatie wat betreft hypercholesterolemie het beste benaderd.

Veel studies naar potentiele therapeutische middelen tegen schadelijke cardiale remodellering maken gebruik van een behandelingsstrategie waarbij de behandeling gestart wordt voordat reperfusie gerealiseerd wordt. In onze ogen is dit niet vergelijkbaar met de klinische situatie van patiënten die een hartinfarct hebben gehad. Daarom hebben wij, in de studies waarin we het MI-R muismodel gebruiken, een behandelingsstrategie gekozen waarbij de behandeling gestart wordt direct na reperfusie.

Doordat wij onze studies hebben verricht in een, wat betreft hypercholesterolemie en behandelingsstrategie, zo realistisch mogelijke klinische situatie, kan er nog meer waarde gehecht worden aan de toch al indrukwekkende beschermende effecten van PC-mAb en AnxA5.

Epigenetische manipulatie tegen vaatwand remodellering

Epigenetische factoren kunnen worden omschreven als factoren die genexpressie kunnen beïnvloeden, en dus het fenotype van een organisme, zonder de DNA sequentie te veranderen. In dit proefschrift belichten we twee epigenetische systemen, namelijk acetylatie en microRNAs. Bij acetylatie wordt een acetylgroep verbonden aan een chemische stof of eiwit, terwijl bij de-acetylatie het omgekeerde gebeurt, namelijk de afsplitsing van een acetylgroep. Genexpressie kan beïnvloed worden door de balans van acetylatie en de-acetylatie van bepaalde eiwitten, zoals histonen, de eiwitten waar het DNA omheen is gewikkeld. Ook andere eiwitten kunnen geacetyleerd en gedeacetyleerd worden, wat kan leiden tot verandering in genexpressie. Acetylatie van histonen zorgt ervoor dat het DNA minder strak om de histonen is gewikkeld waardoor het DNA beter bereikbaar is voor transcriptie, wat leidt tot een verhoging van genexpressie. In het geval van de niet-histon eiwitten kan acetylatie leiden tot zowel verhoging als verlaging van genexpressie. Dit is afhankelijk van de precieze plek in het eiwit waar de acetylering plaatsvindt en het directe gevolg voor dat eiwit. Acetylering van niet-histon eiwitten heeft namelijk invloed op verschillende eiwit eigenschappen, zoals eiwitstabiliteit en eiwit locatie binnen de cel. Verder is bekend dat eiwitten worden geacetyleerd en ge-deacetyleerd op specifieke lysines binnen een eiwit, door specifieke enzymen, namelijk de lysine acetyltransferases en lysine deacetylases.
In hoofdstuk 5 onderzoeken we de rol van lysine acetyltransferase P300/CBP associated factor (PCAF) in schadelijke vaatwand remodellering. Door gebruik te maken van een muismodel voor intimale hyperplasie in PCAF deficiënte muizen hebben we gevonden dat PCAF deficiëntie leidt tot vermindering van intimale hyperplasie. Het is bekend dat PCAF betrokken is bij de acetylatie van histonen waar nuclear factor kappa-beta (NFκB) gereguleerde genen omheen gewikkeld zijn. NFκB is een belangrijke transcriptie factor die de genexpressie van veel pro-inflammatoire genen reguleert, zoals tumor necrosis factor α (TNF-α), wat weer gerelateerd is aan de ontwikkeling van intimale hyperplasie. In een aantal in vitro experimenten laten wij zien dat, in geval van PCAF deficiëntie, verschillende celtypen die betrokken zijn bij vaatwand remodellering, minder

pro-inflammatoire cytokines, zoals TNF-α, interleukine-6 (IL-6) en CCL2, produceren. Deze vermindering van ontstekingsreactie konden wij helaas niet in ons in vivo experiment met PCAF deficiënte muizen bevestigen, waarschijnlijk doordat dit werd geanalyseerd op een moment dat de ontstekingsreactie al grotendeels was uitgedoofd. Om dit toch te onderzoeken hebben we de in vivo ontstekingsreactie onderzocht in hypercholesterolemische ApoE*3-Leiden muizen, waarin de ontstekingsreactie prominenter aanwezig is. Daarnaast hebben we gebruik gemaakt van de farmacologische PCAF remmer garcinol en hebben we de ontstekingsreactie op een eerder tijdspunt geanalyseerd. Hieruit bleek dat de CCL2 expressie was verminderd in de vaatwand na behandeling met garcinol. Daarnaast was zowel leukocyt infiltratie als macrofaag infiltratie in de vaat wand afgenomen na garcinol behandeling. Ook uit in vitro experimenten bleek dat garcinol de TNF-α en CCL2 productie reduceert.

Intimale hyperplasie ontstaat niet alleen onder invloed van ontsteking, ook de migratie en proliferatie van gladde spiercellen speelt een belangrijke rol. Uit ons onderzoek bleek dat PCAF deficiëntie leidt tot een vermindering van gladde spiercellen in de intima (binnenste cellaag) van de vaatwand. De toekomst moet uitwijzen of PCAF deficiëntie direct betrokken is bij de migratie en/of proliferatie van gladde spiercellen, of dat er sprake is van een indirect effect via de ontstekingsreactie.

Concluderend kunnen we stellen dat PCAF een rol speelt in intimale hyperplasie en vaatwandontsteking. Dit wordt veroorzaakt door een direct of indirect effect van PCAF op de ontstekingsreactie en gladde spiercel migratie en proliferatie.

MicroRNAs zijn korte endogene niet-coderende RNA moleculen, die genexpressie kunnen reguleren van specifieke genen (targetgenen), door te binden aan de zogenaamde 3' untranslated regio van die targetgenen. Omdat microRNAs meerdere targetgenen kunnen hebben, soms wel meer dan honderd voor één microRNA, zijn zij in staat om multifactoriële processen te beïnvloeden, zoals schadelijke vaatwand remodellering. In hoofdstuk 6 focussen we ons op de rol van een aantal microRNAs van het 14q32 microRNA cluster in schadelijke vaatwand remodellering. Door gebruik te maken van zogenaamde Gene Silencing Oligo's (GSOs), een relatief nieuwe microRNA-remmer met een hogere specificiteit en minder schadelijke bijwerkingen dan de nu veel gebruikte antagomirs, hebben we de expressie van microRNA-329, -494 en -495 geremd in ons muismodel voor intimale hyperplasie. Hieruit bleek dat remming van microRNA-495 resulteerde in minder intimale hyperplasie. Daarnaast bleek dat remming van microRNA-329, hoewel niet significant, ook resulteerde in een vermindering van intimale hyperplasie. Zowel de ontstekingsreactie als proliferatie van gladde spiercellen spelen een belangrijke rol in de ontwikkeling van intimale hyperplasie. Daarom was het erg interessant dat remming van microRNA-495 zowel de macrofaag influx als gladde spiercel proliferatie in de vaatwand verminderde.

Omdat remming van microRNA-494 geen effect bleek te hebben op intimale hyperplasie,

besloten we ons verder te concentreren op het effect van microRNA-329 en -495 remming op versnelde atherosclerose. Remming van microRNA bleek collar-geïnduceerde plaque formatie te verminderen, terwijl remming van microRNA-329 wederom resulteerde een net niet-significante vermindering van plaque formatie. De stabiliteit van een atherosclerotische plaque wordt bepaald door een aantal eigenschappen. Dit zijn: de grootte van de necrotische kern, macrofaag influx, het percentage gladde spiercellen en het percentage collageen in de vaatwand. Wij observeerden dat remming van microRNA-495 leidde tot een kleinere necrotische kern, minder macrofaag influx en een verhoging van percentage collageen in de vaatwand. Dit betekent dat remming van microRNA-495 niet alleen de ontwikkeling van een atherosclerotische plaque remt, maar ook de stabiliteit van de plaque verhoogd.

Het effect van microRNA remming in versnelde atherosclerose is onderzocht in hypercholesterolemische ApoE-/- muizen. Omdat microRNA-495 een aantal mogelijke targetgenen heeft die een rol spelen in cholesterolmetabolisme, hebben we gekeken of remming van microRNA-495 effect heeft op cholesterolwaardes. Ondanks dat remming van microRNA-495 geen effect heeft op de expressie van de mogelijke targetgenen gerelateerd aan cholesterolmetabolisme (Lrp6, Mttp, Ldlr en Abca1), bleek dat plasma cholesterolwaardes verlaagd waren. Bovendien bleek dat deze verlaging in cholesterol vooral bestaat uit een verlaging van very-low-density-lipoproteïne (VLDL), die, samen met LDL, bekend staat als pro-atherosclerotisch lipoproteïne. Wij denken dat de reductie van VLDL cholesterol, in ieder geval gedeeltelijk, de oorzaak is van de verlaagde plaqueontwikkeling en de verhoging van de plaquestabiliteit.

Naast de bovengenoemde cholesterol gerelateerde targetgenen, hebben we gekeken of microRNA-495 remming effect heeft op de expressie van andere mogelijke targetgenen die invloed kunnen hebben op vasculaire remodellering. Hieruit bleek dat de expressie van Tgfβ2 en Il13ra1 significant verhoogd was, terwijl de expressie van Acvr1 en Il10 in beperkte mate verhoogd bleek. Door gebruik te maken van 'reverse target prediction' hebben we 37 mogelijke targetgenen van microRNA-495 gevonden. Hiervan konden we maar van twee aantonen dat de expressie daadwerkelijk was verhoogd. Het lijkt onwaarschijnlijk dat dit de waargenomen remming van schadelijk vasculaire remodellering kan verklaren. Maar wij denken dat, in plaats van upregulatie van twee targetgenen, de som van vele kleine expressieveranderingen van de targetgenen het effect van microRNA-495 remming op vasculaire remodellering kan verklaren.

Uit eerder onderzoek is gebleken dat remming van microRNA-495 resulteert in therapeutische neovascularisatie na ischemie. Zowel therapeutische neovascularisatie als atherogenese worden beïnvloedt door dezelfde cellulaire mechanismen, zoals de expressie van cytokines en adhesie moleculen. Vaak is het zo dat factoren die therapeutische neovascularisatie verhogen ook de atherogenese verhogen, dit wordt ook wel het Janus fenomeen genoemd. Het feit dat remming van microRNA-495, zowel therapeutische neovascularisatie en atherogenese op een positieve manier beïnvloedt, en dus breekt met het Janus fenomeen, maakt het een extra interessant

therapeutisch middel.

Toekomstperspectieven

Het doel van dit proefschrift was om de rol van ontsteking in vasculaire en cardiale remodellering verder te ontrafelen en daarbij nieuwe mogelijke therapeutische middelen en targets te vinden. Onderzoek naar potentiele immuun modulerende therapieën wordt al tientallen jaren gedaan, maar ondanks veelbelovende preklinische studies, zijn de resultaten in klinische trials vaak tegenvallend. Een van de redenen voor de tegenvallende resultaten is dat de immuun modulerende therapieën vaak gericht waren op één enkele factor uit het ontstekingsproces of op factoren die een rol spelen relatief laat in het ontstekingsproces. Om dit probleem te overwinnen hebben wij onderzoek gedaan naar potentiele targets die een rol spelen vroeg in het ontstekingsproces of factoren die meerdere processen kunnen beïnvloeden. In hoofdstuk 2, 3 en 4 hebben we PC-mAb en AnxA5 onderzocht als behandeling tegen schadelijke cardiale remodellering. Deze potentiele therapeutische middelen hebben beide het vermogen om te binden aan endogene liganden die het aangeboren immuunsysteem kunnen activeren. Doordat deze endogene liganden worden afgeschermd voor het aangeboren immuun systeem, wordt de ontstekingsreactie op het vroegst mogelijke tijdspunt afgeremd. In hoofdstuk 5 en 6 beschrijven we de rol van PCAF en microRNA-495 in schadelijke vasculaire remodellering. Deze factoren zijn in staat om meerdere processen, die gerelateerd zijn aan vasculaire remodellering, te beïnvloeden. In de komende paragraaf zal de huidige status van deze potentiele therapeutische middelen besproken worden. Uit fase 1 klinische trials is gebleken dat PC-mAb veilig is bevonden na toediening bij gezonde vrijwilligers en patiënten die lijden aan perifeer vaatlijden. Daarom wordt PC-mAb nu getest in een fase 2 klinische trial om te effectiviteit te bepalen in een klinisch relevante populatie. Behandeling met AnxA5 heeft in meerdere muismodellen bewezen dat het zeer effectief is als behandeling tegen schadelijke vasculaire remodellering. AnxA5 is op dit moment nog niet getest in een fase 1 klinische trial, maar omdat er een aantal radioactief gelabelde AnxA5 complexen veilig worden gebruikt om de diagnose van verschillende aandoeningen vast te stellen, is het aannemelijk dat AnxA5 niet voor veel bijwerkingen zal zorgen. In hoofdstuk 5 hebben we de rol van PCAF in schadelijk vasculaire remodellering onderzocht, waarbij we gebruik hebben gemaakt van de PCAF remmer garcinol. Door zijn anti-inflammatoire en anti-prolifererende eigenschappen, is garcinol uitvoerig getest als behandeling tegen verschillende ziektes, zoals kanker, bacteriële infectie, maar ook tegen de ziekte van Alzheimer. Klinische data ontbreekt echter nog, en daarom zal er eerst nog meer bekend moeten worden over de farmacokinetiek van garcinol voordat het kan worden getest in een fase 1 klinische trial. Naast garcinol zijn er nog andere PCAF remmers ontwikkelt, wat de kans om een op PCAF gerelateerd medicijn te vinden vergroot. Miravirsen, een microRNA-122 remmer die replicatie van het Hepatitis C virus verminderd, is op dit moment het enige op een microRNA gebaseerd medicijn dat is getest in een klinische trial. Uit de fase 1 klinische trial bleek dat Miravirsen veilig kon worden toegediend bij vrijwilligers. Maar omdat Miravirsen anders is opgebouwd dan de door ons gebruikte GSOs, is meer kennis noodzakelijk

wat betreft de farmacokinetiek van GSOs voordat ze getest kunnen worden in klinische trials.

Conclusie

Dit proefschrift beschrijft nieuwe inzichten in de rol van het onstekingsproces in cardiale en vasculaire remodellering. Daarnaast beschrijven de studies in dit proefschrift potentiele immuun modulerende therapeutische middelen tegen schadelijke cardiale en vasculaire remodellering. Toekomstig onderzoek moet uitwijzen of deze potentiele medicijnen gebruikt kunnen worden in patiënten die lijden aan cardiovasculaire ziekten.

List of publications

Ewing MM, Karper JC, Abdul S, de Jong RCM, Peters HAB, de Vries MR, Redeker A, Kuiper J, Toes RE, Arens R, Jukema JW, Quax PHA. T-cell co-stimulation by CD28-CD80/86 and its negative regulator CTLA-4 strongly influence accelerated atherosclerosis development. *Int J Cardiol.* 2013 Oct 3;168(3):1965-74.

de Vries MR, Seghers L, van Bergen J, Peters HAB, de Jong RCM, Hamming JF, Toes REM, van Hinsbergh VWM, Quax PHA. C57BL/6 NK cell gene complex is crucially involved in vascular remodeling. *J Mol Cell Cardiol.* 2013 Nov;64:51-8.

Bastiaansen AJNM, Karper JC, Wezel A, de Boer HC, Welten SMJ, de Jong RCM, Peters HAB, de Vries MR, van Oeveren-Rietdijk AM, van Zonneveld AJ, Hamming JF, Nossent AY, Quax PHA. TLR4 accessory molecule RP105 (CD180) regulates monocyte-driven arteriogenesis in a murine hind limb ischemia model. *PLoS One.* 2014 Jun 19;9(6):e99882.

Welten SMJ, Bastiaansen AJNM, de Jong RCM, de Vries MR, Peters HAB, Boonstra MC, Sheikh SP, La Monica N, Kandimalla ER, Quax PHA, Nossent AY. Inhibition of 14q32 MicroRNAs miR-329, miR-487b, miR-494, and miR-495 increases neovascularization and blood flow recovery after ischemia. *Circ Res.* 2014 Sep 26;115(8):696-708.

de Jong RCM, Welten SMJ, Wezel A, de Vries MR, Boonstra MC, Parma L, Jukema JW, van der Sluis TC, Arens R, Bot I, Agrawal S, Quax PHA, Nossent AY. Inhibition of 14q32 microRNA miR-495 reduces lesion formation, intimal hyperplasia and plasma cholesterol levels in experimental restenosis. *Atherosclerosis.* 2017 Jun;261:26-36.

de Jong RCM, Ewing MM, de Vries MR, Karper JC, Bastiaansen AJNM, Peters HAB, Baghana F, van den Elsen PJ, Gongora C, Jukema JW, Quax PHA. The epigenetic factor PCAF regulates vascular inflammation and is essential for intimal hyperplasia development. *PLoS One.* 2017 Oct 10;12(10):e0185820.

Hoving LR, de Vries MR, de Jong RCM, Katiraei S, Pronk A, Quax PHA, van Harmelen V, Willems van Dijk K. The Prebiotic Inulin Aggravates Accelerated Atherosclerosis in Hypercholesterolemic APOE*3-Leiden Mice. *Nutrients.* 2018 Feb 3;10(2).

de Jong RCM, Pluijmert NJ, de Vries MR, Pettersson K, Atsma DE, Jukema JW, Quax PHA. Annexin A5 reduces infarct size and improves cardiac function after myocardial ischemia-reperfusion injury by suppression of the cardiac inflammatory response. *Sci Rep.* 2018 Apr 30;8(1):6753.

Dankwoord

Zonder de hulp van veel dierbaren en collega's was het niet mogelijk geweest om dit proefschrift af te ronden en ik wil dan ook iedereen bedanken die mij tijdens dit traject gesteund heeft. Toch wil ik me in dit dankwoord tot een aantal personen in het bijzonder richten.

Professor Quax, beste Paul, al tijdens mijn sollicitatiegesprek voelde ik me gelijk op mijn gemak en dat is in de zes jaar die ik voor jou heb mogen werken nooit veranderd. Op de momenten dat ik niet meer helemaal wist hoe ik verder moest kon je me altijd gerust stellen en verder op weg helpen. Naast de wetenschappelijke begeleiding was je altijd geïnteresseerd in hetgeen waar ik me naast het werken mee bezighield, zoals het voetballen. Het was dan ook heerlijk om zo nu en dan eens lekker te klagen over de bestuurders en trainers van onze voetbalclubs.

Professor Jukema, beste Wouter, ik wil jou bedanken voor jouw bijdragen bij onze werkbesprekingen. Jij kon als geen ander ervoor zorgen dat het klinische aspect van onze studies voldoende aandacht kregen.

Margreet, mede dankzij jouw expertise op het gebied van immuunhistochemie en jouw chirurgische vaardigheden heb ik dit proefschrift af kunnen maken. Daarnaast heb je me ook veel geleerd hoe belangrijk het is om initiatief te blijven nemen. Dank daarvoor.

Yaël, als ik jou een presentatie zag geven was ik tegelijkertijd jaloers en gemotiveerd. Jaloers, omdat ik dat ook zo goed zou willen kunnen, en gemotiveerd, omdat jouw kalme en duidelijke manier van presenteren mij inspireerde bij mijn onderzoek.

Erna, wat ben ik blij dat jij een van mijn paranimfen bent. Na ruim zes jaar kamergenoten te zijn geweest, kunnen we wel stellen dat jij me het beste kent. Niet alleen jouw hulp en lessen op het lab waren waardevol, maar juist ook je luisterend oor op de momenten dat ik dat nodig had. Heel erg bedankt.

Lieve Mariska, mijn grote zus en een van mijn paranimfen. Toen jij 'ja' zei op de vraag of je mijn paranimf wilde zijn, viel er onmiddellijk een last van mijn schouders. Nu weet ik zeker dat het goed gaat komen. Bedankt dat je er altijd bent voor mij of wie dan ook van onze familie.

Gertjan en Michael, lieve broers, naast het plezier dat jullie me hebben gegeven om altijd een maatje te hebben om mee te spelen tijdens onze jeugd, zijn jullie een voorbeeld voor me op het gebied van doorzettingsvermogen.

Lieve Pap en mam, bedankt voor de zorgeloze jeugd die ik dankzij jullie heb gehad. Jullie stonden altijd voor me klaar en mede daardoor ben ik zover gekomen.

Lieve Amber, jij bent mijn zonnetje in huis, altijd vrolijk, altijd lachend. Na een 'mindere' dag op werk ben ik bij jou altijd snel weer opgevrolijkt, zonder jou was het afronden van mijn proefschrift een stuk moeilijker geweest.

Curriculum Vitae

Rob de Jong werd geboren op 1 februari 1985 te Leidschendam. Na het halen van zijn VWO diploma aan het Alfrink College te Zoetermeer in 2003, werd er in september 2004 begonnen met de opleiding Biologisch en Medisch laboratoriumonderzoek aan de Hogeschool Leiden. Nadat deze opleiding was afgerond, werd er in september 2008 begonnen aan de masteropleiding Biologie aan de Universiteit van Leiden. Van november 2009 tot juni 2010 deed hij zijn afstudeerstage aan de afdeling Integratieve Zoölogie aan de Universiteit van Leiden onder leiding van dr. Frans Witte, waar hij afstudeerde op het onderzoek getiteld "Morphological changes of Lake Victoria cichlid *Haplochromis pyrrhocephalus* within in two decades". In Januari 2011 werd hij aangenomen als researchanalist op de afdeling Heelkunde van het Leids Universitair Medisch Centrum (LUMC) in de groep van Prof. Quax. Na twee jaar als researchanalist werkzaam te zijn geweest, startte hij zijn promotieonderzoek in dezelfde onderzoeksgroepmet als onderwerp "The role of inflammation in cardiac and vascular remodelling". Het eindresultaat ligt voor u. Sinds mei 2017 is Rob werkzaam als researchanalist bij de afdeling Hematologie van het LUMC. Hij woont samen met Amber in Stompwijk.